

CR-128919
Jm6

SURFACE ELECTRICAL PROPERTIES EXPERIMENT

STUDY PHASE

FINAL REPORT

NASA CONTRACT NAS 9-10748

January 1973

Vol. 2 of 3

CENTER FOR SPACE RESEARCH
MASSACHUSETTS INSTITUTE OF TECHNOLOGY

(NASA-CR-128919) SURFACE ELECTRICAL
PROPERTIES EXPERIMENT STUDY PHASE, VOLUME
2 Final Report (Massachusetts Inst. of
Tech.) 345 p HC \$19.25 CSCL 22A

G3/30

Unclass
03416

UN73-23836

CSR-TR-73-1

SURFACE ELECTRICAL PROPERTIES EXPERIMENT

STUDY PHASE

FINAL REPORT

NASA CONTRACT NAS 9-10748

January 1973

Vol. 2 of 3

APPENDIX 3.1

TE/TM PATTERNS OF HERTZIAN DIPOLE IN

TWO-OR THREE-LAYERED MEDIUM

TE/TM Patterns of Hertzian Dipole
in Two- or Three-Layered Medium

William W. Cooper

outline

January 1972

- I. Introduction (literature survey, motivation) ✓
- II. Half-space radiation patterns (and power radiated) ✓
- III. Half-space far surface fields (lateral waves) ✓
- IV. Three-layer fields
 - A. Geometrical optics approximation (reflections) ✓
 - B. Surface layer approximation (perturbations, waveguide modes) ✓
- V. Comparison of dipoles on half-space (tabulation)

Appendices

- A. Approximate integration formulas (Bessel transforms, st.-phase) ✓
- B. Multi-layer transmission matrix formulation ✓

References

TE/TM Patterns of Hertzian Dipole in Two- or Three-Layered Medium

William W. Cooper

January 1972

I. Introduction

The choice of an antenna for a sub-surface radio sounding experiment depends heavily on the radiation properties of the antenna as placed on the surface of the medium. The objective of the lunar surface electrical properties experiment (M.I.T. SEP, Contract NAS9-11540) is to determine the complex dielectric permittivity and/or magnetic permeability in a subsurface domain; by use of electromagnetic field measurements between one or more transmitting antennas and a roving receiving station. Thus the problem is one of inversion: given measurements between different points on a surface, to determine the complex electrical parameters $\epsilon(x,y,z)$ and $\mu(x,y,z)$ under the surface. Because of the nonlinearity of the inversion, a commonly used approach is to simplify the model of the subsurface medium, hoping essential properties of the system are preserved, and to interpret the data by matching measurements with predicted curves for the simplified medium.

A commonly used simplification, dating at least to Sommerfeld (1909), is that the medium is planar-stratified. That is, $\epsilon(z) = \epsilon_i$ and $\mu(z) = \mu_i$ in layer i , for each of a finite number of layers. Therefore, the medium is translationally invariant in the remaining two coordinates (x,y) , and a 2-dimensional Fourier transformation of the field

Reproduced from
best available copy.

equations is permissible, as discussed in Clemmow (1966). The resulting equations, for which I am indebted especially to Baños (1966), have a closed solution in \vec{k} -space (k_x, k_y) , for given source current densities. An infinitesimal dipole source is commonly assumed, which can be transformed into a constant current source in \vec{k} -space. Similar solutions for dipoles in stratified media have been reported by Wait (1970), Brekhovskikh (1960), Bahar (1970), Casey (1971), King and Siegel (1971), Hansen and Tai (1971), Wait and Fuller (1971), and by many previous authors; few of whom have discussed the interpretation of measurements in low-loss media. Assuming that the real medium is a planar-stratified medium, we can address the simplified problem of interpreting or inverting electromagnetic measurements to determine the parameters of the simplified medium: ϵ_i , μ_i , and Δ_i , (thickness of layer i) for all i . Because of the assumed translational invariance, we have a choice of interpreting the measurements either in real space or in \vec{k} -space.

Simplified solutions can be investigated in real space, both as a possible aid in interpreting data and as an aid in system design, by estimating field strengths and polarizations. The approach of Baños (1966), extended by Annan (1970) and Sinha (1971), utilizes a closed form of a Hertzian potential $\vec{\pi}$, followed by an approximate Fourier transform into real space to give the field vectors \vec{E} and \vec{H} . In this approach it is possible to show the genesis of the field vectors directly from the source currents, without using any electromagnetic potentials.

Furthermore, the field vectors are seen to be composed of orthogonal TE and TM components (viz., horizontally or vertically polarized components). An additional interesting property of the solutions is that the fields change discontinuously as a vertical Hertzian source is moved from one side of a boundary (boundary⁻) to the other side (boundary⁺). This direct approach is extended to all six (x-, y-, or z-directed electric or magnetic) Hertzian dipoles, allowing, by superposition, a formulation of the fields in real- or in \vec{k} -space for any infinitesimal dipole or turnstile.

A more practical problem than unraveling the theory of a planar-stratified medium is the choice of an antenna for a medium which may not behave like the stratified model. Also, a real antenna may not act like an infinitesimal dipole, when one considers the problems of its finite size, the effect of the medium on its current distribution, and practical impedance matching. For a rough comparison of dipoles, consider an oversimplified model of an infinitesimal dipole located on the plane between two half-spaces. The half-space solutions for different infinitesimal dipoles can be compared on the basis of: (i) surface fields (non-radiating) and (ii) sub-surface radiation patterns, including (a) antenna gain and total power radiated in various lobes (b) radiation peaks or nulls in various directions and (c) azimuthal symmetry or asymmetry of radiation patterns. The comparison is made on the assumption of constant radiated power, not constant dipole current as is commonly done. Special

results for a 3-layered medium are also of interest for initial design purposes, including: (i) sub-surface reflections and (ii) possible low-loss pseudo-waveguide modes.

II. Half-space radiation patterns

Solutions for a Hertzian dipole in a medium of two isotropic half-spaces have been widely reported (including Sommerfeld, 1909 and 1926; van der Pol and Niessen, 1931; Baños, 1966; Wait, 1970), commonly using electromagnetic potentials to obtain asymptotic far fields. A more direct method, without using electromagnetic potentials, to show all six \vec{E} and \vec{H} components for all six (x-, y-, or z-directed electric or magnetic) Hertzian dipoles, is useful. This approach is equivalent to the solution for a Green's dyadic, as in Van Bladel (1964, p. 221).

Starting from the time-harmonic Maxwell's equations, with phasors proportional to $\exp(j\omega t)$, one easily obtains the inhomogeneous wave equations for \vec{E} and \vec{H} given in Van Bladel (1964, p. 200). The solutions, in an isotropic medium, are a superposition of fields harmonic in x and y, with z-component of \vec{k} -vector satisfying dispersion relation:

$$k_{z1} = \pm k_1 = \pm \sqrt{\omega^2 \mu_1 \epsilon_1 - k_t^2} = \pm \sqrt{k_{c1}^2 - k_t^2} \quad (1)$$

in layer 1, with (x,y)-wavevector $= \vec{k}_t = (k_x, k_y)$. Radiation condition, permitting outgoing waves only for $z \rightarrow \pm\infty$, and dissipativeness of the media require that $\text{Im}(k_1) \leq 0$ and $\text{Re}(k_1) \geq 0$.

Very large values of k_t , which are necessary for representing fields of a point source, imply highly attenuated fields in the $\pm z$ -directions.

For any wavevector, $\vec{k}_1 = (k_{x1}, k_{y1}, k_{z1}) = \vec{k}_t \pm \hat{u}_z k_1$, the fields can be either TE (horizontally polarized) or TM (vertically polarized). In either case, \vec{k}_1 , \vec{E}_1 , and \vec{H}_1 are mutually orthogonal, satisfying $\vec{k}_1 \times \vec{E}_1 = \omega \mu_1 \vec{H}_1$, such that the ratio of magnitudes is $|\vec{E}_1|/|\vec{H}_1| = \sqrt{\mu_1/\epsilon_1}$; but the impedance ratio of transverse components differs for TE and TM fields:

$$n_1 = \frac{E_{1,\text{transverse}}}{H_{1,\text{transverse}}} = \begin{cases} \omega \mu_1 / k_1, & \text{TE} \\ k_1 / \omega \epsilon_1, & \text{TM} \end{cases} \quad \begin{matrix} (2)(a) \\ (b) \end{matrix}$$

Solutions for a two-layer medium (two half-spaces) will illustrate methods which are useful for any finitely-layered medium. First, the source current (specifically for a Hertzian dipole below) is represented as a superposition of harmonic current sheets in transverse plane(s). Second, boundary conditions at the source plane(s) can be solved for the unique outgoing wave amplitudes \vec{H}_t^+ and \vec{H}_t^- for $z \rightarrow \pm\infty$. In any layer i , the transverse components \vec{H}_{t1}^+ and \vec{H}_{t1}^- are taken as independent wave amplitudes. This formulation: (a) assumes implicit factor $\exp(-jk_t \cdot r)$ multiplying all field amplitudes and (b) refers wave (\vec{H}_{t1}^+) amplitudes to innermost boundary of layer i . The other field amplitudes are obtained from:

$$H_{z1} = \mp \frac{k_t}{k_1} \text{sign} [\vec{H}_{t1}^+ \cdot \vec{k}_t] H_{t1} \quad (\text{for TE only}) \quad (3)(a)$$

and

$$\vec{E}_1^\pm = -\frac{1}{\omega\epsilon_1} \frac{1}{r_1^\pm} \times (\vec{H}_{t1}^\pm + \vec{u}_z H_{z1}^\pm) \quad (b)$$

Boundary conditions in a source plane are obtained by first transforming the source into harmonic current sheets. For example, an infinitesimal dipole source $\vec{J} = \vec{a} \delta(x) \delta(y) \delta(z)$ transforms to

$$\vec{J}(k_x, k_y) = (\vec{a}_t + \vec{u}_z a_z) e^{-i\vec{k}_t \cdot \vec{r}} \delta(z) \quad (4)$$

(For a similar development, see Baños, 1966, p. 15ff.) Inhomogeneous excitation equations for a source $\vec{a}(k_x, k_y)$ in the plane $z=0$ are:

$$\vec{H}_{t1} - \vec{H}_{t-1} = -\vec{u}_z \times \vec{a}_t \quad (5)(a)$$

$$\vec{E}_{t1} - \vec{E}_{t-1} = -\vec{k}_t a_z / \omega\epsilon_1 \quad (i=\pm 1) \quad (b)$$

where $i=\pm 1$ in (b) depending on whether the current sheet is "thought of" as existing in the upper medium ($i=+1$) or the lower medium ($i=-1$). For a Hertzian dipole, (4) shows that $\vec{a}(k_x, k_y) = \text{constant}$. Equation (5) can be derived by writing field vectors at the boundary in terms of generalized functions $u(z)$ and $\delta(z)$, then using Maxwell's equations and the continuity of charge (Van Bladel, 1964, pp. 82, 200) to determine the fields across a boundary where $\epsilon^+ \neq \epsilon^-$. Then a final limiting process with a vertical current sheet (a_z) imbedded an infinitesimal distance from a boundary where $\epsilon^+ \neq \epsilon^-$, including the contributions of reflected waves in the "small layer", easily yields (b) (Cooper, 1971, pp. 19, 86). By duality, the solutions for a magnetic

source, $\vec{b}(k_x, k_y) = \vec{b}_t + \vec{u}_z b_z$, are obtained from electric solutions simply by replacing: $\vec{E} \rightarrow \vec{H}$, $\vec{H} \rightarrow -\vec{E}$, $\epsilon_1 \leftrightarrow \mu_1$, $\vec{a}(k_x, k_y) \rightarrow \vec{b}(k_x, k_y)$ (Ramo and Whinnery, 1964, p. 404).

Before progressing to a solution of the half-space problem, some generalities for a layered medium are derived from eq. (5):

(a) \vec{a}_t generates both TE and TM waves (Figure 1); the component of $\vec{a}_t \perp \vec{k}_t$ generates only TE, and the component of $\vec{a}_t \parallel \vec{k}_t$ generates only TM. a_z generates only TM. Dual remarks apply for \vec{b}_t , b_z .

(b) (5) implies that a pure TM field is matched only by a pure TM field, and similarly for TE fields, across any boundary, viz. $z = z_1$. TE and TM fields are decoupled at planar boundaries. In addition, the mutual orthogonality of TE and TM fields for each \vec{k} implies that their powers are additive in integrals giving the total power radiated over all values of \vec{k}_t .

The half-space boundary conditions (5) for a Hertzian dipole (4) are easily solved for

$$\begin{bmatrix} \vec{H}_1^+ \\ \vec{H}_1^- \end{bmatrix} = \frac{1}{(n_1 + n_2)} \begin{bmatrix} n_1 & 1 \\ -n_1 & 1 \end{bmatrix} \begin{bmatrix} \vec{u}_z \times \vec{a}_t \\ \vec{u}_z \times \vec{k}_t a_z / \omega \epsilon_1 \end{bmatrix} \quad (6)$$

(6) gives a complete solution in \vec{k}_t -space (k_x, k_y) , given n_1 from (1) and (2). As shown in Fig. 1, TE and TM fields which are excited proportionally to $\sin\theta$ and $\cos\theta$, can be composed along cylindrical coordinates (r, ϕ, z) . A double Fourier inversion

of the \vec{k}_t -space solution (6) can be integrated first on $\psi = \theta - \phi$:

$$\left. \begin{matrix} \vec{E}(r) \\ \vec{H}(r) \end{matrix} \right\} = \frac{1}{(2\pi)^2} \int_{k_t=0}^{\infty} k_t dk_t \int_{\psi=0}^{2\pi} d\psi e^{-jk_t r \cos \psi} \left\{ \begin{matrix} E(k_t, \theta, z) \\ H(k_t, \theta, z) \end{matrix} \right. \quad (7)$$

using the basic identity $\exp(-jk_t r \cos \psi) = J_0(k_t r) - j2 J_1 \cos \psi - 2J_2 \cos 2\psi - \dots$ (Van Bladel, 1964, p. 514), giving the following ^{exact} result for an electric dipole at $z = 0^-$, observer at $z > 0$:

$$\left. \begin{matrix} E_1(r, \phi, z) \\ H_1(r, \phi, z) \end{matrix} \right\} = \frac{1}{2\pi} \int_{k_t=0}^{\infty} dk_t k_t e^{-jk_1 z} \left\{ \begin{matrix} \vec{E}_1(k_t) \\ \vec{H}_1(k_t) \end{matrix} \right. \quad (8)$$

with (TM fields) (TE fields) (TM fields)

$$\tilde{H}_r = -a_t s\phi \left[\frac{\epsilon_{-1}^{k_{-1}}}{(\epsilon_{-1}^{k_1} + \epsilon_{-1}^{k_{-1}})k_t r} \frac{J_1}{k_t r} + \frac{\mu_{-1}^{k_1}}{\mu_{-1}^{k_1} + \mu_{-1}^{k_{-1}}} \left(J_0 - \frac{J_1}{k_t r} \right) \right] \quad (9)(a)$$

$$\tilde{H}_\phi = -a_t c\phi \left[\frac{\epsilon_{-1}^{k_{-1}}}{(\epsilon_{-1}^{k_1} + \epsilon_{-1}^{k_{-1}})k_t r} \left(J_0 - \frac{J_1}{k_t r} \right) + \frac{\mu_{-1}^{k_1}}{(\mu_{-1}^{k_1} + \mu_{-1}^{k_{-1}})k_t r} \frac{J_1}{k_t r} \right] + a_z \left[\frac{\epsilon_{-1}^{k_t} j J_1(k_t r)}{(\epsilon_{-1}^{k_1} + \epsilon_{-1}^{k_{-1}})} \right] \quad (b)$$

$$\tilde{H}_z = -a_t s\phi \left[\frac{\mu_{-1}^{k_t}}{(\mu_{-1}^{k_1} + \mu_{-1}^{k_{-1}})} j J_1(k_t r) \right] \quad (c)$$

$$\tilde{E}_r = -a_t c\phi \left[\frac{k_1^{k_{-1}}}{\omega(\epsilon_{-1}^{k_1} + \epsilon_{-1}^{k_{-1}})} \left(J_0 - \frac{J_1}{k_t r} \right) + \frac{\omega \mu_{-1} \mu_{-1}}{\mu_{-1}^{k_1} + \mu_{-1}^{k_{-1}}} \frac{J_1}{k_t r} \right] + a_z \left[\frac{\epsilon_{-1}^{k_t} k_1 j J_1(k_t r)}{\omega \epsilon_{-1} (\epsilon_{-1}^{k_1} + \epsilon_{-1}^{k_{-1}})} \right] \quad (d)$$

(TM fields)

(TE fields)

(TM fields)

$$\tilde{E}_\phi = +a_t s\phi \left[\frac{k_t k_{-1}}{\omega(\epsilon_{-1} k_t + \epsilon_{-1} k_{-1}) k_{tr}} \frac{J_1}{\mu_{-1} k_t + \mu_{-1} k_{-1}} + \frac{\omega \mu_{-1} \mu_{-1}}{\mu_{-1} k_t + \mu_{-1} k_{-1}} \left(J_0 - \frac{J_1}{k_{tr}} \right) \right] \quad (e)$$

$$\tilde{E}_z = -a_t c\phi \left[\frac{k_t k_{-1}}{\omega(\epsilon_{-1} k_t + \epsilon_{-1} k_{-1})} jJ_1(k_{tr}) \right] + a_z \left[\frac{\epsilon_{-1} k_t^2 J_0(k_{tr})}{\omega \epsilon_{-1} (\epsilon_{-1} k_t + \epsilon_{-1} k_{-1})} \right] \quad (f)$$

abbreviating $s\phi = \sin\phi$ and $c\phi = \cos\phi$. Almost identical expressions can be written for observer at $z < 0$ *and/or dipole at $z = 0$.* Dual results apply for a magnetic Hertzian dipole. This formulation goes no further than previous authors (Baños, 1966, pp. 25-52, 195-235), but (8) and (9) show explicitly the TE and TM contributions to each cylindrical field component in a form to which a simple stationary-phase approximation can be applied to each component, giving leading asymptotic far fields and antenna power gain.

Using large-argument formulas for $J_0(k_{tr})$ and $jJ_1(k_{tr})$ (Van Bladel, 1966, p. 512), the stationary-phase integral derived in Appendix A gives the leading far-field terms, for $\sqrt{k_{c1} r} \gg 1$:

$$\left. \begin{matrix} E_\phi \\ H_\phi \end{matrix} \right\} = \frac{j2k_{c1} z}{R} \frac{e^{-jk_{c1} R}}{4\pi R} \left\{ \begin{matrix} E'_\phi, & \text{TE} \\ H'_\phi, & \text{TM} \end{matrix} \right. \quad (10)$$

in which $R = \sqrt{r^2 + z^2}$ and E'_ϕ, H'_ϕ are coefficients of the leading terms J_0 and jJ_1 in (9). In the far field, \vec{E} and \vec{H} approximate plane waves propagating from source toward observer;

the power radiated/solid angle is proportional to:

$$\frac{dP}{d\Omega} \approx \sqrt{\frac{\mu_1}{\epsilon_1}} \left| \frac{k_1}{k_{c1}} H'_{\phi, TM} \right|^2 + \sqrt{\frac{\epsilon_1}{\mu_1}} \left| \frac{k_1}{k_{c1}} E'_{\phi, TE} \right|^2 \quad (11)$$

$i = \pm 1$

giving the terms listed in Table 1 (from Cooper, 1971, pp. 39-41).

The asymptotic radiated power density has been integrated over all solid angles to give the power gain shown in Figures 2(a)-(d).

Integrals were evaluated numerically using a 100-point trapezoidal sum to approximate the following:

$$P_L^{\pm} = \left\{ \frac{\pi}{2\pi} \right\} \int_{k_t/k_{c\pm} = 0}^{1(=\text{limit for real propagation angles})} \frac{dk_t}{k_{c\pm}} \frac{k_t}{k_{c\pm}} \frac{k_{c\pm}}{k_1} \frac{dP^{\pm}}{d\Omega_L} \quad (12)$$

with $\begin{cases} \pi & \text{for horizontal dipole (integral of } \sin^2\phi, \cos^2\phi) \\ 2\pi & \text{for vertical dipole (integral of } 1 \cdot d\phi) \end{cases}$

Power gain is given by:

$$\text{Gain}^{\pm} = \frac{\sum_L \frac{dP^{\pm}}{d\Omega_L} (\text{angle})}{\frac{1}{4\pi} \sum_L \sum_{\pm} P_L^{\pm}} \quad (13)$$

(sum contains all terms appropriate for given dipole: upper and lower space, TE and TM radiation terms obvious from (9) and Table 1).

(after p.13)

dipole type	field ($z > 0$)	$\frac{dP^+}{d\Omega_L}$ ($z > 0$) proportional to	$\frac{dP^-}{d\Omega_L}$ ($z < 0$) proportional to
Hertzian electric dipoles			
horizontal - \vec{a}_t			
H'_ϕ (TM)	$\frac{-a_t c \phi \epsilon_{1k-1}}{(\epsilon_{1k_1} + \epsilon_{1k_{-1}})}$	$\left \frac{\sqrt{\mu_1} k_1}{\epsilon_1 k_{c1}} \frac{-a_t c \phi \epsilon_{1k-1}}{(\epsilon_{1k_1} + \epsilon_{1k_{-1}})} \right ^2$	$\left \frac{\sqrt{\mu_{-1}} k_{-1}}{\epsilon_{-1} k_{c-1}} \frac{-a_t c \phi \epsilon_{1k-1}}{(\epsilon_{1k_1} + \epsilon_{1k_{-1}})} \right ^2$
E'_ϕ (TE)	$\frac{a_t s \phi \omega \mu_{1k-1}}{(\mu_{1k_1} + \mu_{1k_{-1}})}$	$\left \frac{\sqrt{\epsilon_1} k_1}{\mu_1 k_{c1}} \frac{a_t s \phi \omega \mu_{1k-1}}{(\mu_{1k_1} + \mu_{1k_{-1}})} \right ^2$	$\left \frac{\sqrt{\epsilon_{-1}} k_{-1}}{\mu_{-1} k_{c-1}} \frac{a_t s \phi \omega \mu_{1k-1}}{(\mu_{1k_1} + \mu_{1k_{-1}})} \right ^2$
vertical - a_z			
H'_ϕ (TM)	$\frac{a_z \epsilon_{1k_t}}{(\epsilon_{1k_1} + \epsilon_{1k_{-1}})}$	$\left \frac{\sqrt{\mu_1} k_1}{\epsilon_1 k_{c1}} \frac{a_z \epsilon_{1k_t}}{(\epsilon_{1k_1} + \epsilon_{1k_{-1}})} \right ^2$	$\left \frac{\sqrt{\mu_{-1}} k_{-1}}{\epsilon_{-1} k_{c-1}} \frac{a_z \epsilon_{1k_t}}{(\epsilon_{1k_1} + \epsilon_{1k_{-1}})} \right ^2$
Hertzian magnetic dipoles (by duality)			
horizontal - \vec{b}_t			
E'_ϕ (TE)	$\frac{b_t c \phi \mu_{1k-1}}{(\mu_{1k_1} + \mu_{1k_{-1}})}$	$\left \frac{\sqrt{\epsilon_1} k_1}{\mu_1 k_{c1}} \frac{b_t c \phi \mu_{1k-1}}{(\mu_{1k_1} + \mu_{1k_{-1}})} \right ^2$	$\left \frac{\sqrt{\epsilon_{-1}} k_{-1}}{\mu_{-1} k_{c-1}} \frac{b_t c \phi \mu_{1k-1}}{(\mu_{1k_1} + \mu_{1k_{-1}})} \right ^2$
H'_ϕ (TM)	$\frac{b_t s \phi \omega \epsilon_{1k-1}}{(\epsilon_{1k_1} + \epsilon_{1k_{-1}})}$	$\left \frac{\sqrt{\mu_1} k_1}{\epsilon_1 k_{c1}} \frac{b_t s \phi \omega \epsilon_{1k-1}}{(\epsilon_{1k_1} + \epsilon_{1k_{-1}})} \right ^2$	$\left \frac{\sqrt{\mu_{-1}} k_{-1}}{\epsilon_{-1} k_{c-1}} \frac{b_t s \phi \omega \epsilon_{1k-1}}{(\epsilon_{1k_1} + \epsilon_{1k_{-1}})} \right ^2$
vertical - b_z			
E'_ϕ (TE)	$\frac{-b_z \mu_{1k_t}}{(\mu_{1k_1} + \mu_{1k_{-1}})}$	$\left \frac{\sqrt{\epsilon_1} k_1}{\mu_1 k_{c1}} \frac{-b_z \mu_{1k_t}}{(\mu_{1k_1} + \mu_{1k_{-1}})} \right ^2$	$\left \frac{\sqrt{\epsilon_{-1}} k_{-1}}{\mu_{-1} k_{c-1}} \frac{-b_z \mu_{1k_t}}{(\mu_{1k_1} + \mu_{1k_{-1}})} \right ^2$

Table 1

Asymptotic radiation field coefficients

Figures 2(a)-(d) show an infinite derivative in the antenna pattern near the critical angle $\theta_c = \cos^{-1} (\mu_1 \epsilon_1 / \mu_{-1} \epsilon_{-1})^{1/2}$. This result should not be surprising, because waves propagating near the surface of the upper medium (free space) should generate an infinitely-extending disturbance in the surface, with periodic factor proportional to $\exp(-jk_{c1}r)$, which is equivalent to excitation by a tapered ^{surface} array, with wavelength of the upper medium. Kirchhoff's vector integral (Jackson, 1967, p. 287), with integrand proportional to surface \vec{E} , will show the corresponding "head" wave in the lower medium at an angle corresponding to the tapered periodic surface excitation. The infinite derivative is not surprising for infinite-area "array" excitation. Furthermore, the discontinuity in derivative occurs only as a function of angle at infinite distance, not as a function of any spatial coordinate at any finite radius.

III. Half-space far surface fields

Leading terms of the asymptotic surface fields (which may be important in the interpretation of data at intermediate ranges, where scattering and reflections are relatively small) are obtained from (8) and (9) simply by an approximate real integration near the branch points of the two outermost layers: k_{c1} and k_{c-1} , obtaining the lateral waves of Brekhovskikh (1960, p. 270 ff.) (who used a contour integration). The two lateral waves are proportional to $\exp(-jk_{c1}r)/r^2$ and $\exp(-jk_{c-1}r)/r^2$. My method is an integration of the expression for a Hertzian dipole (8) for $0 < k_t < \infty$, assuming $z > 0$ for convergence. The contribution near each branch point k_{c1} (near the real axis, for assumed low-loss media) is approximated by integrating the leading terms of (9) proportional to $k_1 = \sqrt{k_{c1}^2 - k_t^2}$ and $k_{-1} = \sqrt{k_{c-1}^2 - k_t^2}$. These terms, each a constant $\cdot k_1$, can be subtracted from (9), leaving functions smoother than (9) near the branch points. For similar results, see Rice (1937). The terms $\sim k_1$ and $\sim k_{-1}$ are integrated by (A-5), which is exact for a kernel $J_0(k_tr)$ and asymptotic for $jJ_1(k_tr)$; further questions of my approximations are touched in Appendix A.

The leading terms of (9) are obtained by a geometric series' method, illustrated by an example:

$$H_r = -a_t \sin \phi \left(\frac{\mu_{-1} k_1}{\mu_{1-1} k} \right) \left\{ \left[1 - \left(\frac{\mu_{-1} k_1}{\mu_{1-1} k} \right) - \left(\frac{\mu_{-1} k_1}{\mu_{1-1} k} \right)^2 - \dots \right] \right.$$

(near k_{c1} , $k_1 \rightarrow 0$, $k_{-1} \rightarrow \sqrt{k_{c-1}^2 - k_{c1}^2}$)

$$+ \left[1 - \left(\frac{1^{k_{-1}}}{-1^{k_1}} \right) - \left(\frac{1^{k_{-1}}}{-1^{k_1}} \right)^2 - \dots \right] \} \quad (14)$$

(near $k_{c_{-1}}$, $k_{-1} \rightarrow 0$, $k_1 \rightarrow -j \sqrt{k_{c_{-1}}^2 - k_{c_1}^2}$)

in which the leading terms are circled. The resulting surface field term is:

$$H_r \sim -2a_t \sin \phi \left\{ \frac{\mu_{-1}^{k_{c_1}}}{\mu_1^K} \frac{e^{-jk_{c_1}R}}{4\pi R^2} - \frac{\mu_1^{k_{c_{-1}}}}{\mu_1(-jK)} \frac{e^{-jk_{c_{-1}}R}}{4\pi R^2} \right\} \quad (15)$$

in which $R = \sqrt{r^2 + z^2}$ and $K = \sqrt{k_{c_{-1}}^2 + k_{c_1}^2}$. Final surface coefficients, expressed in terms of dipole current (not radiated power), are listed in Table 2. Assuming $\mu_1 = \mu_{-1}$, the coefficients are functions of $c = \epsilon_{-1}/\epsilon_1$ and $k = \sqrt{c - 1}$. For the horizontal electric dipole in such a medium, $E_z^{\pm}/H_{\phi}^{\pm} = \sqrt{\mu_1/\epsilon_{\pm 1}}$. The imaginary terms in Table 2 imply that: for any dipole, either \vec{E} or \vec{H} or both will be elliptically polarized on the surface.

The coefficients of Table 2 were further adjusted for the condition of constant dipole radiated power leading to the curves of Figure 3 for a horizontal electric dipole. Curves for other dipoles are in Cooper (1971, pp. 62-66).

(after p. 13)

H-coefficient, to be multiplied by		E-coefficient, to be multiplied by	
$\frac{2ck_{c1}}{K} \frac{e^{-jk_{c1}r}}{4\pi r^2}$	$\frac{2ck_{c1}}{K} \frac{e^{-jk_{c1}r}}{4\pi r^2}$	$\sqrt{\frac{\mu}{\epsilon_1}} \frac{2ck_{c1}}{K} \frac{e^{-jk_{c1}r}}{4\pi r^2}$	$\sqrt{\frac{\mu}{\epsilon_1}} \frac{2ck_{c1}}{K} \frac{e^{-jk_{c1}r}}{4\pi r^2}$
electric dipoles horizontal - a_t			
H_r $-c^{-1}$	$jc^{-1/2}$	E_r $-c^{-1} k$	$-c^{-3/2} k$
H_ϕ 1	$-jc^{-3/2}$	E_ϕ $-c^{-1} k$	$c^{-1/2} k$
H_z $c^{-1} k^{-1}$	$-k^{-1}$	E_z 1	$-jc^{-1}$
vertical - a_z			
H_ϕ ck^{-1}	$c^{-1} k^{-1}$	E_r 1	$-jc^{-1}$
		E_z $-ck^{-1}$	$c^{-1/2} k^{-1}$
$\sqrt{\frac{\mu}{\epsilon_1}} \frac{c^2}{c-1} \frac{e^{-jk_{c1}r}}{4\pi r^2}$	$\sqrt{\frac{\epsilon_1}{\mu}} \frac{c^2}{c-1} \frac{e^{-jk_{c1}r}}{4\pi r^2}$	$\frac{c^2}{c-1} \frac{e^{-jk_{c1}r}}{4\pi r^2}$	$\frac{c^2}{c-1} \frac{e^{-jk_{c1}r}}{4\pi r^2}$
magnetic dipoles horizontal - b_t			
H_r $c^{-2} k$	$c^{-3/2} k^2$	E_r $-c^{-1} k$	$jc^{-5/2} k$
H_ϕ 1	$-c^{-5/2}$	E_ϕ $c^{-2} k$	$-jc^{-3/2} k$
H_z $-c^{-2} k$	$jc^{-1} k$	E_z 1	$-c^{-2}$
vertical - b_z			
H_r $c^{-2} k$	$-jc^{-1} k$		
H_z $-c^{-2}$	$c^{-1/2}$	E_ϕ c^{-2}	$-c^{-1}$

Table 2 Asymptotic surface field coefficients

IV. Three-layer fields

Sub-surface reflected fields are of more importance than surface (lateral) waves because of the slower decay of reflected waves at moderate to long ranges. Rather than repeating estimates of field strength (Annan, 1970; Sinha, 1971) involving saddle-point integration of expressions derived from a Hertz vector (a method pioneered by Baños, 1966); two other topics are of interest here: (i) investigation of maximum range at which geometrical optics reflections can be expected and (ii) investigation of effects of a thin surface layer, including (a) perturbation of antenna patterns and (b) possibility of low-loss waveguide modes.

For a geometrical optics' reflection, it is sufficient to consider only the wave components \vec{H}_t , because the other components are given by (3). In a 3-layer medium (formally, a 4-layer medium as illustrated in Figure 4, with layers 1 and -1 electrically identical), the wave amplitudes are found as a solution of (5):

$$\begin{bmatrix} H_2^+ \\ H_{-2}^- \end{bmatrix} = \frac{\begin{bmatrix} (d_{-1}/t_{-1} - s_{-1}t_{-1}) & (d_{-1}/t_{-1} & s_{-1}t_{-1}) \\ (s_1/t_1 - d_1t_1) & (s_1/t_1 & d_1t_1) \end{bmatrix} \begin{bmatrix} \vec{u}_z \times \vec{a}_t(k_x, k_y) \\ -\vec{u}_z \times \vec{k}_t a_z n_1 / \omega \epsilon_1 \end{bmatrix}}{(s_1 s_{-1} t_{-1} / t_1 - d_1 d_{-1} t_1 t_{-1})} \quad (16),$$

where:

$$t_1 = e^{-jk_1 \Delta_1} \quad \text{upward propagation factor of layer 1} \quad (17)(a)$$

$$t_{-1} = e^{-jk_1 \Delta_{-1}} \quad \text{downward propagation factor in layer -1} \quad (b)$$

$$s_1 = 1 + n_2/n_1 \quad (18)(a)$$

$$d_1 = 1 - n_2/n_1 \quad (b)$$

$$s_{-1} = 1 + n_{-2}/n_1 \quad (c)$$

$$d_{-1} = 1 - n_{-2}/n_1 \quad (d)$$

k_1 and n_1 (TE or TM) are defined in (1) and (2). (16) is exact and therefore applicable to thick or thin layers, TE or TM waves, horizontal sources. Exactly as for the half-space solutions (6)-(9), the solutions for a magnetic source are written by duality. By letting $\Delta_1 = 0$ or $\Delta_{-1} = 0$ one obtains a special result for a buried layer or a raised layer. (By letting $\Delta_{-1} = \Delta_1 = 0$, the half-space solution (6) results.)

A. Geometrical optics approximation

Denominator of (16) can be expanded in a geometric series (19) (in lossless media, this is valid if k_1 k_{-1} is real and k_2 and/or k_{-2} is real). Restriction to lossless media is not necessary to ensure convergence of geometric series; however, this simple sufficient condition simplifies things.

$$\frac{1}{(s_{1-1-1} t/t_{-1} - d_{1-1} t/t_{-1})} = \frac{t_1}{s_{1-1-1} t} \left[1 + \left(\frac{d_{1-1} t^2}{s_{1-1-1} t^2} \right) + \left(\frac{d_{1-1} t^2}{s_{1-1-1} t^2} \right)^2 + \dots \right] \quad (19).$$

(16) will not be completely expanded (see Cooper, 1971, pp. 76-79) but typical terms, for example the terms of H_2^+ are

flections, replacing Δ_1 by $(m\Delta_1 + n\Delta_{-1})$. An equivalent statement is that the total vertical change (Δ_1 for the direct ray as shown in Fig. 4) projected along the ray path in the 3-layer medium, must be large with respect to the wavelength. Beyond r_{\max} , the fields are approximated by lateral waves ($\sim r^{-2}$) (as in Table 2) if low-loss waveguide modes ($\sim r^{-1/2}$) can be excluded, as discussed in B.

Higher reflections (near vertical incidence, with $z \approx R$) may be approximated by geometrical optics, using a contour integration, as in Baños (1966, pp. 159-172); the stationary-phase integration with real k_t is not valid here. For our purposes, such higher reflections are not important because the fields should be attenuated greatly due to multiple transmission losses (leakage) and geometrical spreading (since $z \gg r$).

As discussed in Annan (1970, pp. 54-61), the geometrical optics approach applied in his thesis should be superior to the normal mode approach for thick sub-surface layers which cannot sustain total internal reflection of plane waves at both upper and lower boundaries. In such a medium, lateral waves ($\sim r^{-2}$) will predominate at long ranges.

proportional to:

$$\frac{t_1}{s_1} \cdot \left(\frac{d_1 d_{-1}}{s_1 s_{-1}} \frac{t_1^2}{t_{-1}^2} \right)^N \quad (20)(a)$$

$$\text{and } \frac{d_{-1}}{s_{-1}} \frac{t_1}{t_{-1}} \cdot \left(\frac{d_1 d_{-1}}{s_1 s_{-1}} \frac{t_1^2}{t_{-1}^2} \right)^N ; N = 0, 1, 2, \dots \dots (b)$$

A Fourier inversion of (16) , integrated first over angle ψ as in (7), followed by a stationary-phase approximation of the single integrals involving Bessel functions and exponential factors t_1 and t_{-1} , will yield the geometrical optics fields as in (10); but with z and R corresponding to the specular reflected path (shown in Figure 4) and with amplitude factors from (20) which includes multiple reflection factors $(d_1 d_{-1} / s_1 s_{-1})^N$ at upper and lower boundaries. As in the half-space media, the results apply to both TE and TM fields, when the corresponding impedances (2) and angular factors (ϕ) as in (9) are included.

The stationary-phase approximation of Appendix A is good only if the argument of the exponential factor (which is k_1 for the first term in (20), $k_1(\Delta_1 - 2\Delta_{-1})$ for the next term, etc.) exceeds roughly 2π for the specular ray path. Translated to geometrical terms, the limit of range is

$$r_{\max} \approx \frac{2\Delta_1^2}{\lambda_1} = \frac{k_{c1} \Delta_1^2}{\pi} \quad (21),$$

for a thick layer ($\Delta_1 / \lambda_1 \gg 1$) and similarly for multiple re-

B. Surface layer approximation

A thin surface layer, for example a photoelectron layer above a planetary surface, may produce a noticeable perturbation of the antenna patterns and surface fields of an infinitesimal dipole. The solution (16) in k_t -space can be simplified when $k_{c1}(\Delta_{-1} + \Delta_1) \gg 1$ giving first-order approximations:

for TE waves

$$H(0) \simeq \frac{[k_2 + j(k_2 k_{-2} \Delta_{-1} + k_1^2 \Delta_1)](-u_z \times a_t)}{(k_2 + k_{-2}) + j(\Delta_1 + \Delta_{-1})(k_1^2 + k_2 k_{-2})} \quad (22)(a)$$

$$E(0) \simeq \frac{[1 + j(k_{-2} \Delta_{-1} + k_2 \Delta_1)] \omega u(-u_z \times a_t)}{(k_2 + k_{-2}) + j(\Delta_1 + \Delta_{-1})(k_1^2 + k_2 k_{-2})} \quad (b)$$

for TM waves

$$H(0) \simeq \frac{[k_2 \epsilon_1 \epsilon_{-1} + j(k_1^2 \epsilon_2 \epsilon_{-2} \Delta_{-1} + k_2 k_{-2} \epsilon_1^2 \Delta_1)](-u_z \times a_t) + [\epsilon_2 \epsilon_{-2} + j(k_2 \epsilon_1 \epsilon_2 \Delta_{-1} + k_2 \epsilon_1 \epsilon_{-2} \Delta_1)](-u_z \times k_t a_z)}{\epsilon_1(k_2 \epsilon_{-2} + k_{-2} \epsilon_2) + j\Delta(k_1^2 \epsilon_2 \epsilon_{-2} + k_2 k_{-2} \epsilon_1^2)} \quad (c)$$

$$E(0) \simeq \frac{[k_2 k_{-2} \epsilon_1^2 + jk_1^2(k_2 \epsilon_1 \epsilon_{-2} \Delta_{-1} + k_{-2} \epsilon_1 \epsilon_2 \Delta_1)](-u_z \times a_t)/\omega \epsilon_1 + [k_2 \epsilon_1 \epsilon_{-2} + j(k_2 k_{-2} \epsilon_1^2 \Delta_{-1} + k_1^2 \epsilon_2 \epsilon_{-2} \Delta_1)](-u_z \times k_t a_z)/\omega \epsilon_1}{\epsilon_1(k_2 \epsilon_{-2} + k_{-2} \epsilon_2) + j\Delta(k_1^2 \epsilon_2 \epsilon_{-2} + k_2 k_{-2} \epsilon_1^2)} \quad (d)$$

In these expressions, perturbations first order in Δ_1 and Δ_{-1} are apparent (provided $k_2 + k_{-2}$ does not approach zero). A sample perturbed radiation pattern is shown in Figure 5.

Low-loss real or pseudo-waveguide modes will be manifested

in spikes of (22) on the real k_t -axis. It is not necessary for a pole to exist near the real axis in order for the integrand (22) of the real-integral formulation (8) to exhibit finite spikes which lead to pseudo-waveguide fields: surface fields with approximate $r^{-1/2}$ decay, to a maximum range of approximately $1/\delta k$ where δk is the half-width of the spike. If $(\Delta_1 + \Delta_{-1})$ is made arbitrarily small, then the only rapid changes in (22) are $\sim k_2$ and $\sim k_{-2}$ producing lateral waves (III, Table 2). If $k_2 \approx k_{-2}$, then the existence and amplitude of spikes and/or poles near the branch points depends in a complicated manner on the magnitudes of $k_{c_1}(\Delta_1 + \Delta_{-1})$ and on the loss tangents in the media, and is probably of academic interest. A radio sounding situation where $k_2 \approx k_{-2}$ is unlikely; and, if it occurred, the amplitude of the surface fields probably would be much less than other contributions. Early references to surface waves in a thin dielectric are in Attwood (1951) and Barlow (1956).

V. Comparison of dipoles

A summary of half-space field properties of different infinitesimal dipoles is shown in Table 3. Peak sub-surface directivity, azimuthal symmetry, sub-space power as a fraction of total, and relative field amplitudes are shown; all normalized for constant dipole radiated power and with $\mu_1 = \mu_{-1}$, $\epsilon_{-1}/\epsilon_1 = 4$. The upper and lower lateral wave amplitudes in Table 3 are for fields $\sim \exp(-jk_{c_1}r)$ and $\sim \exp(-jk_{c_{-1}}r)$ respectively. Here; VED = vertical electric dipole, HED = horizontal electric dipole, VMD = vertical magnetic dipole, HMD = horizontal magnetic dipole,

Dipole Type	Max. Gain	Symmetry	Power Rad.	Surface Fields r^{-2}					
				H_r	H_ϕ	H_z	E_r	E_ϕ	E_z
VED	10.6		.661		1.174 -.073		.508 -j.127		-1.174 .147
HED-TM	2.4		.276		1.000 -j.125		-.433 -.217		1.000 -j.062
HED-TE	5.1		.460	-.250 j.500		.125 -.577		-.143 .289	
VMD	3.7		.938	.131 -j.523		-.075 .604		.075 -.302	
HMD-TM	10.1		.227		1.624 -.050		-.704 j.088		1.624 -.101
HMD-TE	1.9		.239	.304 .152		-.304 j.704		.176 -j.088	
HET	2.5		.736	-.177 j.353	.707 -j.085	.085 -.408	-.306 -.153	-.101 .204	.707 -j.044
HMT	5.0		.466	.215 -.107	1.149 -.035	-.215 j.487	-.487 j.062	.124 -j.062	1.149 -.071

Table 3 Summary of half-space Hertzian dipole properties

HET = horizontal electric turnstile, HMT = horizontal magnetic turnstile.

cylindrical symmetry

cylindrical asymmetry with TE & TM lobes
90° apart with power \cos^2 , \sin^2 .

Conclusions from Table 3 will not be drawn, because of
(i) conflicting desirable properties of different dipoles and
(ii) various practical problems of dipole and system design
which were not considered here. No such comparison of dipoles
normalized for constant radiated power has been seen in the lit-
erature, although Baños (1966, Ch. 7) makes a good comparison
based on constant excitation current.

Appendix A Approximate integration formulas

The real integral formulation (8) for the half-space fields
can be approximated simply in three cases: (a) asymptotic radia-
tion fields; by a stationary-phase approximation, (b) asymptotic
surface fields (lateral waves) by a Bessel-function identity
and (c) very near fields, by use of integration formulas from
Magnus and Oberhettinger (1966, p. 91). The very near fields (c)
will not be presented here, although it will be mentioned that:
for $\mu_1 = \mu_{-1}$, the \vec{E} -field approaches that of a Hertzian electric
dipole in a medium with $\epsilon = (\epsilon_{-1} + \epsilon_1)/2$, but the \vec{H} -field lines
are denser in the sub-space (for $\epsilon_{-1} > \epsilon_1$) and are distorted from
their bilateral symmetry (in an isotropic medium) to satisfy

Maxwell's displacement equation ($\vec{\nabla} \times \vec{H} = j\omega\epsilon_1 \vec{E}$).

The stationary-phase approximation (b) used to derive (10) will only be sketched. Van Bladel (1964, p. 512) gives

$$J_B(k_t r) \sim \sqrt{2/\pi k_t r} \cos(k_t r - n\pi/2 - \pi/4) \quad (A-1)$$

which is written in exponential form to combine with the exponential term of (8) to give a term

$$e^{j\Phi}, \quad \Phi = - (k_t r + k_1 z) \quad (A-2)$$

exhibiting stationary phase ($d\Phi/dk_t = 0$) where $k_t/k_1 = r/z$ and $d^2\Phi/dk_t^2 = R^3/k_{c1} z^2$ (in which $R = \sqrt{r^2 + z^2}$) so that (8) can be approximated by the Fresnel integral formula:

$$\int_{-\infty}^{\infty} e^{jk^2} dk = (1+j) \frac{\pi}{2} = \sqrt{\pi} e^{j\pi/4} \quad (A-3)$$

giving (10). Higher derivatives of the amplitude and phase of the integrand in (8) could be included but are unnecessary for first-order fields.

A Bessel function identity (b) for the surface fields is derived from the free-space dipole integral formulation. As shown in Cooper (1971, pp. 88-91), the fields of a Hertzian dipole (4) in free space is derived simply from the vector wave equations for \vec{E} and \vec{H} in Cartesian coordinates (Van Bladel, 1964, p. 200),

by operation on a scalar Green's function, $G = \exp(-jk_c R)/4\pi R$.

The integral formulation (8) for \vec{H}_t (in same plane as dipole \vec{a}_t) implies the exact integral:

$$\frac{1}{2\pi} \int_{k_t=0}^{\infty} dk_t k_t e^{-jk_1 z} J_0(k_t r) = -2\partial_z G = 2 \left(\frac{jk_c z}{R} + \frac{z}{R^2} \right) \cdot G \quad (A-4)$$

(A-4) leads directly to

$$\frac{1}{2\pi} \int_{k_t=0}^{\infty} dk_t k_t e^{-jk_1 z} k_1 J'_0(k_t r) = -j2\partial_z^2 G = 2 \left(\frac{k_c}{R} + \frac{1}{R^2} \right) \cdot G \text{ at } z=0 \quad (A-5)$$

A number of other identities can be derived from (A-4), principally involving derivatives of (A-4) with respect to r or z . However, the additional formula used in deriving Table 2 from (8) and (9) is the same as (A-4) except that J_0 is replaced by jJ_1 which is valid for large r as implied by (A-1).

The validity of a geometric series approximation of (9), as shown in (14), allowing the use of (A-5) for the surface fields will not be discussed in detail. A qualitative argument is as follows. (A) the exact integral (8) includes: (a) an envelope factor $E(k_t)$ including (i) the rational functions of k_1 and k_{-1} in (9), (ii) the asymptotic amplitude $(\sqrt{2/\pi k_t r})$ of (A-1) and (iii) $\exp(-jk_1 z)$ which $\sim \exp(-k_t z)$ for large k_t and for $z > 0$, and (b) a rapid oscillatory factor, $\cos(k_t r - n\pi/2 - \pi/4)$, also from

(A-1). (B): after subtracting the terms $\sim k_1$ and $\sim k_{-1}$ which give the singularities in the derivative (dE/dk_t), the envelope of the remainder ($E - c_1 k_1 - c_2 k_{-1}$) is smooth and integrable for $0 < k_t < \infty$. (C): as $r \rightarrow \infty$, the integral transform of the smooth remainder (continuous first derivative) will approach zero at least as $r^{-5/2}$. In fact, the next asymptotic terms are $\sim r^{-3}$, obtained by integrating terms $\sim k_1^3$ and $\sim k_{-1}^3$, leaving a still smoother remainder (continuous second derivative).

Appendix B Multi-layer transmission matrix formulation

Formal solutions for horizontally and vertically polarized wave amplitudes in finitely-layered media long have been known (see Bahar, 1970; references in Wait, 1970 and in Brekhovskikh, 1960). Here the formal solution is stated simply in terms of our own TE/TM, \vec{H}_t -amplitude formalism, and indexing of layers. Starting from source at $z=0$, layers are indexed upward from $i=1$ to I and downward from $i=-1$ to $-J$, with planar boundaries at $z=z_i$. Wave amplitudes, \vec{H}_{t1}^+ and \vec{H}_{t1}^- for upgoing and down-going waves respectively, both are referred to innermost boundary of layer 1. For a layer above the source ($i > 0$), the transmission of wave amplitudes is determined by continuity of transverse \vec{E}_t and \vec{H}_t :

$$\begin{bmatrix} \vec{H}_{t1}^+ \\ \vec{H}_{t1}^- \end{bmatrix} = \frac{1}{2} \begin{bmatrix} s_1/t_1 & d_1/t_1 \\ d_1 t_1 & s_1 t_1 \end{bmatrix} \begin{bmatrix} \vec{H}_{t1+1}^+ \\ \vec{H}_{t1+1}^- \end{bmatrix} \quad (A-5)$$

where t_1 , s_1 , d_1 are defined as in (17), (18). The same expression applies for $i < 0$ but with $(i+1)$ replaced by $(i-1)$. Satisfaction of boundary conditions (5) at $z=0$ simply requires a solution of 2×2 linear equations for \vec{H}_I^+ and \vec{H}_J^- , from which \vec{E} and \vec{H} directly can be found at any z by use of transmission matrices (A-5) and wave relations (3).

References

1. Annan, A. P., M. S. thesis: Radio interferometry depth sounding, Dep't. of Physics, U. of Toronto, Jan. 1970.
2. Attwood, S. S., Surface wave propagation over a coated plane conductor, J. Appl. Phys. 22, 504-509, 1951.
3. Bahar, E., Propagation of radio waves over a non-uniform layered medium, Radio Sci. 5 #7, 1069-1076, July 1970.
4. Baños, A., Dipole Radiation in the Presence of a Conducting Half-Space, Pergamon Press, Oxford, 1966.
5. Barlow, H. M. and Cullen, A. L., An investigation of the properties of radial surface waves launched over a flat reactive surface, Proc. I. E. E. (British) 103B, 307-318, 1956.
6. Brekhovskikh, L. M., Waves in Layered Media, Academic Press, N. Y., 1960.
7. Casey, K. F., Two-dimensional fields in azimuthally inhomogeneous media, I.E.E.E. Trans. on AP 19 #4, 571-572, July 1971.
8. Cagniard, L. Basic theory of the magneto-telluric method of geophysical prospecting, Geophysics 18 #3, 605-635, 1953.
9. Cooper, W. W., M.I.T. Center for Space Research: TR71-3, Patterns of dipole antenna on stratified medium, June 1971.
10. Hansen, P. M. and Tai, C. T., Radiation from sources in the presence of a flat earth, I.E.E.E. Trans. on AP 18 #3, 423-424, May 1970.
11. Jackson, J. D., Classical Electrodynamics, Wiley, N. Y., 1966.
12. King, R. W. P. and Siegel, M., Radiation from linear antennas in a dissipative half-space, I.E.E.E. Trans. on AP 19 #4, 477-485, July 1971.

13. Magnus, W., Oberhettinger, F., Soni, R. P., Formulas and Theorems for the Special Functions of Mathematical Physics, Springer, N.Y., 1966.
14. Ramo, S. and Whinnery, J. R., Fields and Waves in Modern Radio, Wiley, N.Y., 1964.
15. Rice, S. O., Series for the wave function of a radiating dipole at the earth's surface, Bell Sys. T. J. 16, 101-109, 1937.
16. Sinha, A. K., Theoretical studies of the radio-frequency interferometry method of sounding, Dep't. of Physics, U. of Toronto, Mar. 1971.
17. Sommerfeld, A. N., "Über die Ausbreitung der Wellen in der drahtlosen Telegraphie, Ann. Physik 28, 665-737, 1909.
Sommerfeld, A. N., (same title), Ann. Physik 81, 1135-1153, 1926.
18. Van Bladel, J., Electromagnetic Fields, McGraw-Hill, N.Y., 1964.
19. Van der Pol, B. and Niessen, K. F., "Über die Raumwellen von einem vertikalen Dipolsender auf ebener Erde, Ann. Physik 10, 485-510, 1931.
20. Wait, J. R., Electromagnetic Waves in Stratified Media, Pergamon Press, Oxford, 1970.
21. Wait, J. R. and Fuller, J. A., "On radio propagation through earth, I.E.E.E. Trans. on AP 19 #6, Nov. 1971.

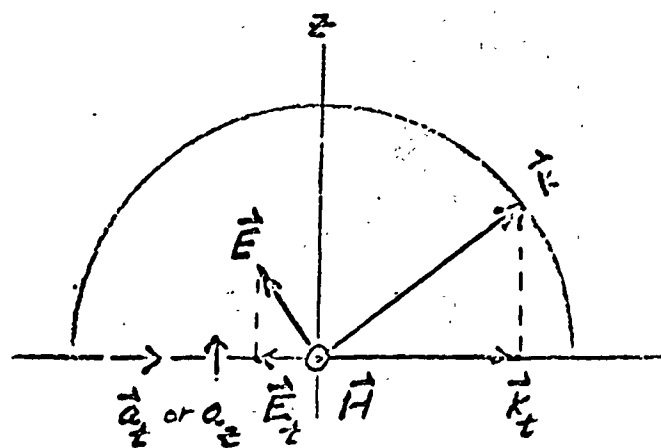
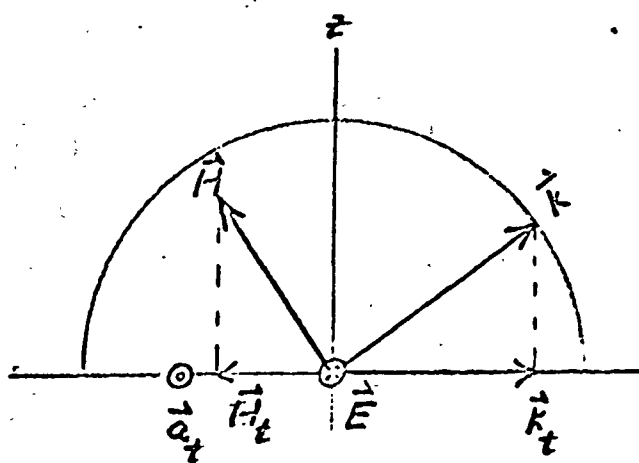
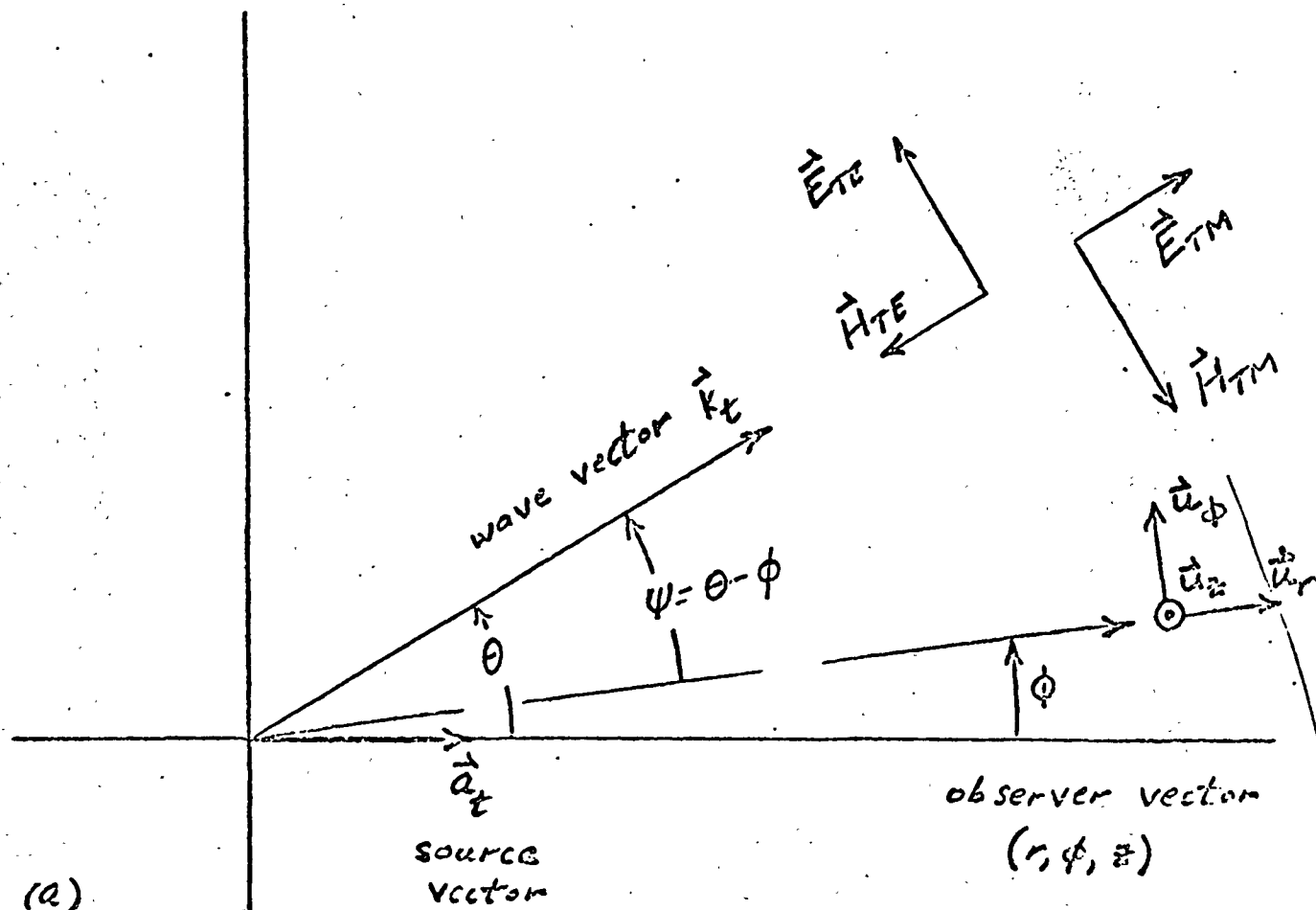
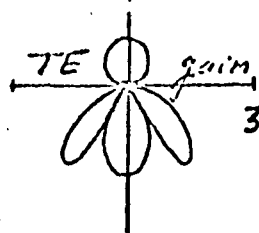
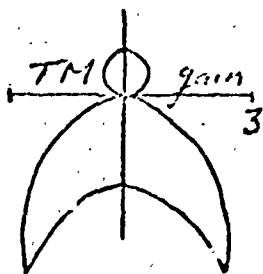


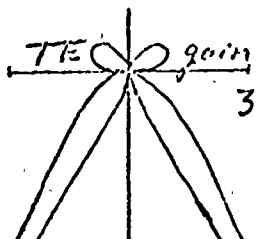
Fig. 1. TE & TM wave excitation by current sheet
 should be re-drawn with lettering $\geq 3/16$ "

TM patterns TE patterns

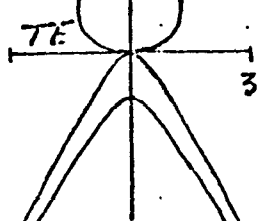
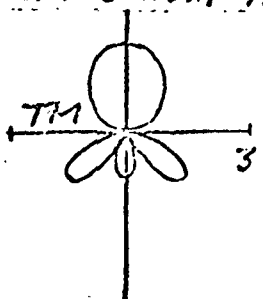
(a) horizontal electric dipole



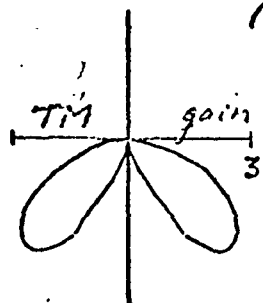
(b) vertical electric dipole



(c) horizontal magnetic dipole



(d) vertical magnetic dipole



all for $\mu_1 = \mu_2$
 $\epsilon_1/\epsilon_2 = 4$

power split
upper space & lower space

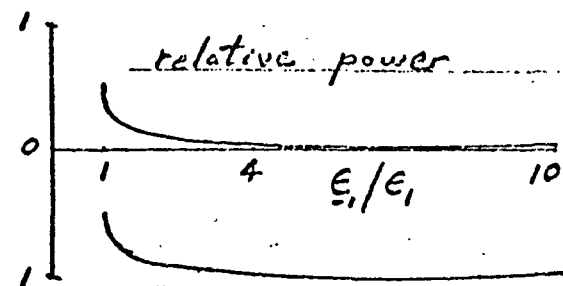
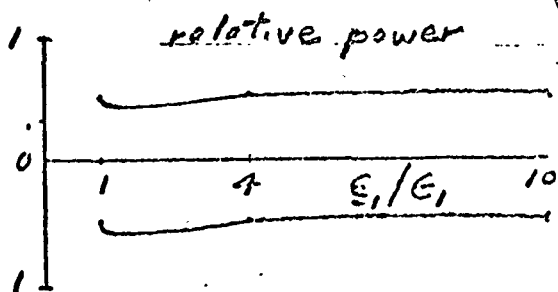
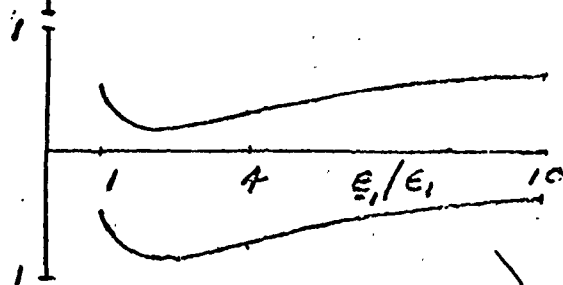
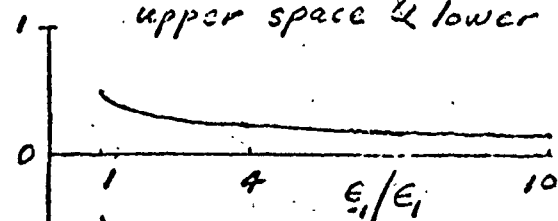


Fig. 2. Hertzian dipole power gain and power split

Page 42, 43, 45, 48

These plots are the most important part of the report and should be re-plotted accurately from TR 11-3 Figures 3-3 & A, B, D, E (curve for 4.00) and 3-2 A, B, D, E (take total power in upper two curves [= 1 - total lower power] to plot parallel curves of upper & lower power). Preferably, plots should be double size with letters $\geq 5/16$ " for later reduction to $8\frac{1}{2} \times 11$ ".

P. 48, 49, 51, 52

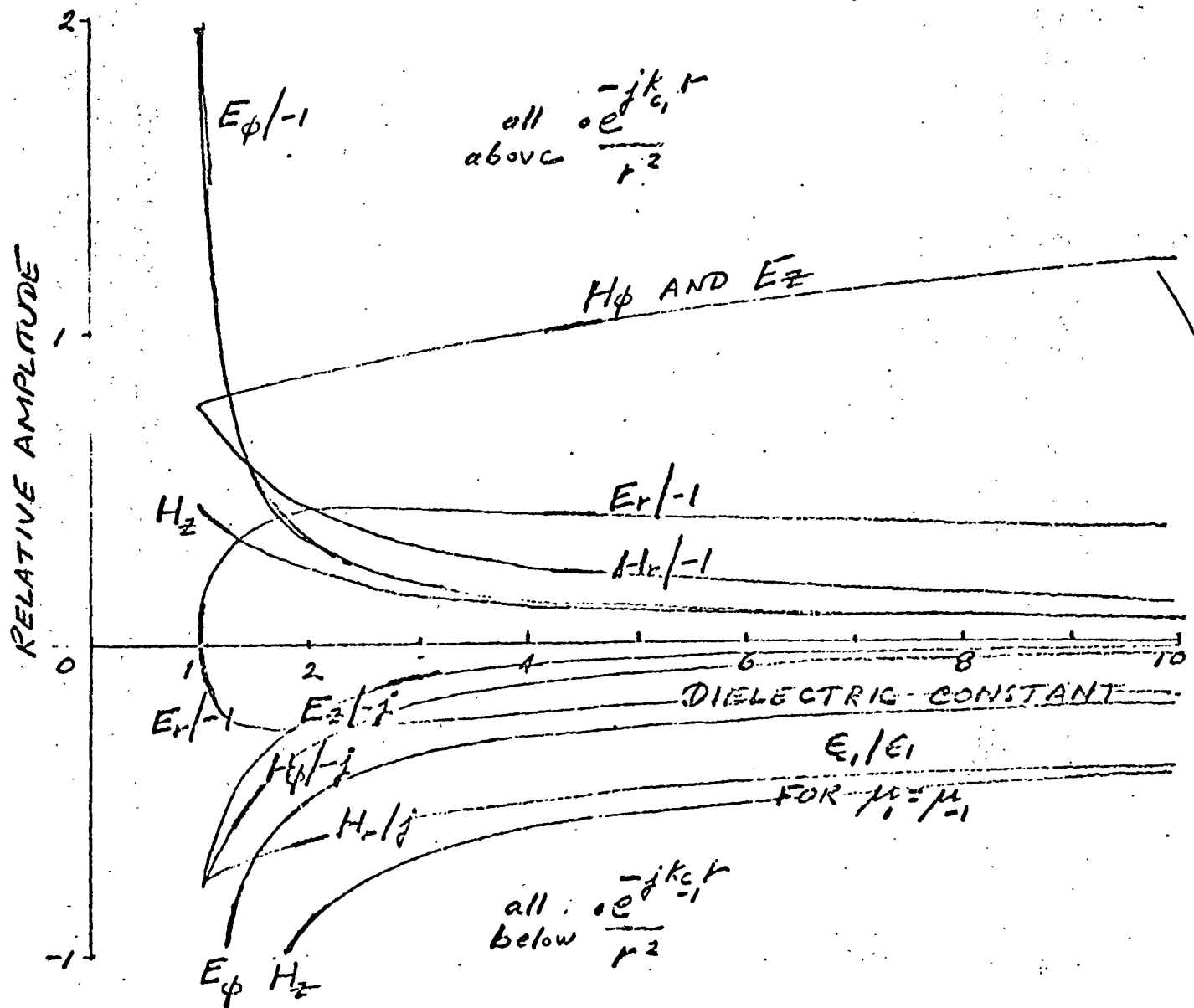


Fig 3. Surface (lateral wave) coefficients

- Should be plotted accurately from 3-5 A, B with lettering $\geq 3/16"$.

(Page 61 & 62)

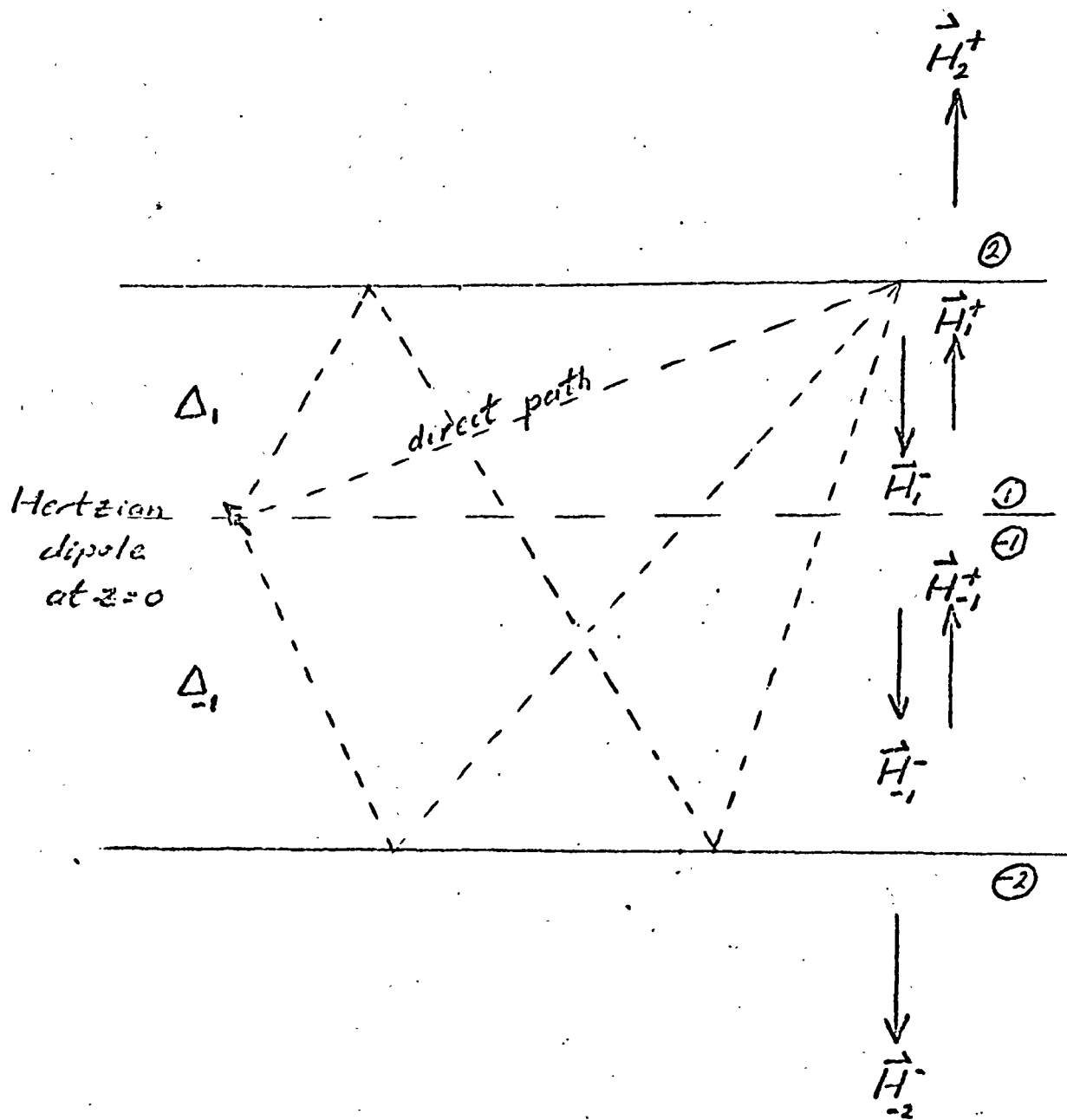


Fig. 4. Three layer geometry

Should be re-drawn with lettering $\geq 3/16"$.

THREE LAYER MEDIUM : $.05\lambda$ $\epsilon_r = .250$,
 UPPER SPACE $\epsilon_r = 1.00$, LOWER SPACE $\epsilon_r = 4.00$
 - HERTZIAN ELECTRIC DIPOLE, $\mu_r = \mu_0$

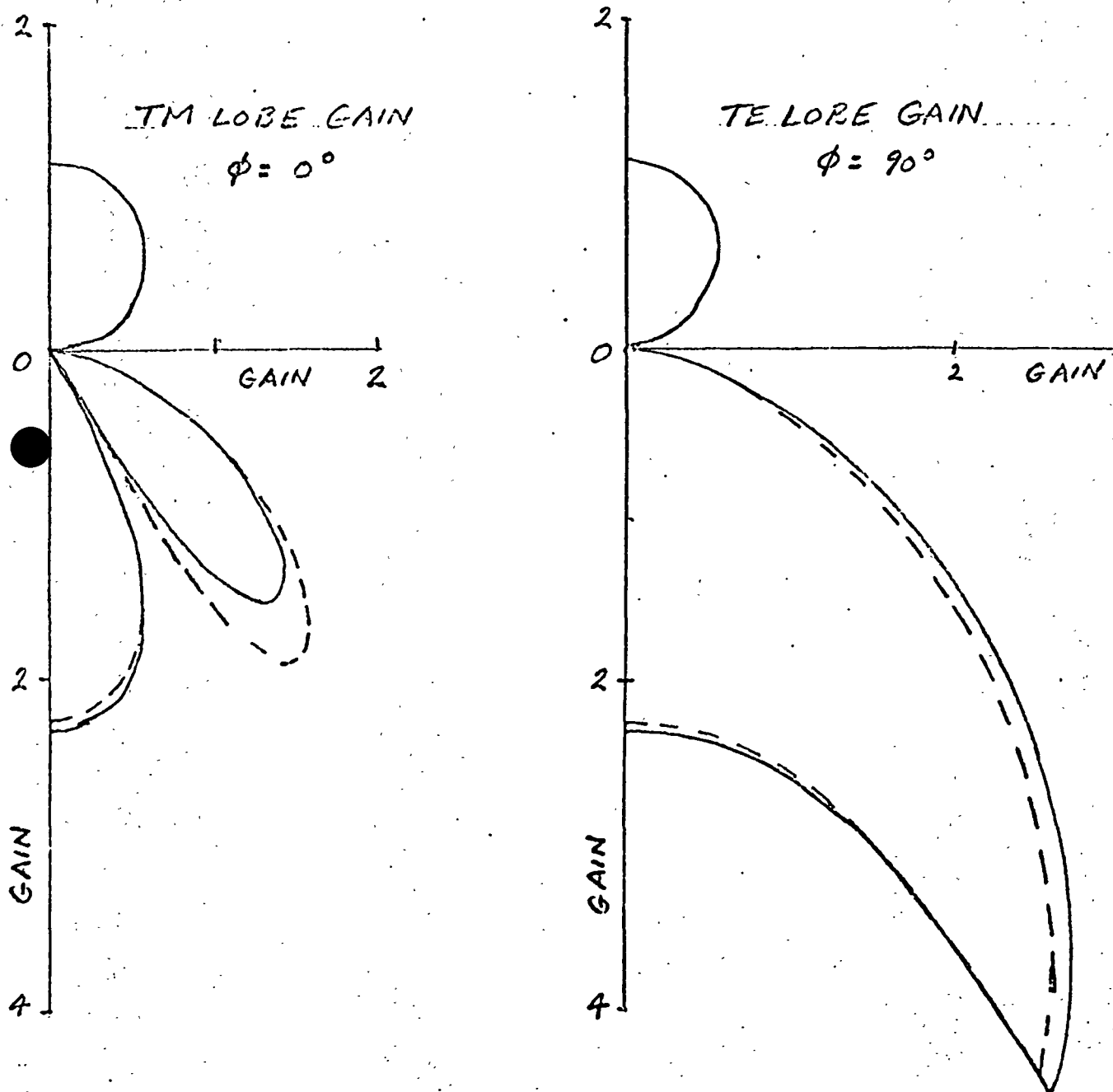


Fig. 5. Perturbed radiation patterns.
 should be re-plotted accurately from 3-7 with lettering 7, 3/16"
 (Pg. 69)

APPENDIX 3.2

MODEL STUDY OF LUNAR SUBSURFACE

ELECTRIC PROPERTIES

Memo 13 & 14 are identical

RECEIVED

MASSACHUSETTS INSTITUTE OF TECHNOLOGY 00664

NOV 8 1971

Research Laboratory of Electronics

SEP-PMO

Electrodynamics Memo No. 13

February 17, 1971

MODEL STUDY OF LUNAR SUBSURFACE ELECTRIC PROPERTIES

I. Formal Solutions of Radiation from Dipole Antennas over Stratified Media.

by

Jin Au Kong

Abstract--The proposed research work deals with data interpretation of an experiment designed to detect subsurface electric properties of the moon. Dipole antennas radiated at discrete radio frequencies are placed on the lunar surface and the electromagnetic field components are measured as a function of distance from the antennas. In order to interpret the interference pattern, the moon is modeled as a stratified medium, and a thorough study is made by varying geometrical configurations and physical constituents of this medium. In this report, an exact solution is presented for all electromagnetic field components due to radiation from dipole antennas over a stratified n -layer medium. The antennas considered are vertical and horizontal dipoles and horizontal turnstile antennas. The solution is facilitated by decomposing total wave field into TE and TM modes. There is no need to introduce either Hertzian or vector potential functions.

I. Introduction

This series of reports deals with data interpretation of an experiment to be performed on the lunar surface. The experiment is designed to detect subsurface electric properties of the moon. Dipole antennas are placed on the surface of the moon and the electromagnetic field components are measured as a function of distance from the antennas which radiate at discrete radio frequencies. In order to interpret the interference pattern, the moon is modeled as a stratified medium, and a through study is made by varying geometrical configurations and physical constituents of this medium. This problem of radiation from dipole antennas in the presence of a stratified medium has been studied for many simple cases under various approximations (Sommerfeld 1949, Annon 1970). Traditionally, it is solved by employing Sommerfeld's Hertz potential which by itself has no direct physical meaning.

Since the proposed experiment directly measures the field components, we present in this report a formal solution for all electromagnetic field components due to radiation of dipole antennas over a stratified medium. The dipole antennas considered are 1.) vertical electric and magnetic dipoles, 2.) horizontal electric and magnetic dipoles, and 3.) horizontal electric and magnetic turnstile antennas. An arbitrarily oriented dipole can be treated as a linear combination of one vertical and two horizontal dipoles. Solutions are facilitated by recognizing

that outside the source, two scalar functions are sufficient to determine all field components. Instead of using potentials, we choose the two scalar functions to be the electric and magnetic field components perpendicular to the plane of stratification. They have direct physical significance and are used to characterize TE and TM solutions. All other components are derived from them and written explicitly in integral form which separates the primary excitation of the radiating antenna from contributions due entirely to the presence of the medium. The solution is exact and includes both far fields and near fields.

2. Transversal Electric and Magnetic Waves

Governing equations for electromagnetic fields in a region outside any source are the Maxwell's source free equations

$$\nabla \times \vec{E} = -j\omega\mu\vec{H} \quad (1)$$

$$\nabla \times \vec{H} = (j\omega\epsilon + \sigma)\vec{E} \quad (2)$$

where μ , ϵ and σ are, respectively, permeability, permittivity, and conductivity of the medium. Time harmonic excitations with dependence $\exp(j\omega t)$ are assumed. Since cylindrical coordinate systems will be employed throughout this study, we designate the longitudinal direction to be z -direction. The transversal plane are characterized by ρ and ϕ . Longitudinal electric and magnetic components E_z and H_z satisfy wave equation

$$(\nabla^2 + k^2) \begin{Bmatrix} E_z \\ H_z \end{Bmatrix} = 0, \quad k^2 = \omega^2 \mu \epsilon (1 - j\sigma/\omega\epsilon) \quad (3)$$

which is derived from (1) and (2). We note in particular that

wave equations for transversal components do not take the form of (3) by simply writing E_ρ , E_ϕ and H_ρ , H_ϕ in place of E_z and H_z .[†]

Solutions of E_z and H_z to the wave equation (3) in cylindrical coordinates are well-known (Harrington 1964). In our problems we are interested in wave solutions which are outgoing in $\hat{\rho}$ -direction and travelling or standing in \hat{z} -direction. Therefore we write, for a fixed separation constant n ,

$$E_z = \int_{-\infty}^{\infty} dk_\rho \{ A(k_\rho) e^{-jk_z z} + B(k_\rho) e^{jk_z z} \} H_n^{(2)}(k_\rho \rho) S_n(\phi) \quad (4)$$

$$H_z = \int_{-\infty}^{\infty} dk_\rho \{ C(k_\rho) e^{-jk_z z} + D(k_\rho) e^{jk_z z} \} H_n^{(2)}(k_\rho \rho) S_n(\phi) \quad (5)$$

where

$$k_z^2 = k^2 - k_\rho^2 \quad (6)$$

and $S_n(\phi)$ stands for sinusoidal functions of ϕ . $H_n^{(2)}(k_\rho \rho)$ is the n^{th} order Hankel function of second kind which, with our choice of time dependence $\exp(j\omega t)$, represents an outgoing wave in $\hat{\rho}$ -direction. The k_ρ dependent functions A , B , C and D are to be determined by the appropriate boundary conditions.

[†] For instance, the wave equation for an electric field which has E_ϕ component only will take the form $(\nabla^2 + k^2 - \frac{1}{\rho^2}) E_\phi = 0$.

As a consequence of the Maxwell's equations (1) and (2), all transversal electric and magnetic field components can be expressed in terms of the longitudinal components E_z and H_z . After some manipulations, we find that, with solutions for E_z and H_z written in the form of (4) and (5),

$$E_\rho^{TM} = \int_{-\infty}^{\infty} dk_\rho \left(j \frac{k_z}{k_\rho} \right) \{ -Ae^{-jk_z z} + Be^{jk_z z} \} H_n^{(2)'}(k_\rho \rho) S_n(\phi) \quad (7)$$

$$E_\phi^{TM} = \int_{-\infty}^{\infty} dk_\rho \left(j \frac{k_z}{k_\rho} \right) \{ -Ae^{-jk_z z} + Be^{jk_z z} \} \frac{1}{\rho} H_n^{(2)}(k_\rho \rho) S_n'(\phi) \quad (8)$$

$$H_\rho^{TM} = \int_{-\infty}^{\infty} dk_\rho \left(j \frac{\omega \epsilon}{k_\rho} \right) \{ Ae^{-jk_z z} + Be^{jk_z z} \} \frac{1}{\rho} H_n^{(2)}(k_\rho \rho) S_n'(\phi) \quad (9)$$

$$H_\phi^{TM} = \int_{-\infty}^{\infty} dk_\rho \left(j \frac{\omega \epsilon}{k_\rho} \right) \{ -Ae^{-jk_z z} - Be^{jk_z z} \} H_n^{(2)'}(k_\rho \rho) S_n(\phi) \quad (10)$$

where superscript TM indicates that solutions are TM waves derived from E_z alone, and

$$E_\rho^{TE} = \int_{-\infty}^{\infty} dk_\rho \left(-j \frac{\omega \mu}{k_\rho} \right) \{ Ce^{-jk_z z} + De^{jk_z z} \} \frac{1}{\rho} H_n^{(2)}(k_\rho \rho) S_n'(\phi) \quad (11)$$

$$E_\phi^{TE} = \int_{-\infty}^{\infty} dk_\rho \left(-j \frac{\omega \mu}{k_\rho} \right) \{ -Ce^{-jk_z z} - De^{jk_z z} \} H_n^{(2)'}(k_\rho \rho) S_n(\phi) \quad (12)$$

$$H_\rho^{TE} = \int_{-\infty}^{\infty} dk_\rho \left(j \frac{k_z}{k_\rho} \right) \{ -Ce^{-jk_z z} + De^{jk_z z} \} H_n^{(2)'}(k_\rho \rho) S_n(\phi) \quad (13)$$

$$H_{\phi}^{TE} = \int_{-\infty}^{\infty} dk_{\rho} \left\{ j \frac{k_z}{k_{\rho}} \right\} \left\{ -C e^{-jk_z z} + D e^{jk_z z} \right\} \frac{1}{\rho} H_n^{(2)}(k_{\rho} \rho) S_n'(\phi) \quad (14)$$

which are TE waves derived from H_z alone. Total wave fields are obtained by superposition of both the TM and TE solutions.

3. Primary Excitation

The explicit solution to the problem of dipole radiation over stratified medium depends on field excitations of the source, and the geometrical configuration and physical constituents of the medium. In the absence of the stratified medium, the solution of electromagnetic fields due to a dipole antenna, which we refer to as the primary excitation, is well-known (Adler, Chu and Fano 1959). The solution is usually written in spherical coordinates. It can be transformed into cylindrical coordinates and represented by Hankel functions in the integral form. Writing in the general form, we have

$$E_z = \int_{-\infty}^{\infty} dk_{\rho} E_0(k_{\rho}) \left\{ \begin{matrix} e^{jk_z z} \\ e^{-jk_z z} \end{matrix} \right\} H_n^{(2)}(k_{\rho} \rho) S_n(\phi) \quad \begin{cases} z \leq 0 \\ z \geq 0 \end{cases} \quad (15)$$

$$H_z = \int_{-\infty}^{\infty} dk_{\rho} H_0(k_{\rho}) \left\{ \begin{matrix} e^{jk_z z} \\ e^{-jk_z z} \end{matrix} \right\} H_n^{(2)}(k_{\rho} \rho) S_n(\phi) \quad \begin{cases} z \leq 0 \\ z \geq 0 \end{cases} \quad (16)$$

where E_0 and H_0 characterize the structure and excitation of the dipole. Other field components are determined by Eqs. (7)-(14) with $B = D = 0$, $A = E_0$, $C = H_0$ for $z \leq 0$, and $A = C = 0$, $B = E_0$, $D = H_0$ for $z \geq 0$.

For the three types of antennas under consideration, we obtain for:

1.) Vertical electric dipole; $n = 0$, $S_n(\phi) = 1$

$$E_o = \frac{-I l k^3 \rho}{8 \pi \omega \epsilon k_z} \quad (17)$$

$$H_o = 0 \quad (18)$$

2.) Horizontal electric dipole along \hat{x} -direction; $n = 1$

$$E_o = \pm j \frac{I l k^2 \rho}{8 \pi \omega \epsilon} \quad S_1 = \cos \phi \quad \begin{cases} k_z \leq 0 \\ k_z \geq 0 \end{cases} \quad (19)$$

$$H_o = -j \frac{I l k^2 \rho}{8 \pi k_z} \quad S_1 = -\sin \phi \quad (20)$$

3.) Horizontal turnstile antenna; $n = 1$, $S_1 = e^{j\phi}$

$$E_o = \pm j \frac{I l k^2 \rho}{8 \pi \omega \epsilon} \quad \begin{cases} k_z \leq 0 \\ k_z \geq 0 \end{cases} \quad (21)$$

$$H_o = \frac{I l k^2 \rho}{8 \pi k_z} \quad (22)$$

To obtain solutions for the three types of magnetic dipoles, we apply duality to above by changing $\vec{E} \rightarrow \vec{H}$, $\vec{H} \rightarrow -\vec{E}$, and $\mu \leftrightarrow \epsilon$.

We observe the following: 1.) The \pm signs in (19) and (21) do not imply discontinuities of E_z at $z = 0$ plane, in fact, $E_z = 0$ at $z = 0$. 2.) For a horizontal electric dipole along \hat{y} -direction, we merely change $\cos \phi$ to $\sin \phi$ and $\sin \phi$ to $-\cos \phi$. 3.) For vertical antennas, there is TE to z waves only and involves Hankel functions of zeroth order. 4.) For horizontal dipoles, we have Hankel functions of first order and both TE and TM waves are present. 5.) An arbitrary oriented dipole can now be treated as a linear combination of three dipoles along \hat{x} , \hat{y} and \hat{z} axes which are just described.

4. Dipole Antennas Over Stratified Mediums

Because the Hankel functions involved are of different order, we consider vertical and horizontal antennas separately. Geometrical configuration of the problem is shown in Fig. 1. There are n slab regions, and the last region is numbered t instead of $n+1$, for the sake of simplifying writings. In each region labelled i , solutions of electromagnetic field components take the form of Eqs. (4)-(14) with all quantities subscripted by i . In the 0th region where we have the antennas, $A_0 = E_0$ and $C_0 = H_0$ which are known from (17)-(22) for the three types of antennas under consideration. In the last region, namely region t , it is semi-infinite and we do not expect reflected waves, therefore $B_t = D_t = 0$.

Boundary conditions at all interfaces are that all tangential electromagnetic field components must be continuous for all ρ and ϕ . This implies that k_ρ 's in all regions must be equal.

We consider first the vertical electric antenna. Since the primary excitation has only a TM wave, we choose $H_{zi} = 0$ for $i = 0, 1, 2, \dots, n, t$, and E_z of the form (4) with 0th order Hankel functions. Our main interest is in the 0th region where measurements are taken. We thereby want ultimately to know B_0 which is due entirely to the presence of the stratified medium. Solutions can be facilitated by introducing propagation matrices (Kong, 1970). The propagation matrix from i th region to $(i+1)$ th region is defined to be

$$M_i^{(i+1)} = \frac{1}{2} \begin{bmatrix} \left(\frac{\kappa_{i+1}}{\kappa_i} + \frac{k_{z(i+1)}}{k_{zi}} \right) e^{-jk_{z(i+1)}(d_i - d_{i+1})} \\ \left(\frac{\kappa_{i+1}}{\kappa_i} - \frac{k_{z(i+1)}}{k_{zi}} \right) e^{-jk_{z(i+1)}(d_i - d_{i+1})} \\ \left(\frac{\kappa_{i+1}}{\kappa_i} - \frac{k_{z(i+1)}}{k_{zi}} \right) e^{jk_{z(i+1)}(d_i - d_{i+1})} \\ \left(\frac{\kappa_{i+1}}{\kappa_i} + \frac{k_{z(i+1)}}{k_{zi}} \right) e^{jk_{z(i+1)}(d_i - d_{i+1})} \end{bmatrix} \quad (23)$$

where $\kappa_i = \epsilon_i(1 - j\sigma_i/\omega\epsilon_i)$ and $k_{zi} = \sqrt{k_i^2 - k_0^2}$, $i = 0, 1, 2, \dots, n, t$.

Matching boundary conditions at $z = d_i$, we obtain

$$\begin{bmatrix} A_i e^{-jk_{zi}d_i} \\ B_i e^{jk_{zi}d_i} \end{bmatrix} = M_i^{(i+1)} \begin{bmatrix} A_{i+1} e^{-jk_{z(i+1)}d_i} \\ B_{i+1} e^{jk_{z(i+1)}d_i} \end{bmatrix} \quad (24)$$

for $i = 0, 1, 2, \dots, n$.

There are $n+1$ such pairs of equations to solve for the $2n+2$ unknowns A_i and B_i . The solution is thus unique. Note that $B_t = 0$ and $A_0 = E_0$ is known.

We see from (24) that the propagation matrix $M_i^{(i+1)}$ relates field components in i^{th} region to field components in the $(i+1)^{\text{th}}$ region. Field components in region 0 are related to those in the last region by successive multiplication of the propagation matrices

$$\begin{bmatrix} E_0 e^{-jk_{z0}d_0} \\ B_0 e^{jk_{z0}d_0} \end{bmatrix} = M_0^t \begin{bmatrix} A_t e^{-jk_{zt}d_n} \\ 0 \end{bmatrix} \quad (25)$$

where

$$M_0^t = \prod_{i=0}^n M_i^{(i+1)} \quad (26)$$

Equation (25) consists of two equations to solve for the two unknowns B_0 and A_t . Let

$$M_0^t = [M_{jk}] \quad j, k = 1, 2 \quad (27)$$

We obtain from (25)

$$B_0 = E_0 \frac{M_{21}}{M_{11}} e^{-j2k_{z0}d_0} \quad (28)$$

Thus the problem is reduced to the evaluation of the propagation

matrix M_o^t . Once B_o is determined, all field components can be evaluated from Eqs. (4), (7), and (10). There are no E_ϕ and H_ρ components because $S_n' = 0$.

Next, we consider horizontal electric antennas. This time both TM and TE waves will exist. The primary excitation involves 1st order Hankel function. We choose accordingly solutions for E_z and H_z with same Hankel function and same $S_n(\phi)$ as the primary excitation whether it be due to a horizontal dipole or a turnstile antenna. Following a parallel analysis of the above, we define a propagation matrix $N_i^{(i+1)}$ for TE waves

$$N_i^{(i+1)} = \frac{1}{2} \begin{bmatrix} \left(\frac{\nu_{i+1}}{\nu_i} + \frac{k_{z(i+1)}}{k_{zi}} \right) e^{-jk_{z(i+1)}(d_i - d_{i+1})} \\ \left(\frac{\nu_{i+1}}{\nu_i} - \frac{k_{z(i+1)}}{k_{zi}} \right) e^{-jk_{z(i+1)}(d_i - d_{i+1})} \\ \left(\frac{\nu_{i+1}}{\nu_i} - \frac{k_{z(i+1)}}{k_{zi}} \right) e^{jk_{z(i+1)}(d_i - d_{i+1})} \\ \left(\frac{\nu_{i+1}}{\nu_i} + \frac{k_{z(i+1)}}{k_{zi}} \right) e^{jk_{z(i+1)}(d_i - d_{i+1})} \end{bmatrix} \quad (29)$$

As a consequence of the boundary conditions, we obtain, at the interface where $z = d_i$, Eq. (24) and

$$\begin{bmatrix} C_i e^{-jk_{zi}d_i} \\ D_i e^{jk_{zi}d_i} \end{bmatrix} = N_i^{i+1} \begin{bmatrix} C_{i+1} e^{-jk_{z(i+1)}d_i} \\ D_{i+1} e^{jk_{z(i+1)}d_i} \end{bmatrix} \quad (30)$$

B_o is determined as before by Eq. (23) with the same propagation

matrix defined in (23). Note that E_ϕ^{TM} and H_ρ^{TM} are no longer zero because $S_n \neq 0$. D_0 is likewise determined by a successive multiplication of the propagation matrix (29) which yields

$$N_0^t = \prod_{i=0}^n N_i^{(i+1)} = [N_{jk}] \quad j, k = 1, 2 \quad (31)$$

$$D_0 = H_0 \frac{N_{21}}{N_{11}} e^{-j2k_{z0}d_0} \quad (32)$$

It is seen that for the horizontal antennas, all the field components will now be present. Applying duality, we can easily obtain solutions for all the three types of magnetic dipoles.

5. Summary

In the preceding sections, we have succeeded in: 1) decomposing total wave solutions into TE and TM waves and 2) separating primary excitations from effects due to the presence of the stratified medium. In the following, we assume $\sigma = 0$ in region 0 and write solutions for $z < 0$.

1.) Vertical electric dipole:

$$\vec{E} = \int_{-\infty}^{\infty} dk_\rho \begin{bmatrix} j \frac{15k_\rho^2}{8\pi\omega\epsilon} (1 + R^{TM}) e^{jk_z z} H_1^{(2)}(k_\rho \rho) \\ 0 \\ - \frac{12k_\rho^3}{8\pi\omega\epsilon k_z} (1 + R^{TM}) e^{jk_z z} H_0^{(2)}(k_\rho \rho) \end{bmatrix} \quad (33)$$

$$\bar{H} = \int_{-\infty}^{\infty} dk_{\rho} \begin{bmatrix} 0 \\ -j \frac{I l k_{\rho}^2}{8 \pi k_z} (1 + R^{TM}) e^{jk_z z} H_1^{(2)}(k_{\rho} \rho) \\ 0 \end{bmatrix} \quad (34)$$

where the reflection coefficient R^{TM} accounts for contributions solely due to the presence of the stratified medium.

$R^{TM} = (M_{21}/M_{11}) \exp(-j2k_z d_0)$, and M_{21} and M_{11} are to be evaluated from the propagation matrix (26).

2.) Horizontal electric dipoles:

$$\bar{E} = \bar{E}^{TM} + \bar{E}^{TE} \quad (35)$$

$$\bar{H} = \bar{H}^{TM} + \bar{H}^{TE} \quad (36)$$

$$\bar{E}^{TM} = \int_{-\infty}^{\infty} dk_{\rho} \begin{bmatrix} j \frac{k_z}{k_{\rho}} E_0 (1 + R^{TM}) e^{jk_z z} H_1^{(2)}(k_{\rho} \rho) S_1(\phi) \\ j \frac{k_z}{k_{\rho}} E_0 (1 + R^{TM}) e^{jk_z z} \frac{1}{\rho} H_1^{(2)}(k_{\rho} \rho) S_1'(\phi) \\ E_0 (1 + R^{TM}) e^{jk_z z} H_1^{(2)}(k_{\rho} \rho) S_1(\phi) \end{bmatrix} \quad (37)$$

$$\bar{H}^{TM} = \int_{-\infty}^{\infty} dk_{\rho} \begin{bmatrix} j \frac{\omega \epsilon}{k_{\rho}} E_0 (1 + R^{TM}) e^{jk_z z} \frac{1}{\rho} H_1^{(2)}(k_{\rho} \rho) S_1'(\phi) \\ -j \frac{\omega \epsilon}{k_{\rho}} E_0 (1 + R^{TM}) e^{jk_z z} H_1^{(2)}(k_{\rho} \rho) S_1(\phi) \\ 0 \end{bmatrix} \quad (38)$$

$$\vec{E}^{TE} = \int_{-\infty}^{\infty} dk_{\rho} \begin{bmatrix} -j \frac{\omega \mu}{k_{\rho}} H_0 (1 + R^{TE}) e^{jk_z z} \frac{1}{\rho} H_1^{(2)}(k_{\rho} \rho) S_1'(\phi) \\ j \frac{\omega \mu}{k_{\rho}} H_0 (1 + R^{TE}) e^{jk_z z} H_1^{(2)}(k_{\rho} \rho) S_1(\phi) \\ 0 \end{bmatrix} \quad (39)$$

$$\vec{H}^{TE} = \int_{-\infty}^{\infty} dk_{\rho} \begin{bmatrix} j \frac{k_z}{k_{\rho}} H_0 (1 + R^{TE}) e^{jk_z z} H_1^{(2)}(k_{\rho} \rho) S_1(\phi) \\ j \frac{k_z}{k_{\rho}} H_0 (1 + R^{TE}) e^{jk_z z} \frac{1}{\rho} H_1^{(2)}(k_{\rho} \rho) S_1'(\phi) \\ H_0 (1 + R^{TE}) e^{jk_z z} H_1^{(2)}(k_{\rho} \rho) S_1(\phi) \end{bmatrix} \quad (40)$$

where E_0 , H_0 and $S_1(\phi)$ are determined from Eqs. (19)-(22) for the cases of a horizontal electric dipole along \hat{x} -direction and a turnstile antenna. The case of a horizontal antenna along \hat{y} -direction is obtained from (19) and (20) by changing $\cos\phi$ to $\sin\phi$ and $\sin\phi$ to $-\cos\phi$. The reflection coefficients are $R^{TM} = (M_{21}/M_{11}) \exp(-j2k_{z0}d_0)$ and $R^{TE} = (N_{21}/N_{11}) \exp(-j2k_{z0}d_0)$. M_{21} , M_{11} , N_{21} and N_{11} are determined by evaluation of the propagations matrices (26) and (31).

We note the following: 1) In the absence of the medium, $R^{TM} = R^{TE} = 0$. 2) The problem of dipole radiation over a stratified medium has been reduced to the task of evaluation of the propagations matrices (26) and (31) and the integrals (33)-(40). 3) An arbitrarily oriented dipole can be decomposed

into one vertical dipole and two horizontal dipoles perpendicular to one another. The total solution is a superposition of contributions due to each of them. 4) Solutions for magnetic dipoles are obtained by applying duality. 5) When the antennas are lied on the surface, we have $d_0 = 0$. 6) To calculate R^{TM} and R^{TE} , numerical methods can now be directly applied to evaluate the integrals. Both far field and near field solutions are obtained from the same integrals under different approximations.

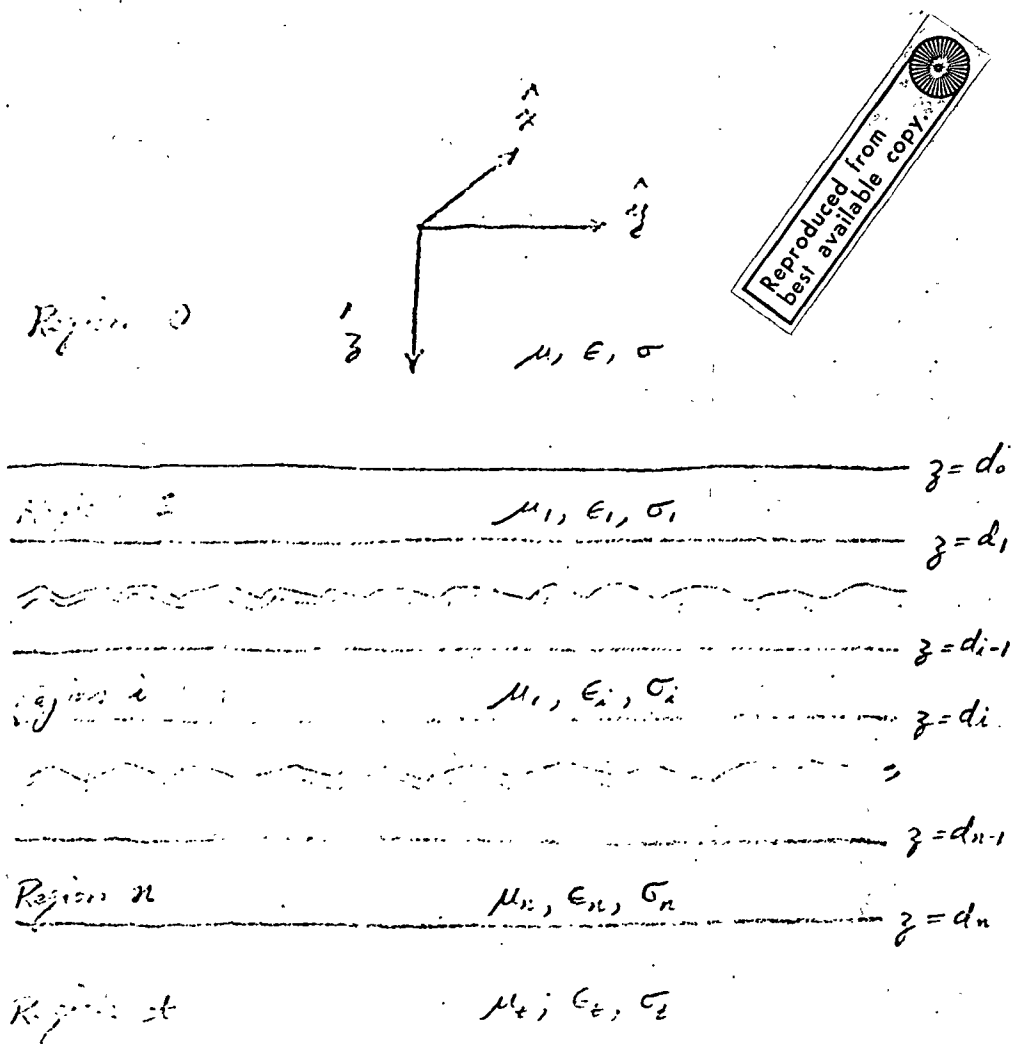


Fig. 1 Geometrical configuration of the problem

REFEPENCES

Adler, R. B., Chu, L. J., and Fano, R. M.; (1960), Electromagnetic Energy Transmission and Radiation, John Wiley & Son, Chapt. 10.

Annan, A. P.; (1970), Radio Interferometry Depth Sounding,
S. M. Thesis, Toronto University.

Harrington, R. F.; (1961), Time-Harmonic Electromagnetic Field,
McGraw Hill, Chapt. 5.

Kong, J. A.; (1970), Interaction of Acoustic Waves with Moving
Media, J. Acoust. Soc. Am., v. 48, pp. 236-241.

Sommerfeld, A.; (1949), Partial Differential Equations in Physics,
Academic Press, Chapt. 6.

APPENDIX 3.3

RESONANT DIPOLE ON SURFACE

OF A DIELECTRIC

Jim Meyer

Massachusetts Institute of Technology
Charles Stark Draper Laboratory

23S Memo 70-81

TO: L. B. Johnson
FROM: J. B. Lozow
DATE: 23 December 1970
SUBJECT: Resonant Dipole on the Surface of a Dielectric
Half Space

References:

1. Radio Interferometry Depth Sounding; Annan, A.P.;
Masters Thesis, Physics Department, University
of Toronto.
2. Dipole Radiation in the Presence of a Conducting
Half-Space; Baner A.; Pergamon Press 1966.
3. Field Analysis and Electromagnetics; M. Savid
and P. Brown; McGraw-Hill, 1963.
4. Antenna Theory Part 2; R.E. Collin and F.J. Zucker;
McGraw-Hill 1969.

Summary: What is presented here can be regarded as a straightforward extension and/or application of earlier work done by many investigators. The results of Reference 1, in particular, are exploited. In this memo we attempt to derive expressions for the far-field electromagnetic vectors of an elementary dipole antenna located on the surface of a dielectric half-space. Once the electric vector ("E-field") is determined it is a simple, though perhaps tedious, task to calculate quantities such as the Poynting vector, radiation resistance etc. . In this analysis we ignore any terms that fall off at a rate greater than $1/R$ since any attempt to include higher order terms results in terrific complication.

Analysis

As shown in Figure 1, it is postulated that the horizontal plane

i.e., $Z=0$ coincides with the interface between two homogeneous isotropic media. The region $Z>0$ is assumed to be free space while the region for $Z<0$ is assumed to be a very low conducting media of complex permittivity ϵ_1 , and permeability μ_1 , equal to free space that is $\mu_1 = \mu_0$.

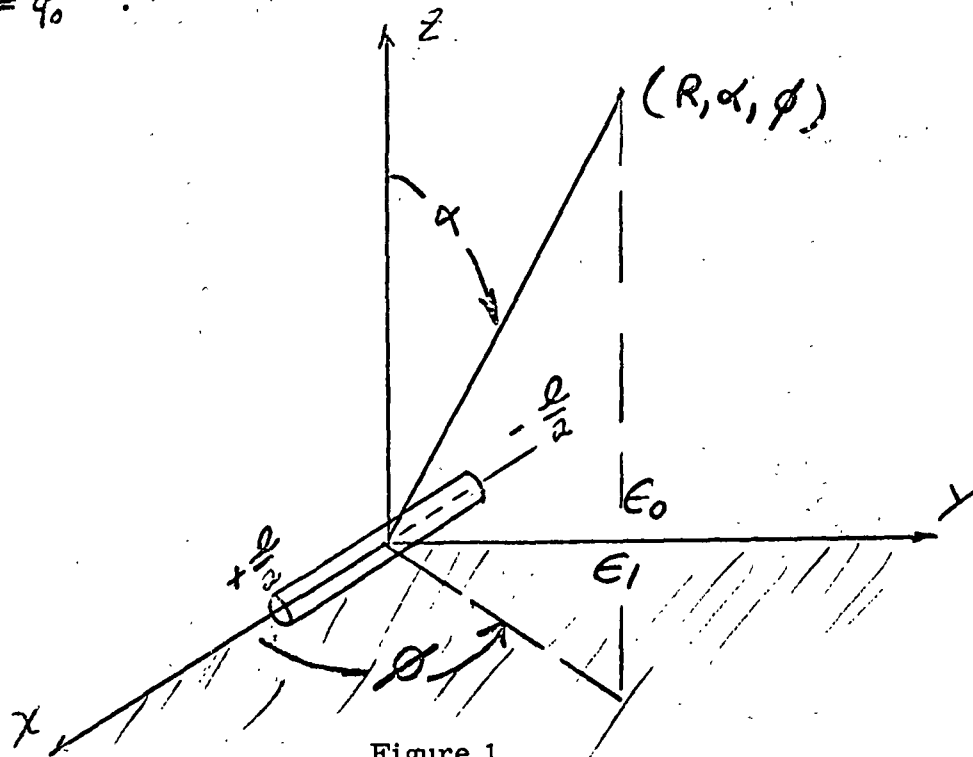


Figure 1

As in Figure 1 the dipole of length " l " is aligned along the x -axes with its midpoint coinciding with the origin of our $x - y - z$ system. A current distribution $I(x) \cdot e^{-j\omega t}$ is assumed to flow in the dipole. We will first consider the E/H field set up by an element Δl of the antenna and then integrate over its whole length to get the total effect.

The classical treatment of this problem is to solve the Helmholtz wave equation in both regions for the "Hertz vector" $\vec{\Pi}$. These vector equations take the form:

$$(1) (\nabla^2 + K^2) \vec{\Pi} = \vec{F}(x, y, z)$$

where $K = \omega \sqrt{\mu \epsilon} =$ propagation
constant particular to
the medium

\vec{F} = source of the electro-
magnetic field

The quantity $\vec{\Pi}$ in the present case is taken to be an "electric type" Hertz vector. Once $\vec{\Pi}$ is evaluated by means of solving (1) subject to the appropriate boundary conditions the \vec{E} and \vec{H} (electric and magnetic vectors respectively) are shown to be given by the following expressions:

$$(2) \vec{E} = \nabla(\nabla \cdot \vec{\Pi}) + K_1^2 \vec{\Pi}$$

$$(3) \vec{H} = -j\omega \epsilon_i \nabla \times \vec{\Pi}$$

where: ω = radian frequency

$i = 0$ for $Z > 0$

$i = 1$ for $Z < 0$

Annan (Ref. 1) has solved expression 1 approximately for the cartesian components of the Hertz vector for $Z < 0$ and $Z > 0$. It should be noted in the following that the Hertz vector has a Z-component which arises primarily due to the plane interface and thus disappears as $\epsilon_0 \rightarrow \epsilon_1$ as expected. The Hertz vector from page 46 of Ref. 1 written in terms of its cartesian components is given for $Z > 0$

$$(4) \vec{\Pi} = \Delta M \frac{e}{R} j k_0 R \Gamma_{01}(\alpha) \vec{U}_x + \Delta M \frac{e}{R} j k_0 R \left(\frac{\epsilon_0 - \epsilon_1}{2\epsilon_0} \right) \cos \phi \sin \phi A(\alpha) \vec{U}_z$$

and for $Z < 0$

$$(5) \vec{\Pi} = \Delta M \frac{e}{R} j k_1 R \Gamma_{10}(\alpha) \vec{U}_x + \Delta M \frac{e}{R} j k_1 R \left(\frac{\epsilon_0 - \epsilon_1}{2\epsilon_0} \right) \cos \phi \sin \phi B(\alpha) \vec{U}_z$$

where \vec{U}_x, \vec{U}_z - unit vectors in the x and z directions

$$\Gamma_{01}(\alpha) \equiv \frac{2 \cos \alpha}{\cos \alpha + \left(\frac{k_1^2}{k_0^2} - \sin^2 \alpha \right)^{1/2}}$$

$$\Gamma_{10}(\alpha) \equiv \frac{2 \cos \alpha}{\cos \alpha + \left(\frac{k_0^2}{k_1^2} - \sin^2 \alpha \right)^{1/2}}$$

$$A(\alpha) \equiv \frac{\epsilon_1 \cos \alpha}{\left[\epsilon_1 \cos \alpha + \epsilon_0 \left(\frac{k_1^2}{k_0^2} - \sin^2 \alpha \right)^{1/2} \right] \left[\cos \alpha + \left(\frac{k_1^2}{k_0^2} - \sin^2 \alpha \right)^{1/2} \right]}$$

$$B(\alpha) \equiv \frac{\epsilon_0 \cos \alpha}{\left[\epsilon_0 \cos \alpha + \epsilon_1 \left(\frac{k_0^2}{k_1^2} - \sin^2 \alpha \right)^{1/2} \right] \left[\cos \alpha + \left(\frac{k_0^2}{k_1^2} - \sin^2 \alpha \right)^{1/2} \right]}$$

$$\Delta M \equiv I(\alpha) \Delta x / j 4 \pi \epsilon_0 \omega$$

Note that only terms of $\frac{1}{R}$ dependence are included in equation (4) and (5).

For the sake of expediency we now transform expressions (4) and (5) to spherical coordinates:

Thus

$$(6) \quad \vec{\pi} = \pi_x \vec{U}_x + \pi_z \vec{U}_z \rightarrow \pi_R \vec{U}_R + \pi_\alpha \vec{U}_\alpha + \pi_\phi \vec{U}_\phi$$

where U_R , U_α , U_ϕ are orthogonal unit vectors in the r , α , ϕ system shown in Figure 1.

and

$$(7) \quad \pi_R = \pi_x \sin \alpha \cos \phi$$

$$\pi_\alpha = \pi_x \cos \alpha \cos \phi - \pi_z \sin \alpha$$

$$\pi_\phi = -\pi_x \sin \phi$$

We can now proceed to calculate the \vec{E} and \vec{H} vectors by means of the relationships (2) and (3). For the \vec{E} field:

$$(2) \quad \vec{E} = \nabla (\nabla \cdot \vec{\pi}) + K_i^2 \vec{\pi}$$

$$(8) \nabla \cdot \vec{\pi} = \frac{1}{R^2} \frac{\partial}{\partial R} (R^2 \pi_R) + \frac{1}{R \sin \alpha} \frac{\partial}{\partial \alpha} (\sin \alpha \pi_\alpha) + \frac{1}{R \sin \alpha} \frac{\partial \pi_\phi}{\partial \phi}$$

and

$$(9) \nabla(\nabla \cdot \vec{\pi}) = \frac{\partial(\nabla \cdot \vec{\pi})}{\partial R} \vec{U}_R + \frac{1}{R} \frac{\partial(\nabla \cdot \vec{\pi})}{\partial \alpha} \vec{U}_\alpha + \frac{1}{R \sin \alpha} \frac{\partial(\nabla \cdot \vec{\pi})}{\partial \phi} \vec{U}_\phi$$

Performing the above operations and ignoring all but " $\frac{1}{R}$ " terms it is found that with $\vec{E} = E_R \vec{U}_R + E_\alpha \vec{U}_\alpha + E_\phi \vec{U}_\phi$

$$(10) E_R \approx 0$$

$$E_\alpha \approx K_i^2 (\cos \alpha \cos \phi F_i(\alpha) - \sin \alpha \sin \phi \cos \phi G_i(\alpha)) \Delta M \frac{e}{R} \downarrow K_i R$$

$$E_\phi \approx -K_i^2 F_i(\alpha) \sin \phi \Delta M \frac{e}{R} \downarrow K_i R$$

where

$$(11) F_i(\alpha) \equiv \begin{cases} P_{01}(\alpha) & z > 0 \\ \Gamma_{10}(\alpha) & z < 0 \end{cases}$$

$$G_i(\alpha) = \begin{cases} A(\alpha) & z > 0 \\ B(\alpha) & z < 0 \end{cases}$$

$$K_i = \begin{cases} \omega \sqrt{\epsilon_i \epsilon_0} & z > 0 \\ \omega \sqrt{\epsilon_i \epsilon_0} & z < 0 \end{cases}$$

to solve for the magnetic field H. It is then shown that

$$(12) \vec{H} = H_R \vec{U}_R + H_\alpha \vec{U}_\alpha + H_\phi \vec{U}_\phi = -j\omega \epsilon_i (\nabla \times \vec{\pi})$$

where

$$H_R \approx 0$$

$$H_\alpha \approx K_i \omega \epsilon_i \sin \phi F_i(\alpha) \Delta M \frac{e}{R} \downarrow K_i R$$

$$H_\phi \approx K_i \omega \epsilon_i [\cos \alpha \cos \phi F_i(\alpha) - \sin \alpha \sin \phi \cos \phi G_i(\alpha)] \Delta M \frac{e}{R} \downarrow K_i R$$

We have thus calculated the \vec{E} and \vec{H} fields at a distant point (r, α, ϕ) due to a current distribution $I(x')$ in an incremental dipole source Δl . It now remains to calculate the total effect due to the entire source, i. e., an elementary dipole source of length l .

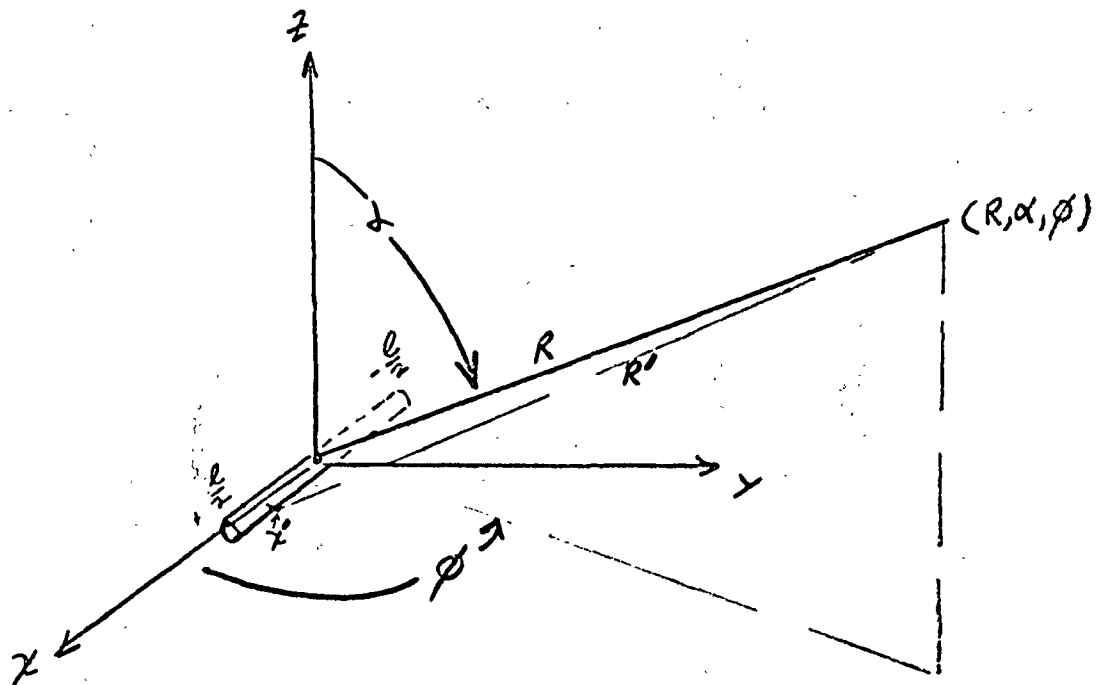


Figure 2

The procedure for utilizing the superposition principle to calculate the total field can be found in any text on electromagnetics (See Ref. 3 for example). Basically the method consists of ignoring all differences between the coordinate R and the distance R' (that being the distance from point (r, α, ϕ) to any point on the line source) except in the phasing consideration. (See Fig. 2).

Suppose we examine the geometry at the source.

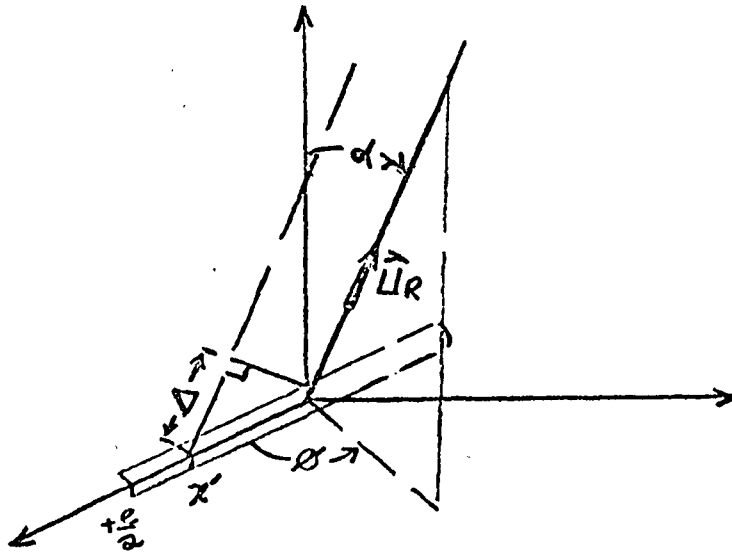


Figure 3

Using Figure 3 as a reference, we can write vectors \vec{R} and \vec{R}' as

$$(13) \quad \begin{aligned} \vec{R} &= R \vec{U}_r \\ \vec{R}' &= R' \vec{U}_r \end{aligned}$$

Also it is approximately true that

$$(14) \quad \vec{R}' - \vec{R} \approx \Delta \vec{U}_r$$

where the scalar " Δ " is shown in Fig. 3. If the vector \vec{R}' originates at point $(X', 0, 0)$ and the far field point is at (R, α, ϕ) it is easily shown that

$$(15) \quad \Delta \approx X' (\vec{U}_r \cdot \vec{U}_x) = x' \sin \alpha \cos \phi$$

If Δ is the path difference the phase difference is $Ki\Delta$ and it remains to evaluate the definite integral $Q(\alpha, \phi)$.

$$(16) \quad \varphi(\alpha, \phi) \equiv \frac{1}{j4\pi\epsilon_0\omega} \int_{-\frac{\ell}{2}}^{+\frac{\ell}{2}} I(x') e^{jKi\Delta} dx' = \frac{1}{j4\pi\epsilon_0\omega} \int_{-\frac{\ell}{2}}^{+\frac{\ell}{2}} I(x') e^{jKi x' \sin\alpha \cos\phi} dx'$$

and it can be shown that we replace the ΔM in equations (10) and (12) by $Q(\alpha, \phi)$ to find the respective \vec{E} and \vec{H} vectors. Here we must assume a form for the current distribution $I(x')$ in order to continue. It is known that generally, the current will consist of a superposition of standing waves. For present purposes it will suffice to consider a single standing wave which vanishes at the ends of the line source.

Then let's suppose that

$$(17) \quad I(x') = I_0 \cos\left(\frac{\pi x'}{\ell}\right)$$

Inserting (17) into (16) we get

$$(18) \quad \varphi(\alpha, \phi) = \frac{1}{j4\pi\epsilon_0\omega} \int_{-\frac{\ell}{2}}^{+\frac{\ell}{2}} I_0 \cos\left(\frac{\pi x'}{\ell}\right) e^{jKi x' \sin\alpha \cos\phi} dx'$$

$$= \frac{I_0}{j2\ell\epsilon_0\omega} \frac{\cos\left(Ki \frac{\ell}{2} \sin\alpha \cos\phi\right)}{\left(\frac{\pi}{\ell}\right)^2 - (Ki \sin\alpha \cos\phi)^2}$$

Finally replacing ΔM in expressions (10) and (12) by $Q(\alpha, \phi)$ we get

$$(19) \vec{E} = k_i^2 (\cos \alpha \cos \phi F_i(\alpha) - \sin \alpha \sin \phi \cos \phi G_i(\alpha)) \varphi(\alpha, \phi) \frac{e^{-jk_i R}}{R} \vec{U}_\alpha \\ - k_i^2 F_i(\alpha) \sin \phi \varphi(\alpha, \phi) \frac{e^{-jk_i R}}{R} \vec{U}_\phi$$

$$(20) \vec{H} = k_i \epsilon_i \omega F_i(\alpha) \sin \phi \varphi(\alpha, \phi) \frac{e^{-jk_i R}}{R} \vec{U}_R \\ + k_i \epsilon_i \omega [\cos \alpha \cos \phi F_i(\alpha) - \sin \alpha \sin \phi \cos \phi G_i(\alpha)] \varphi(\alpha, \phi) \frac{e^{-jk_i R}}{R} \vec{U}_\phi$$

Now suppose that the antenna under consideration is a "half-wave" dipole. That is $l = \frac{\lambda}{2} = \frac{\pi}{k_0}$ and $\varphi(\alpha, \phi)$ becomes

$$(21) \varphi(\alpha, \phi) = \frac{I_0 k_0}{j 2 \pi \epsilon_0 \omega} \cdot \frac{\cos\left(\frac{k_0 \pi}{2} \sin \alpha \sin \phi\right)}{k_0^2 - (k_i \sin \alpha \cos \phi)^2}$$

It now follows that the average Poynting vector $\vec{P}(\alpha, \phi)$ is given by

$$(22) \vec{P} = \frac{1}{2} \operatorname{Re} \{ \vec{E} \times \vec{H}^* \}$$

where

Re - real part of

()* indicates complex conjugate.

Performing the operation indicated in (22) we get for $\vec{P}(\alpha, \phi)$:

$$(23) \vec{P}(\alpha, \phi) = \frac{k_i^3 |\varphi(\alpha, \phi)|^2 \epsilon_i \omega}{2 R^2} \left[\cos \alpha \cos \phi F_i(\alpha) - \sin \alpha \sin \phi \cos \phi G_i(\alpha) \right]^2 \\ + |F_i(\alpha)|^2 \sin^2 \phi \vec{U}_R$$

Note that $F_1(\alpha)$ and $G_1(\phi)$ are in general complex variables of α and ϕ .

The total power radiated into free space ($z > 0$) is therefore found by integrating the Roynting vector over the region $z > 0$ or

$$(24) \quad P_{(z>0)} = \int_0^{2\pi} \int_0^{\pi/2} |\vec{P}(\alpha, \phi)|_{z=0} R^2 \sin \alpha \, d\alpha \, d\phi$$

and the power radiated into the region $z < 0$ is

$$(25) \quad P_{(z<0)} = \int_0^{2\pi} \int_{\pi/2}^{\pi} |\vec{P}(\alpha, \phi)|_{z=1} R^2 \sin \alpha \, d\alpha \, d\phi$$

The antenna "gain function" or power pattern is by definition

$$(26) \quad G(\alpha, \phi) \equiv \frac{4\pi R^2 |\vec{P}(\alpha, \phi)|}{P_{(z<0)} + P_{(z>0)}}$$

and the radiation resistance R_{RAD} can be found by equating the total radiated power ($P_{(z<0)} + P_{(z>0)}$) to the average power delivered to the antenna:

$$(27) \quad \frac{1}{2} I_0^2 R_{RAD} = P_{(z<0)} + P_{(z>0)}$$

or

$$(28) \quad R_{RAD} = \frac{2}{I_0^2} [P_{(z<0)} + P_{(z>0)}]$$

Obviously a digital computer must be employed to get meaningful results from the above expressions. It is interesting however to let $\epsilon_1 \rightarrow \epsilon_0$ in the preceeding equations because as $\epsilon_1 \rightarrow \epsilon_0$

$$\lim_{\epsilon_1 \rightarrow \epsilon_0} G_1 = 0$$

$$\lim_{\epsilon_1 \rightarrow \epsilon_0} F_1 = 1$$

The results then are identical to the classical problem of a half wave dipole radiating in free space.

APPENDIX 4.1

- (1) PRELIMINARY REPORT ON THE ATHABASCA
GLACIER FIELD EXPEDITION
- (2) A HEURISTIC INTERPRETATION OF THE MARCH 1970
ATHABASCA GLACIER FIELD TRIAL DATA

(1)

~~ATHABASCA~~
~~GLACIER~~

PRELIMINARY REPORT
ON THE
ATHABASCA GLACIER FIELD EXPEDITION
April 1970

by
E.A. Johnston, G.A. LaTorraca,
J.R. Rossiter and D.W. Strangway

NASA Grant NGL 22-009-257
Principal Investigator - Gene Simmons

INTRODUCTION

There were two outstanding reasons for planning an expedition to depth-sound a glacier using the radio-frequency interferometry technique. First, the glacier provides a reasonable geological environment in which to prove the method. Second, it provides a full-scale area in which prototypes of the lunar instruments can be tested and evaluated.

Most geological environments on earth are too conductive to make the interferometry approach feasible. However, ice is a highly resistive dielectric medium, and radar waves are known to be reflected through it from depths of over 1000 meters (e.g. Evans, 1963). It is for this reason that a glacier study can furnish convincing data to show that the interferometry technique is feasible scientifically, and that the necessary instrumentation performs satisfactorily. Both these objectives were reached on this trip.

The following information was obtained from the expedition:

- 1) The technique is feasible for depth sounding in low loss geological environments;
- 2) Actual field data compare favorably with theoretical and scale model studies;
- 3) In a typical geological environment, scattering is an important factor in the use of this technique;

- 4) The prototype transmitter performed flawlessly;
- 5) A method of tuning a multiple-frequency antenna on the surface of a dielectric was developed.

This information is essential to the development of the interference technique.

PREVIOUS WORK

Considerable previous work led up to this expedition. Theoretical results had been derived and computed for a two-layer earth. A model experiment had been set up at the University of Toronto which gave reasonable agreement with theory. An initial glacier experiment had been conducted in September 1969, and a prototype transmitter had been developed at the Center for Space Research at M.I.T.

The basic transmitter-receiver configuration planned for the lunar experiment is a horizontal electric dipole transmitting antenna laid on the surface, and orthogonal loop receivers. The receivers measure the vertical H_z and radial H_ρ field components, as the distance from the transmitter is increased. The theory has been derived for a homogeneous, isotropic dielectric layer over a perfect conductor. Model results correspond quite well with this theory, and suites of curves for both the H_z and

H_p components have been plotted.

The trip to the Gorner Glacier last year did not give a complete test of the theory. Although the frequency of the peaks and troughs accurately gave the dielectric constant of ice (see Figure 1), the depth to the bottom was too great to obtain reflections. Therefore this expedition was made to a shallower glacier. A more powerful transmitter was used, readings were taken over a wider frequency range, and care was taken to insure that the antenna was properly tuned before each traverse.

CHOICE OF GLACIER

The Athabasca Glacier, near Jasper, Alberta, was chosen for this experiment. Although this glacier is not within the United States, it has many advantages. It is probably one of the most accessible glaciers in the world, since it is less than a mile from the Glacier Highway, between Banff and Jasper. It has been extensively studied and drilled over a period of many years, and is a safe glacier on which to work. The location of the glacier is shown in Figures 2 and 3.

Of course, equally important for this experiment is the availability of accurate information on the depth to the bot-

tom of the ice. A gravity survey has been conducted by Kanasewich (1963); seismic and drilling studies have been made by Paterson and Savage (1963); and electromagnetic and resistivity soundings have been run by Keller and Frischknecht (1960 and 1961). These results are shown in Figures 4, 5, and 6 respectively. The depth is seen to vary from less than 100 m. at the tongue, to some 350 m. higher up.

Electrical properties of the Athabasca Glacier have been studied by Watt and Maxwell (1960). They give a value of $\tan \delta = 3$ at 0.1 MHz., which agrees entirely with the dielectric profiles of ice as reviewed by Evans (1965). Moreover, Keller and Frischknecht found that, except for a shallow surface layer, the ice on this glacier had the very high resistivity of 30 Megohm-m. They also mention that the ice is fairly pure, except for several lateral moraines, and some surface dust. Both these groups worked during the summer, when large amounts of water were present sitting on the surface and running off. Therefore, it was expected that the losses would be even less in winter.

FIELD RESULTS

The transmitter was set up at the position 000 shown in Figure 7. The traverse line was chained out along the glacier,

away from the toe, and the antennas were laid out perpendicular to the traverse line. For each frequency, readings were made about every $1/6$ wavelength, along the traverse line to a distance of approximately 20 wavelengths, or until the signal could not be detected.

The traverses made are shown in Figure 7. They start near the toe of the glacier and head toward the higher ice-field, approximately along the center of the glacier. As can be seen from the profile, initial reflections will be from the ridge approximately 100 m. from the surface. Continuing along the traverse line, there is then a fairly steep slope into a basin with a depth of approximately 200 m. The ice thickness is constant for a distance, then slopes down to around 300 m. at the extreme end of the traverse line.

Preliminary results are shown in Figures 8 to 18, along with corresponding theoretical curves. In each curve, field strength is plotted on the vertical axis, against transmitter-receiver separation on the horizontal axis. The vertical scales are arbitrary; the horizontal scale is in wavelengths for every curve.

The lowest frequency used, 2 MHz., with a free-space wavelength of 150 m., had fairly low relative signal strengths.

(see Figures 8 and 9). This corresponds to the theoretical results, shown for the H_z component. As shown, the fit is reasonable, with the exception of one point at the top of the experimental H_z curve. This is probably spurious, since it is not found in the H_p results.

For frequencies greater than 2 MHz. the curves show more character. Unlike the Gorner Glacier results (Figure 1), which tended to drop off exponentially, these curves show an initial drop in amplitude, followed by an increase as transmitter-receiver separation is increased. This increase in amplitude is due to an increase in reflected energy received from a critical angle.

The field curves for both H_z and H_p components at 4 MHz. match fairly well to theoretical curves for 2 wavelengths or 150 m. depth (Figure 1). The major inconsistency in Figure 10 is in the amplitudes of the major peaks of the empirical and theoretical curves. This is probably due to approximations in the theoretical model, which tend to show the peak larger than it should be. Scale model results have confirmed this discrepancy. The other inconsistency is that the field curves show a split in the peak between 7 and 8 λ separation. This could be caused by scattering from the basin shown in Figure 7.

The 8 MHz. field data for the H_p component fits extremely well to the theoretical curve for 3 wavelengths or 115 m. depth

(Figure 12). This is reasonable, since the shorter traverse at this frequency would be largely confined to the ledge shown in Figure 7. Moreover, the fact that the field curve is "pulled" slightly towards the end of the traverse is indicative of the fact that the bottom is sloping downwards at this point. With the exception of the major peak at about 6λ , the H_z field curve matches a theoretical curve for about 4 wavelengths depth (Figure 13). Although this is a greater depth than that indicated by the H_ϕ results, it is not unreasonable for the farther reaches of the traverse.

At this point adequate matches have not been made for the 16 and 24 MHz. results. They are shown in Figures 14 to 18 in order to point out the effects of scattering in this experiment. The free-space wavelengths of these frequencies are only 19 m. and 12 m. respectively, and it is reasonable to assume that the roughness of the glacier bottom is the same order of size as this. Thus it is expected to contribute some scatter into the results. As can be seen, there are few clearly defined peaks in these curves. However, it must be pointed out that the theoretical curves (and model results) indicate that as the depth increases (in terms of number of wavelengths), the number of interference peaks also increases. This effect is clear in the field results. One feature which indicates that scattering, although definitely present, is not an overwhelming problem, is that the E_ϕ component is basically similar to the

H₂. This is expected if there are no scattering bodies present; however, it is not necessarily true if there is a large amount of scattered energy.

A preliminary investigation shows that reflections were obtained from the bottom of the glacier. These gave interference patterns agreeing with theoretical models, when the known parameters for ice and depth of the glacier are substituted. Scattering is present, as would be expected in a geological environment, and although it should be studied further, it was not serious enough to make a preliminary interpretation impossible.

Further work will include computation of more precise theoretical curves for the particular field results shown, reduction of the remaining field data, and comparison of curves run at various places along the traverse line at the same frequency. Data was also taken to investigate the effect of human bodies near the receiver, and this will be analyzed.

ANTENNA CONFIGURATION

Several antenna experiments were done on the Athabasca Glacier to determine the feasibility of using, and tuning procedure for, the "ribbon wire" antenna. This would determine

the effect of a dielectric interface on the radiation impedance of the antenna.

One test consisted of feeding a standard ($\lambda/2$) dipole antenna at its resonant frequency (50 MHz.) when elevated above the surface of the ice. Then, lowering this antenna to the ice surface, the change in its resonant frequency was about 2%. Next the same experiment was done using 100 MHz., and again the shift was downward by about 2%.

Using two strands of #22 wire in parallel for each element of a dipole for 4 MHz., and a similar set of wires for an 8 MHz. dipole, it was found that the required length for resonance was 90% of that calculated for free space. This includes the effect of the dielectric half space noted above.

In the ribbon wire configuration, elements were cut to resonance at 2, 4, and 8 MHz. and found to average about 75% of the free space half-wavelength. This amount of detuning is apparently due to the wire capacity, lowering the resonant frequency of all of the elements.

The tuning procedures used for the ribbon wire were as follows. The longest element (1) was connected to the feed network (Merrimack HSM-110) and all elements were cut for resonance at the desired frequency f_1 . Then the next ele-

ment (2) was added in parallel, and fed at the second desired frequency f_2 , cutting all elements except that used for f_1 , until resonance is achieved at f_2 . There was no noticeable change in the tuning of element 1. Element 3 was then connected in parallel with elements 1 and 2, and all elements except 1 and 2 were cut for resonance at f_3 , noting that the tuning of elements 1 and 2 did not change. Thus the antenna was well tuned for each frequency.

This antenna tuning method indicates that the natural current division due to the element impedance is taking place at the feed point, and that a ribbon wire type of antenna is therefore feasible.

] The feed network used was not quite optimum since it was designed to be used in a 50Ω system and the dipole impedance is near 72Ω . This should have produced a minimum vswr of about 1.4:1 which represents about 3% reflected power. On the glacier the reflected power was typically between 5 and 10%, or a vswr of 1.6:1 to 2:1. A 72Ω hybrid would lower the reflected power to 5% or less, which is quite tolerable.

The plastic insulation on the ribbon wire used was found to be too brittle, and unsuitable in the extreme cold of the glacial environment. However, teflon insulation would solve this problem. The breadboard transmitter used for this experi-

ment was found to be entirely satisfactory. The receiver IF bandwidth of 2 KHz was considered to be too sharp, and a bandwidth of the order of 10 KHz is recommended for future work. In addition, the crystal oscillator should be temperature controlled or compensated to minimize drift.

CONCLUSION

It is therefore concluded that the technique, with present instrumentation, will give satisfactory results in a geological environment in which the electromagnetic losses are small. In spite of mathematical approximations in the theoretical models, the theory seems to be justified with few modifications. Future work should investigate more fully the effects of scattering.

(Note: The assistance of Dr. W.S.B. Paterson, Dr. Ron Goodman, and Mr. K.G. Neave in providing information on the Athabasca Glacier is gratefully acknowledged. We are also grateful to the National Parks Service for permission to work in Jasper National Park and for the support provided.)

LIST OF FIGURES

1. Determination of the dielectric constant of ice from Gorner Glacier field data.
2. General location map of the Athabasca Glacier.
3. Detail location map of the Athabasca Glacier, showing connecting highways.
4. Sketch of the Athabasca Glacier and gravity profile.
5. Contour map of the Athabasca Glacier and seismic profile.
6. Electromagnetic and resistivity cross-section of the Athabasca Glacier.
7. Sketch map and profile of the Athabasca Glacier, showing the expedition's traverse position.
8. Field results; $f=2\text{MHz}$, H_z and Theoretical curve of H_z for a depth of 1 wavelength.
9. Field results, $f=2\text{MHz}$, H_p .
10. Field results, $f=4\text{MHz}$, H_z and Theoretical curve of H_z for depth of 2 wavelengths.
11. Field results, $f=4\text{MHz}$, H_p and Theoretical curve of H_p for depth of 2 wavelengths.
12. Field results, $f=8\text{MHz}$, H_p and Theoretical curve for H_p for depth of 3 wavelengths.
13. Field results, $f=8\text{MHz}$, H_z and Theoretical curve of H_z for depth of 4 wavelengths.
14. Field results, $f=16\text{MHz}$, H_z .
15. Field results $f=16\text{MHz}$, H_p .
16. Field results, $f=24\text{MHz}$, H_z .

FIGURES (cont.)

17. Field results, $f=24\text{MHz}$, $E\phi$.

18. Field results, $f=24\text{MHz}$, H_ϕ .

REFERENCES

✓ Evans, S., "Radio Techniques for the Measurement of Ice Thickness", Polar Record, v. 11, pp. 406-410 & 795, 1963.

✓ Evans, S., "Dielectric Properties of Ice and Snow - A Review", J. Glaciol., v. 5, pp. 773-792, 1965.

✓ Kanasewich, E.R., "Gravity Measurements of the Athabasca Glacier, Alberta, Canada", J. Glaciol., v. 4, pp. 617-631, 1963.

Keller, G.V. and Frischknecht, F.C., "Electrical Resistivity Studies on the Athabasca Glacier, Alberta, Canada", J. Res. U.S. Nat. Bur. Stan., v. 64D, pp. 439-448, 1960.

Keller, G.V. and Frischknecht, F.C., "Induction and Galvanic Resistivity Studies on the Athabasca Glacier, Alberta, Canada:", Geology of the Arctic (International Symposium), ed. G.O. Raasch, v. 2, pp. 809-832, U. of T. Press, 1961.

Paterson, W.S.B. and Savage, J.C., "Geometry and Movement of the Athabasca Glacier", J. Geophys. Res., v. 68, pp. 4513-4520, 1963.

✓ Watt, A.D. and Maxwell, E.L., "Measured Electrical Properties of Snow and Glacial Ice", J. Res. U.S. Nat. Bur. Stan., v. 64D, pp. 357-363, 1960.

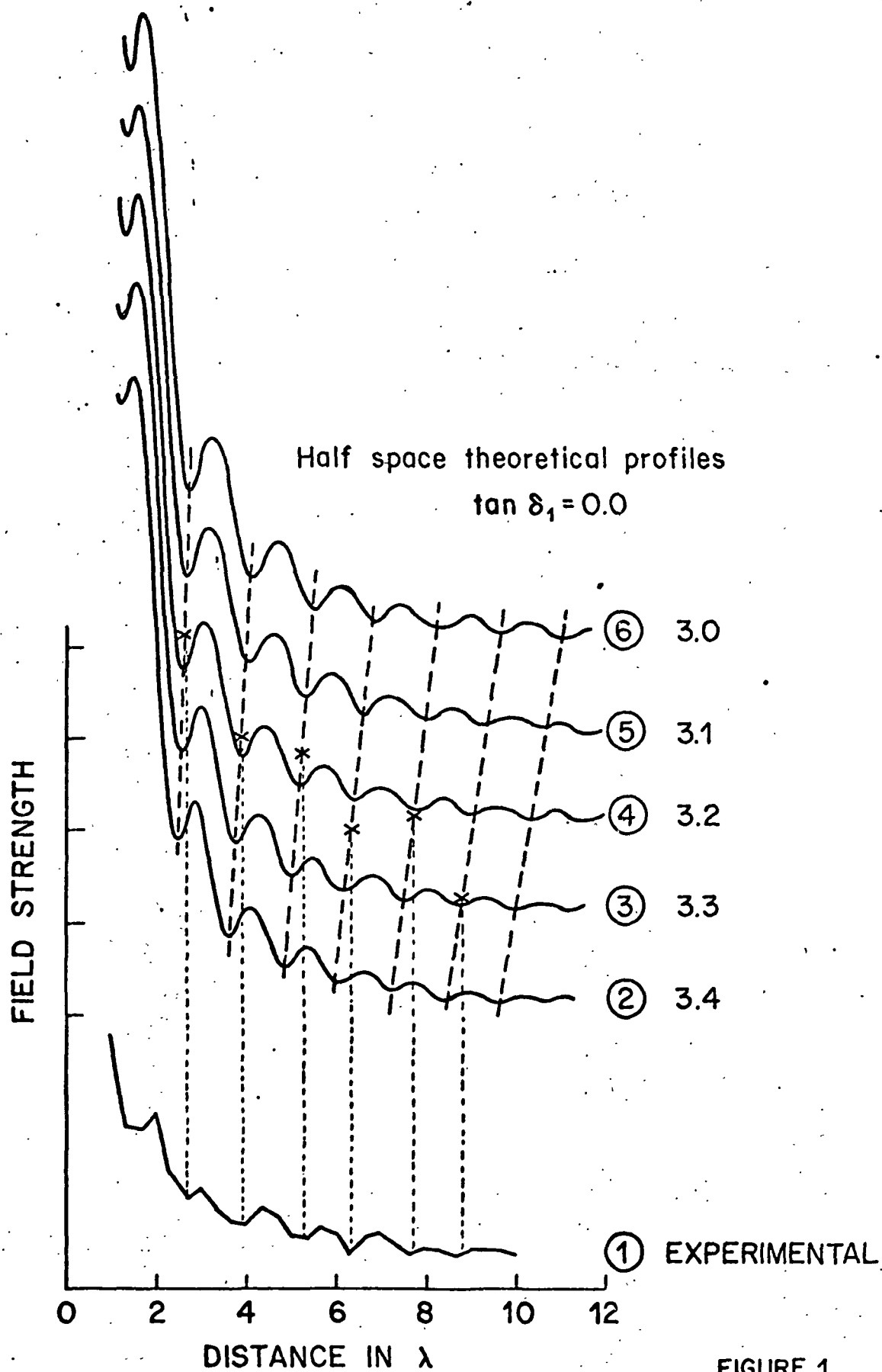
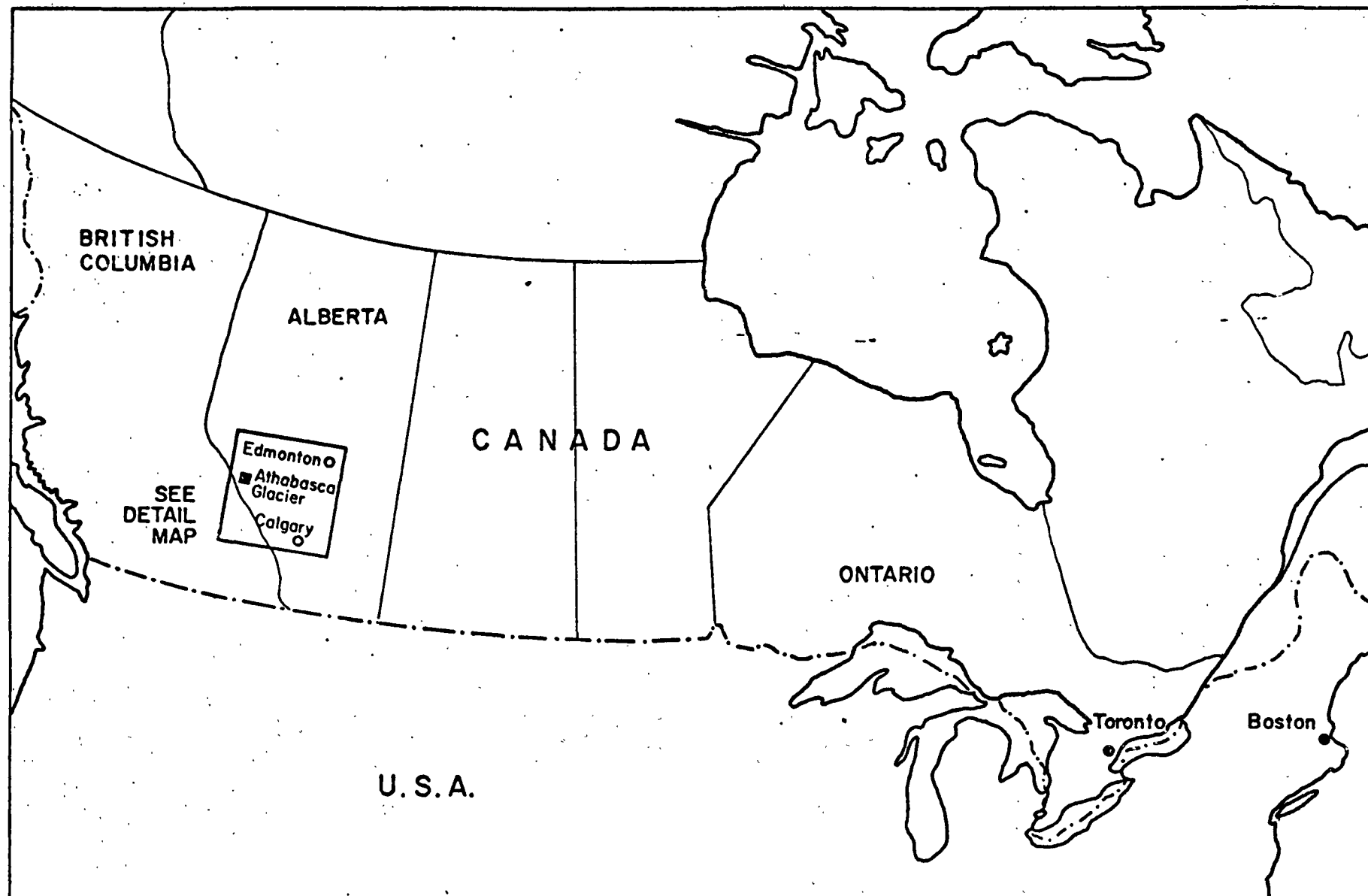
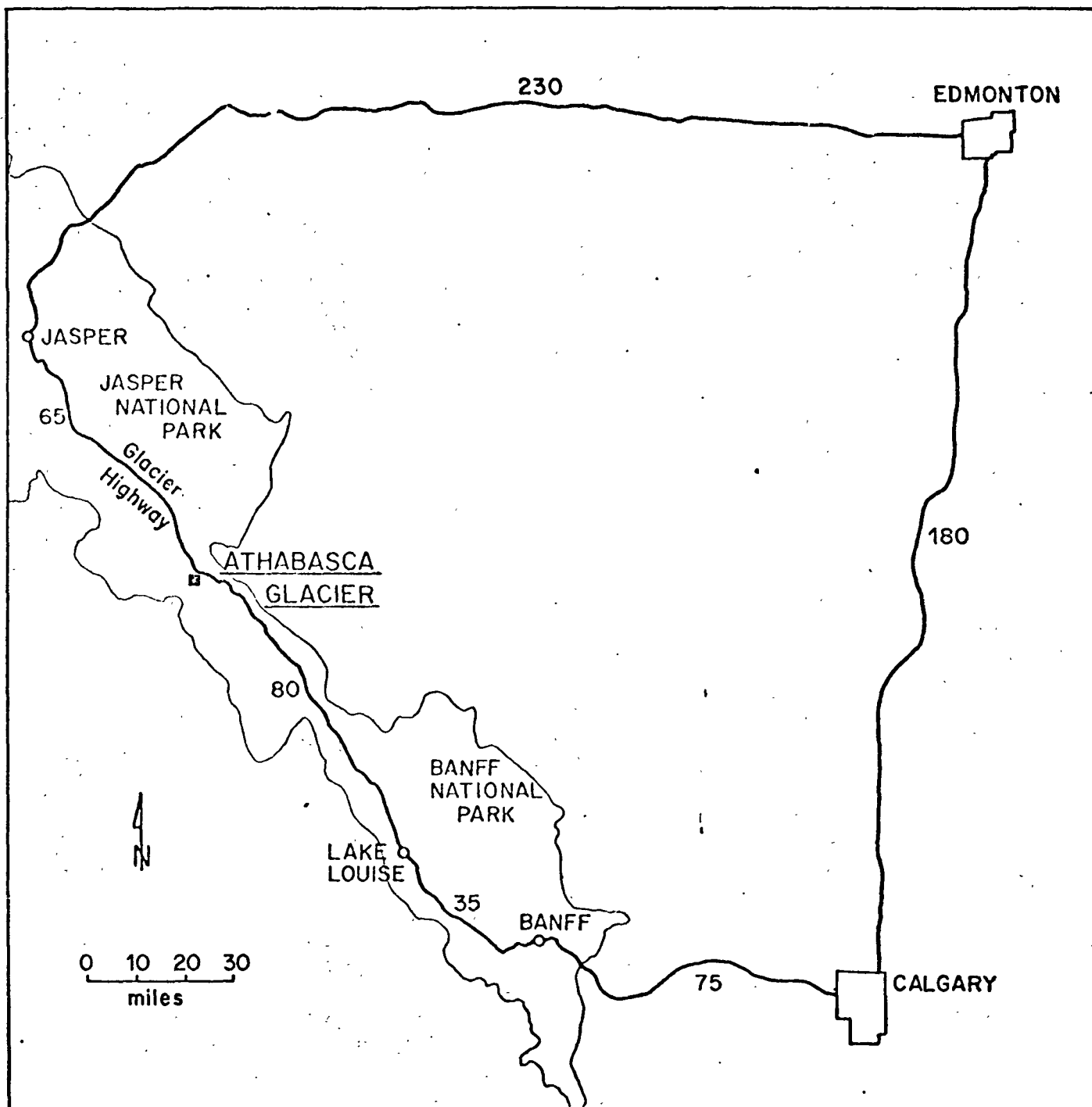


FIGURE 1



GENERAL LOCATION MAP

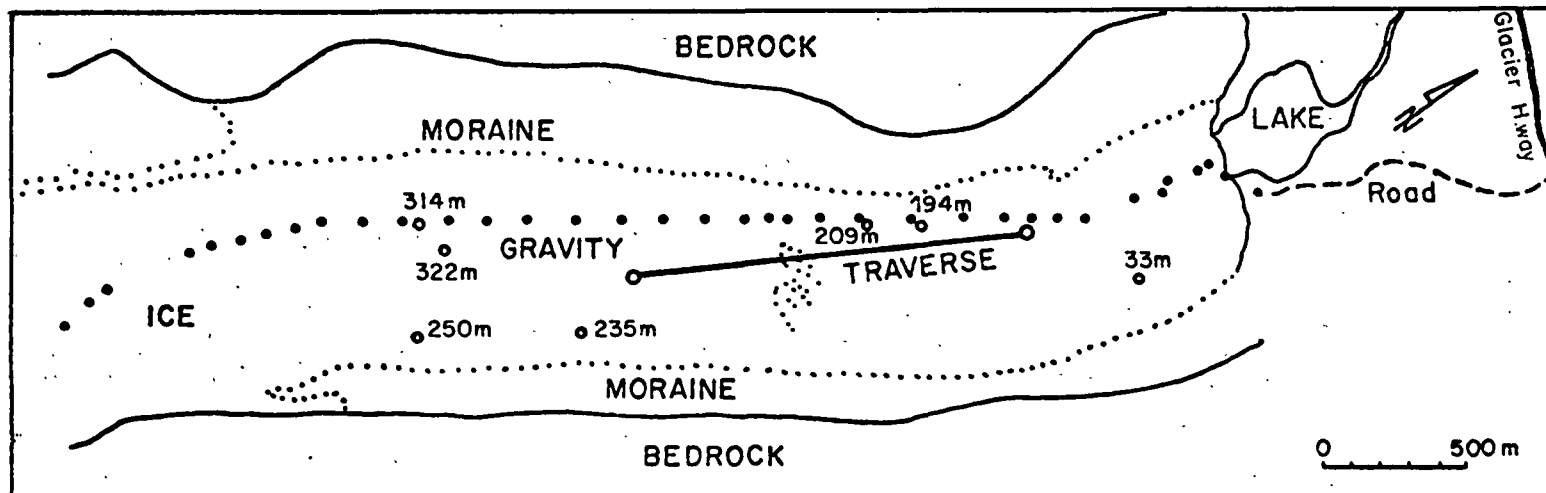
FIGURE 2



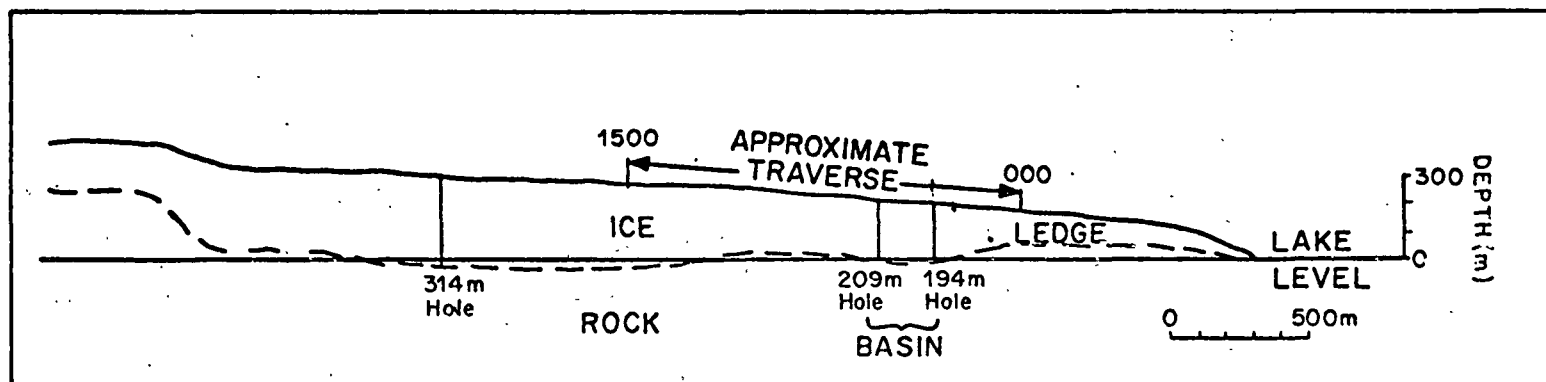
ATHABASCA GLACIER LOCATION MAP

Highway distances shown in miles

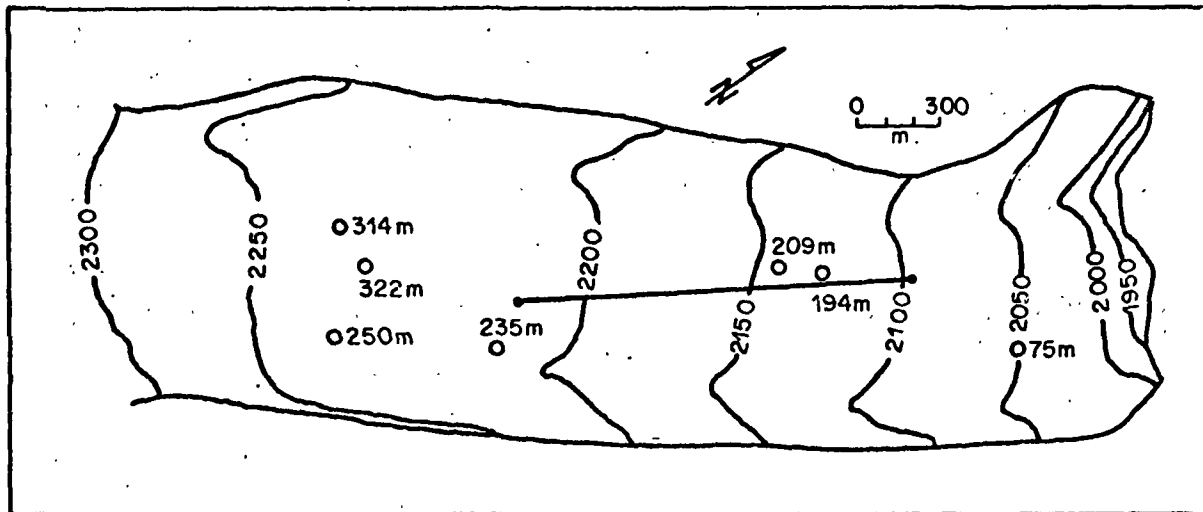
FIGURE 3



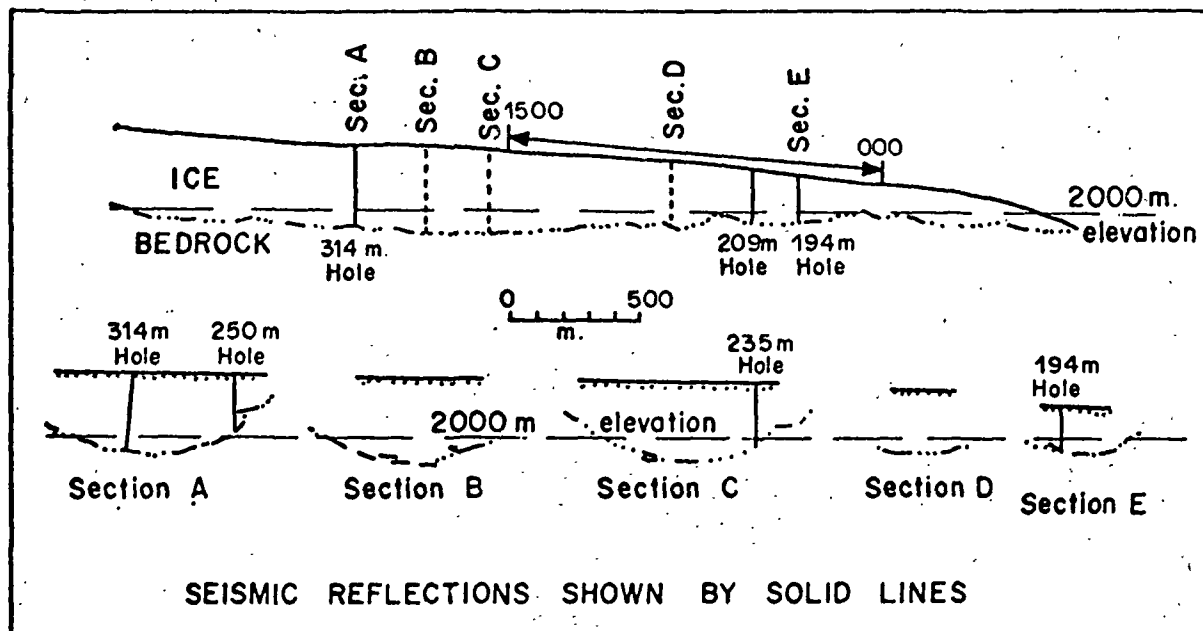
Sketch map of the Athabasca Glacier, showing gravity station (•) and boreholes (o).
After Kanasewich (1963)



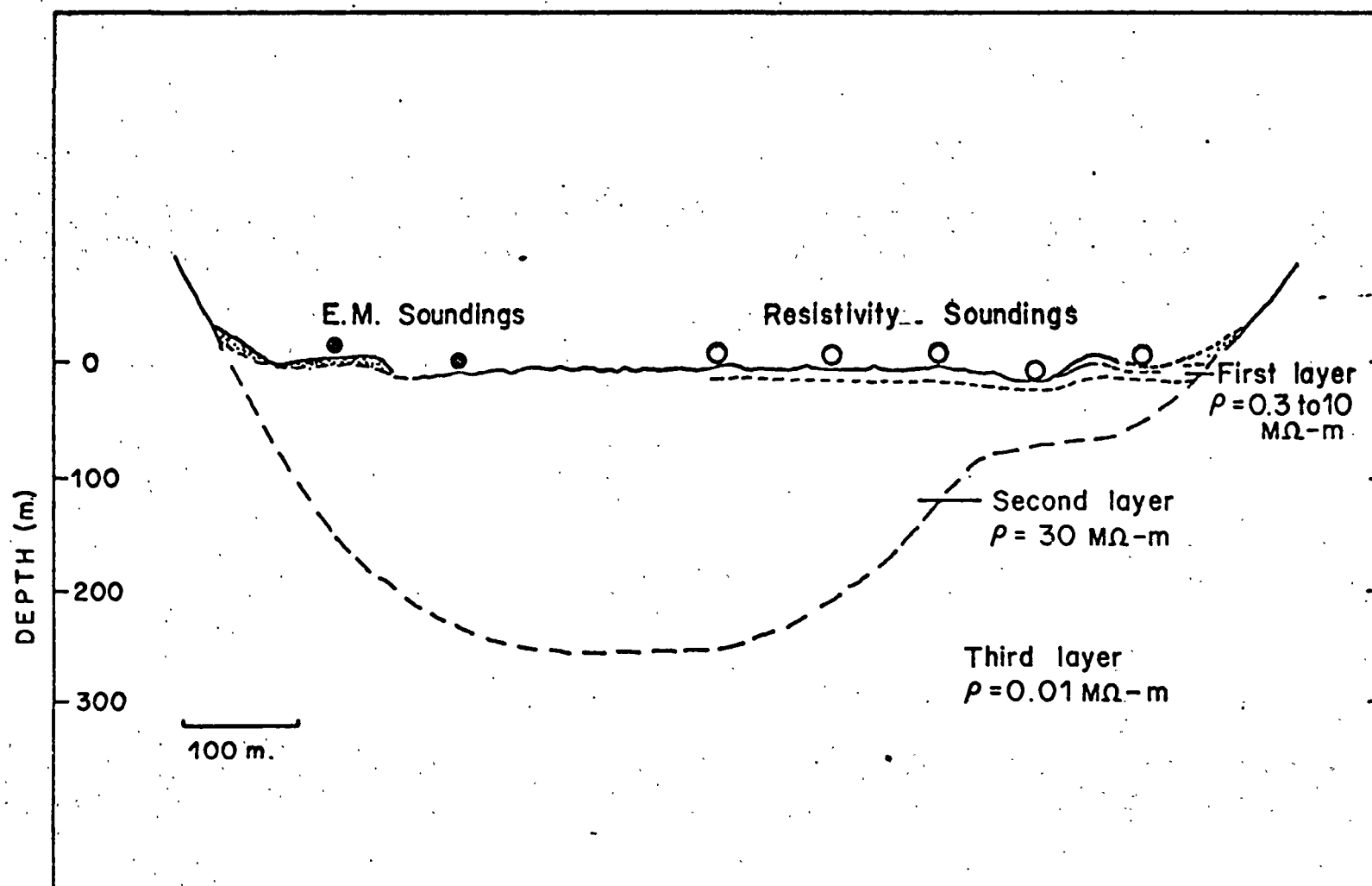
Longitudinal profile of the Athabasca Glacier from gravity results.
as proposed by Kanasewich (1963)



Contour map of the Athabasca Glacier,
after Paterson and Sarage (1963)
Elevations above sea level in (m). Boreholes shown (o).

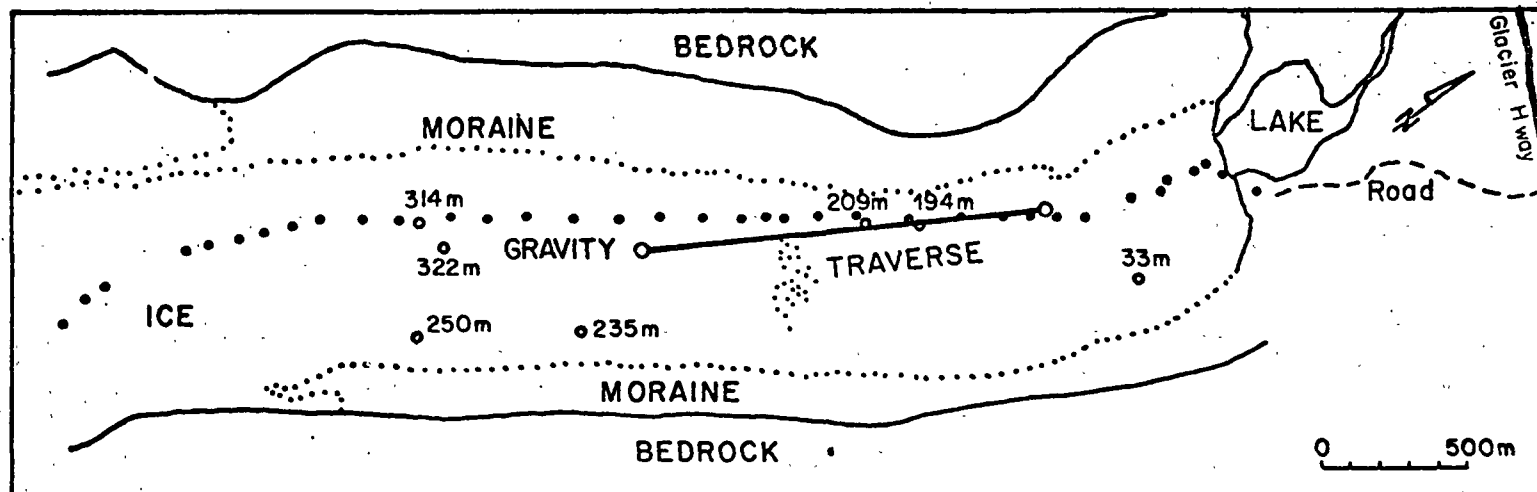


Longitudinal and transverse sections of the Athabasca Glacier,
proposed from seismic and drilling results
by Paterson and Sarage (1965)

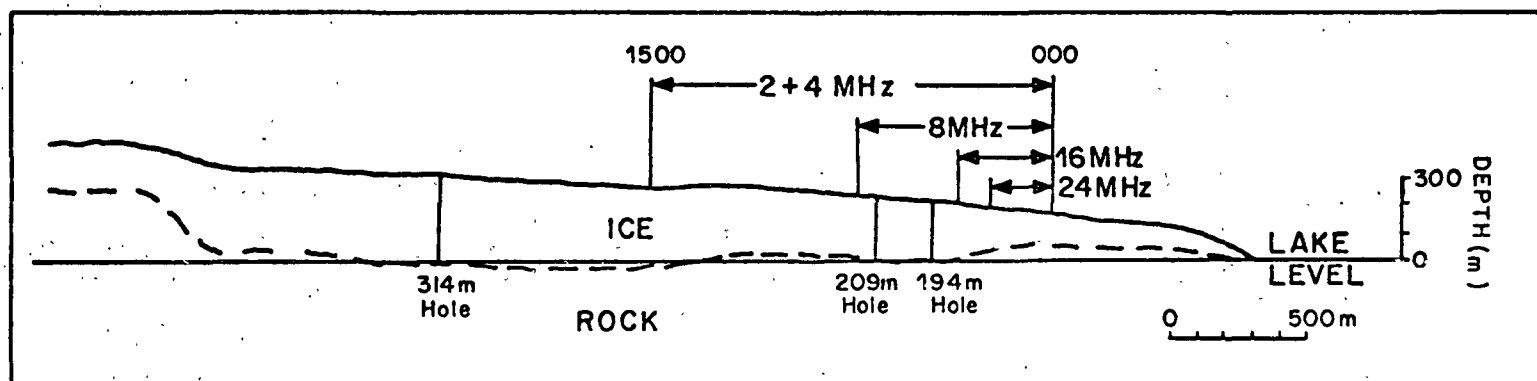


Cross-section of the Athabasca glacier, as postulated by Keller and Frischknecht (1961)

FIGURE 6



APPROXIMATE INTERFEROMETRY TRAVERSE ALONG ATHABASCA GLACIER



INTERFEROMETRY TRAVERSES SHOWN FOR EACH FREQUENCY

FIGURE 7

Hp

FIELD STRENGTH

ATHABASCA GLACIER

Hp, RADIAL FIELD
STRENGTH COMPONENT

$f = 2\text{MHz}$

$\lambda_0 = 150\text{m}$

0

2

4

6

8

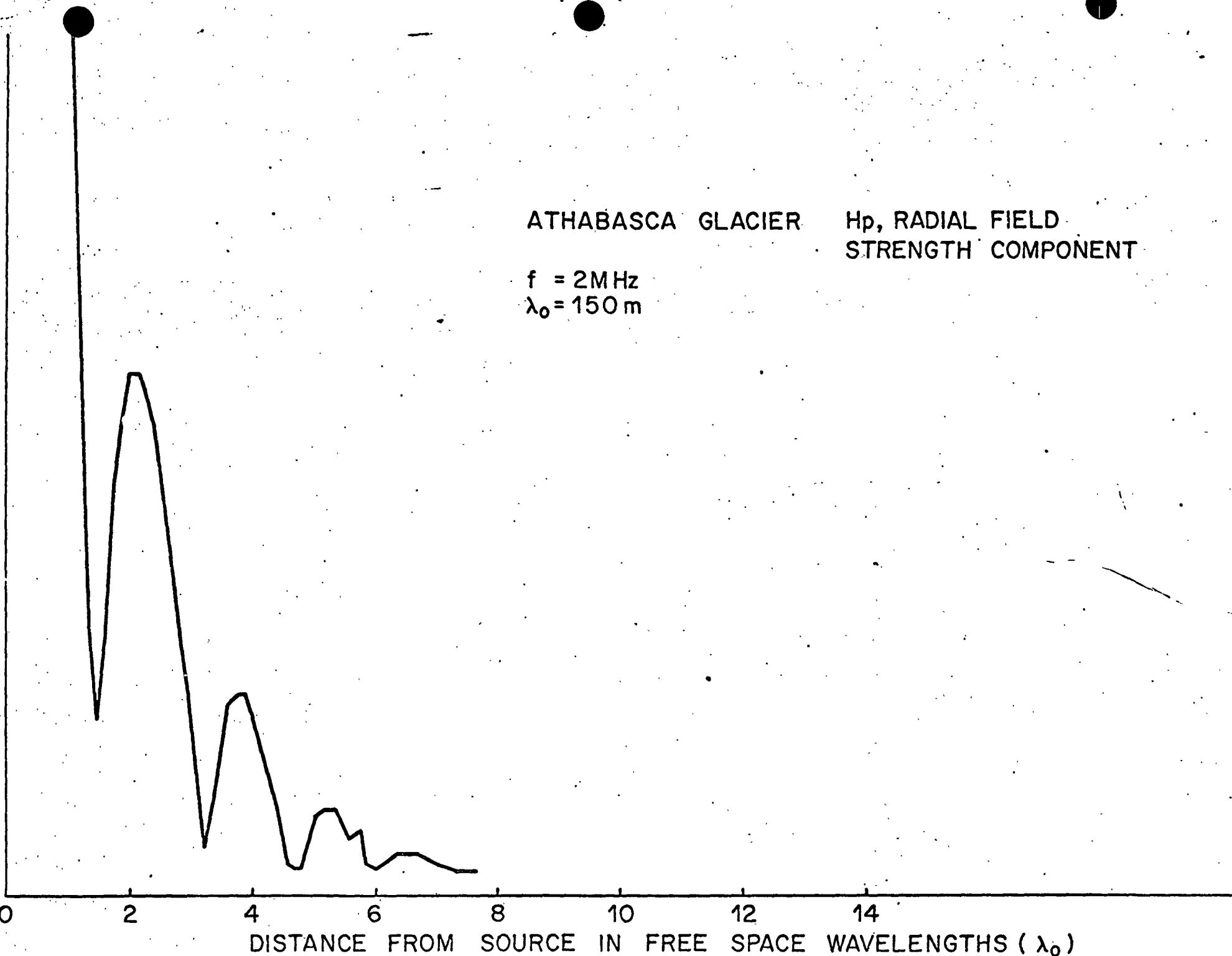
10

12

14

DISTANCE FROM SOURCE IN FREE SPACE WAVELENGTHS (λ_0)

FIGURE 8



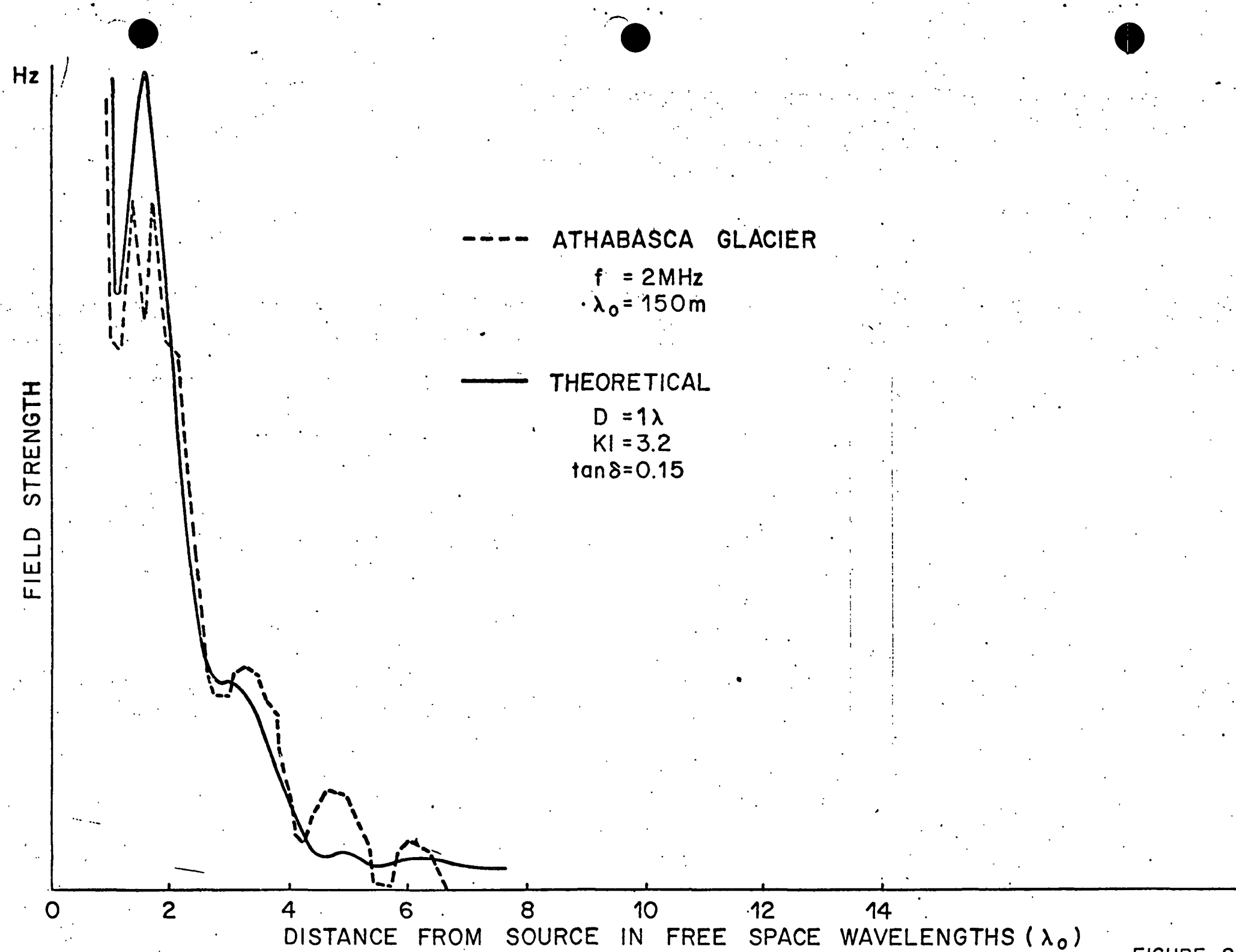


FIGURE 9

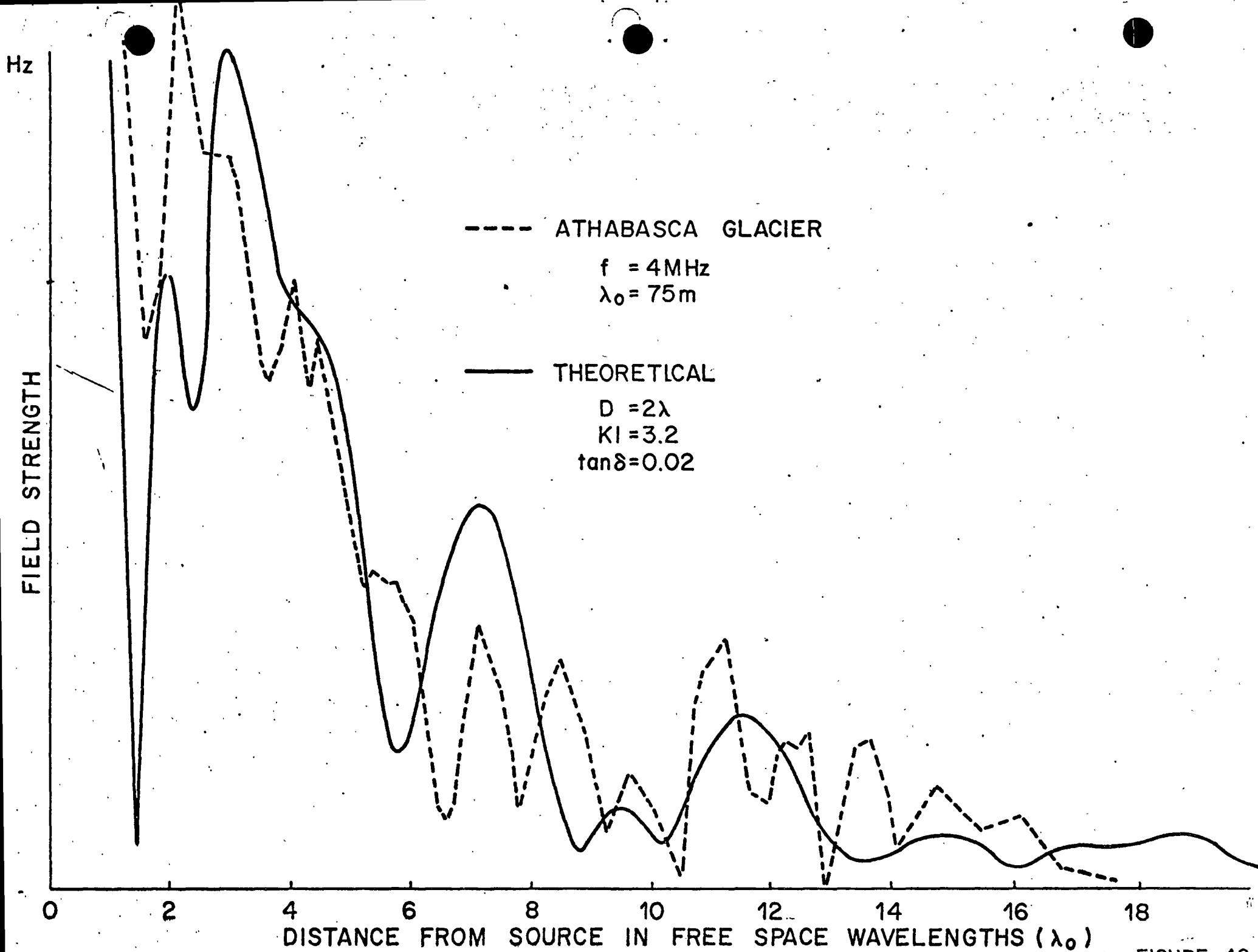


FIGURE 10

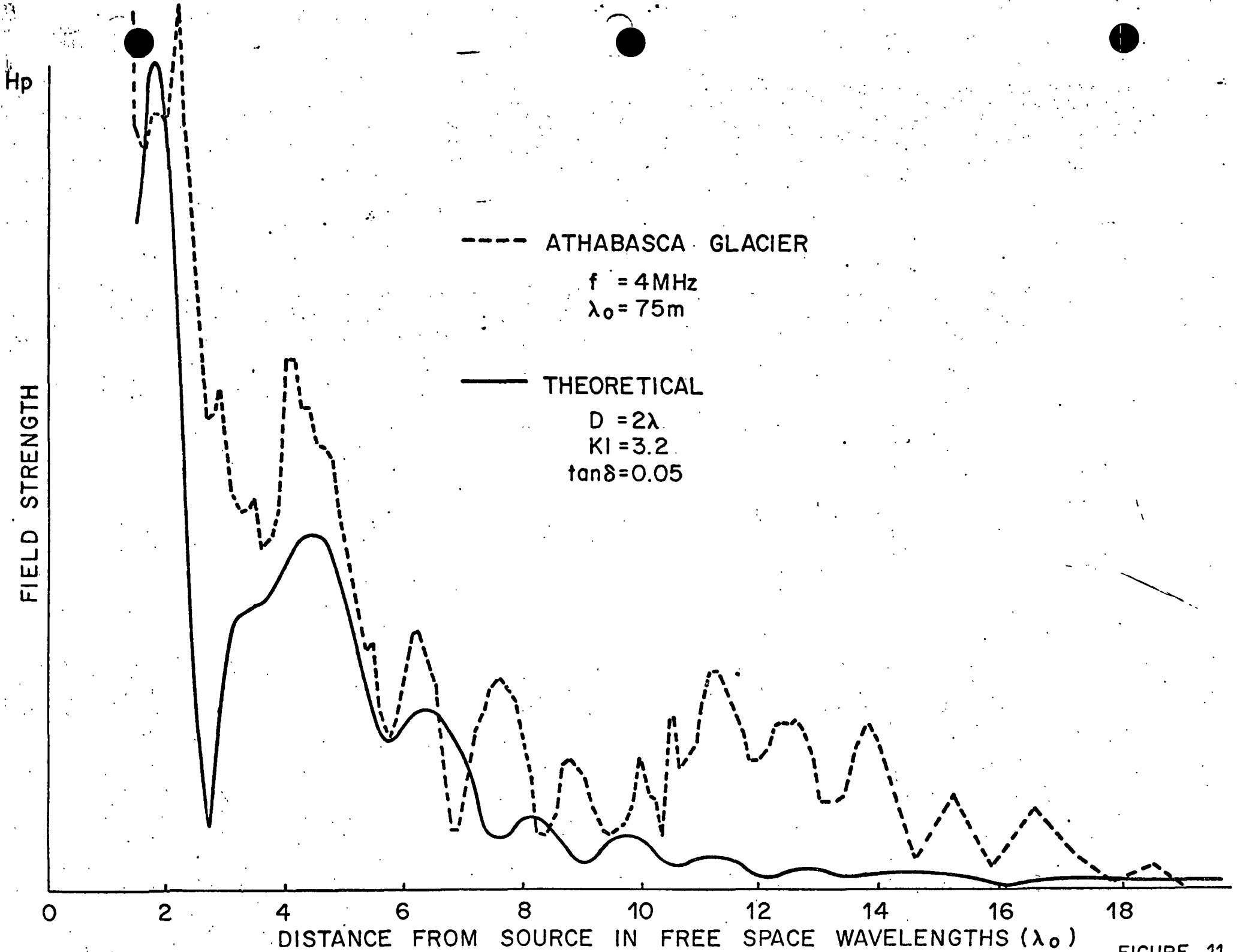


FIGURE 11

Hp

FIELD STRENGTH

----- ATHABASCA GLACIER

 $f = 8\text{MHz}$ $\lambda_0 = 38\text{m}$

—— THEORETICAL

 $D = 3.0\lambda$ $KI = 3.2$ $\tan\delta = 0.03$

0

2

4

6

8

10

12

14

16

18

DISTANCE FROM SOURCE IN FREE SPACE WAVELENGTHS (λ_0)

FIGURE 12

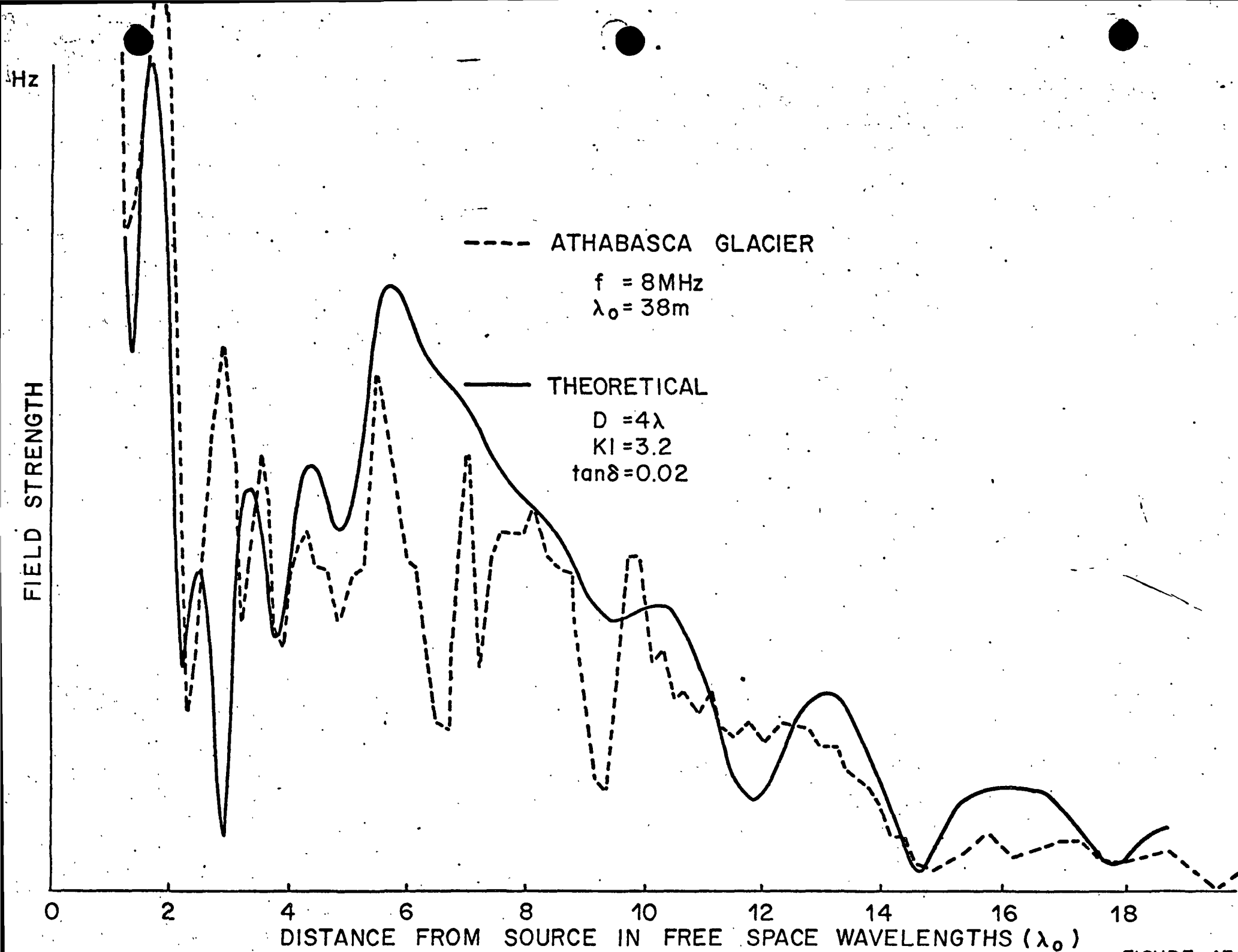


FIGURE 13

Hz

FIELD STRENGTH

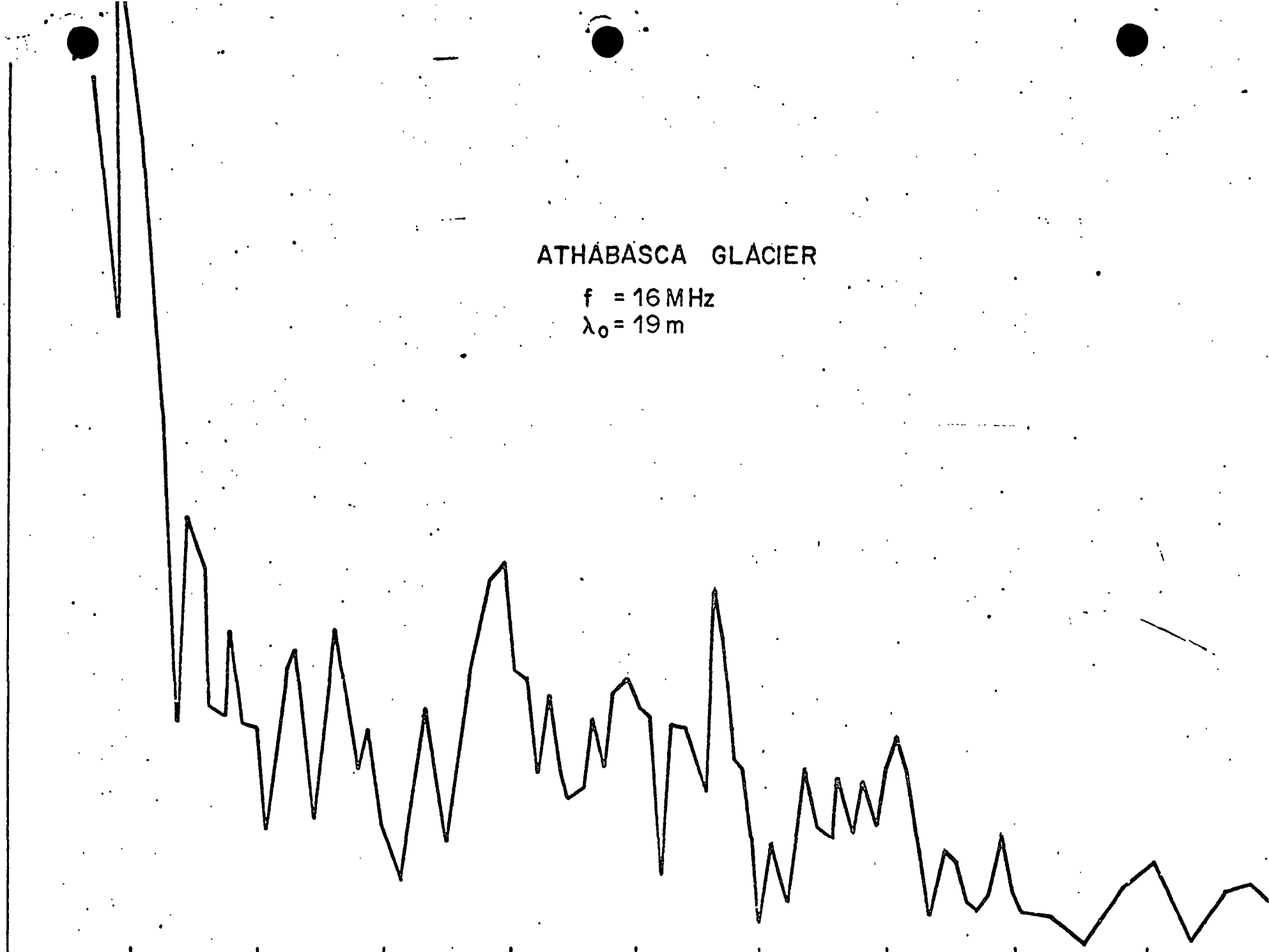
ATHABASCA GLACIER

$f = 16 \text{ MHz}$

$\lambda_0 = 19 \text{ m}$

0 2 4 6 8 10 12 14 16 18
DISTANCE FROM SOURCE IN FREE SPACE WAVELENGTHS (λ_0)

FIGURE 14



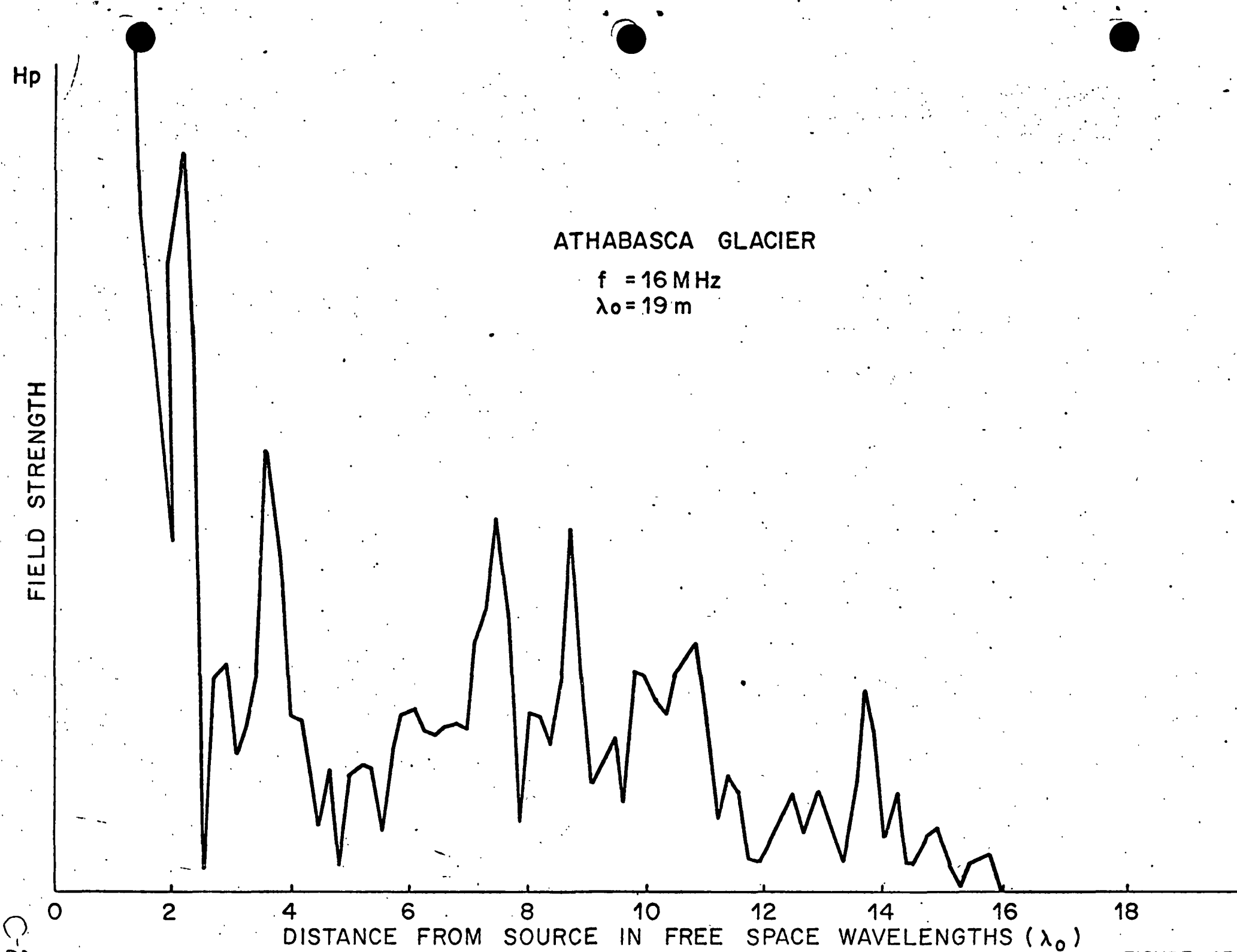


FIGURE 15

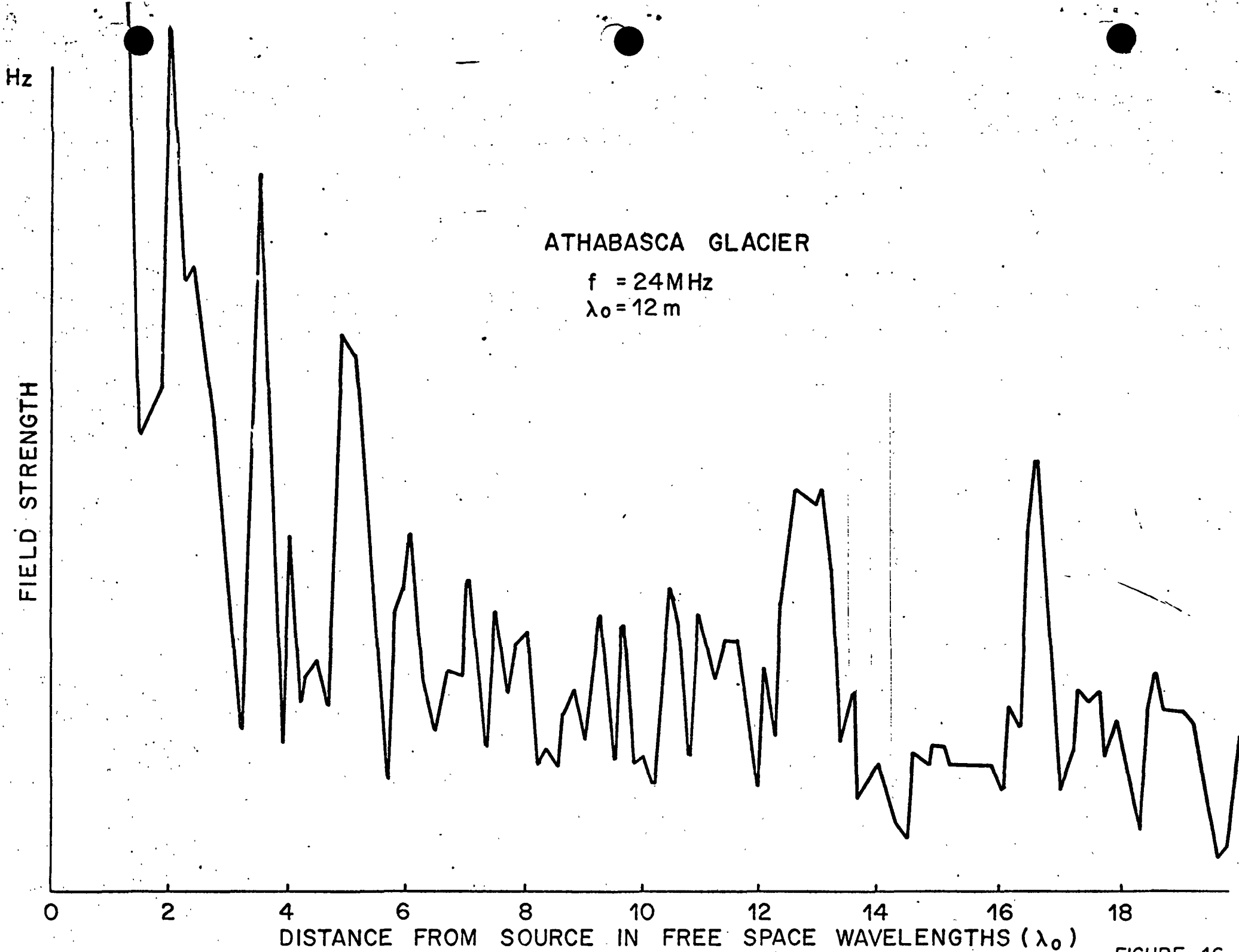


FIGURE 16

E_0

ATHABASCA GLACIER

$f = 24 \text{ MHz}$

FIELD STRENGTH

0

2

4

6

8

10

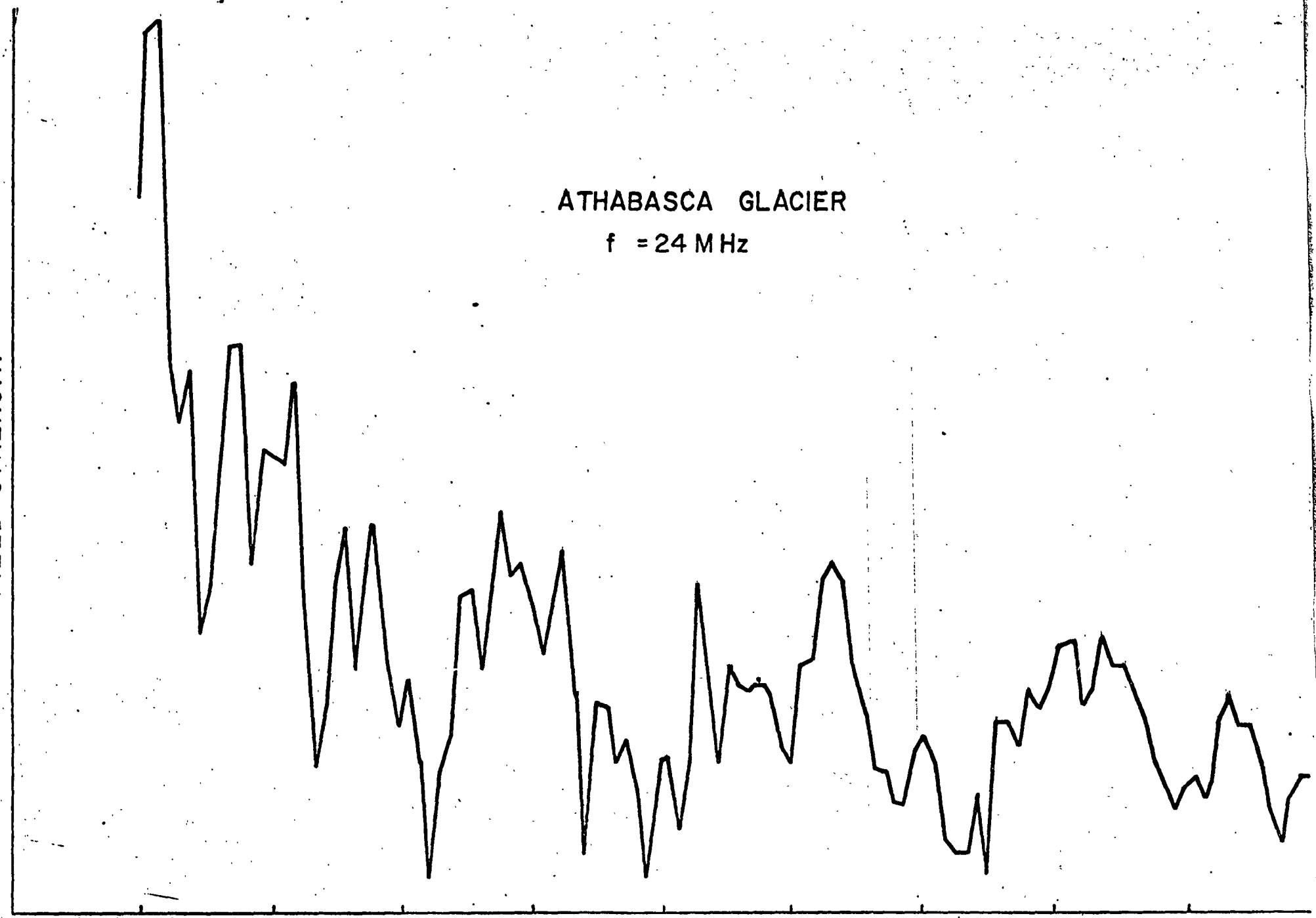
12

14

16

18

DISTANCE FROM SOURCE IN FREE SPACE WAVELENGTHS (λ_0)



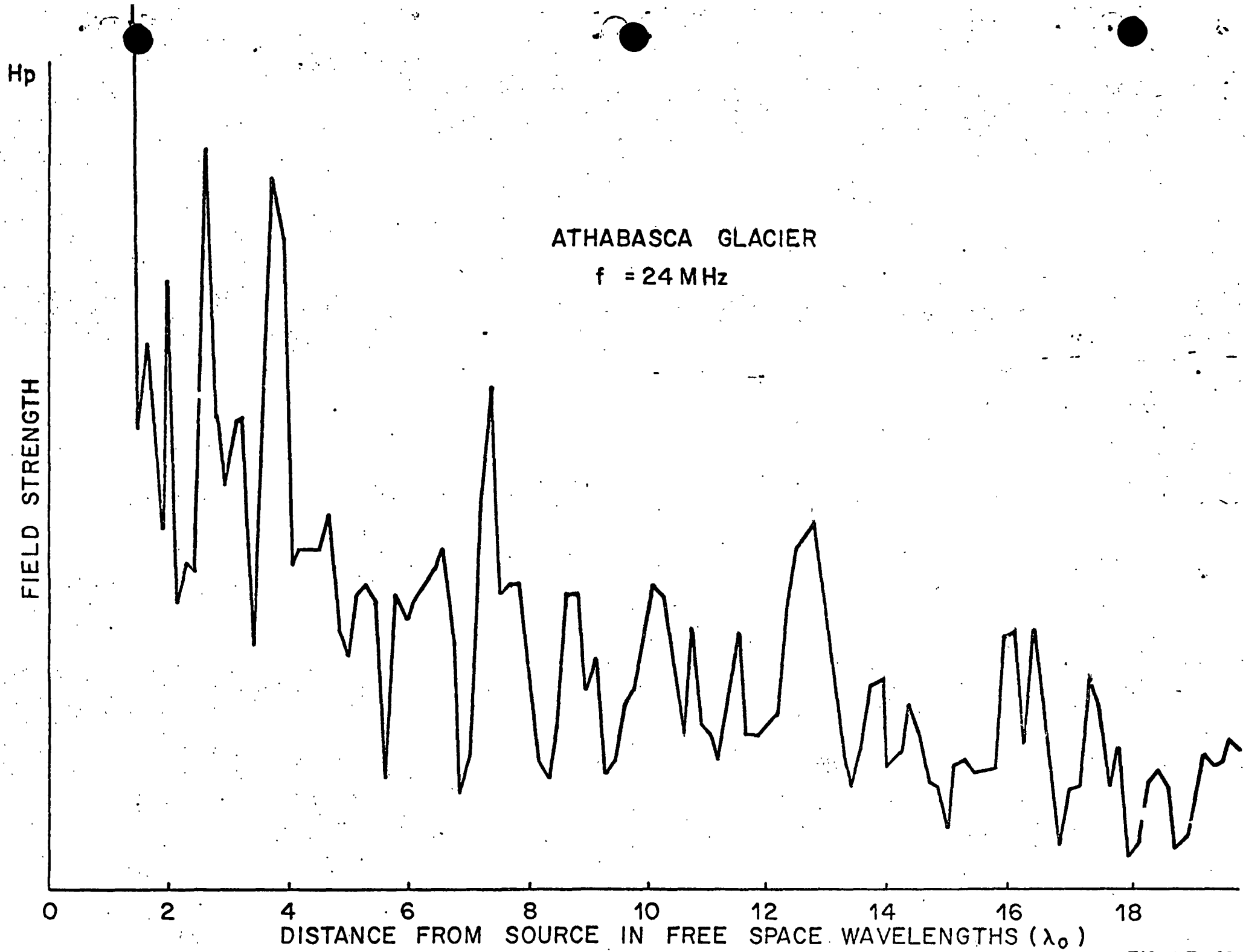


FIGURE 18

(2)

J.W. MEYER

(4)

Surface Electrical Properties Experiment

A heuristic interpretation of the March 1970
Athabasca Glacier field trial data

Lawrence H. Bannister

26 March 1971

(Draft issued 12 March 1971)

Distribution:

- R. Baker
- W. Cooper
- A. England
- J. Gronier
- J. Harrington
- L. Johnson
- E. Johnston
- G. LaTorraca
- J. Meyer (4)
- V. Nanda
- J. Rossiter
- G. Simmons
- D. Strangway
- R. Watts

✓ HAND DEL'D COPIES TO:

J. URNER ✓
D. CUBLEY ✓

1. Summary

A heuristic argument is presented which seems to yield a plausible fit to the Athabasca Glacier field trial data of March 1970. Although the data base is limited, and the quantitative arguments used here cannot be said to prove anything definitively, some conclusions emerge which are believed to be important to the design of future field trials and the lunar experiment hardware.

The situation of interest is that a transmitter is deployed in a fixed position on the surface of the glacier, and a small receiving antenna is moved along a line that is radial to the transmitter.

In this memo, a qualitative exposition is used to predict the manner in which the received signal might be expected to vary with range.

Quantitative values then are derived, and it is shown that there is very good agreement between the developed theory and the empirical data.

It is recommended that 4MHz be reinstated in the list of experiment frequencies.

It is concluded that the transmitting antenna should lie flat on the lunar surface, and that the receiving antenna should be mounted as low as possible on the LRV.

2. Conclusions

According to the argument developed in this memo:

- (1) the mean path attenuation is independent of frequency;
- (2) An effective line-of-sight exists between the receiver and the transmitter to a range of about 100 meters;
- (3) in the line-of-sight regime, the mean value of the received power varies in accordance with:

$$P_r = K_1 R^{-2}$$

- (4) in the line-of-sight regime, the observed interference pattern is attributable to interaction between a surface wave and a subsurface wave, and provides an excellent measure of the dielectric constant of the ice;
- (5) in a regime extending from about 100 to about 300 meters, the received power is influenced markedly by reflections which provide a good measure of the depth to the interface underlying the glacier;
- (6) at ranges greater than about 300 meters, the mean value of the received power varies in accordance with:

$$P_r = K_2^{-R}$$

- (7) in this distant regime, the observed interference pattern is caused by multiple reflections and scattering and cannot be interpreted unambiguously, but the mean path attenuation provides an excellent measure of the dissipative loss in the ice.

3. Hypotheses

The arguments to be developed in this memo will make use of the following hypotheses:

- (1) The dielectric constant of ice is about 3.2 at the glacier surface temperature of about -0.1°C and is not much affected by the slightly lower temperatures encountered in the glacial body.
- (2) Within the frequency range of interest, the loss tangent in solid ice is inversely proportional to frequency.
- (3) At the glacier surface temperature the magnitude of the loss tangent is given by:

$$\tan \delta = \frac{3 \cdot 10^5 \text{ Hz}}{f} = \frac{\lambda}{1000 \text{ meters}}$$

where f is the signal frequency, in Hertz

λ is the free space wavelength, in meters

- (4) The loss tangent is sensitive to temperature and at the slightly lower temperatures encountered in the glacial body is given by:

$$\tan \delta = \frac{2.5 \cdot 10^5 \text{ Hz}}{f} = \frac{\lambda}{1200 \text{ meters}}$$

4. Qualitative evaluation of received power

Generally, for any situation in which a transmitting antenna is deployed at an air-ice interface, it may be said that some part of the radiated power will flow 'upward' into the essentially lossless atmospheric medium while the remainder will flow 'downward' into the dissipative ice.

If the transmitting antenna and the atmospheric medium were both isotropic, the power radiated 'upward' would disperse uniformly in a hemispherical pattern bounded by the line-of-sight. The consequent power density at the surface of a hemisphere centered on the transmitting antenna then would be uniform, and would be simply the ratio of the power radiated 'upward' to the total surface area of the hemisphere.

Because the actual transmitting antenna is anisotropic, the observed power density will not be uniform, but will be modified by the figure-of-eight radiation pattern of a short dipole. At any point on a surrounding hemispherical surface, therefore, the observed power density occasioned by the 'upward' radiated power will be the product of the average power density at the hemispherical surface and the gain of the transmitting antenna in the direction of the chosen point.

Strictly speaking, the power radiated 'upward' cannot be said to propagate into an isotropic hemisphere because the Athabasca valley glacier is ringed by mountains. However, the test configuration used in the March 1970 field trials was such that the effect of these mountains was minimized.

The relevant topography is shown as Figure 4-1. The transmitting dipole was deployed on the surface of the ice, with the axis of the dipole normal to the intended traverse line, and roughly transverse to the glacier. A small loop receiving antenna then was deployed on the surface of the ice and moved on a traverse line roughly longitudinal to the

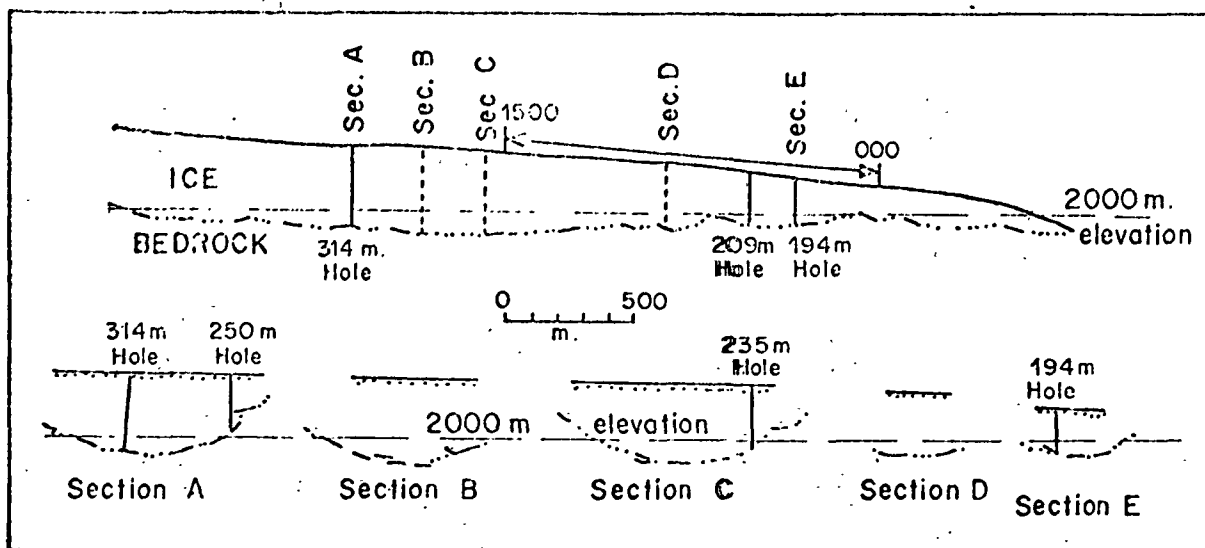
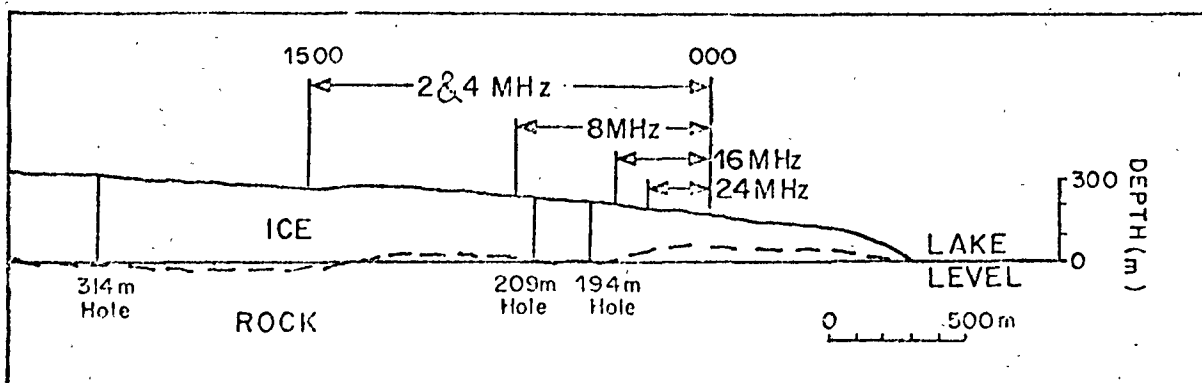
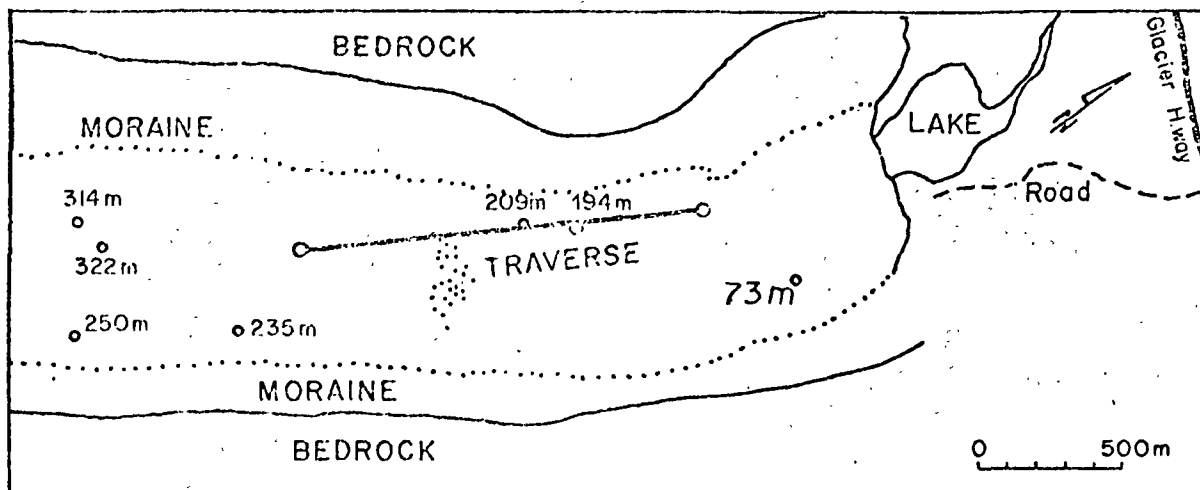


FIGURE 4-1 INTERFEROMETRY TRAVERSE ALONG ATHABASCA GLACIER

glacier and extending to about 1500 meters from the transmitter site.

The nearest mountains, roughly parallel to the traverse line and some 500 meters distant, were thus in the minimum intensity portion of the dipole radiation pattern, while the nearest mountains included within the half-power beamwidth of the transmitting dipole were at least 3000 meters distant from the transmitter site.

With this configuration, the relative magnitude of the power reflected from the surrounding mountains is small enough to be neglected, so, for a line-of-sight propagation path, the power density caused by the 'upward' radiated power may be taken as:

$$P_u = \frac{P_t U G_t}{2\pi R^2} \quad (4.1)$$

where P_u is the power density, in watts per meter²

P_t is the total transmitted power, in watts

U is the fraction of the total transmitted power which is radiated 'upward'

G_t is the gain of the transmitting antenna in the direction defined by the receiver

R is the range from transmitter to receiver, in meters.

The dispersion of the 'downward' radiated power is complicated both by distortions of the antenna radiation pattern caused by refraction effects at the interface, and by multiple reflections and scattering occurring in the ice. However, some illustrative approximations can be made.

Consider, first, the situation at very short ranges. Successive power contours, or surfaces of constant power density, initially will have a form similar to the field intensity pattern of a dipole but modified by refraction effects occurring at the interface. Importantly, prior theoretical work (Annan, 1970) suggests that, in the plane normal to the dipole, the radiation pattern will exhibit a significant lobe of the form shown in Figure 4-2 where the tilt angle is given by:

$$\sin \beta = \sqrt{\frac{k_o}{k_i}} \quad (4.2)$$

where k_o is the dielectric constant of the atmospheric medium
 k_i is the dielectric constant of the ice

As illustrated by Figure 4-3, this lobe may be expected to affect significantly the power density observed at the surface of the glacier at some critical range where the geometry permits the propagating wave to be observed after one reflection. Assuming a horizontal reflecting layer, this range will be of the order of:

$$R = 2 D \tan \beta \quad (4.3)$$

where R is the range from transmitter to receiver, in meters
 D is the depth to the reflecting interface, in meters
 β is the tilt angle defined by (4.2) above

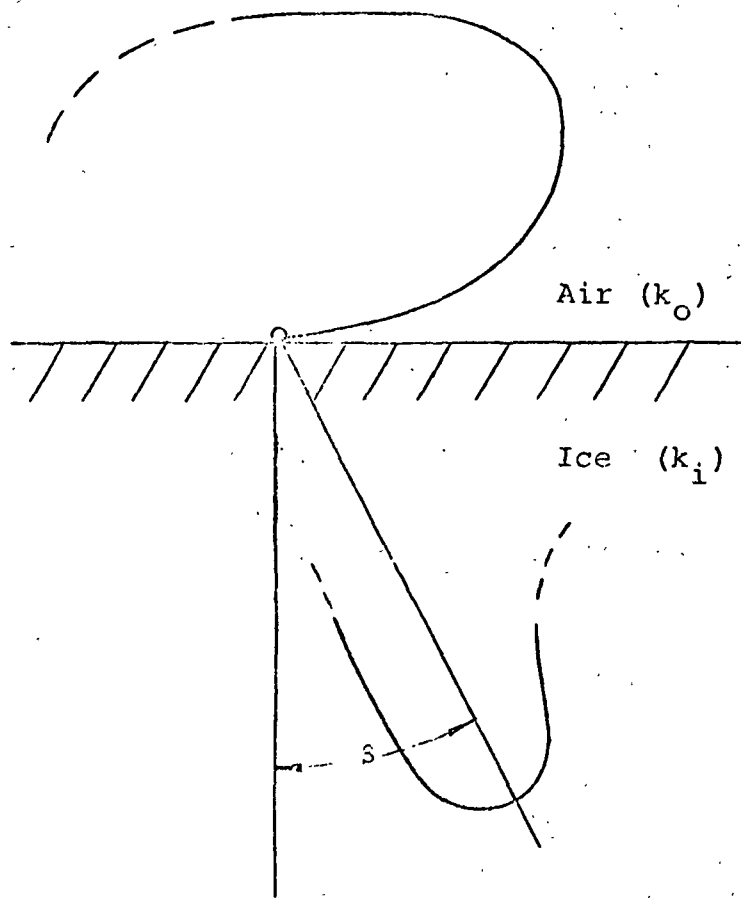


Figure 4-2 Approximate radiation pattern

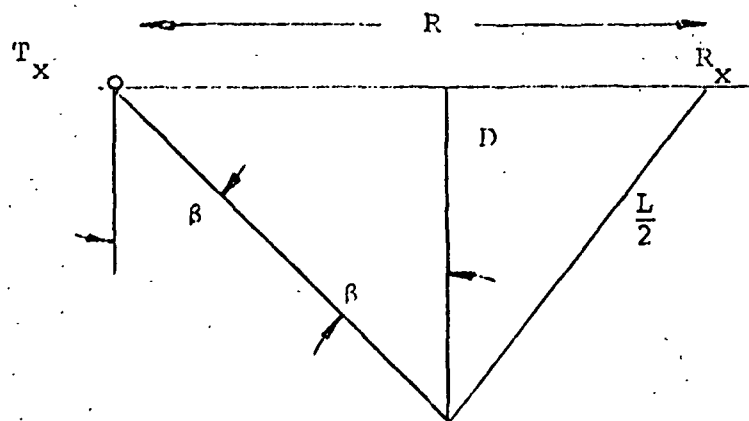


Figure 4-3 Geometry for one reflection

Now, according to the geometry of Figure 4-3, the path length traversed by a wave reaching the receiver after one reflection is given by:

$$L = \sqrt{R^2 + 4 D^2} \quad (4.4)$$

It should be noted that this path length has a minimum value of $2D$ as the range tends to zero.

So, at ranges shorter than that defined by (4.3) the effect of reflections from the underlying bedrock will be small for two reasons. First, the absolute magnitude of the reflected power will be small because the radiation pattern has a minimum in the vertical direction. And, second, because of the substantial difference in path lengths, a wave propagating to and from the reflecting layer will be attenuated dramatically relative to a wave propagating over or close to the glacier surface.

At medium ranges, perturbations caused by reflections from the underlying bedrock will be significant and the radiation pattern, as defined by successive surfaces of constant power density, will be even more complicated. A first approximation, however, can be made by noting that the pattern will tend to be similar to that existing at short ranges but truncated at the bottom bedrock line; thus a surface of constant power density will tend to have the form of a solid figure-of-eight with near vertical walls extending down through the ice. The exact shape is not critical to the present argument and this subject will not be pursued here.

At sufficiently long ranges, however, the situation permits a very simple approximation. Some friction induced melting occurs at the ice-bedrock interface of the valley

glacier. The presence of this water at the interface will cause a large dielectric contrast which will cause the interface to act as a good reflector. Very little power will flow across the interface and so the rock valley will behave like a waveguide in which the principal loss is due to the dissipative attenuation in the ice. Power injected into the ice will divide equally to flow longitudinally toward the toe and the headwall of the glacier. And successive surfaces of constant power density will simply be successive vertical cross-sections of the ice stream.

With this approximation, the power density caused by the 'downward' radiated power may be taken as:

$$P_d = \left[\frac{P_t (1 - U) G_t}{2 A_c} \right] \left[10^{-\left(\frac{A_s R}{10} \right)} \right] \quad (4.5)$$

where P_d is the power density, in watts per meter²

P_t is the total transmitted power, in watts

U is the fraction of the total transmitted power which is radiated 'upward'

G_t is the gain of the transmitting antenna in the direction defined by the receiver

A_c is the cross-sectional area of the ice stream, in meters²

A_s is the specific dissipative attenuation of the ice, in decibels per meter

R is the range from transmitter to receiver, in meters

Now, a small receiving antenna operated in the vicinity of the glacier-air interface will be coupled both to the 'upward' radiated signal propagating over the line-of-sight and to the 'downward' radiated signal propagating through the ice. In particular, a horizontal loop deployed on the surface of the glacier (as in the March 1970 field trials) will be operating right at the interface and so will be coupled about equally to the two signals.

In this situation, the apparent power density will be subject to localized disturbance as a result of the multipath interference effects which are of prime interest in this experiment; but the mean power density along the traverse will be simply the sum of the power densities appropriate for the line-of-sight and the subsurface propagation paths.

So the mean power density incident on a receiving antenna within the line-of-sight may be taken as:

$$\begin{aligned}
 P_r &= P_u + P_d \\
 &= \left[\frac{P_t U G_t}{2 \pi R^2} \right] + \left[\frac{P_t (1 - U) G_t}{2 A_c} \right] \left[\frac{-(0.1 A_s R)}{10} \right] \\
 &= \left(\frac{P_t G_t}{2} \right) \left\{ \left[\frac{U}{\pi R^2} \right] + \left[\frac{(1 - U)}{A_c} \right] \left[\frac{-(0.1 A_s R)}{10} \right] \right\} \quad (4.6)
 \end{aligned}$$

while the mean power density incident on an antenna beyond the line-of-sight will be that shown by (4.5) as due to the 'downward' radiated power alone.

Two major qualifications must be made to the preceeding assertion.

First, the term 'line-of-sight' should not be taken literally. The effective line-of-sight may be much shorter than the optical line-of-sight because of distortions of the 'upward' radiated power pattern caused by the proximity of the air-ice interface; or it may be much longer than the optical line-of-sight because of ground wave effects. This subject is worthy of investigation but will not be pursued here.

Second, when the distance between the transmitter and the receiver is very short, the relative effect of a wave reflected from the underlying bedrock will be very small because such a wave will suffer significant relative attenuation in the passage to and from the reflecting layer. In this situation, therefore, the mean received power may be taken, without much error, as that due to the line-of-sight propagation alone.

The second qualification has an important corollary. Any major perturbation in the field intensity observed at short range cannot be ascribed to reflections from a distant interface, but must be due to interaction between a wave propagating over the glacier surface and a wave propagating laterally just under the surface.

5. Parameter evaluation

In this section the physical properties of the glacier will be used to derive values for the parameters involved in the range equations. The principal quantities to be determined are the dissipative attenuation in the ice, the relevant dimensions of the glacier, and the effect of the major lobe in the subsurface radiation pattern.

5.1 Dissipative attenuation

A plane RF wave propagating wholly in a lossy medium can be represented as:

$$E(R) = E_0 e^{-jKR} \quad (5.1)$$

where R is the range measured from the radiating source

E_0 is the electric field amplitude at $R = 0$

K is the complex propagation constant

For a homogeneous, isotropic, linear, non-magnetic medium, the propagation constant may be written as:

$$\begin{aligned} K &= \omega \sqrt{\mu_0 (\epsilon' - j\epsilon'')} \\ &= \omega \sqrt{\mu_0 \epsilon' (1 - j \frac{\epsilon''}{\epsilon'})} \\ &= \omega \sqrt{\mu_0 \epsilon'} - j \frac{\omega \sqrt{\mu_0 \epsilon'}}{2} \left(\frac{\epsilon''}{\epsilon'} \right) \quad \{\epsilon'' \ll \epsilon'\} \\ &= \omega \sqrt{\mu_0 \epsilon_0 k} - j \frac{\omega \sqrt{\mu_0 \epsilon_0 k}}{2} \left(\frac{\epsilon''}{\epsilon'} \right) \\ &= \frac{2\pi}{\lambda} \sqrt{k} - j \frac{\pi}{\lambda} \sqrt{k} \tan \delta \end{aligned} \quad (5.2)$$

where k is the dielectric constant of the medium

λ is the free space wavelength

$\tan \delta$ is the loss tangent of the medium, defined as the ratio of the energy dissipated to the energy stored per cycle, or, equivalently, as the ratio of the imaginary to the real part of the complex permittivity.

Substituting (5.2) in (5.1), the propagating electric field is:

$$E(R) = E_0 e^{-\frac{\pi \sqrt{k} \tan \delta R}{\lambda}} e^{-j \frac{2\pi \sqrt{k} R}{\lambda}}$$

The dissipative attenuation at a particular distance R is:

$$\begin{aligned} \alpha(R) &= \frac{|E(0)|}{|E(R)|} \\ &= e^{\left(\frac{\pi \sqrt{k} \tan \delta R}{\lambda}\right)} \end{aligned}$$

Or, expressing the attenuation in decibels, the dissipative attenuation is:

$$\begin{aligned} A &= 20 \log_{10} [\alpha(R)] \\ &= 20 \log_{10} \left[e^{\frac{\pi \sqrt{k} \tan \delta R}{\lambda}} \right] \\ &= 20 \left[\log_{10} (e^{\pi}) \right] \left(\frac{\sqrt{k} \tan \delta R}{\lambda} \right) \\ &= 27.26 \left(\frac{\sqrt{k} \tan \delta R}{\lambda} \right) \text{ dB} \end{aligned} \tag{5.3}$$

According to the hypotheses listed earlier:

$$\sqrt{k} = \sqrt{3.2} = 1.79$$

$$\tan \delta = \frac{\lambda}{1200 \text{ meters}}$$

Substituting these values in (5.3), the specific dissipative attenuation in the glacial ice is:

$$A_s = 27.26 \frac{1.79}{1200} = 0.04 \text{ dB/meter} \quad (5.4)$$

5.2 Glacier dimensions

A sketch map of the portion of the glacier used for the March 1970 traverses has been shown previously as Figure 4-1.

The ice depth varies monotonically and fairly linearly from about 130 meters underneath the transmitter site to about 150 meters at a range of 200 meters. So, in this range regime the average ice depth is:

$$D = (130 + 150)/2 = 140 \text{ meters} \quad (5.5)$$

This result will be used later.

From a range of 200 meters to a range of 1000 meters the ice depth varies fairly linearly from about 150 meters to about 230 meters. The surface width is about 1000 meters but the sides of the valley slope significantly, and there is a ledge at one side of the glacier, so the average width of the ice in this range regime is about 600 meters. For the region of interest, then, the average cross-sectional area of the ice is:

$$A_c = 600 (150 + 230)/2 = 1.1 \cdot 10^5 \text{ meters}^2 \quad (5.6)$$

Parenthetically, it should be noted that the area to be used when evaluating the far range equation of (4.5) should include the range dependence implied above. However, in the situation considered here, the effect of this range dependence is very much smaller than the effect of the dissipative attenuation, so without significant error the area may be taken as a constant having the value given by (5.6) above.

5.3 Subsurface radiation lobe

According to (4.2), the subsurface radiation pattern will exhibit a significant lobe at a tilt angle given by:

$$\sin \beta = \sqrt{\frac{k_o}{k_i}}$$

And, according to the hypotheses listed earlier:

$$k_i = 3.2$$

So the tilt angle is:

$$\beta = \sin^{-1} \sqrt{\frac{1}{3.2}} = \sin^{-1} 0.56 = 34^\circ \quad (5.7)$$

According to (4.3), this lobe will have a maximum effect on the power density observed at the surface of the glacier at a range of:

$$R = 2 D \tan \beta$$

Substituting values in accordance with (5.5) and (5.7), the maximum effect will occur at a range of:

$$R = 2 \cdot 140 \tan 34^\circ \approx 190 \text{ meters} \quad (5.8)$$

5.4 Effect of subsurface geometry at medium range

The attenuation suffered by a wave reaching the receiver after one reflection is proportional to the path length which, according to (4.4), is given by:

$$L = \sqrt{R^2 + 4 D^2}$$

Substituting values in accordance with (5.4) and (5.5) yields the following tabulation which shows the signal power received at various ranges relative to that received at a range of 300 meters.

Range (meters)	Path length (meters)	Relative signal (dB)
150	320	+ 3.7
200	346	+ 2.6
250	378	+ 1.4
300	412	Reference

According to this tabulation, the effect of a singly reflected wave will increase by about 3.7 dB as the separation between receiver and transmitter is reduced from 300 to 150 meters.

It should be noted that this is an upper bound. The actual signal increase will be less than 3.7 dB because the vertical minimum in the subsurface radiation pattern will cause an offsetting decrease in the magnitude of the signal as the range is decreased below the critical value defined by (5.8). As a practical approximation, therefore, it may be assumed that this signal component will remain sensibly constant at ranges less than that defined by (5.8).

6. Comparison with empirical data

Rossiter has compiled an extensive set of data smoothed by a three point averaging procedure. The data to be used here is abstracted from his set of curves.

In particular, using his cataloging system, the data used here is the field intensity of the H_z component as measured in traverses 1, 3, 8, and 17 at frequencies of 2, 4, 8, and 24 MHz respectively.

One important adjustment is made. The field intensity data taken from Rossiter's curves is scaled in accordance with the following table:

Traverse	Frequency	Field intensity multiplied by
1	2	1.0
3	4	2.4
8	8	0.64
17	24	4.0

These scale factors were selected on the basis of a preliminary iterative curve fitting procedure. They can be defended by the following rationale. ~~First, the reflectometer~~ system used to measure transmitter output during the March trials was shown in the September glacier trials to give inconsistent and grossly erroneous readings because of cable problems, so there is no valid reason to accept the power normalization used by Rossiter. Second, these scale factors are well within the range that could be ascribed to differing antenna coupling and radiation efficiencies. Third, these factors yield a cohesive set of data with no anomalous discontinuities.

The selected, and adjusted, data is shown as Figure 6-1.

Superposed on the data are three best-fit lines which are in accord with the near range equation of (4.1), the comments of section 5.4, and the far range equation of (4.5). It is apparent that these yield a plausible fit at ranges of less than 100 meters, from 100 to 300 meters, and more than 300 meters, respectively.

This good fit provides powerful confirmation that the heuristic arguments developed earlier properly describe the fundamental mechanisms involved.

Another significant effect may be seen in the data of Figure 6-1. According to the arguments developed earlier, perturbations occurring at short range may be attributed to interaction between a wave propagating over the surface and one propagating just below the surface. At 24 Mhz the phase retardation in free space is:

$$\phi = \frac{2\pi}{\lambda} \approx \frac{360}{12.5} = 28.8 \text{ degrees/meter}$$

In a medium having a dielectric constant of 3.2, the phase retardation is:

$$\phi = \frac{2\pi}{\lambda} \sqrt{k} \approx \frac{360 \sqrt{3.2}}{12.5} = 51.5 \text{ degrees/meter}$$

Two parallel propagating waves would add constructively at intervals where the relative phase difference becomes an integer multiple of 2π . In the present situation, this would imply constructive addition at intervals of:

$$\Delta R = \frac{360}{51.5 - 28.8} = \frac{360}{22.7} = 15.8 \text{ meters}$$

The data of Figure 6-1 shows pronounced peaks at 45, 60, 75, and 90 meters which are in good agreement with this postulated value.

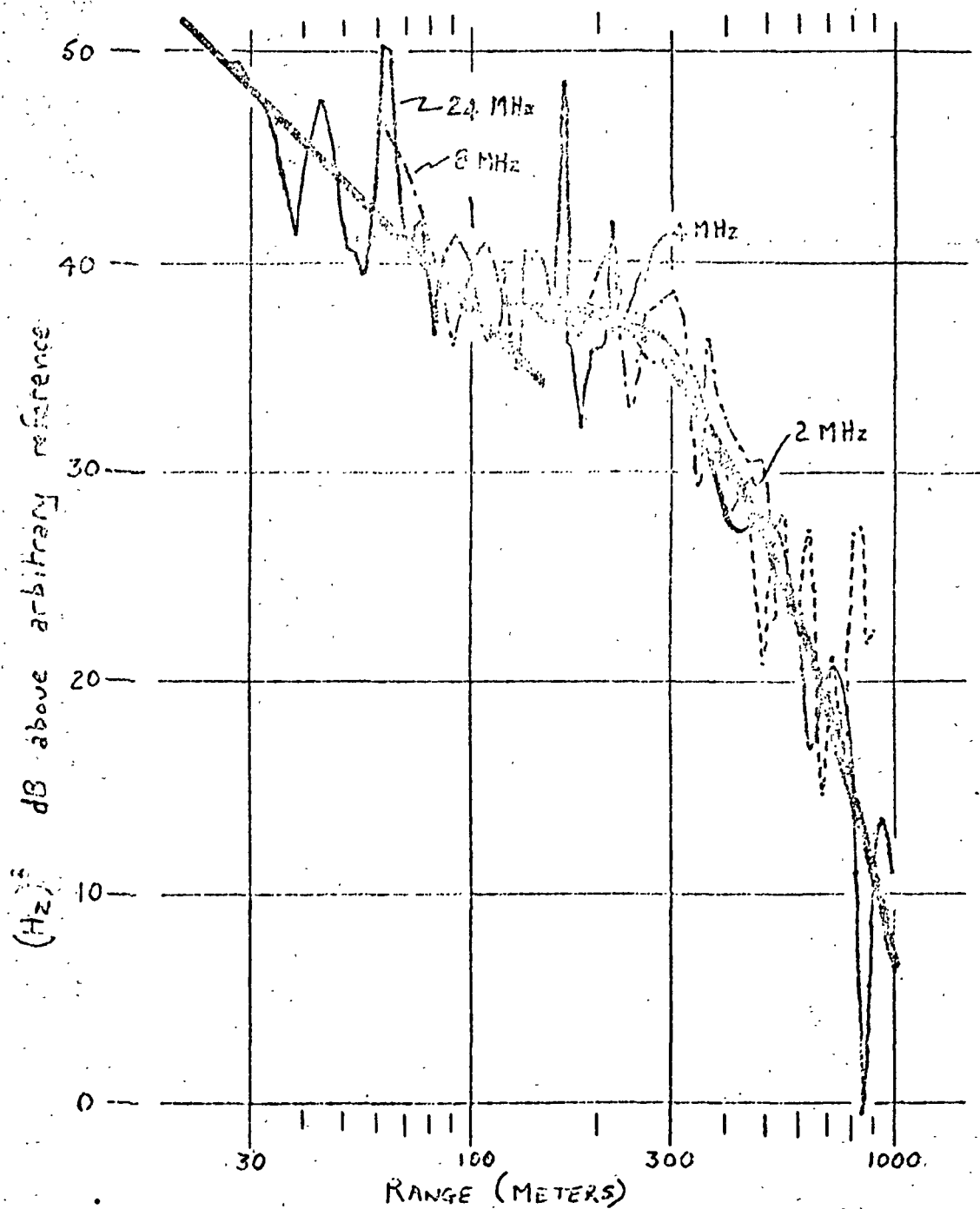


FIGURE 6-1 EMPIRICAL DATA AND POSTULATED FUNCTIONS

The fraction of the total transmitted power which is apparently radiated 'upward' can be evaluated by considering the ratio of the powers received at two widely separated ranges. From the functions fitted to the data of Figure 6-1:

$$P_r(10 \text{ meters}) = 1.35 \cdot 10^4 \cdot P_r(1000 \text{ meters})$$

Comparing the near range and far range equations of (4.1) and (4.5) yields:

$$\frac{U}{\pi R_1^2} = 1.35 \cdot 10^4 \cdot \frac{(1 - U)}{A_c} \cdot 10^{-(0.1 A_s R_2)}$$

or, substituting previously derived values:

$$\frac{U}{\pi 10^2} = 1.35 \cdot 10^4 \cdot \frac{(1 - U)}{1.1 \cdot 10^5} \cdot 10^{-(0.1 \cdot 0.04 \cdot 1000)}$$

which yields:

$$U = 0.004$$

It should be noted that this fraction does not purport to show the relative fraction of the total power that is radiated 'upward'. Considering the radiation pattern and geometry shown previously by Figures 4-2 and 4-3, it may be seen that the far range evaluation provides a good measure of the total power radiated 'downward' and propagating by multiple reflections along the ice channel, but the near range evaluation measures only the limited power radiated in the minimum of the radiation pattern existing just above the interface.

7. Review

The heuristic arguments presented here and the empirical data available from the March 1970 Athabasca glacier trials show good agreement.

Some salient features may be noted:

- (1) The propagating mechanism is independent of frequency, subject only to a power normalizing adjustment;
- (2) An apparent line-of-sight exists to a range of about 100 meters;
- (3) Perturbations in the short range data are compatible with a dielectric constant of 3.2 for the glacial ice;
- (4) The character of the mid-range data is compatible with an ice depth of 150 meters;
- (5) Perturbations in the long range data are the result of multiple reflections and scattering and cannot be interpreted unambiguously;
- (6) Attenuation of the long range data is compatible with a loss tangent that is inversely proportional to frequency and has a value of 0.25 at 1 MHz.

8. Recommendations

The theory developed here extends previous explanatory models to include the effect of a finite line-of-sight and the effect of geometry related deviations from the simplistic half-space assumed in prior analyses.

An important consequence of this theory is that the depth to a reflecting interface can be measured only in the mid range regime. At short ranges, the line-of-sight signal obscures the reflected signal; at long ranges, any physically plausible geometry which is likely to be encountered will cause multiple reflections which will make the data ambiguous.

It follows that the lunar experiment should be designed to optimize the mid range performance: in particular, 4 MHz must be reinstated in the list of experiment frequencies.

It follows also that the effective line-of-sight must be restricted as much as possible: it is very important that the transmitting antenna lie flat on the lunar surface and the receiving antenna should be mounted as low as possible on the LRV, preferably underneath the vehicle. Continued theoretical and experimental work is required to define the extent to which the placement of the antennas can depart from the intimate contact used in these glacier trials without reducing the validity of the experiment.

It follows, also, that the transmitting antenna must be held to the smallest possible dimensions so that there is an adequate range interval between the near field of the antenna and the end of the line-of-sight so as to permit a good measure of the dielectric constant of the medium.

APPENDIX 5.1

CHARLES STARK DRAPER LABORATORY
CONCEPTUAL DESIGN REPORT JULY 21, 1970

SURFACE ELECTRICAL
PROPERTIES EXPERIMENT

PRELIMINARY

JUL 21 1970

- 0. Tape Recorder ✓
- 0.1 Requirements ✓
- 0.2 Proposed Recorder ✓
- 0.3 Operation ✓
- 0.4 Data Retrieval ✓
- 0.5 Preflight and Postflight ✓
- 0.6 Modifications ✓
- 1.0 Envelope Description ✓
- 1.1 Transmitter Mechanical ✓
- 1.2 Receiver Mechanical ✓
- 1.3 Stowed Configuration ✓
- 2.0 Deployment ✓
- 2.1 Calibration ✓
- 2.2 Operation ✓
- 2.3 Time Estimate for Deployment by One Astronaut ✓
- 3.0 Thermal
- 3.1 Transmitter
- 3.2 Receiver

4.0 Weight Estimates ✓

4.1 Transmitter ✓

4.2 Receiver ✓

4.3 Totals ✓

5.0 Power Requirements ✓

5.1 Transmitter Power ✓

5.2 Receiver Power ✓

5.2.1 Example

6.0 Required Equipment ✓

6.1 Ground Support Equipment ✓

0. Tape Recorder

0.1 Requirements

A typical late Apollo mission could involve three EVA's, each of six-hour duration, with traverses lasting five or more hours. To allow the receiver to run without attention, for two traverses, ten hours of recording time would be highly desirable.

For this application, power consumption and operating time directly affect battery weight. Since a relatively long operating time is desired, power consumption should be small.

Additionally the recorder should be small and light-weight, it should contain enough tape so that tapes need not be changed, and should be sealed to maintain a proper environment for its mechanical parts and lubricants.

0.2 Proposed Recorder

The tape recorder proposed for the receiver is the Leach 11-14000 Data Storage Electronics Assembly (DSEA). This unit was designed as a voice recorder for use aboard the LM, and has been qualified for use in the LM and for return to earth in the CM cabin environment. The unit is used in the Lunar Module to record voice-keyed audio with superimposed time information. A reference frequency is recorded for operating the speed-control servo in the reproduce transport. Specifications for this recorder are:

Size: 6.22 x 2.05 x 4.0 in.

Weight: 2.3 lb.

Power: 2.4 watts at 115v, 400Hz, or 26v, 400Hz.*

Channels: One. (The DSEA uses 4 tracks with track switching to realize the recording time.)

Recording Time: 10 hours.

Tape Speed: 0.6 inches per second.

Tape: 450 ft. of 1/4 inch, 1/2 mil tape.

Frequency Response: 300Hz to 5.2KHz, with audio compressed into 300Hz to 3KHz, a time-code modulated FM carrier at 4.4KHz \pm 5%, and a reference at 5.2KHz.

Signal to Noise Ratio: 35dB.

Operational Environment: Temperature: 0° to 160°F.

Pressure: Atmospheric to hard vacuum.

Acceleration: 15g

Random Vibration: 9g rms for 3% p-p flutter

Shock: 52g for 11ms, 1/2-sine shock (survival only)

Non-operational Temperature: -20°F to 160°F

Start Time: 50 msec

Track Switching and Reversal Time: 100 msec

Life: 5000 hrs.

Storage: 5 years, provided recorder is operated once every 120 days for a minimum of one minute.

Survival Probability for 10-hr. mission: 0.9998

The DSEA also meets salt spray and sand and dust requirements.

* See 0.6, Modifications

0.3 Operation

Once loaded and initialized for operation, the DSEA operates automatically for up to 10 hours, with track switching and tape motion reversal accomplished by logic circuitry using latching relays. Track switching at the end of each of the 2.5 hour passes occurs in less than 100 milliseconds. The latching relays provide a memory function and ensure that recording will resume on the same track in the same direction after a power interruption so that no special attention need be given the tape unit before or after the shut-down between traverses.

The voice-operated-keying (VOX) feature of the DSEA will not be required in this application, and will be wired out.

An indication of recorder operation is given by a tape motion amplifier which provides a relay closure when signals are sensed on the tape in the range of 300Hz to 3KHz; this signal may be used to drive a go/no-go indicator, since the VCO will continuously supply a signal to the recorder regardless of the received signal strength.

0.4 Data Retrieval

Following the final traverse, the recorder is removed from the receiver package and returned to earth. No attempt at handling the tape magazine need be made and the seal need not be opened, alleviating the problems of dust and mishandling. The weight of the recorder is small (2.3 lb.) and the recorder itself serves as a protective carrying case for the return trip. This procedure is essentially the same as that used to return the LM's DSEA, and experience has indicated that the tape is suitably protected by the recorder.

1.0 Envelope Description

The experiment package consists of two assemblies, a transmitter (assembly I) and a receiver (assembly II). Before deployment the transmitter assembly contains the transmitting antennas on four reels, and the receiver assembly contains the receiving loops folded in a flat configuration. The transmitter is to be deployed a short distance from the LM and the receiver may be mounted on the Mobile Equipment Transport, on the Lunar Roving Vehicle, or may be hand carried for a walking traverse.

1.1 Transmitter Mechanical

The transmitter assembly, Fig. 1.1, contains the transmitter electronics, the antennas reels, and a solar panel for a power source. The transmitter case is a cylinder of 6-inch diameter mounted on a 9x9 inch base which serves as a protective cover for the solar panel before deployment and as a foot for the assembly after deployment.

The four elements of the transmitting antennas mount on four reels stowed around the transmitter. Each reel measures 6.25 in ID, 8.5 in OD, and 1 inch thick, and weighs less than 1/3-lb without wire; the weight of the wire and insulation on one reel is estimated to be 0.7 lbs. Handling of the reels may be done using a universal handling tool or a special tool may be supplied to interface conveniently with the reel hubs.

The solar panel provides continuous power to the transmitter and also serves as a sun screen for the transmitter's radiating (top) surface. The panel measures 9x9 inches and weighs approximately 1 lb with its fixtures.

Essentially all the volume in the transmitter case is allotted for the transmitter electronics. The interior dimensions, after thermal blanketing, are 5.5 dia x 4.5 in high or 107 in³.

0.5 Preflight and Postflight

The DSEA is intended for use as a recorder only, although a monitoring signal is available for each tape track. Playback after recording is done with a reproduce transport in a test set provided by the manufacturer; Leach, NASA/MSD and KSC have playback equipment for the DSEA as configured for the LM, so it is obviously desirable to maintain interface compatibility.

The DSEA is tested by recording a test tape magazine for playback in the reproduce transport. Following test, a clean tape magazine is installed, the head shield realigned and the DSEA is sealed using a fresh O-Ring and a coat of sealant. A "reset" pulse is applied to set the control logic to track 1 forward (this need be done only on the ground) to prepare the recorder for operation. After the fourth pass is completed the DSEA will stop until another reset is applied, thus preventing overwriting of data.

0.6 Modifications

The DSEA will work in this application with minimal modification; indeed it will operate satisfactorily with no modification at all, although a few simple changes are desirable.

Since playback equipment for the DSEA is available, no modification should be made that will require changing it. This implies that the servo reference signal should be left at 5.2KHz, and the input frequency response should be left at 300KHz. The time code carrier is not needed for this experiment, but could be put to use to indicate the beginnings of major receiver cycles.

The following minor modifications to the DSEA would be worthwhile:

1. Permitting 26-volt operation by bringing two leads from the motor winding to spare pins on the connector.

2. Carry leads from the VOX circuit to the connector to permit disabling by a jumper wire.
3. Make provision for driving the 5.2KHz reference externally.

The above modifications can be made without affecting existing interfaces to the GSE and LM.

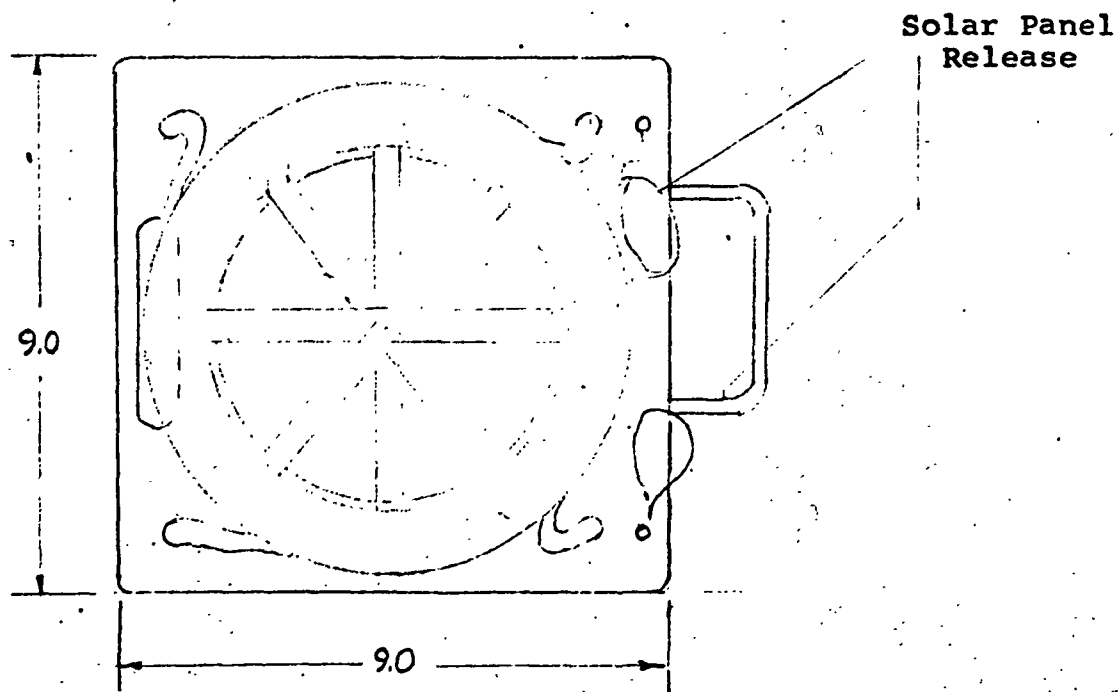
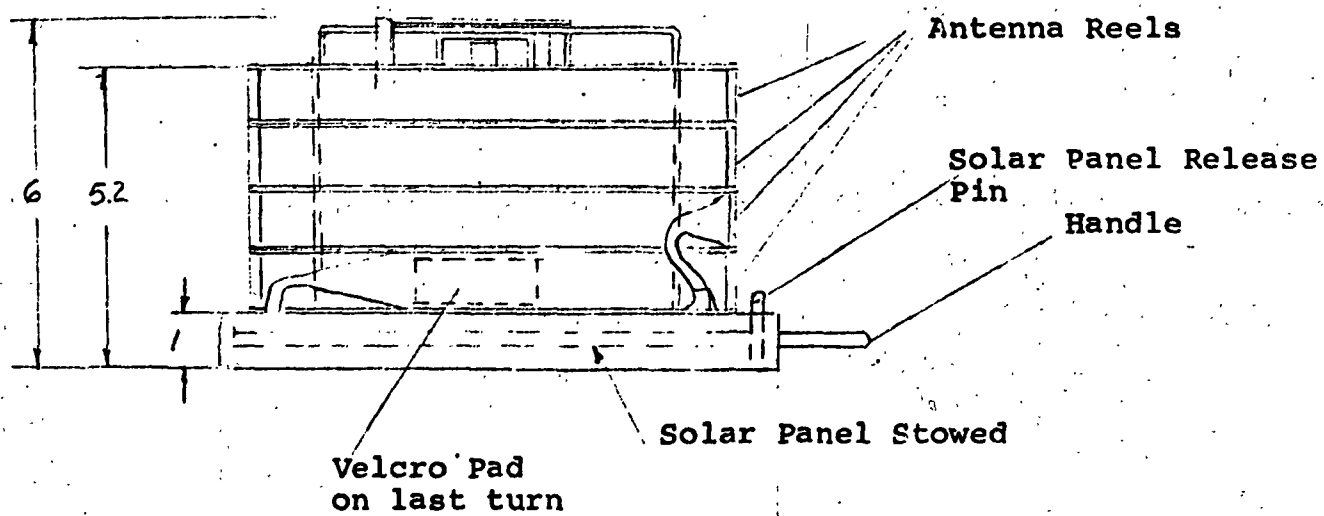
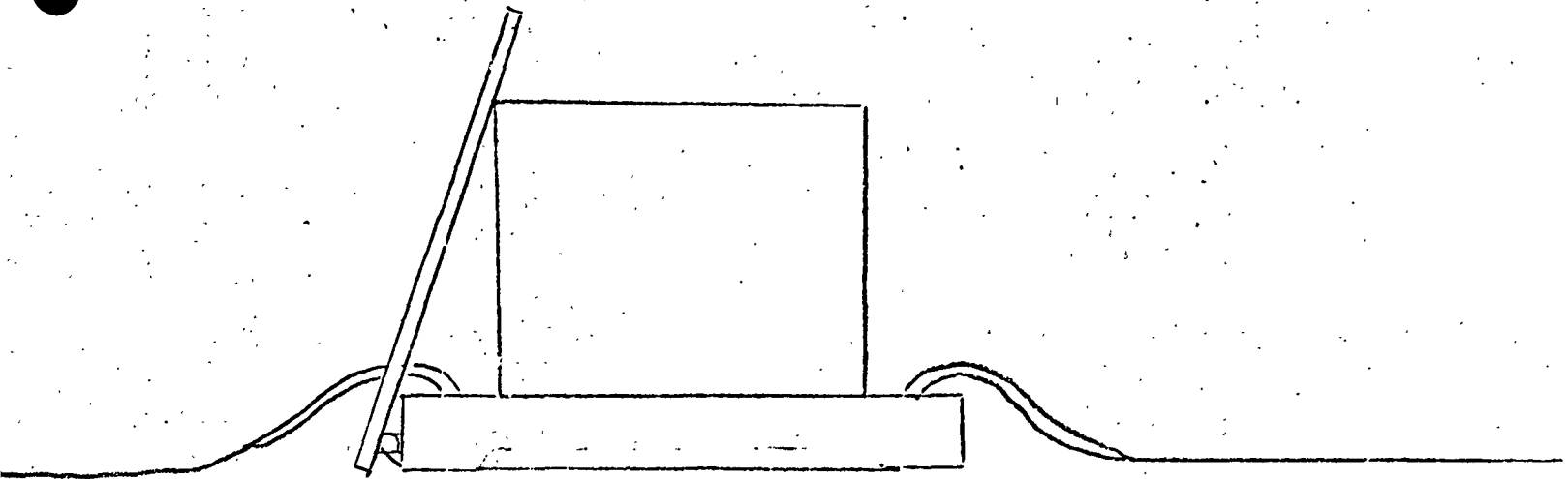
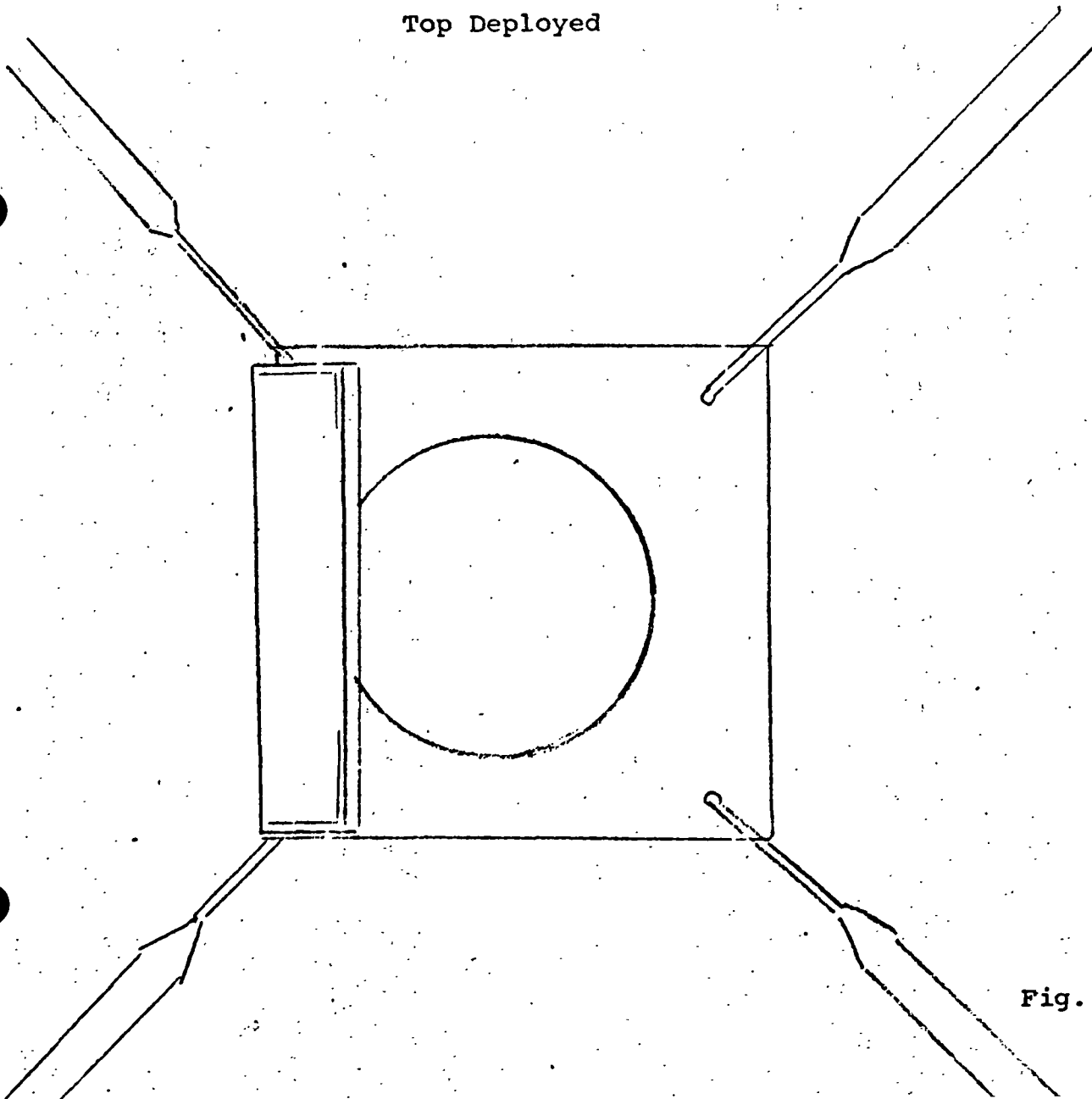


Fig. 1.1.1 Transmitter Stowed

Side Deployed



Top Deployed



1.2 Receiver Mechanical

The major features of the receiver assembly (Fig. 1.2) are the case (a), containing the electronics, tape recorder, and batteries, the antenna assembly (b), and an extendable mast (c) for Rover use. The antennas and mast will be sufficiently strong to permit handling of the package by the antennas.

The space remaining in the receiver case after the thermal blanketing is $4.5 \times 8 \times 8$ in. (256 in^3). The allocation of this volume is as follows:

Recorder with interconnect block: $2.1 \times 5 \times 7$ (73.5 in^3)

Energy source (Silver-Zinc battery): $2 \times 4 \times 7$ (56 in^3)
and power conditioning

Receiver Electronics: $2 \times 5 \times 7$ (70 in^3)

The arrangement of subassemblies within the case is shown in Fig. 1.3. A central web serves as the medium for conducting heat from the subassemblies to the heat switch. The tape recorder is mounted by means of slide fasteners, and is released after the last traverse by opening a door and pulling a lanyard. The recorder is removed in the direction shown.

A three-position lever-type control and an indicator are located on the side of the receiver case (mounting on the top of the case would increase the possibility of contaminating the radiator with dust). Position 1 of the control (Fig. 1.2) turns the receiver off; position 2 places the receiver in the semi-active thermal control mode between traverses, and position 3 turns the receiver on. When the receiver is on, the indicator is illuminated when there is satisfactory output from the tape motion sensor and a measurable receiver signal. When the receiver is placed in

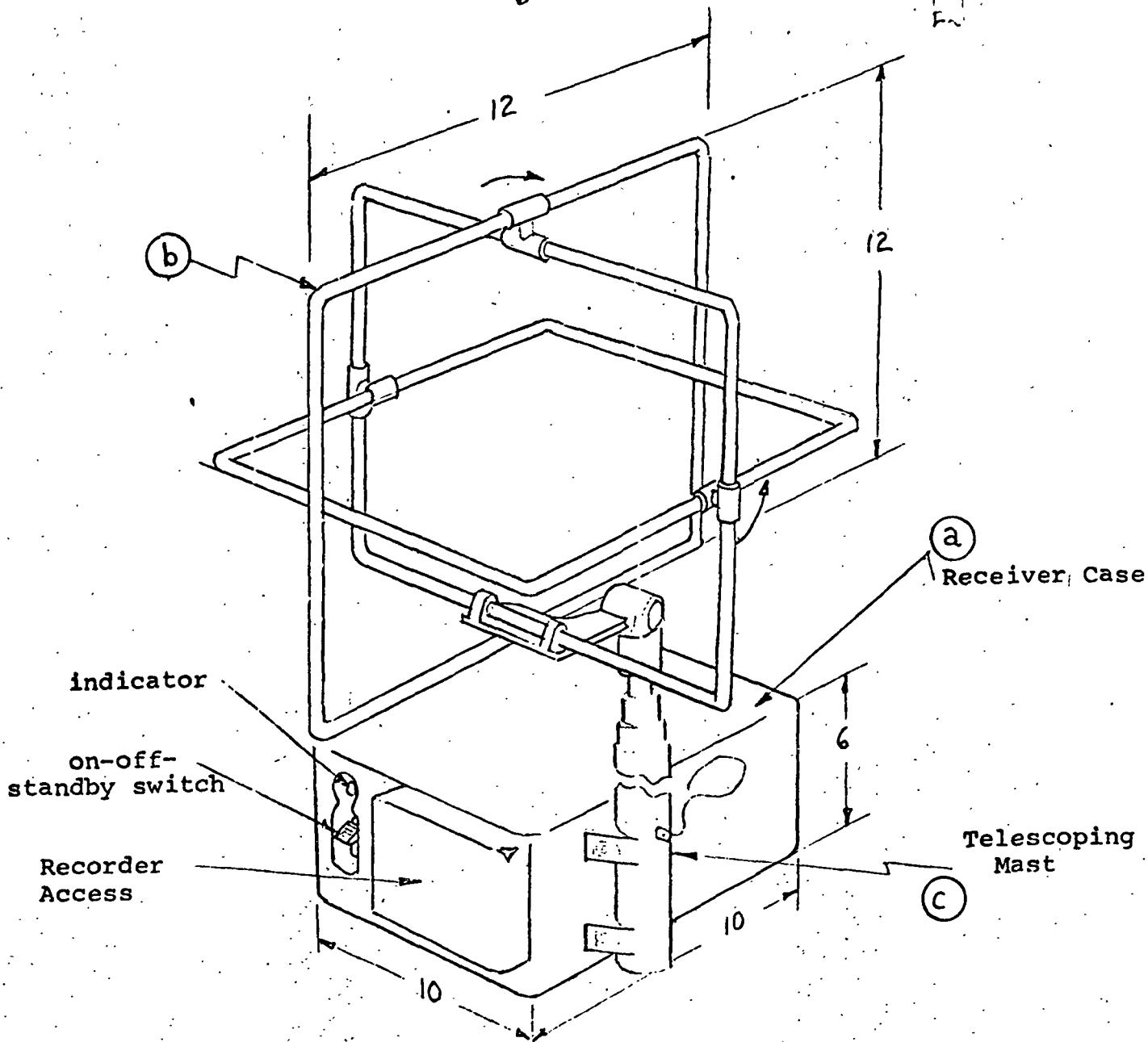
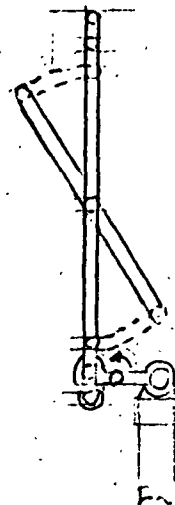
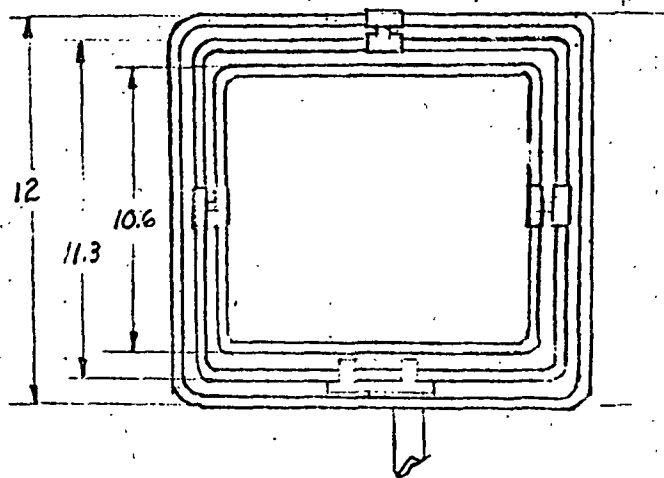


Fig. Receiver

RECEIVER, STOWED

SIDE

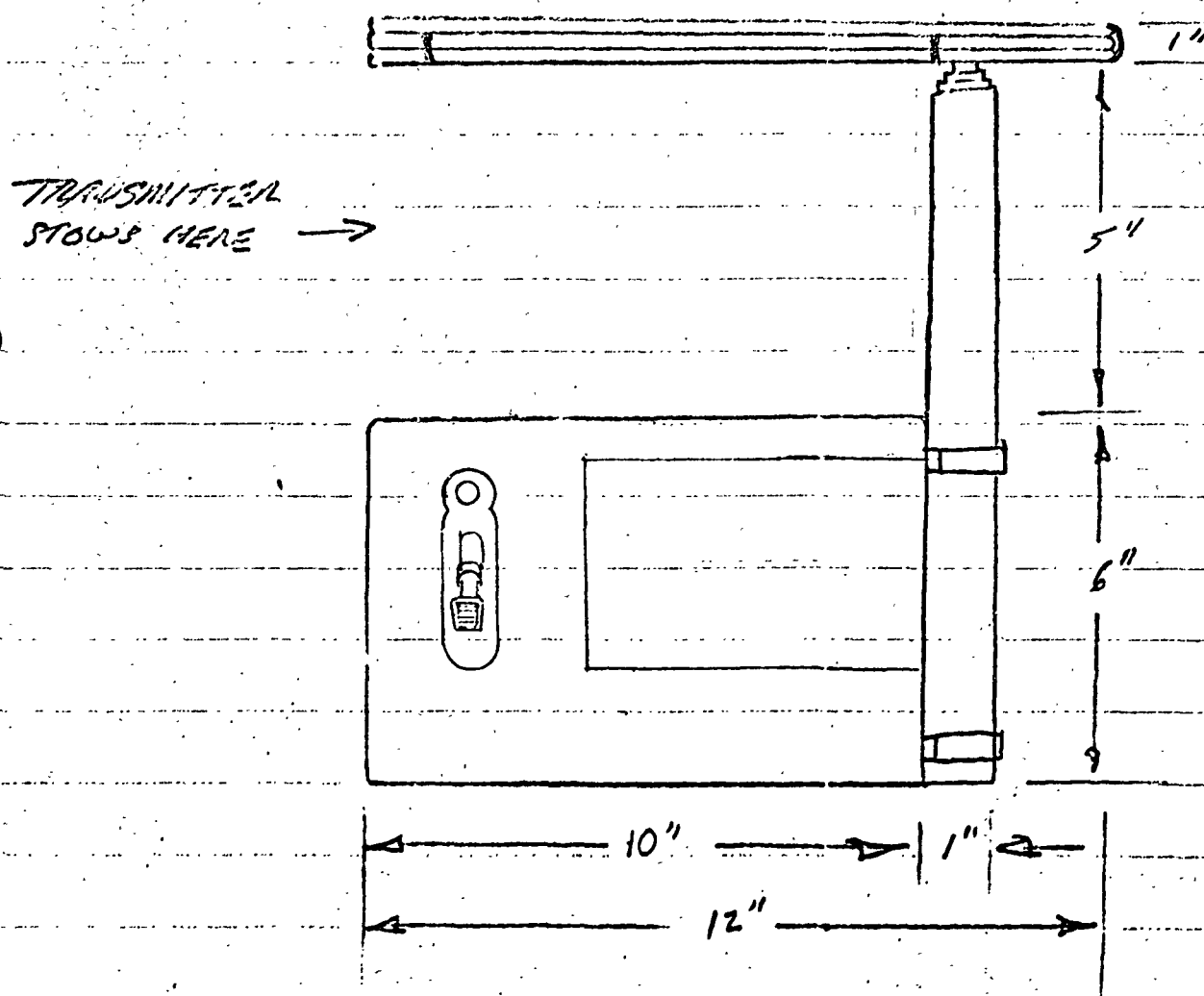


Fig. 1.2 Cont'd.

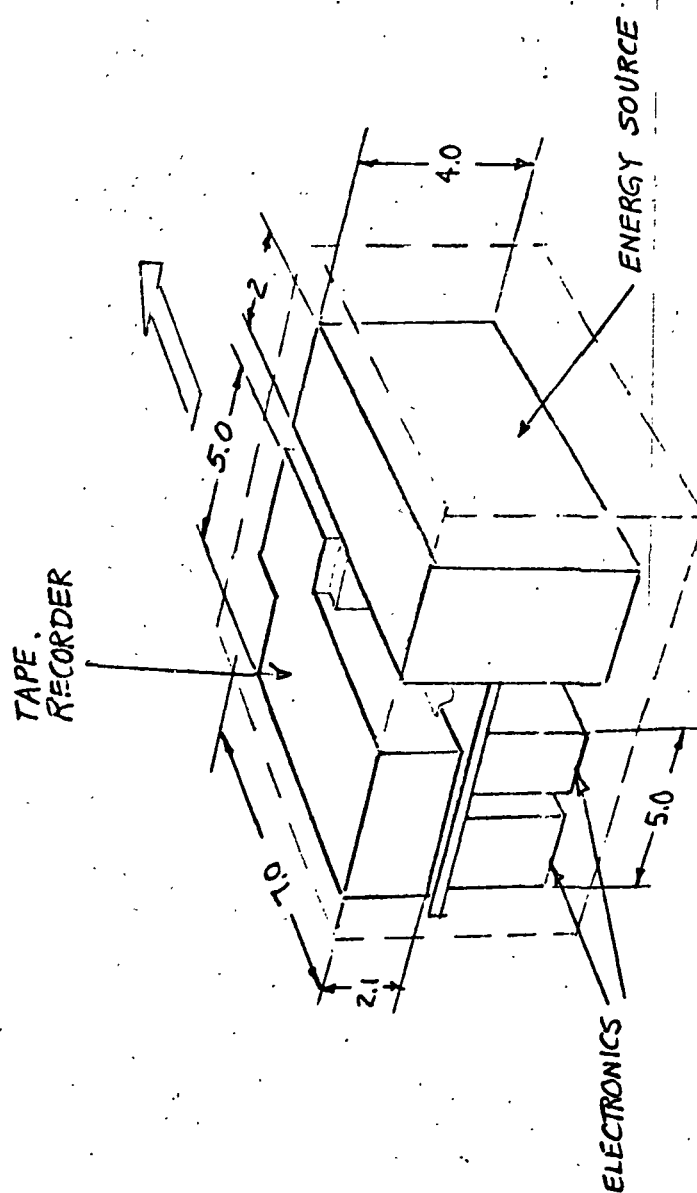


Fig. 1.3 Receiver Electronic Subassemblies

the semi-active thermal control mode, the indicator remains lit for several seconds after the switch is thrown, and then is extinguished; and when the receiver is shut off, the indicator goes off immediately.

1.3 Stowed Configuration

In the stowed configuration, the complete package occupies a volume of less than 1.0 ft³. The transmitting antennas occupy four reels, the receiving loops are folded flat, and the solar panel for the transmitter is stowed beneath the transmitter foot. The solar panel and the radiating surfaces for both the transmitter and receiver are covered by protective sheets until deployment is complete to prevent dust contamination.

2.0 Deployment

The stowed assembly is taken from the LM descent stage and carried approximately 200m from the LM. The transmitter is released from the package by a lanyard pull, the covered solar panel is unfolded and the transmitter assembly placed so that the solar panel is facing in the general direction of the sun. The topmost antenna reel is lifted from the transmitter by the handling tool and carried in a straight line for 35m. The antenna wire will be color coded near the end to prevent overstress when the reel is fully unwound. The reel is placed hub down on the surface and may be anchored by stepping on it. This procedure is repeated for the other three antenna sections.

The astronaut then returns to the transmitter, and removes the protective covering on the transmitter radiator surface and solar panel. After verifying that the solar panel is aimed properly (within approximately 15° of a horizontal line to the sun and aimed approximately 10° above horizontal), the receiving loops are unfolded, the mast is extended, and the protective cover removed from the radiator.

The receiver is then turned on and its operation verified by observing the indicator. The astronaut should indicate when the receiver is turned on over the voice link.

2.1 Calibration

The receiver is then carried along one leg of the antenna, and pauses are made at several points indicated by markings on the antenna. The receiver is then placed in the thermal-control mode until the first traverse.

2.2 Operation

Following the calibration, the receiver is mounted in the MET or on the LRV. When the first traverse is to be made, the receiver is turned on and left on until the traverse is complete. Again, for data correlation purposes, the astronaut should indicate, by voice, the time at which the receiver is turned on. Following the traverse, the receiver is returned to the thermal-control mode.

The above procedure is repeated for each traverse but the last. Following the final traverse, the receiver is turned off and the tape recorder is removed for return to earth.

2.3 Time Estimate for Deployment by One Astronaut

a. Deployment

Remove equipment from Descent Stage	60 sec
Carry to deployment site (200m @ 0.8m/sec)	250 sec
Separate package and set up transmitter	120 sec
Deploy antennas (see Fig. 2.1)	
230m @ 0.8m/sec	350 sec
Remove transmitter dust covers	60 sec
Extend receiver mast, remove dust cover, and turn on. Indicate over voice link	60 sec
Verify receiver operation	60 sec
Carry receiver for calibration (35m @ 0.5m/sec + 10 stops @ 10 sec)	170 sec
Set receiver to standby mode	30 sec
Return receiver to vicinity of LM, LRV or MET	250 sec
Install receiver on LRV or MET	120 sec
	<hr/>
	1530 sec =
	25.5 min.

b. Other activities

Turn receiver on or off at beginning 30 sec
or end of traverse

Remove tape recorder at the end of last 180 sec
traverse

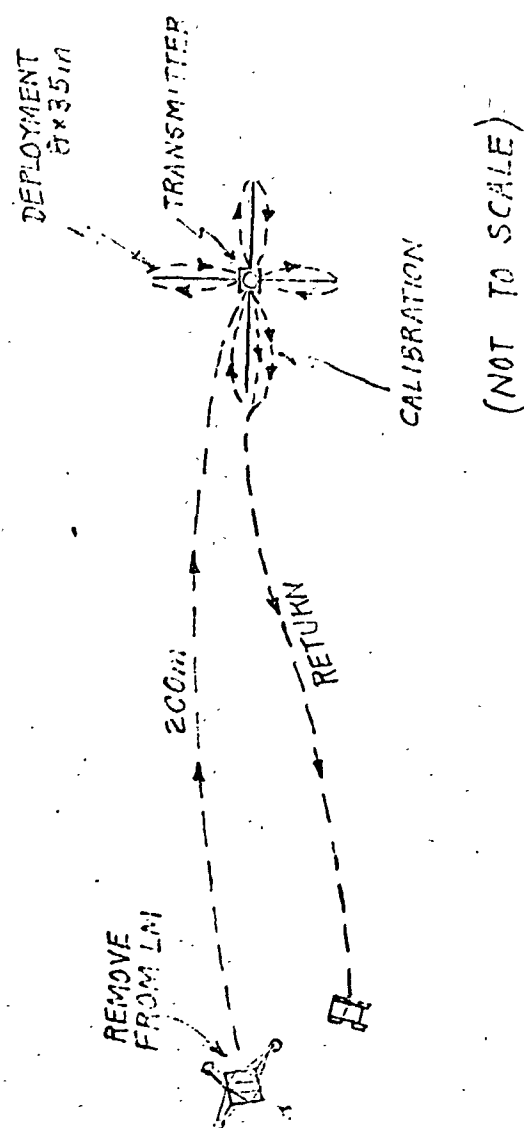


Fig. 2.1 Deployment, Plan View

3.0 Thermal

In writing a heat balance equation for an object on the lunar surface we must consider the following:

1. Heat generated in a piece of equipment.
2. Heat absorbed by direct radiation from the sun.
3. Heat absorbed from reflected radiation from lunar surface.
4. Heat absorbed from IR radiation from lunar surface.
5. Heat conducted to or from lunar surface.
6. Heat transferred to or from man-placed objects on lunar surface.
7. Heat loss from object by radiation.

The surface temperature of the moon varies between 90° and 310°K for a sun angle variation from 0 to 25° . Since the amount of heat transferred to an object by IR from the moon's surface can be quite high and is obviously a large variable, the thermal control problem can be reduced if the equipment can be insulated from this effect. This could be done by applying insulation to the bottom and sides of the equipment.

Although epoxy-glass legs have been used in the past to reduce heat transfer to or from the equipment, this is not felt necessary because of the very poor thermal conductivity of the lunar surface material.

Since we have insulated all equipment surfaces but the top, it is this surface that we will examine in detail.

3.1 Transmitter

We will look at the transmitter first. Although we have a sun shield on this surface (the solar panel) we will look at two extreme cases which will neglect the shield. The first case is for 0° sun angle and the second case is for the 25° sun angle. We will assume a 5-watt dissipation in the transmitter and that the top surface is painted with an 8-mil thickness of S13-G paint which has an absorption, α of .20 for sunlight and an emissivity, ϵ of .87 for IR. The surface area is .01825 meters². The heat balance equation is:

$$\epsilon A \sigma T^4 = Q + \alpha A S \sin \phi$$

$$(.87)(.01825)(5.675 \times 10^{-8})T^4 = 5 + (.20)(.01825)1375 \sin \phi$$

$$\text{For } \phi = 0^\circ \quad T = 273^\circ\text{K or } 0^\circ\text{C}$$

$$\text{For } \phi = 25^\circ \quad T = 298^\circ\text{K or } 25^\circ\text{C}$$

If α increases to .50 because of dust contaminating the heat transfer surface, then:

$$\text{For } \phi = 25^\circ \quad T = 327^\circ\text{K} = 54^\circ\text{C}$$

$$\alpha = .5$$

This range of temperatures is reasonable for the heat sink surface. However, some important effects have not yet been taken into account.

1. At what temperature will the electronics stabilize during deployment before the solar cells can supply power to the heater or transmitter?
2. Is there any problem during stowage on the way to the moon if the top surface sees mostly space?
3. What thermal effect can be expected due to thermal paths through antenna wires, power wires, switch,

and indicator light wires? Also what effect will conductive paths between the radiating surface and the rest of the case have?

The first two problems above may be solved by providing a temporary thermal blanket and dust shield over the top surface which can be removed at the time the transmitter or heaters are turned on.

At the 25° sun angle the antennas and other wires will be cooler than the 50°C calculated for a dirty radiating surface and therefore tend to lower the temperature of the transmitter as desired. At the 0° sun angle these wires may be as cold as 100°K. We should calculate the thermal effect to see that the transmitter will not be cooled too much under these conditions. We will assume 30 number 25 gage copper wires conducting heat to the outside with a $\frac{\Delta T}{\Delta x}$ of 20°C per cm. It is felt that this figure of 20°C can easily be maintained by proper design. The thermal balance is then

$$\epsilon A \sigma T^4 + K A_c \frac{\Delta T}{\Delta x} = 5$$

$$(.87)(.01825)(5.675 \times 10^{-8})T^4 + 3.8(.039)(20) = 5$$

$$T^4 = 22.5 \times 10^8$$

$$T = 218^\circ\text{K or } -55^\circ\text{C}$$

It is apparent that these losses are very significant and will have to be reduced either by thermally insulating the cable for some distance (~ 1 foot) or reducing the number and/or size of wires used.

The conductive paths between the radiating surface and the rest of the case can be minimized by proper insulation and materials selection.

3.2 Receiver

The receiver poses a different problem in that its orientation is not fixed; it may or may not be shaded; it will be turned off for periods of time, and since it is battery powered, a high-powered heater cannot be used for thermal control. Also, the tape recorder and batteries impose a more limited temperature range than required by the transmitter: ideally, these elements should be maintained between $+20$ and $+150^{\circ}\text{F}$ (-7 to $+65^{\circ}\text{C}$). The number of wires emanating from the receiver is less but the thermal leakage paths provided by them is most significant. If we assume 6 wires of 8-mil diameter with the 20°C per centimeter gradient, the loss would be 0.15 watt.

Obviously we should not continue to radiate heat from the radiation heat transfer surface under the off condition as the electronics and battery would very quickly cool down below the point where the battery could supply power, if the receiver were in shade. This means that the radiation heat transfer surface must be as thermally isolated as possible except for a "thermal switch" which allows heat to flow when the receiver heats up during operation. Either a heat pipe, or insulating shutters, or a contacting type switch might be used. The contacting type switch, we believe, will offer the lowest leakage.

For design purposes it appears that something on the order of $1/4$ watt will be required to maintain the receiver

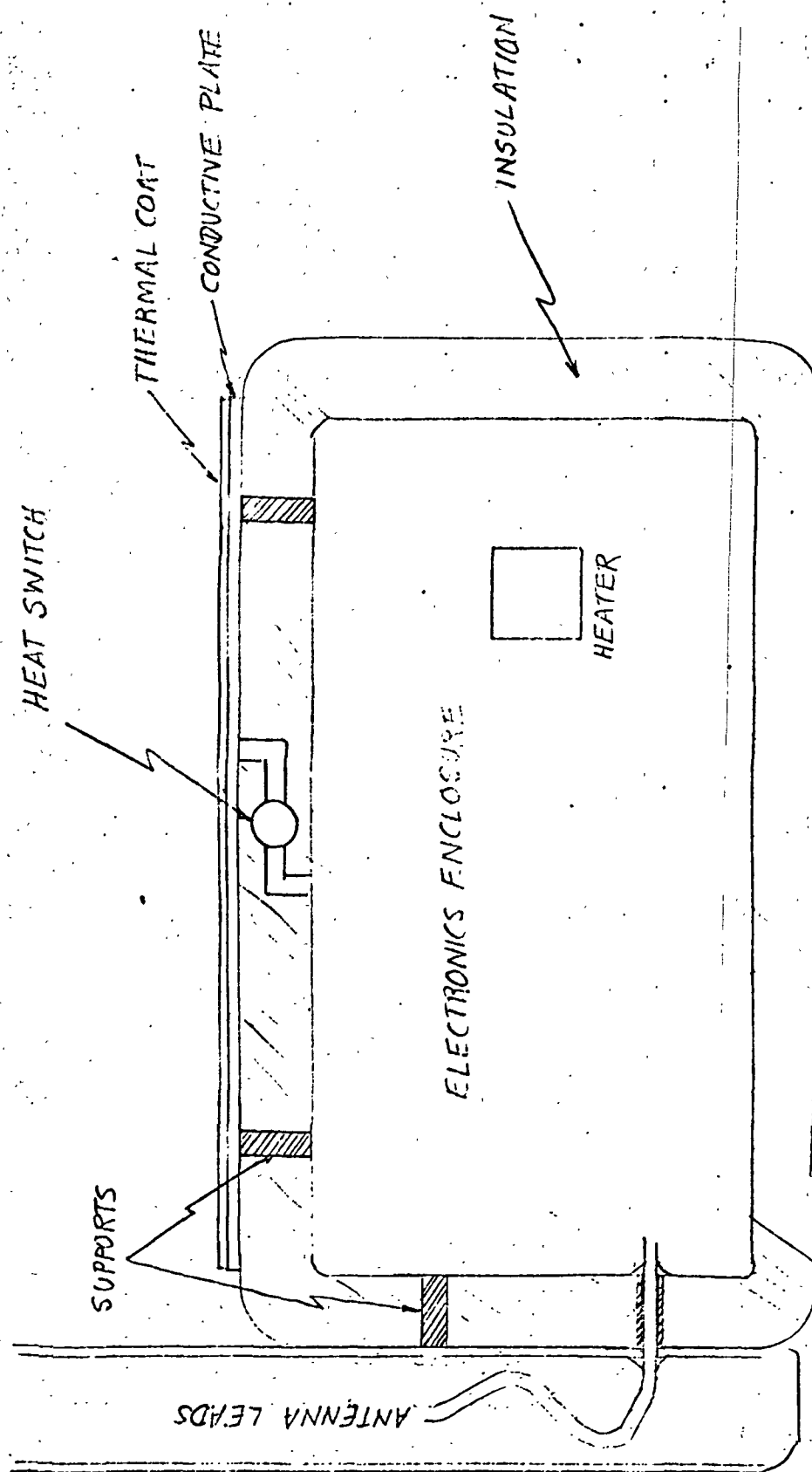


Fig. 3.1 Receiver Thermal

thermal environment when it is turned off.

The thermal configuration proposed for the receiver is a semi-active system, and is illustrated in Fig. 3.1. The electronics, tape unit, and battery are mounted in a container thermally insulated on all sides and from the radiator as well. The radiator surface is designed so that its temperature will never exceed approximately 80°F. A heat switch is used to provide a heat path from the internal heat sink to the radiator whenever the internal temperature approaches say, 80°F. We expect to be able to build a heat switch with thermal resistance in the "on" state of less than 10°F/watt and with a leakage in the off state of less than 1 mw/°F.

In the operational state the receiver's thermal system must eliminate approximately 5 watts plus the heat evolved from the batteries; assuming 7 watts total for now, the temperature drop across the closed thermal switch would be 70°F (21°C) for a maximum internal temperature of 150°F (65°C). In the standby state, the internal power is small, and the thermal switch is usually open.

4.0 Weight Estimates

4.1 Transmitter

Antennas: a.) Reels, 4 at 0.3	1.2 lb
b.) Ribbon, 4 35-m lengths	2.8 lb
Solar Panel with Fixtures	1.0 lb
Case and Thermal	1.4 lb
Electronics	1.9 lb
	<hr/>
	8.3 lb

4.2 Receiver

Loops	0.9 lb
Mast	1.0 lb
Recorder	2.3 lb
Case and Insulation	2.4 lb
Batteries (Silver Zinc, 60wH @ 40wH/lb)	1.5 lb
Electronics	2.5 lb
	<hr/>
	10.8 lb

4.3 Totals

Launch and Lunar Descent weight:	19.1 lb
Receiver Weight for LRV, MET, or carrying:	10.8 lb
Tape Recorder Weight for Data Retrieval	2.3 lb

5.0 Power Requirements

The SEP equipment contains its own power sources and requires no external power.

5.1 Transmitter Power

The transmitter power source is a solar panel measuring approximately 9x9 inches. Using a derated (for dust) density of 6.5 watts/ft², the power available to the transmitter electronics is 3.66 watts, continuous.

Using the power vs. frequency profile discussed previously, the transmitter output power is

$$0.1 (2w + 0.5w + 6(0.125w)) = 0.325 \text{ watts}$$

Taking an efficiency of 50%, the power input to the RF amplifier is 0.65 watts. Additional electronics might require 1.0 watt, and the logic is expected to consume less than 0.5 watt, for a total power dissipation of 2.15 watts. There is then 1.5 watts available for operation of a thermostatically-controlled heater for temperature control; the variation possible is from 2.15 to 3.66 watts (a 70% increase), under derated conditions.

5.2 Receiver Power

The receiver power source is a silver-zinc battery of the secondary type. Silver-zinc cells exhibit energy densities of from 20 to 95 watt-hours/lb; manufactured silver-zinc batteries exhibit energy densities from 15 to 60 watt-hours/lb.

These batteries are rechargeable and have a cycle life of a few hundred cycles.

The receiver's power budget is as follows:

a. Operational (10 hours total)

Tape Recorder:	2.4 watts (max)
Tape Recorder Power Supply (2/3 eff)	1.2 watts
Receiver Electronics:	1.0 watt
Receiver Logic:	<u>0.4 watts</u>
	5.0 watts, or 50 watt-hours

b. Non-Operational (heater mode)

Assuming that 0.25 watts average is required to maintain the electronics temperature satisfactorily, and permitting 40 hours of operation in this mode, an additional 10 watt-hours will be required.

Using a typical energy density of 40 watt-hours/lb. and 2.8 watt-hours/in.³, 1.5 lb. and 21.5 in³ of batteries will be required.

5.2.1 Example

The voltages required by the receiver electronics are as follows:

Logic and IC amplifiers	5 vdc
PLL IC's	18 vdc
Tape recorder with slight modification	26 vac 400Hz

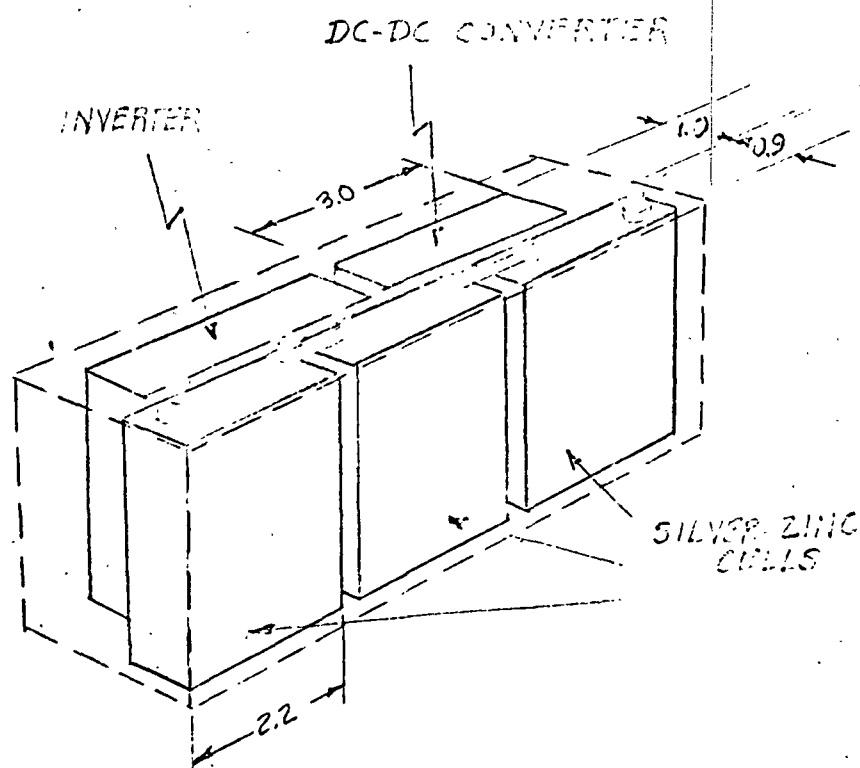
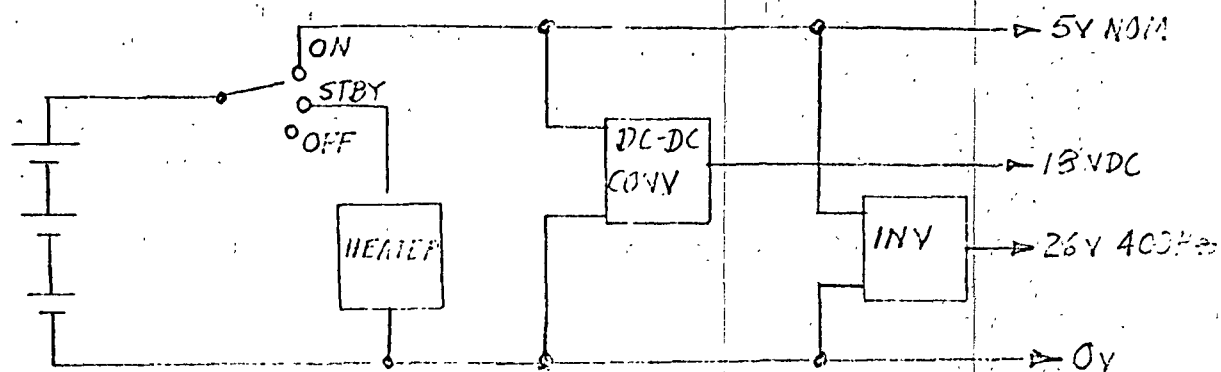


Fig. 5.1 Receiver Energy Source

Silver-zinc cells exhibit an initial voltage per cell of approximately 1.8v , and a final voltage of 1.5v at 80°F. The voltage of low-rate cells is fairly constant at 1.5v from 25% to 100% discharge. For a 6-volt battery, then, four cells would be required; 3 cells would yield a 4.5v battery. Using a three-cell battery entails operating the 5-volt electronics directly from the battery (5.4 volts initial to 4.5v discharged) and using power converters for the 18 and 26-volt supplies.

A number of available cells fit this application closely. The Eagle-Picher SZLR 20.0 cell is a 20A-hour device at the 10-hour discharge rate with initial energy densities of 60 watt-hours/lb and 4.05 wH/in³. Each cell measures 0.89 x 2.20 x 3.75 in and weighs 8.1 oz. A configuration of these cells for the receiver is shown in Fig. 2.1. The three cells used give a battery with an initial available energy of 90 watt hours, 50% more than required. The additional capacity covers the effects of self-discharge during wet stand, and low temperature.

6. Required Equipment

A. Breadboard

To assist in early design effort and preliminary concept evaluation.

B. Engineering Unit

A non-production electrical equivalent of the SEP apparatus to be used for design verification and evaluation of changes.

C. Structural/Thermal Mockups

As required for proof of the mechanical and thermal design. The primary thermal mockup unit is to be used for thermal/vacuum testing, and requires internal heat sources (in lieu of electronics and tape recorder) and sufficient instrumentation (i.e., temperature sensors) to prove the soundness of the thermal design.

D. System Interface Mockups

For simulation and demonstration of S/C and lunar vehicle interfacing. The following are contemplated:

- a. A stowed configuration mockup for the LM.
- b. A receiver mockup for the LRV or MET.
- c. A mockup of the tape recorder.

E. Astronaut Training Mockup

Since the operation of the SEP equipment requires minimal attention and there are no real-time display or operational requirements, the training equipment may be functionally simple and may be made one-sixth the weight of the flight hardware to simulate lunar gravity. To demonstrate the transmitting antenna deployment, this unit will require reels and ribbons identical to those designed for the flight equipment.

The form factor and handling will be exactly that of the flight equipment, although this unit will contain no actual electronics or tape recorder.

F. Prototype Unit

This unit is a non-production prototype fabricated insofar as possible to the flight hardware design. The unit is intended for a glacier test of the experiment concept and design in March, 1971, and will require a tape recorder and full electronics, although not necessarily flyable hardware. The equipment will be identical to the flight equipment as defined by October, 1970.

G. System Compatibility Model

This is the first production equipment; following evaluation it will be delivered for compatibility testing as directed by the Contracting Officer.

H. Qualification Unit

The second production unit is intended for qualification testing, following acceptance testing; this is the first unit requiring all flight-qualified components.

J. Flight Unit

K. Flight Spare

L. Flight Unit

M. Flight Spare

UNIT	DESCRIPTION	ELECTRONICS	MECHANICAL	THERMAL	RECORDER
A	Breadboard	N			
B	Eng'g Unit	N,F			
C	Structural/ Thermal		N	N	
D	Mockups				
E	Training				
F	Prototype	N	N	N	N
G	Compatibility	N,F*	F	F	N,F*
H	Qualification	F	F	F	F
J	Flight	F	F	F	F
K	Flight	F	F	F	F
L	Flight	F	F	F	F
M	Flight	F	F	F	F

N: non-flyable hardware

F: flyable hardware

* Flyable if schedule permits

Table 6.1 SEP Hardware

6.1 Ground Support Equipment

The equipment required to evaluate the transmitter and receiver must perform the following:

a. For the transmitter

1. Provide adjustable metered power to the transmitter electronics.
2. Provide adjustable or switchable dummy loads.
3. Measure and display power output at each frequency as a function of time.
4. Measure transmitter clock frequency.

b. For the receiver

1. Provide adjustable metered power.
2. Measure battery voltage for determination of state of charge.
3. Provide to the antenna terminals adjustable signals simulating those transmitted for evaluation of sensitivity, noise figure, and frequency characteristics. Sufficient adjustment should exist to permit receiver calibration.
4. Provide a battery-charging capability.
5. Display recorder VCO output and input.
6. Provide facilities for evaluating the tape recorder and for reproducing tapes.

The GSE will consist largely of rack-mounted commercial instruments. Specialized hardware will be required for commutating and decommutating signals, simulating loads, and switching among the various functions.

The transmitter and receiver will have test connectors for interfacing with the GSE.

Three sets of GSE are proposed; two for delivery (to MSC and KSC) and one to be used at MIT for acceptance, qualification, and production final testing.

APPENDIX 5.2

SEP MEMO SEP-4-T, JUNE 8, 1970

SEP MEMO SEP-5-T, JUNE 12, 1970

C. Eldon

Charles S. Draper Laboratory
Massachusetts Institute of Technology
Cambridge, Massachusetts

SEP-4-T

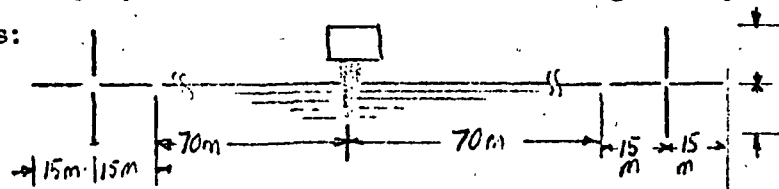
Memo

To: Distribution
From: J. McKenna
Date: 8 June 1970
Subject: Strawman Conceptual Design of SEP Equipment

The apparatus for the Surface Electrical Properties Experiment is as described in CSR's proposal, with the following changes:

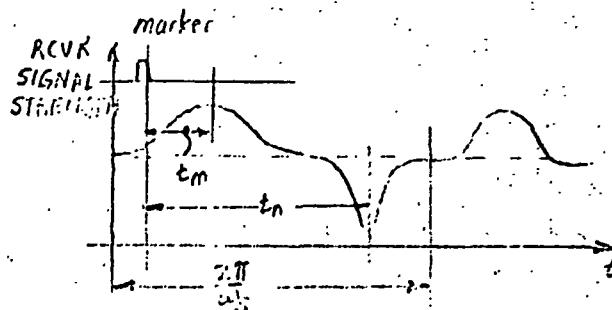
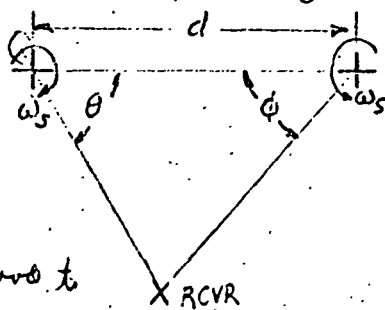
1. Ranging

An attempt to use a ranging system employing rotating-beam antennas will be made. CSR has suggested using turnstile antennas with elements excited at slightly different frequencies to produce a field pattern rotating at the difference frequency. The antennas might be deployed at the ends of the existing multiple dipole as follows:



The ranging antennas are placed in null points of the dipoles, and interference should be minimal. The choice of frequency for the ranging transmitters is somewhat open: too low a frequency gives too large an antenna, while too high a frequency leads to scattering effects and excessive attenuation with distance. The arrays shown above assume a transmitter frequency of 5.0 MHz.

A marker tone is transmitted, using the same antennas, to indicate when the pattern is pointing in a certain direction; the time delay from the marker to a field-strength maximum or minimum at the receiver is a measure of angle θ or ϕ , depending on which antenna is being driven:



ranging goes to

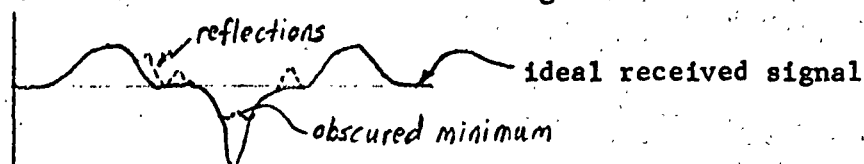
1.5 Km

The distance between the antennas is known, permitting calculation of range and azimuth.

Problems:

a. This system is subject to interference patterns of the sort being measured by the experiment itself; that is, there will probably be points where the ranging signals drop out; this is not considered to be a problem, however.

b. The system is subject to lateral multipath effects; reflections from objects may obscure the minima in the received signal, or add additional variations in the received signal:

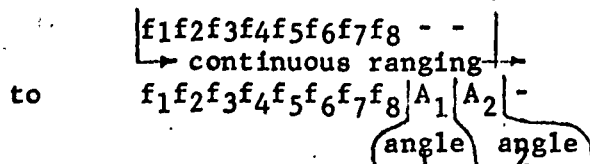


These effects may make direct readout during the experiment difficult; however, since it is intended to record the ranging signal directly on the tape, the information may be extracted post-flight.

c. Will the antenna produce a suitable rotating pattern? How accurately must the alignment of the antennas be made?

2. Transmitter Stepping

In light of the above, the transmitter stepping will change from



This will permit simpler multiplexing onto the tape (permitting single-track tape) and a reduction in transmitter power, because the ranging transmitters need not operate continuously.

3. Receiver Stepping

The receiver stepping will change from

	f_1	f_2	f_3	f_4	f_5	f_6	f_7	f_8	CAL 1	CAL 2
each loop { 33 msec	$L_1 \quad L_2 \quad L_3$	$L_1 \quad L_2 \quad L_3$	$L_1 \quad L_2 \quad L_3$	---	---	---	---	$L_1 \quad L_2 \quad L_3$		
to	f_1	f_2	f_3	f_4	f_5	f_6	f_7	f_8	A_1	A_2
each loop { 33 msec	$L_1 \quad L_2 \quad L_3$	---	---	---	---	---	---	$L_1 \quad L_2 \quad L_3$		$CAL \quad 1$ $CAL \quad 2$

what is the rate of rotation. Should have several 1000 points. Discern beam fact enough where is the time zone

$$T_A, \quad C, \quad T_A, \quad f_5, \quad f_9$$

4. Transmitter power:

The transmitter output power on any frequency will be 1.5 watts, $\pm 20\%$, initially, and degrading less than 10% over the EVA (4 hours).

5. Receiver sensitivity:

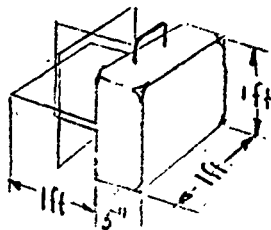
The expected minimum field strength is 18uV/M.

6. Receiver Bandwidth Reduction

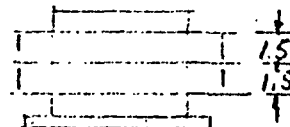
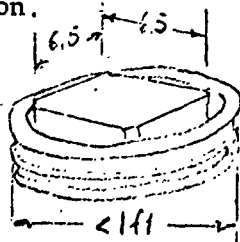
The strawman calls for continued use of crystal filters. The use of other techniques (heterodyning, phase-locked loops) will be considered.

7. Package Configuration

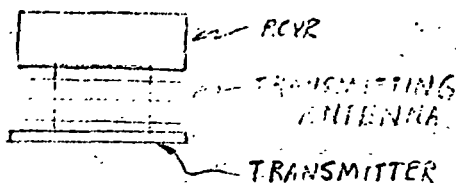
Moving the receiver carrying handle from the top of the loop antennas to a side of the receiver case will facilitate carrying. The possible effects of the case shielding the antennas will need to be considered; however, it does not seem that the presence of the case will add any effect since layers of the astronaut's suit are conductive.



For the transmitter, the small reels for the antenna are removed from the transmitter case (thus making the case smaller) and are replaced by larger reels which fit around the transmitter in the stowed configuration.



Stowed configuration:



Reproduced from
best available copy.

The primary intent here is to reduce the amount of bending required to mount the antenna section on a reel, so that deployment will be simplified and the tendency of the antenna to roll up after deployment will be reduced.

8. Tape Unit

by timing signal
A somewhat representative listing of tape recorders having characteristics suitable for this application appears on the following page. The strawman contains the following allocation for the recorder:

Weight: 8 lbs.

Dimensions: 9 x 6 x 5 in.

Power: 8W

The target operational characteristics are:

EVA length: 2 hours

number of EVA's: 2

No changing of tapes because of the dust problem.

Number of tracks: flexible

Tape speed variation: not critical

9. Energy Source

The energy source for both transmitter and receiver will be Nickel-Cadmium batteries. These are rechargeable and permit a thorough evaluation and test before actual use.

10. AGC

The Automatic Gain Control will not be a slow loop, as shown in the proposal, but will be a fast loop (approx. 15 MSEC) to prevent loss of data due to large differences between successively received signals.

Distribution

J.F. McKenna
E.C. Hall
L.D. Hanley
J. Partridge
J.H. Martin
R.R. Ragan
L.E. Larson
R.H. Baker
L.H. Bannister
M.G. Murley
A.C. Metzger
G.W. Mayo, Jr.
D.J. Grief
Central Files (2)

DESCRIPTION	TAPE & HEADS IN L TRACKS (CHLS)	E SPEED	REC. TIME	OP. TEMP. *NON-OP	SHOCK/ VIB.	FREQ RESPON	DIM'S IN [cu in]	WEIGHT	POWER (RECORD)	SEALED	EST. COST
B-N R210 310	-	1500 (1) to 2200	1-7/8	200min	-	(dgtl) 3400BPI	8x8 x4-1/2 [288]	8 lbs	3 W	Herm	
B-N R304 9001	1/4	300 4	-	130 min.	.25" 8g, 20gV 15gA	DC 50 HZ	-	7 lbs	4.4W		
RXP SIR940	1/4	1100 x 2	1-4	228 min	40g ⁺ .07g ⁺ /HZ	D 2000 BPI DC 720HZ	7.5x 9x3.6 [243]	8 lbs	5-7W	O-Ring	62K/ recorder
KINELOGIC Proposal McGel RSL?	1/2	400 5			-	D 2000b/in 2Kb/sec	5x6x5 [150]	6 lbs	<5W		162 Dev. +25K/1
LEACH Proposal -	1/4	1800 1		180 min	.07/.13 g/HZ 8/20g V	D 2040 b/i	5.25x 7.1x 7.6 [283]	<10 lb	<10W	Solder Strip	58K dev. +18K/
SONY TC-50	1/4	-	1	60 min	Apollo Profiles	80HZ - 8 KHZ	7x3x1.5 [31.5]	20 oz		No	119.50
KINELOGIC LL From CSR's Proposal	1"	400' (8) 4/dir.		1-7/8	-	50HZ - 10 KHZ	9x6x4 [216]	<10 lb	10W	-	50K
KINELOGIC LL NSC	1/4	700' 7		15/32 IPS to 16 IPS	5g OP 12g non	Dgtl. 1500 b/in An. 6000 b/in bw: DC-150HZ @ 15/32 DC-5KHZ @ 15 IPS	11x5x 3-1/2 [193]	11 lbs	15 to 18W	O-Ring not Hermetic	150K
DSC Syn., Dgtl.	-	1200' 16		-	-	-	[324] 6x6x9	7 lbs	1 W	No	
DSC 3800 Record only annals	1/4	1200 4		-	-	-	5x7x7 [245]		-	-	

Eldon

Charles S. Draper Laboratory
Massachusetts Institute of Technology
Cambridge, Massachusetts

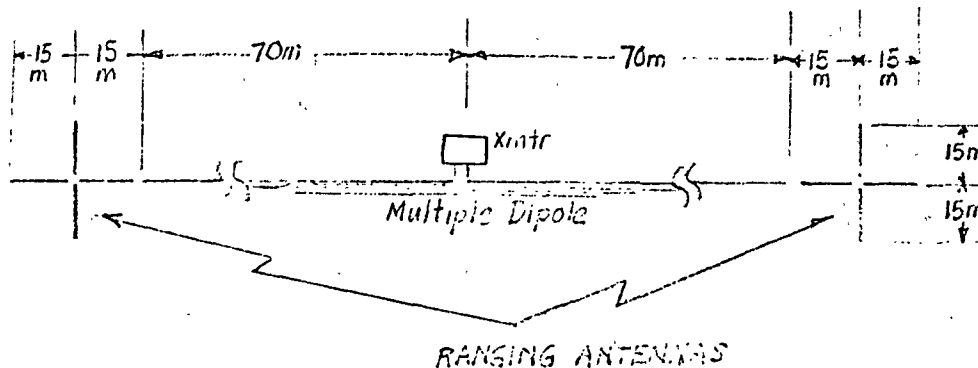
SEP-5-T MEMO

To: Distribution
From: J. McKenna
Date: 12 June 1970
Subj: Conceptual Design of SEP Equipment - Rev. 1

The apparatus for the Surface Electrical Properties Experiment is as described in CSR's proposal, with the following changes:

1. Ranging

An attempt to use a ranging system employing rotating-beam antennas will be made. CSR has suggested using turnstile antennas with elements excited at slightly different frequencies to produce a field pattern rotating at the difference frequency. The antennas might be deployed at the ends of the existing multiple dipole as follows:

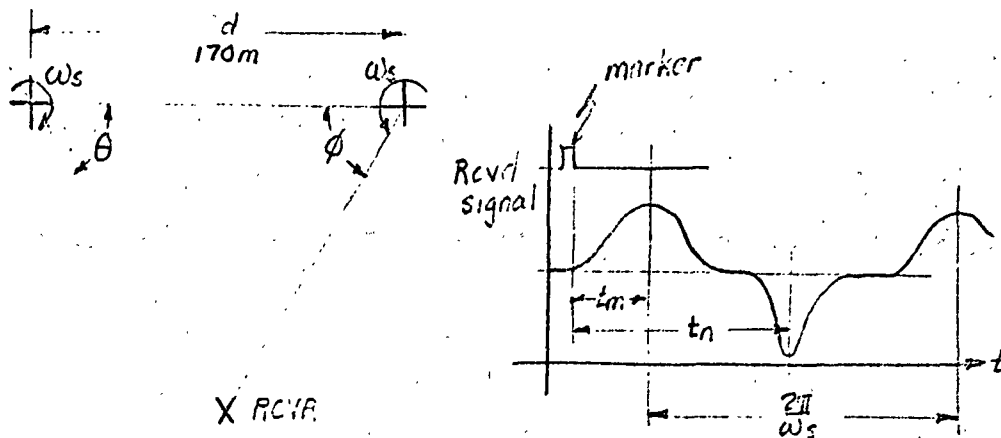


It may be possible to overlap the inboard elements of the turnstiles with the outer ends of the low-frequency dipole to shorten the overall length by 30 m.

The ranging antennas are placed in null points of the dipoles, and interaction should be minimal. The choice of frequency for the ranging transmitters is somewhat open: too low a frequency gives too large an antenna, while too high a frequency leads to scattering effects and excessive attenuation with distance. The arrays shown above assume a transmitter frequency of 5.0 MHz.

1

A marker tone is transmitted, using the same antennas, to indicate when the pattern is pointing in a certain direction; the time delay from the marker to a field-strength maximum or minimum at the receiver is a measure of angle θ or ϕ , depending upon which antenna is being driven:



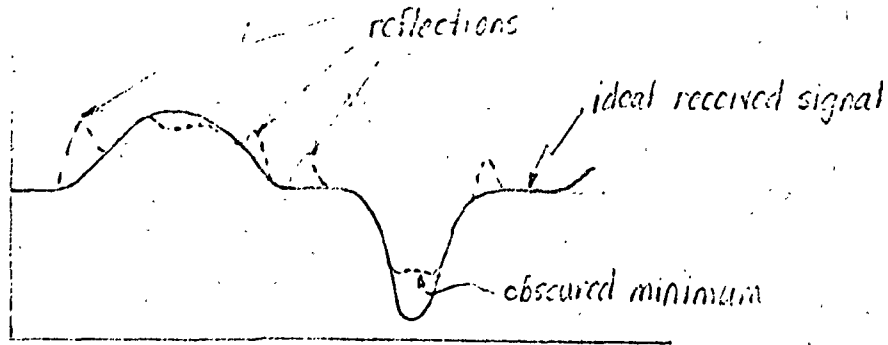
It may not be necessary to transmit a marker at all, because the receiver is inherently synchronized to the transmitter and the beginnings of the ranging time slots may serve as implied markers as long as the rotating pattern always starts at a given angle.

The distance between the antennas is known, permitting calculation of range and azimuth.

Problems:

a. This system is subject to interference patterns of the sort being measured by the experiment itself; that is, there will probably be points where the ranging signals drop out; this is not considered to be serious, since an absolute measurement of range is available wherever sufficient field strength is available, and interpolation may be done.

b. The system is subject to lateral multipath effects; reflections from objects may obscure the minima in the received signal, or add additional variations in the received signal:

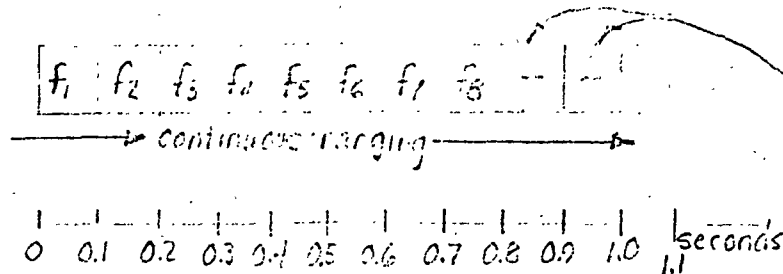


These effects may make direct readout during the experiment difficult; however, since it is intended to record the ranging signal directly on the tape, the information may be extracted post-flight. This technique will also provide information on multipath effects.

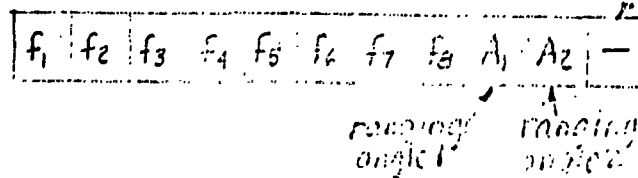
c. Will the antenna produce a suitable rotating pattern? How accurately must the alignment of the antennas be made?

2. Transmitter Stepping

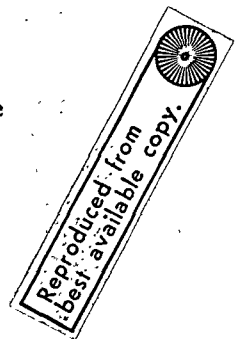
In light of the above, the transmitter stepping will change from



To:

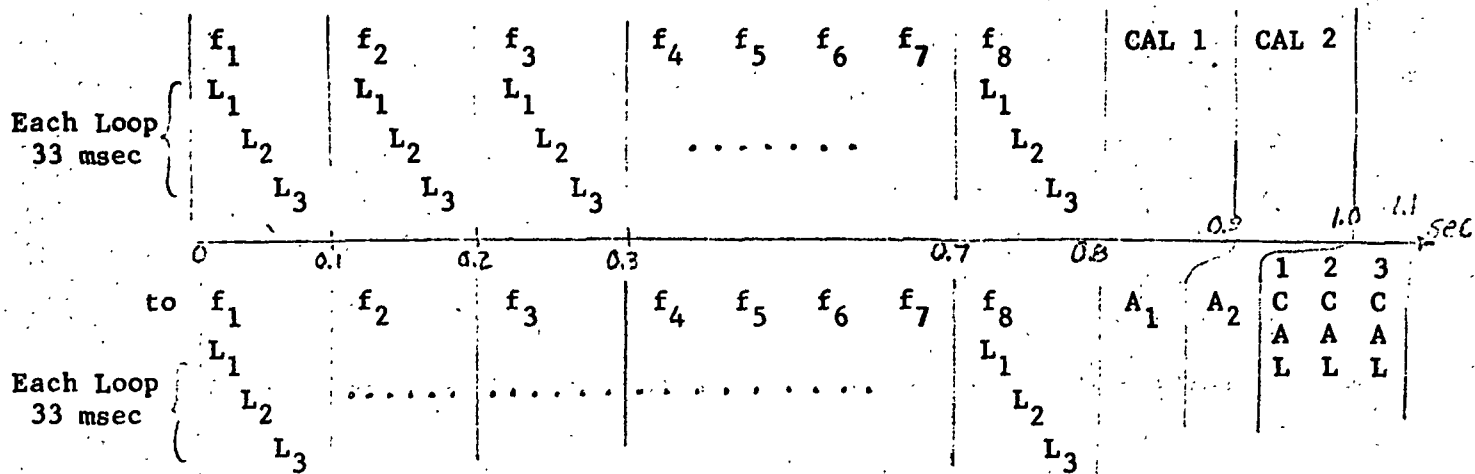


This will permit simpler multiplexing onto the tape (permitting single-track tape) and a reduction in transmitter power, because the ranging transmitters need not operate continuously. The ranging transmitters may operate at a lower duty cycle than shown above (e.g., by operating them only on alternate cycles) if it is demonstrated that a higher power level is desirable.



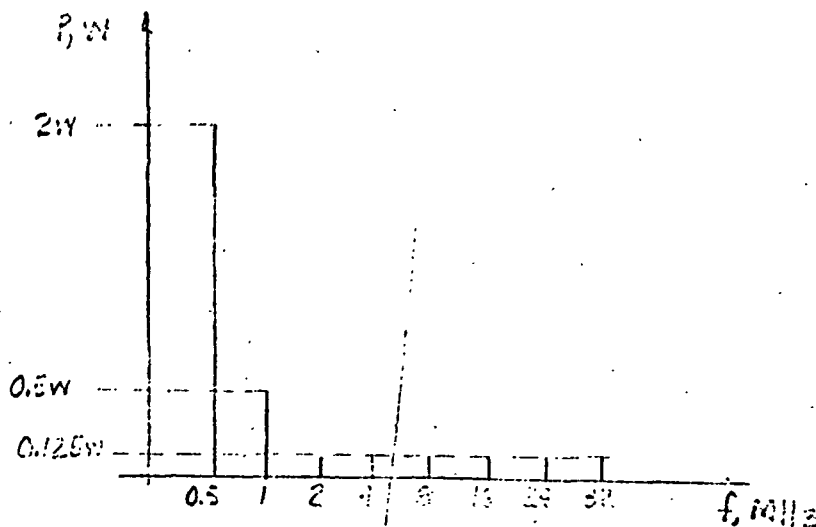
3. Receiver Stepping

The receiver stepping will change from



4. Transmitter Power

Since it is not worthwhile to record field strength at a distance of more than 40λ from the source, the transmitter power at the higher frequencies need not be as large as at the lower frequencies. Considering this fact with the frequency response of the receiver's loop antennas, it is possible to establish a required transmitter output power proportional to λ^3 . Thus, if one watt at 0.5 MHz were acceptable, 0.125 watts at 1 MHz and 62.5 mW at 2 MHz would do. The following transmitter power profile is proposed:



Thus the average transmitter power has been reduced from 0.8 watts (not including ranging) to $\frac{1}{11}$ ($2+0.5 \times 6 \times 0.125$) = 0.295 watts while increasing the power by a factor of two at the lowest frequency.

For the ranging antennas, it may be desirable to deliver as much as 25 watts on a pulsed basis (the acceptable power level needs to be defined). If we take 10 watts, pulsed, as being acceptable, and assume that the ranging transmitters are operated every second major cycle, the average power output for ranging is approximately 0.91 watts.

5. Receiver

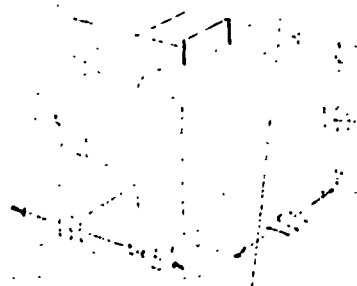
Receiver Noise Figure	< 6dB
Receiver Sensitivity	< 1 μ V.

6. Receiver Bandwidth Reduction

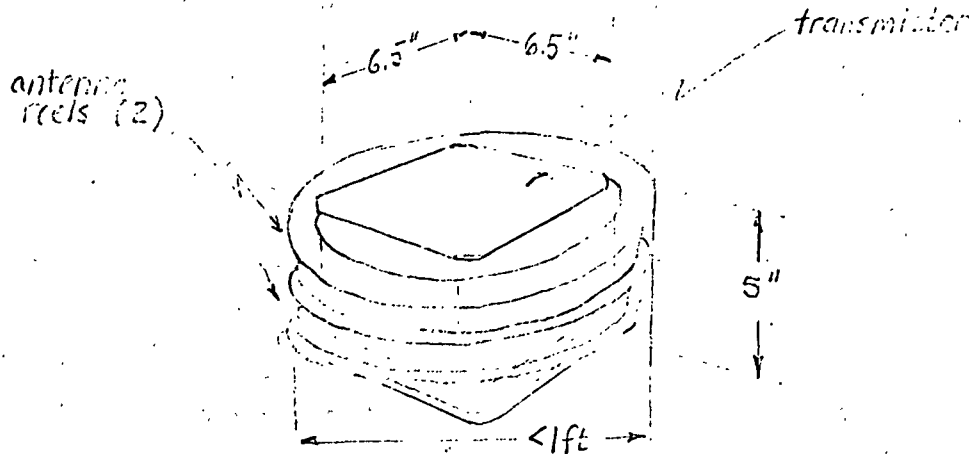
Crystal filters are the present candidate. The use of other techniques (heterodyning, phase-locked loops) will be considered.

7. Package Configuration

Moving the receiver carrying handle from the top of the loop antennas to a side of the receiver case will facilitate carrying. The possible effects of the case shielding the antennas will need to be considered; however, it does not seem that the presence of the case will add any effect since layers of the astronaut's suit are conductive.



For the transmitter, the small reels for the antenna are removed from the transmitter case (thus making the case smaller) and are replaced by larger reels which fit around the transmitter in the stowed configuration.



The primary intent here is to reduce the amount of bending required to mount the antenna section on a reel, so that deployment will be simplified and the tendency of the antenna to roll up after deployment will be reduced.

8. Tape Unit

A somewhat representative listing of tape recorders having characteristics suitable for this application appears on the following page. The present conceptual design contains the following allocation for the recorder:

Weight:	8 lbs
Dimensions:	9 x 6 x 5 in.
Power:	8 W.

The target operational characteristics are:

EVA length:	2 Hours
Number of EVA's:	2

No changing of tapes because of the dust problem.

Number of tracks:	Flexible
-------------------	----------

Tape speed variation:	Not critical, if a timing reference is used.
-----------------------	--

Depending upon the nature of the EVA, the receiver will often remain in the same location, continuously recording the same data. In the interests of conserving tape (and energy used to move the tape) it would be desirable to turn off the tape unit after the receiver has remained in one location for, say, 10 full cycles. The following techniques of accomplishing this have been suggested:

1. A motion sensor, such as a g-switch, would keep the tape operating continuously if motion were sensed every minute or so; if no motion were sensed for one minute, the tape would operate in a second mode of one minute off, 10 seconds on.
2. If the receiver is hand-carried, a switch coupled to the carrying handle would turn on the tape whenever the receiver is being carried.
- 3a. If the received signal pattern does not change over, say, 10 cycles, the tape would automatically be switched to a low duty-cycle mode of, perhaps, one cycle per minute.
- 3b. If the ranging information does not change over, say, 10 cycles, the tape would automatically be switched to the low duty-cycle mode.

9. Energy Source

The energy source receiver will be Nickel-Cadmium batteries. These are rechargeable and permit a thorough evaluation and test before actual use.

Since the transmitter is stationary, solar cells could be used with a possible weight saving for the entire assembly. Nickel Cadmium batteries consume approximately 0.1 (0.2 with derating) lbs/watt-hour, and solar panels approximately 0.1 lbs/watt. A four-hour EVA, with a transmitter consuming 4 watts, would require 1.6 to 3.2 lbs of batteries or less than 1/2-lb of solar panel. A solar panel does need to be deployed, however, and could be susceptible to lunar dust.

DESCRIPTION	TAPE & HEADS		TAPE SPEED	REC. TIME	OP. TEMP. *NON-OP	SHOCK/ VIB.	FREQ. RESPONSE	DIM'S in	WEIGHT	POWER (RECORD)	SEALED	EST. COST
	"	L TRACKS (CHLS)										
2-K K210 310	-	1500 (1) to 2200	1-7/8	200min	-	-	(dgtl) 3400BPI	8x8 x4-1/2 [288]	8 lbs	3 W	Herm	
2-K R304 9001	1/4	300 4	-	130 min.	0 → 120F	.25" 8g, 20gV 15gA	DC 50 HZ	-	7 lbs	4.4W		
2-K SIR940	1/4	1100 x 2 1-4	1 IPS	228 min	+55 → 195F	40gS ² .07g ² /HZ	D 2000 BPI DC 720HZ	7.5x 9x3.6 [243]	8 lbs	5-7W	O-Ring	62K/ recorder
KINELOGIC Proposal Model RSL?	1/2	400 5	.22 IPS		-	-	D 2000b/in 2Kb/sec	5x6x5 [150]	6 lbs	<5W		162 Dev. +25K/1
LEACH Proposa -	1/4	1800 1	1 IPS (1/2 - 4 avail)	180 min	0 → 130F	.07/.13 g ² /HZ 8/20g V	D 2040 b/i	5.25x 7.1x 7.6 [283]	<10 lb	<10W	Solder Strip	58K dev. +18K/
SONY TC-50	1/4	- 1	1-7/8	60 min	(32 → 120°F) Batts.?	Apollo Profiles	80HZ - 8 KHZ	7x3x1.5 [31.5]	20 oz		No	119.50
KINELOGIC LL From CSN's Proposal	1" 400'	(8) 4/dir.	1-7/8	120 min	-20F → 160F	-	50HZ - 10 KHZ	9x6x4 [216]	<10 lb	10W	-	50K
KINELOGIC LL NSC	1/4 700'	7	15/32 IPS to 16 IPS	-	-20 → +120°F	5g OP 12g non	Dgtl. 1500 b/in An. 6000 b/in bw: DC-150HZ @ 15/32 DC-5KHZ @ 15 IPS	11x5x 3-1/2 [193]	11 lbs	15 to 18W	O-Ring not Hermetic	150K
DSC Sync. Dgtl.	- 1200'	16	.16 IPS	-	-	-	-	[324] 6x6x9	7 lbs	1 W	No	
DSC 3800 Record only analog	1/4 1200 4		-	-	-	-	-	5x7x7 [243]	-	-	-	

10. AGC

The Automatic Gain Control will not be a slow loop, as shown in the proposal, but will be a fast loop (approx. 15 msec response) to prevent loss of data due to large differences between successively received signals.

11. Synchronization

A system of synchronization between the transmitter and receiver that does not require a hard-wire connection to establish or continuous reception of a reference signal to maintain, will be employed.

Dist.

J. McKenna
E. Hall
D. Hanley
J. Partridge
J. Martin
R. Ragan
L. Larson
R. Baker
L. Bannister
M. Murley
A. Metzger
G. Mayo
D. Grief
E. Johnston
J. Barker
R. Cushing
C. Files -2

APPENDIX 5.3

CHARLES STARK DRAPER LABORATORY

WEEKLY MEMOS

NOS. 1 & 2

THE CHARLES STARK DRAPER LABORATORY
A DIVISION OF MASSACHUSETTS INSTITUTE OF TECHNOLOGY
68 ALBANY STREET
CAMBRIDGE, MASSACHUSETTS 02139

SEP-16-A

To: Distribution
From: J. McKenna
Date: 18 November 1970
Subject: Draper Laboratory Weekly Memo No. 1

During the MIT/NASA meeting of November 2 I agreed to provide weekly letters concerning Draper Laboratory's SEP activities. This memo (No. 1) serves as a brief status report of SEP to date; following memos will appear weekly and will contain, for the most part, information concerned with the preceding week's activities.

1. Design/Development

1.1 Receiver Electrical

- a. Front-end amplifiers: designed and breadboarded; presently under test.
- b. Diode Switches: breadboarded and tested.
- c. Switching VCO for Tape Recorder Interface: designed and breadboarded; design now being optimized.
- d. Logic and Countdown: designed; breadboarding begun.
- e. Sync Circuits and Logic: design initiated.
- f. Power Converter: design initiated.

1.2 Transmitter Electrical

Oscillator: Purchase order initiated

Countdown and Logic: Ready for breadboard build

Filters and power-profiling amps: design initiated;
breadboards have been built
at several frequencies.

RF Switches: breadboarded and tested

Baluns, balanced modulators, power dividers: purchase orders
being prepared.

Sine shaping for 15Hz: a section of a piecewise-linear sine
function generator has been breadboarded
and is currently being optimized for
operation at temperature extremes.

Linear Amplifiers: Negotiation with vendors continuing.

1.3 Structural/Thermal

Two structural/thermal models of the transmitter and two
of the receiver have been built; one of each is intended for
mechanical testing (e.g., vibration) and one of each for thermal
testing. One version of the receiver model has undergone and
survived vibration testing (sinusoidal and random). Solar-cham-
ber thermal testing is expected to commence next week.

Antennas have been built in the tri-loop configuration for
CSR's use on the glacier and a loop was fabricated for the MSFC
EMI test. Wooden mockups of the SEP instrument have been completed.

1.4 EMI Test Receiver

The design of the EMI test receiver has begun and purchase orders are being prepared for necessary items. This receiver will use a Sony TC-50 tape recorder resulting in 45 minutes recording time for each tape change.

2. EMI Test at Huntsville

An EMI test was conducted by CSDL personnel at NASA/MSFC on an LRV traction drive motor with its drive electronics. Details may be found in SEP-10-T.

3. The Proposal for SEP Phase II has been submitted.

4. RFQ issued to Leach for tape unit procurement.

5. Support proposals from Raytheon and RCA are being evaluated.

Distribution

R.H. Baker

H.D. Cubley

R.R. Ragan

G. Simmons

D. Hanley

E.C. Hall

D. Hoag

E. J. Don

THE CHARLES STARK DRAPER LABORATORY
A DIVISION OF MASSACHUSETTS INSTITUTE OF TECHNOLOGY
68 ALBANY STREET
CAMBRIDGE, MASSACHUSETTS 02139

SEP-17-A

To: Distribution
From: J. McKenna
Date: 27 Nov. 1970
Subj: Draper Laboratory Weekly Memo #2

1. DESIGN/DEVELOPMENT

1.1 Receiver Electrical

- a. Front-End Amplifiers - breadboarding completed. Amplifiers suitable for use as front-end and post-filter amplifiers are now being built in gated and non-gated configurations for the Field - evaluation receiver. Advance information on these circuits has been transmitted to packaging and R/QA.
- b. Diode Switches - A build effort is under way for the field-evaluation receiver and transmitter. Advance information has been transmitted to packaging and R/QA.
- c. Switching VCO - Design completed; breadboard of final configuration will be initiated.
- d. Clock and Logic Section - Design will be available about December 1.
- e. Sync Section - We are pursuing a synchronization approach using close oscillators and a counter reset on detection of the 0.5 MHz signal. This has been designed and breadboarded but testing has not yet begun.
- f. Calibration Circuits - Calibration circuits using a single frequency (4.0 MHz) have been designed;

no breadboarding yet.

- g. Mixer Preamp - Designed in lieu of a too-power-consuming unit from an outside vendor.
- h. Local oscillators, clock oscillator, IF amplifier dividers/combiners, and mixer have been ordered, as have crystal filters for evaluation breadboarding and for the field evaluation receiver.

1.2 Transmitter Electrical

- a. Oscillator - A TXCO with self-contained frequency multiplication circuitry has been ordered.
- b. Baluns, Power Dividers, and balanced modulators ordered.
- c. Linear Amplifiers - A procurement spec for linear amplifiers with increased efficiency (Class AB) has been generated and a quote received. A purchase order for these will be processed shortly; preliminary information to packaging and R/QA.
- d. Diode Switches - A build effort is under way for the field-evaluation receiver and transmitter. Advance information has been transmitted to packaging and R/QA.
- e. Bandpass Filters - Design continuing. A problem with the buffers (not the filters) at the high frequency end has appeared and some modification will be required.
- f. 15 Hz sine-shaping - A glitch at the temperature extremes will slip release of this circuit one week.

1.3 Structural/Thermal

The transmitter mockup (without solar panel) was vibration tested and withstood 8g random vibration in the vertical and horizontal positions. During sine sweep resonances showed up at 170 cycles in the horizontal position (transmissibility 6.5) and at 170 and 320 cycles in the vertical position (transmissibility 5). The antenna reel holding system was judged not good enough because of excessive reel chatter and will be redesigned.

The technique of suspending the receiver electronics with supports under compression from the corners of the outside case has been abandoned in favor of the technique using supports under tension.

1.4 EMI Test Receiver

1. Diode Switches - being built.
2. Fron End Amplifiers - being built.
3. VCO - designed and built; not yet tested.
4. Detectors and Switchable Active Filters - designed; build will start shortly.
5. Local and Timing Oscillator - ordered and received.
6. Timing and Countdown - A previously-built breadboard of the countdown logic is being modified for use in the EMI receiver.
7. Tape Recorder - The TC-50 procured last summer is available for use.

2.0 DSEA

Quote received from Leach Corp. We are generating a procurement specification in concurrence with R/QA and purchasing. Some get-started funding may be necessary for Leach to begin procurement of long-lead items.

Dist.

R.H. Baker
H.D. Cubley
R.R. Ragan
G. Simmons
L.D. Hanley
E.C. Hall
D.G. Hoag
T. White
A.C. Metzger
J.F. McKenna
Sep File -2

APPENDIX 5.4

M.I.T./CSDL

SURFACE ELECTRICAL PROPERTIES

PRESENTATION

DECEMBER 11, 1970

Jack

MASSACHUSETTS INSTITUTE OF TECHNOLOGY

APOLLO

GUIDANCE, NAVIGATION AND CONTROL

MIT/DL

SEP PRESENTATION

December 11, 1970

MIT

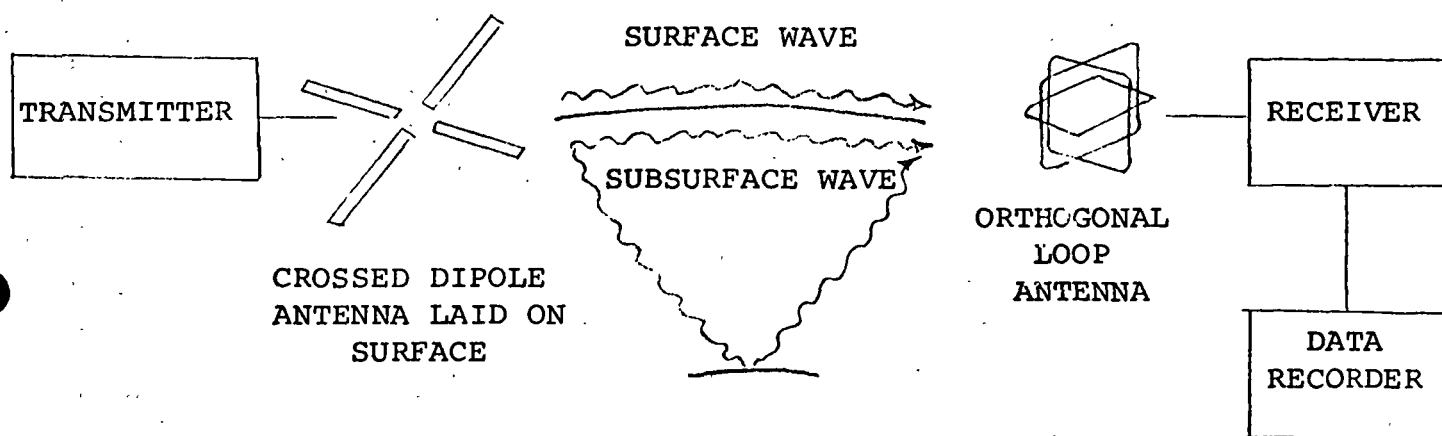
CAMBRIDGE, MASSACHUSETTS, 02139

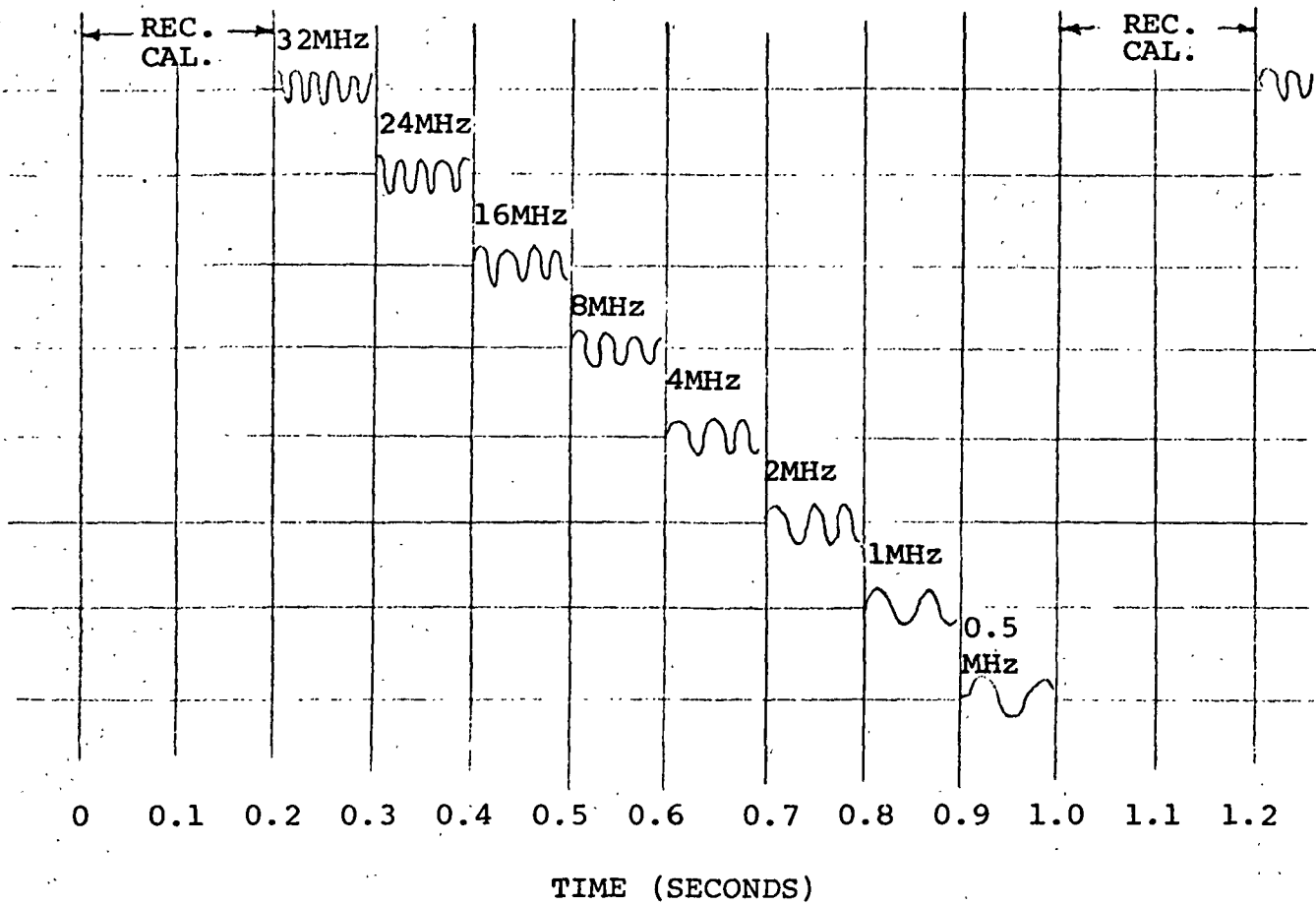
**CHARLES STARK DRAPER
LABORATORY**

INTRODUCTION

1. Experiment Definition.
2. Key Milestones.
3. Hardware Requirements. E.C. Hall
4. Proposed Division of Effort.
5. Technical Presentation.
 - a. Electronic Design. R. Cushing
 - b. Mechanical Design. J. Martin
 - c. Systems Integration. L. Johnson
6. Summary. E.C. Hall

OBJECTIVE: MEASURE FIELD STRENGTH AS A FUNCTION OF RANGE

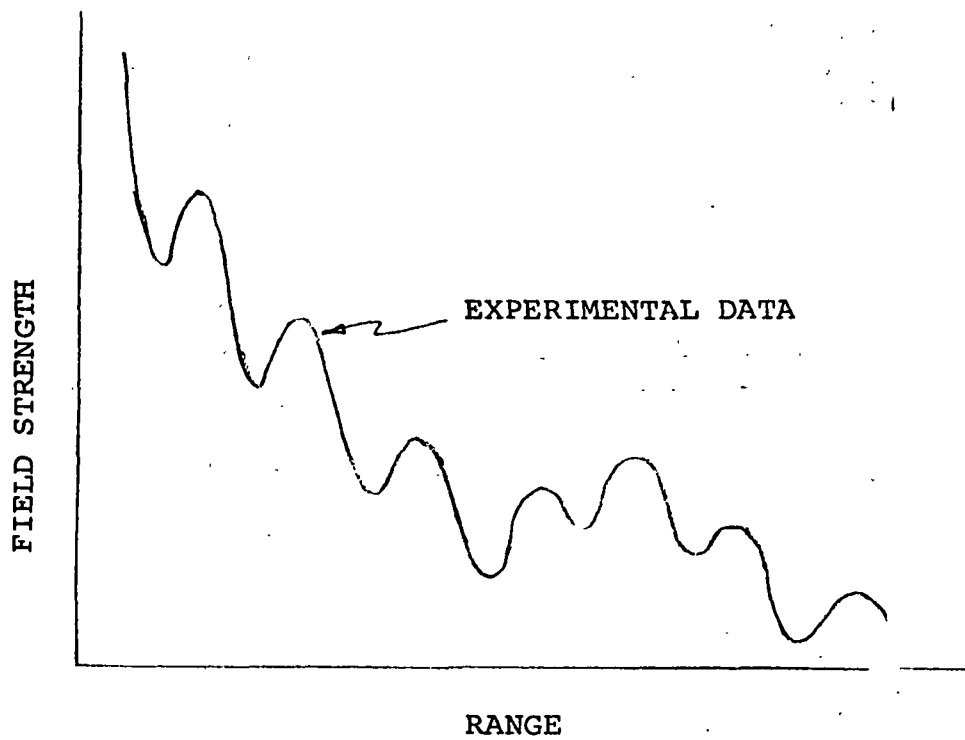




PROBLEM AREAS

Power Levels/Antenna Coupling
Hardware Deployment
Output Stability
Output Modulation (Rotating Beam)

RECEIVED FIELD STRENGTH



PROBLEMS

- Measurement Stability
- Data Dynamic Range
- Antenna Characteristics
- Rover Disturbances

KEY MILESTONES

<u>ITEM</u>	<u>NEED DATE</u>
MIT (Go Ahead)	15 Dec. '70
END ITEM SPECIFICATION - PART I	Dec. '70
Experiment/Mission Requirements	
Antenna Requirements	
Human Factors/Hardware Interface	
SUBCONTRACTS	
Tape Recorder (9 Month Delivery ARO)	Dec. '70
Raytheon (Go Ahead)	Jan. '71
MSC SCHEDULE FOR ROVER EMI TEST	Jan. '71
SEP EMI Receiver	Jan. '71
NASA CRITICAL DESIGN REVIEW	Apr. '71
Fabrication Design Release	
(Subcontractor Req.)	May '71
QUALIFICATION TEST	Jan. '72
FIRST FLIGHT MODEL	Jan. '72
INSTALLATION (Lead Time 4 Months Assumed)	Mar. '72
FLIGHT 17	July '72

HARDWARE

<u>ITEM</u>	<u>NEED DATE</u>	<u>BUILT BY</u>
EMI RECEIVER (Rover Noise)	Jan. '71	CSDL
FIELD EVALUATION UNIT (Electrical Integration)	Jan. '71	CSDL
ENGINEERING PROTOTYPE UNIT (Mechanical Integration)	May '71	CSDL
TRAINING AND INTERFACE MODEL	June '71	CSDL
FIRST G.S.E. OF THREE REQUIRED	Aug. '71	RAYTHEON
COMPATIBILITY MODEL (First Production Unit)	Sept. '71	RAYTHEON
QUALIFICATION MODEL	Nov. '71	RAYTHEON
FIRST FLIGHT MODEL OF TWO REQUIRED	Jan. '72	RAYTHEON
TAPE DATA REDUCTION EQUIPMENT	Sept. '71	CSDL

PI/CSR EFFORT

1. Verify Satisfaction of Scientific Requirements.
2. Define Design Requirements.
3. Tape Data Reduction.
4. Monitor Hardware Development.
5. Support the PI.

HARDWARE DEVELOPMENT EFFORT

CSDL

1. Management of hardware development, R&QA and subcontracts.
2. Design, design verification, and top level spec.
3. Development prototypes and models.
4. Provide tape recorder.

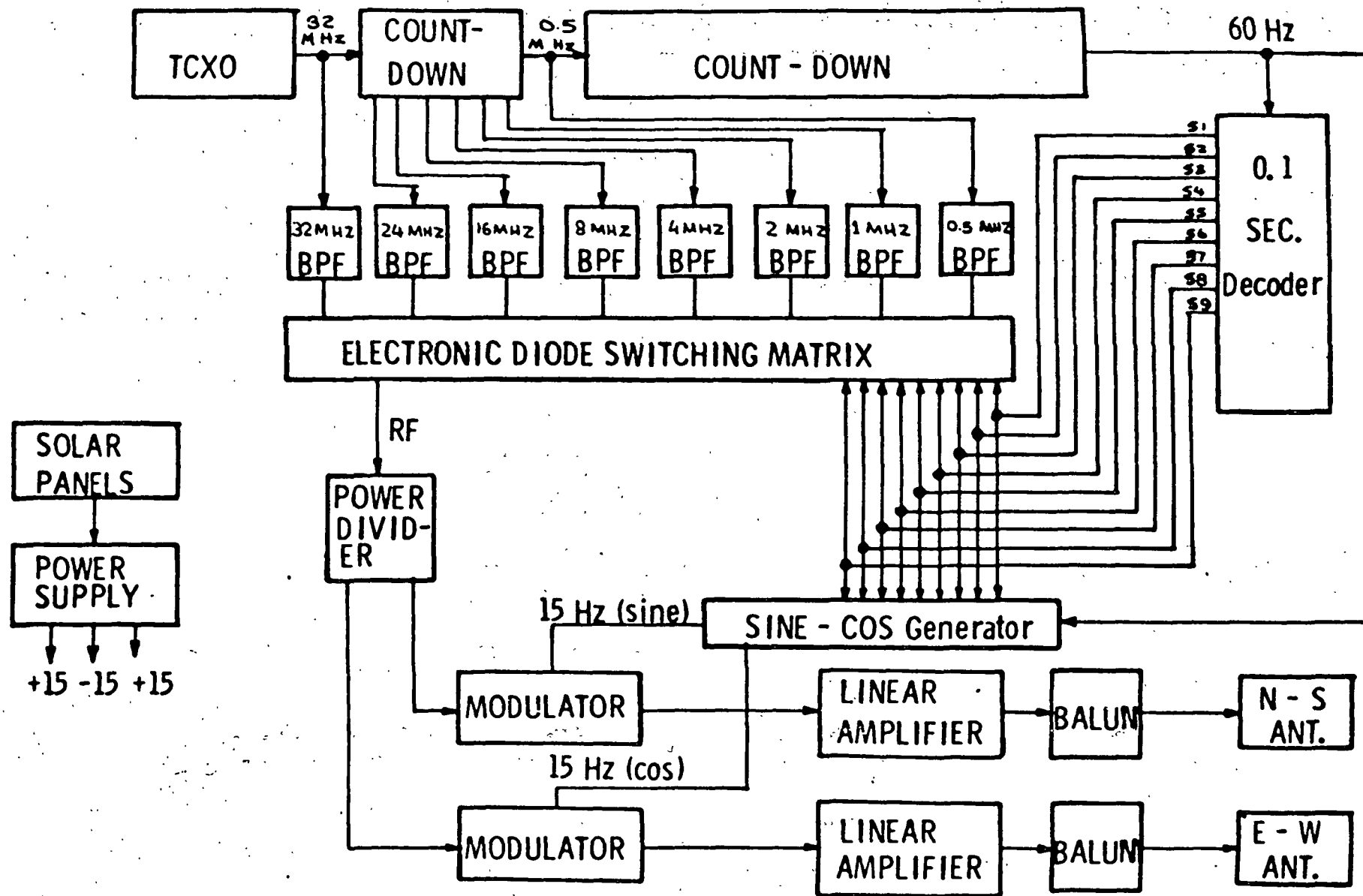
LINCOLN LAB

1. Electrical design for antennas and coupling electronics.
2. Antenna design verification tests.

RAYTHEON

1. Production management.
2. Design support.
3. GSE design.
4. Fabricate, assemble and acceptance test all deliverable hardware.
5. Conduct qualification test.

BLOCK DIAGRAM OF SEP TRANSMITTER



TRANSMITTER PROBLEM AREAS

1. Linear Amplifier Efficiency:

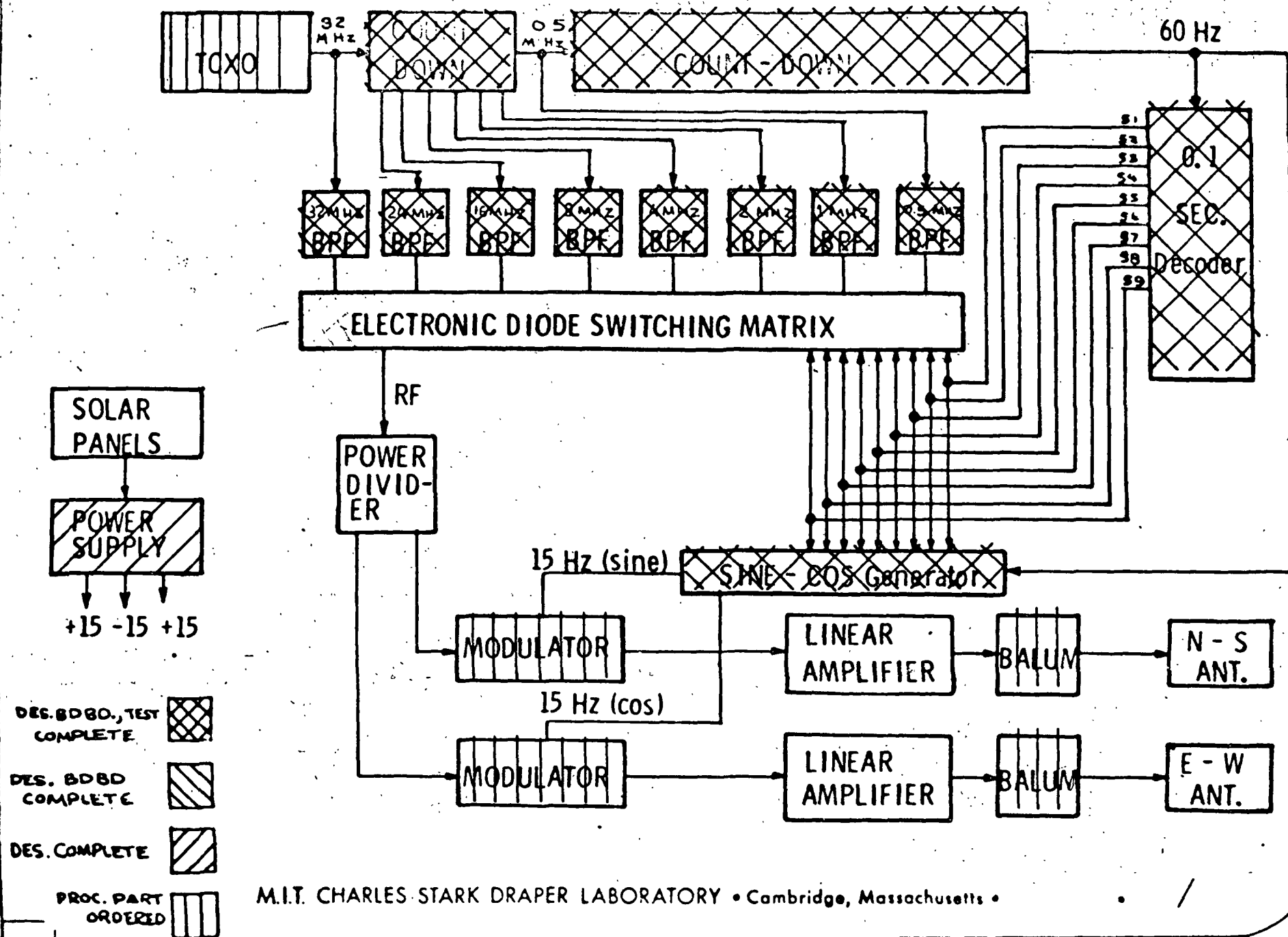
Applies to original concept only; 10-15% efficiency can be improved to $> 30\%$;

Status: Specification complete; one affirmative response to date.
Held for finalization of concept for .5mhz, 1mhz, 2mhz frequencies.

2. Finalization of concept may require automatic impedance matching of antenna.

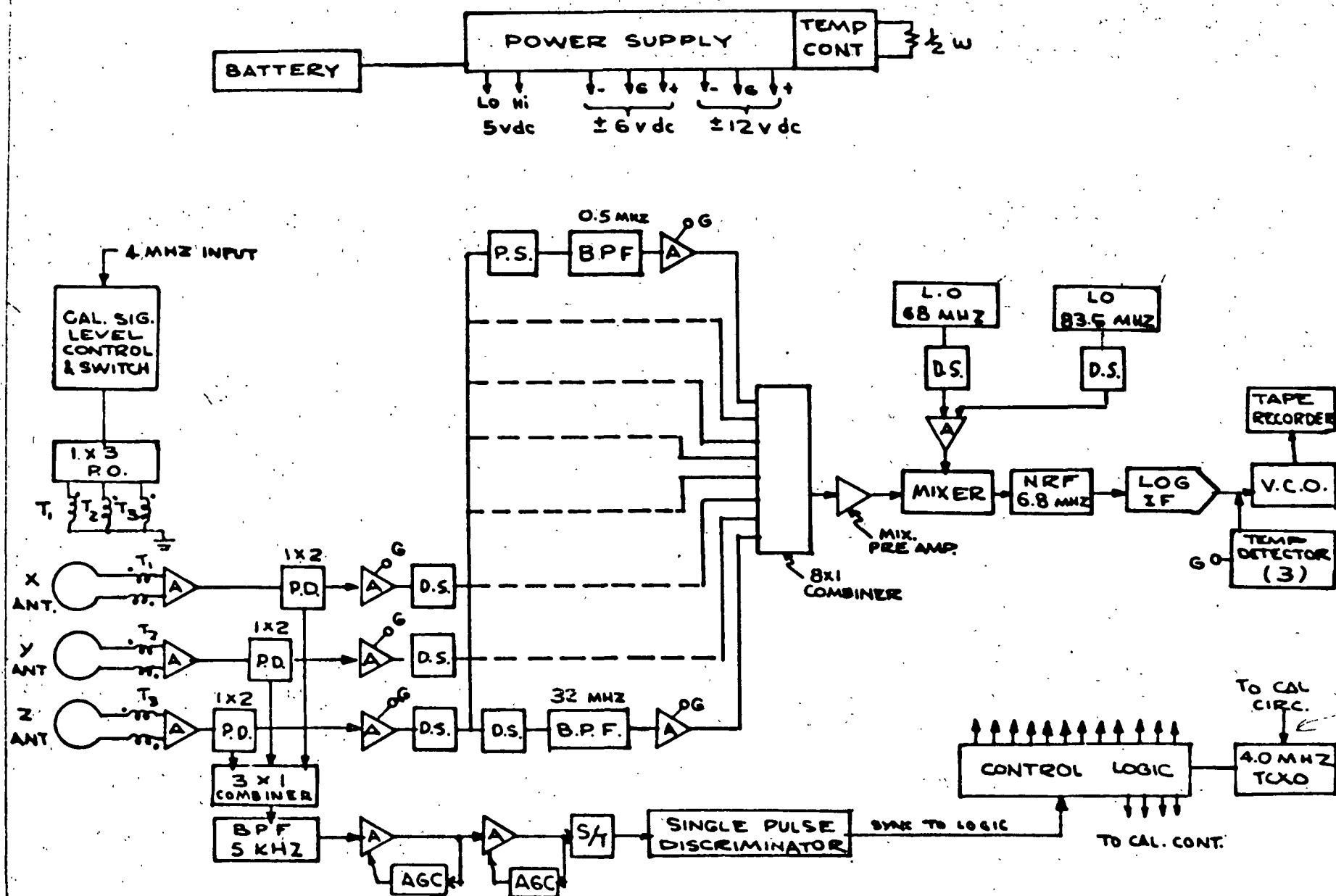
3. Above problems or implied changes will not seriously impact work complete to date. High power drive for .5, 1, 2mhz frequencies, may be thru separate amplifiers (possibility of Class C being investigated).

BLOCK DIAGRAM OF SEP TRANSMITTER



M.I.T. CHARLES STARK DRAPER LABORATORY • Cambridge, Massachusetts •

S.E. P FIELD EVALUATION RECEIVER



RECEIVER PROBLEMS TO DATE

1. Front End Overdrive At Near Range.

Probable Solution - Front End Limiting, for signal levels above usable dynamic range.

2. AGC Range (40db) in Sync Front End Inadequate Per Test.

Solution: Modify Front End to 90db and add over-range limiting.

Status: Breadboard modified awaiting test.

3. 68mhz Feed Thru To Log I.F.

Solutions: A. Notch out 68mhz - Filter on order, will assure 100db suppression of 68mhz.

B. Double Mix 1/2, 1, 2, 4, 8 mhz using nominal 20 mhz 1st I.F. - notch out 1st L.O. - assures > 140 db suppression.

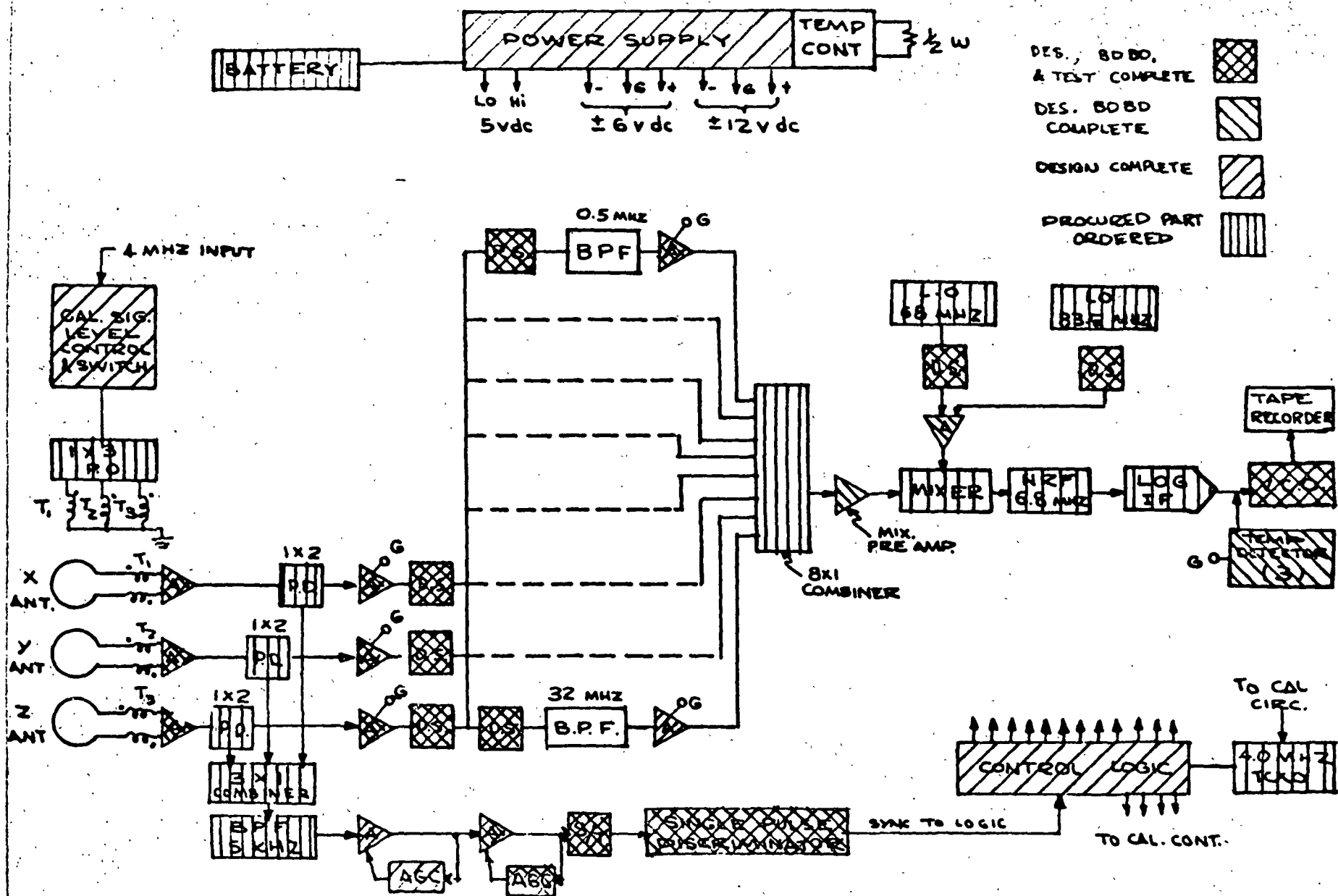
C. By pass Mix Problems with wideband Log Video.
Vendor available who can modify an existing design.
Further analysis required.

4. Gated Amplifier Transient - Post Crystal Only.

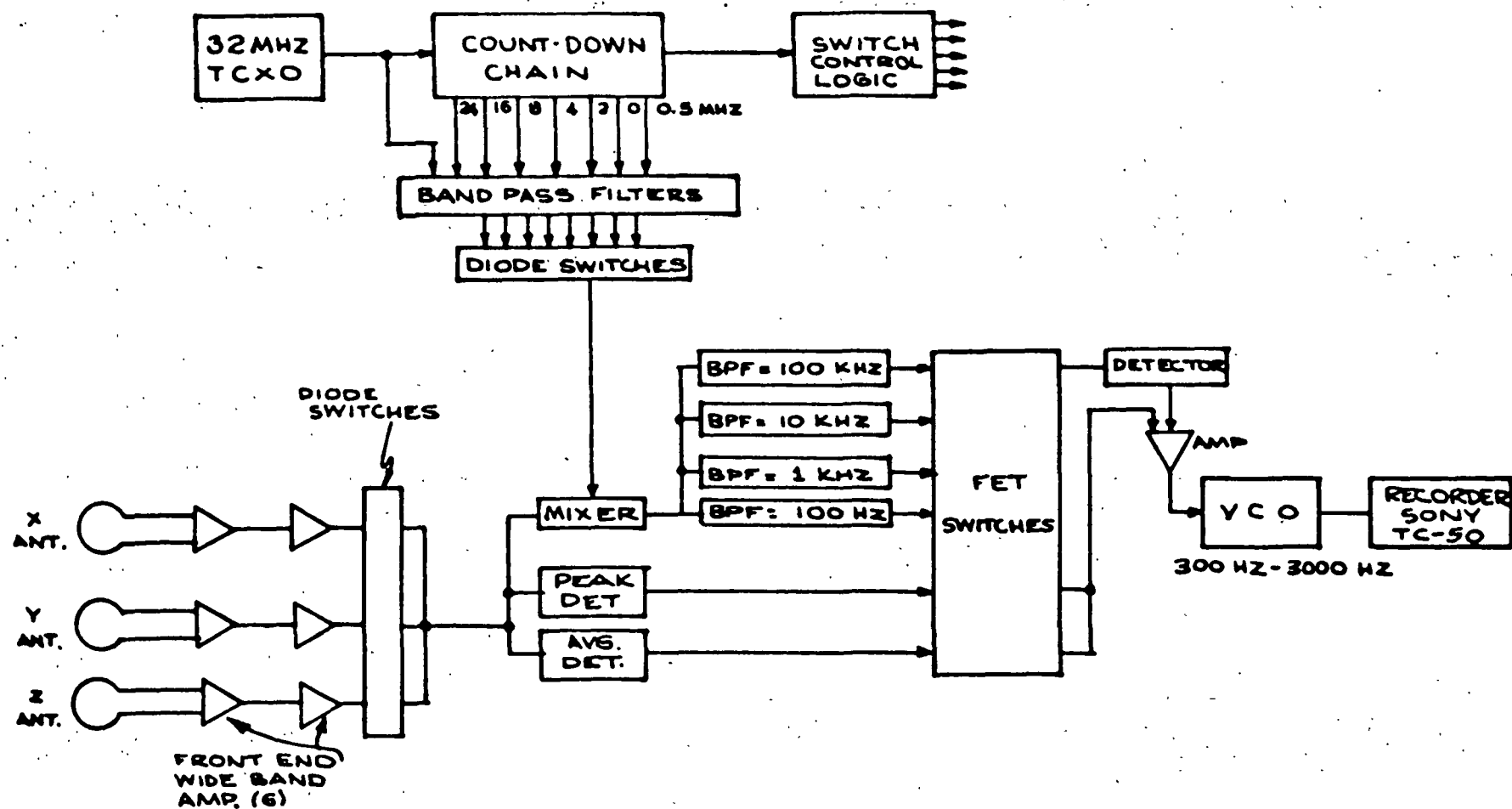
Solution: Brute force RC squelch finally required.

Status: Breadboard modified, test complete, problem considered solved.

S.E. P FIELD EVALUATION RECEIVER



EMI NOISE TEST RECEIVER



**PRIMARY RESPONSIBILITIES
OF
MECHANICAL DESIGN**

1. ASSEMBLY OF DESIGN INFORMATION:

NASA

MIT/CSR

MIT/DL ELECTRICAL DESIGN GROUP

MIT/LL ANTENNA DESIGN GROUP

2. STRUCTURAL DESIGN:

FOR EASE OF HANDLING BY ASTRONAUTS

TO MATE WITH LEM AND LRV

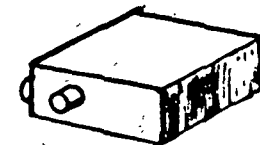
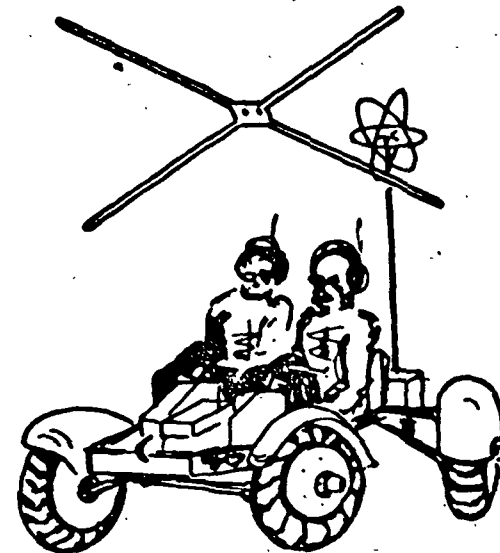
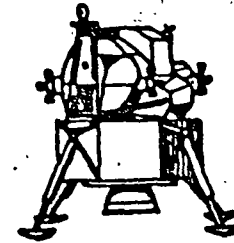
TO WITHSTAND MECHANICAL STRESSES

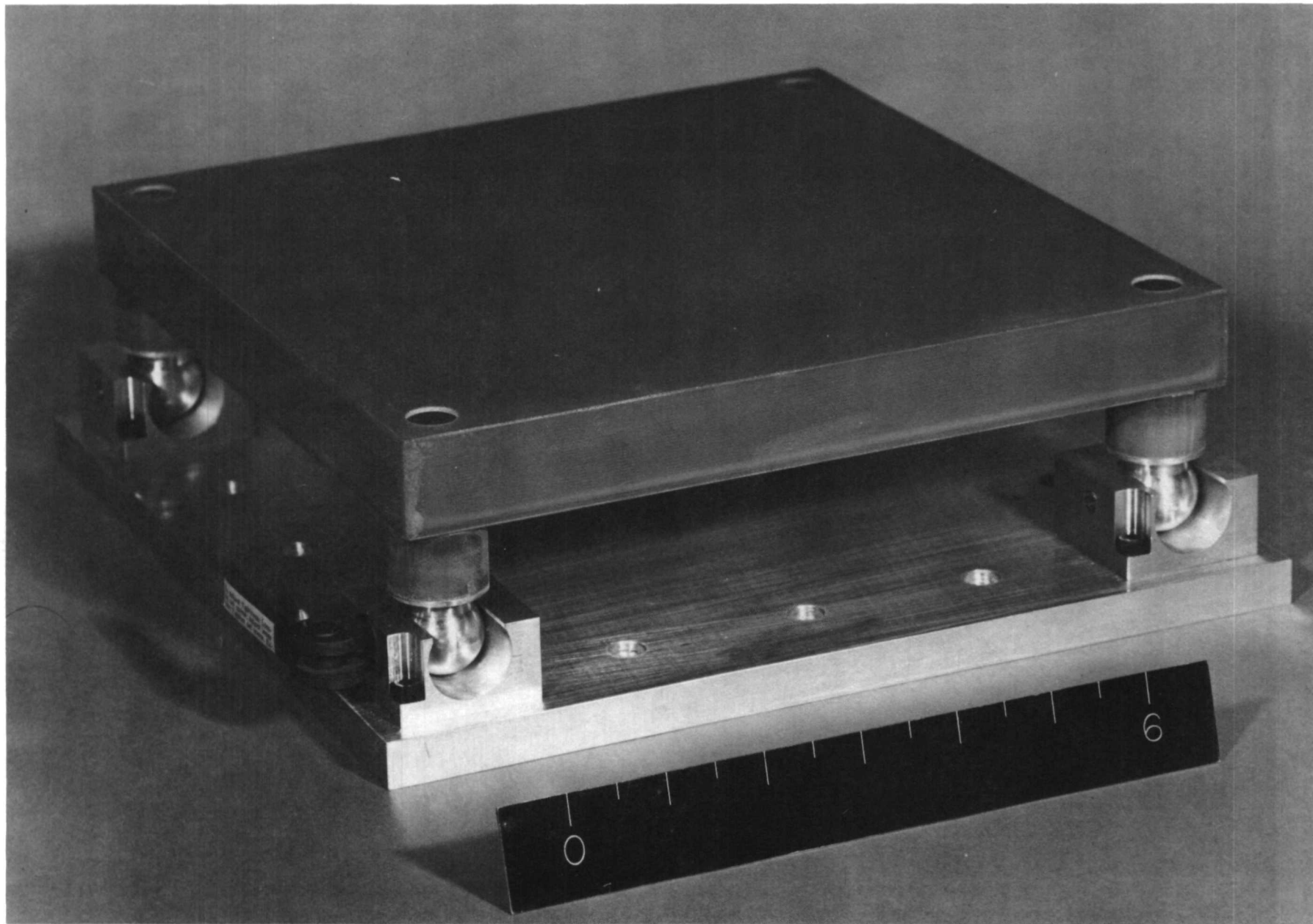
3. THERMAL DESIGN:

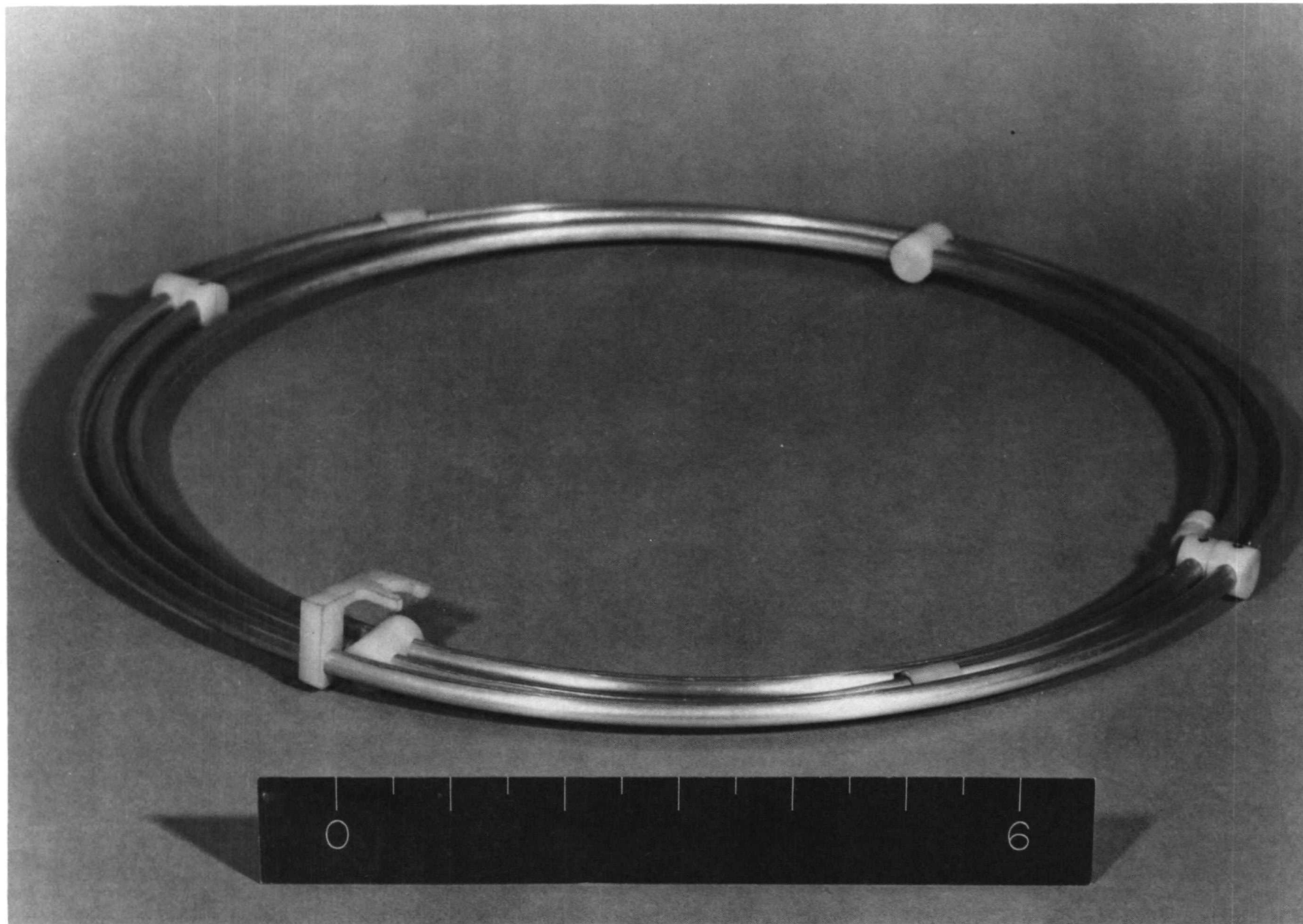
TO ASSURE RELIABLE OPERATION OF THE ELECTRONICS,
RECORDER, BATTERIES, AND SOLAR CELLS

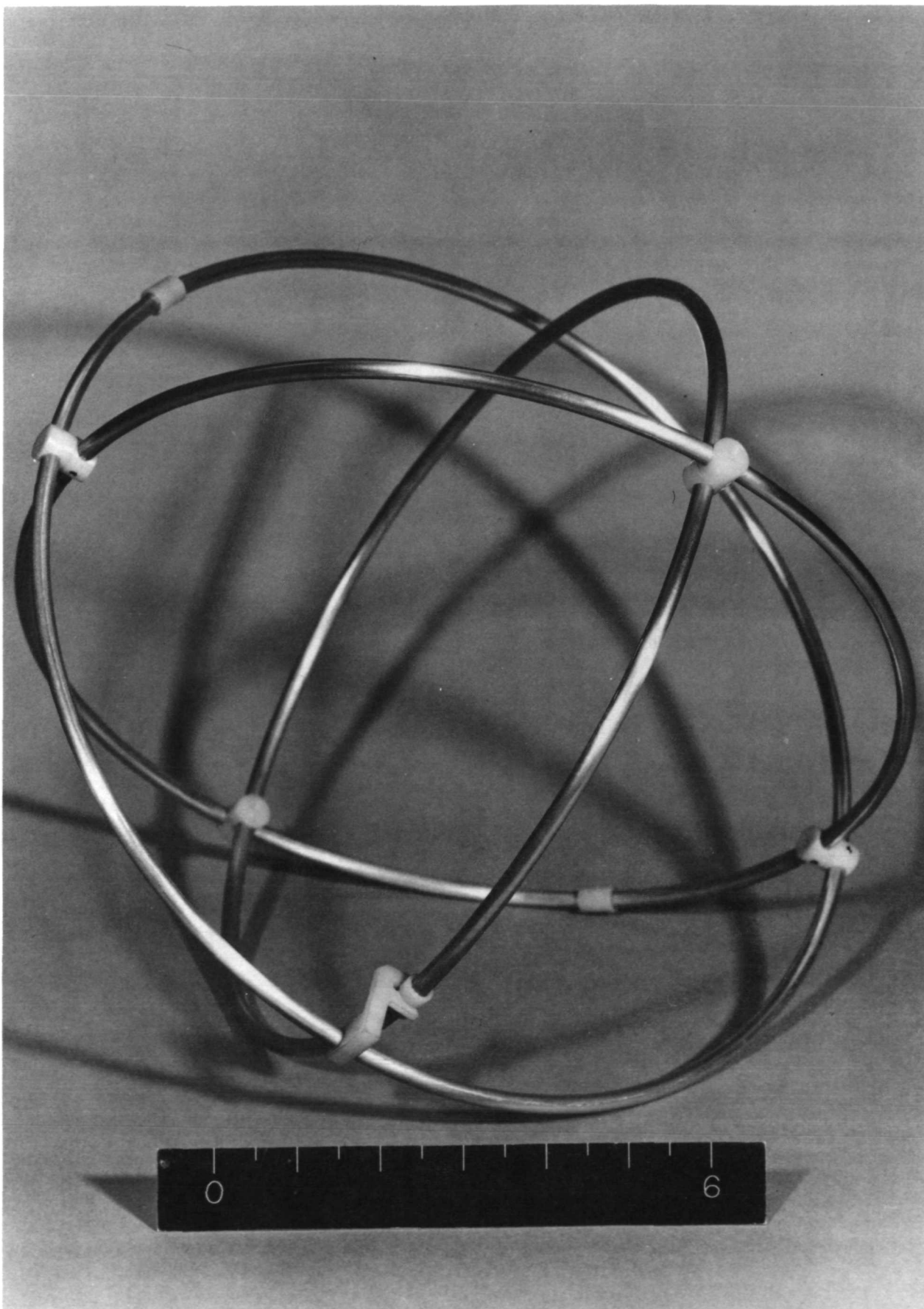
SEP DEPLOYMENT

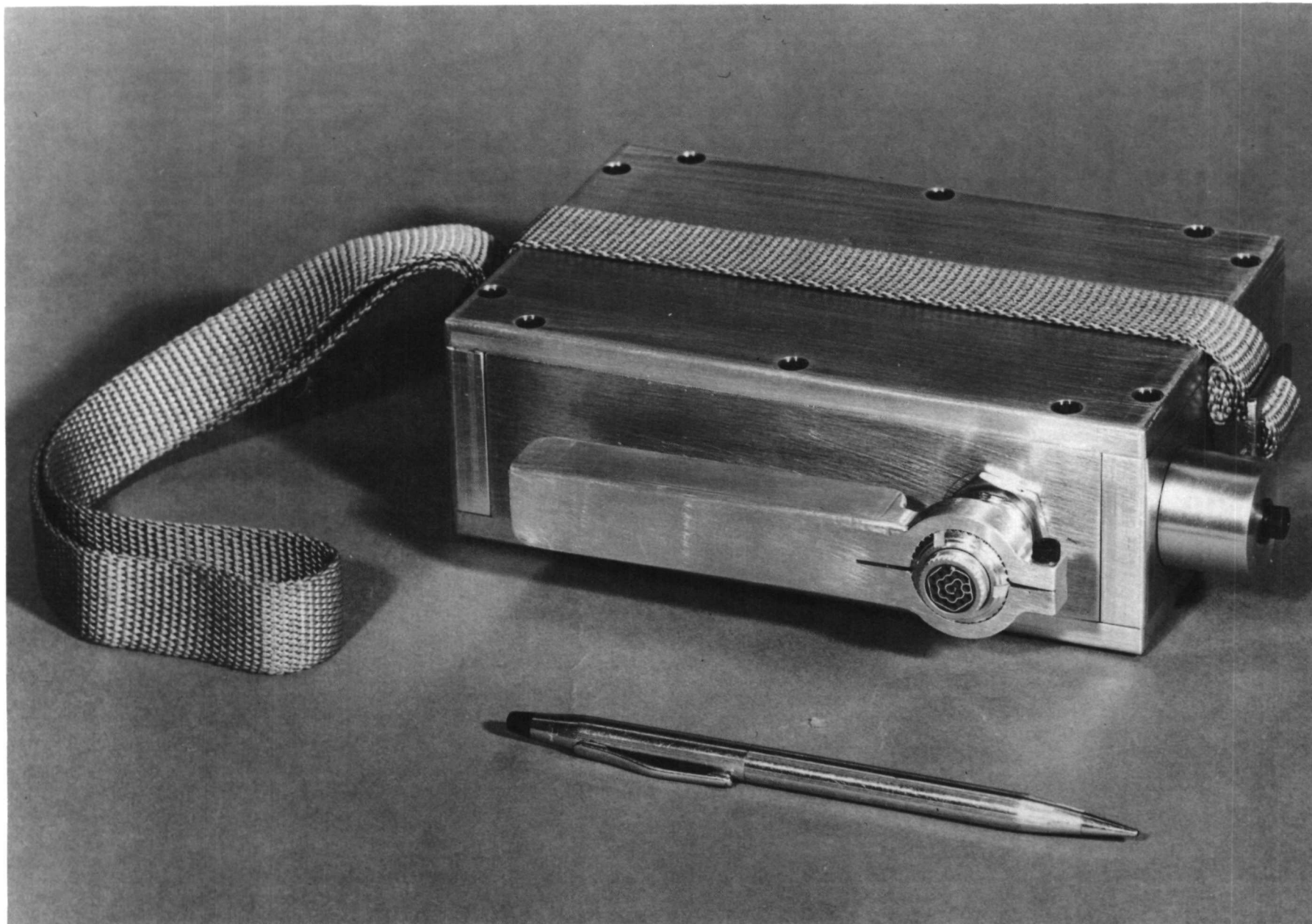
1. REMOVE TRANS & RCV FROM PALLET
2. DEPLOY TRANS ANTENNA
3. DEPLOY SOLAR PANEL
4. SWITCH ON TRANS
5. MOUNT RCV ON ROVER
6. DEPLOY RCV ANTENNA
7. REMOVE RCV THERMAL BLANKET
8. TURN ON RCV
9. REMOVE TAPE RECORDER

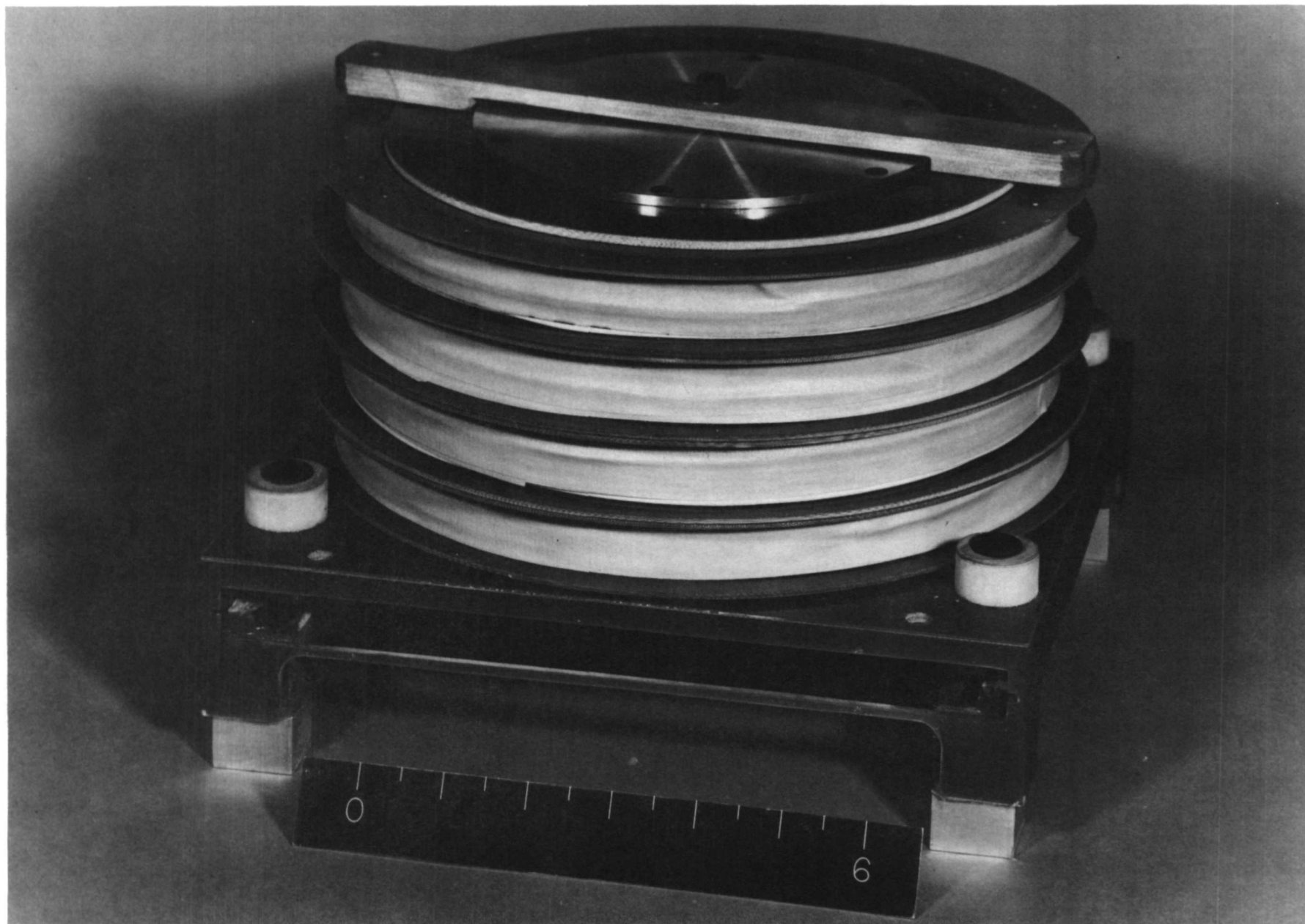


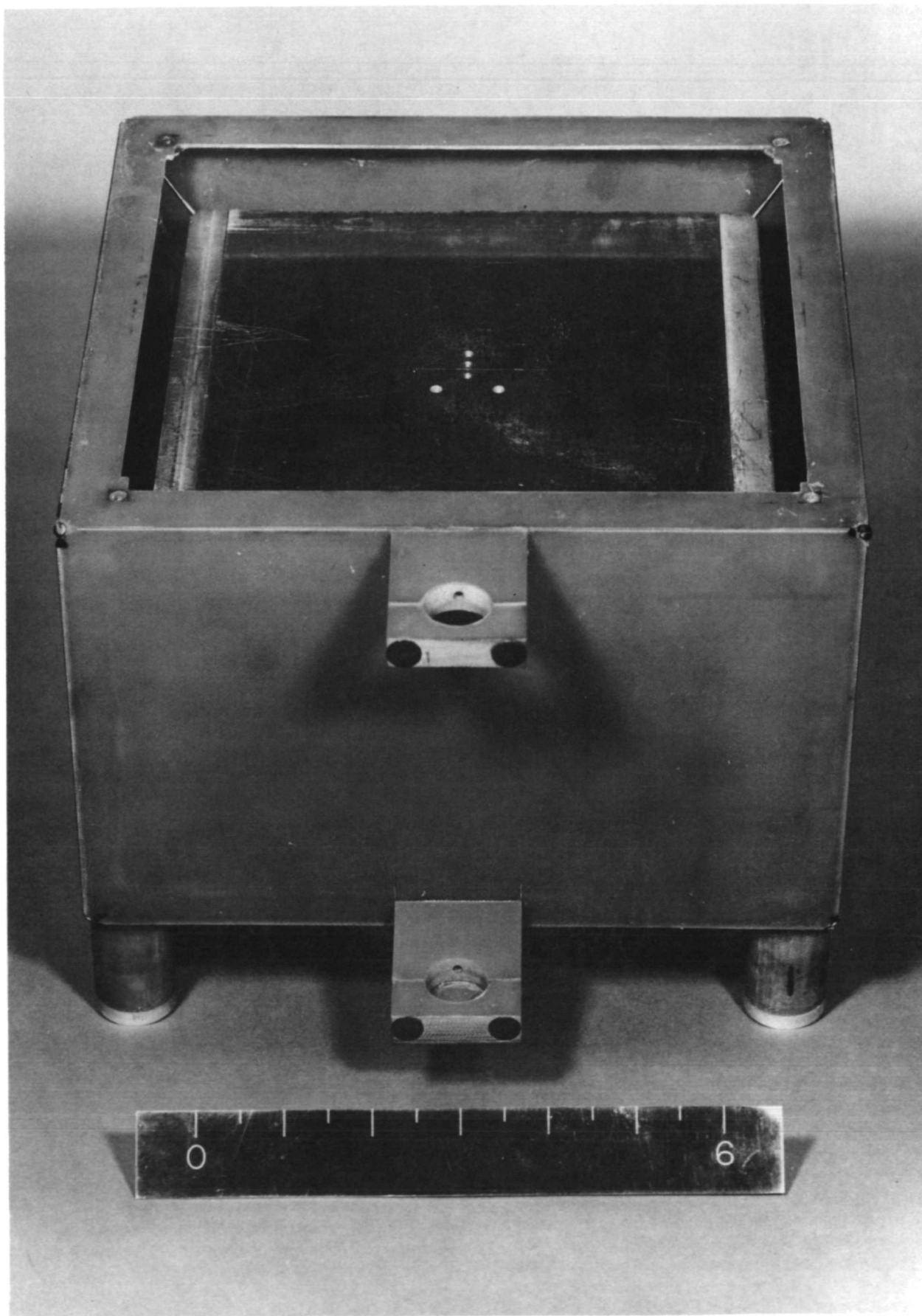


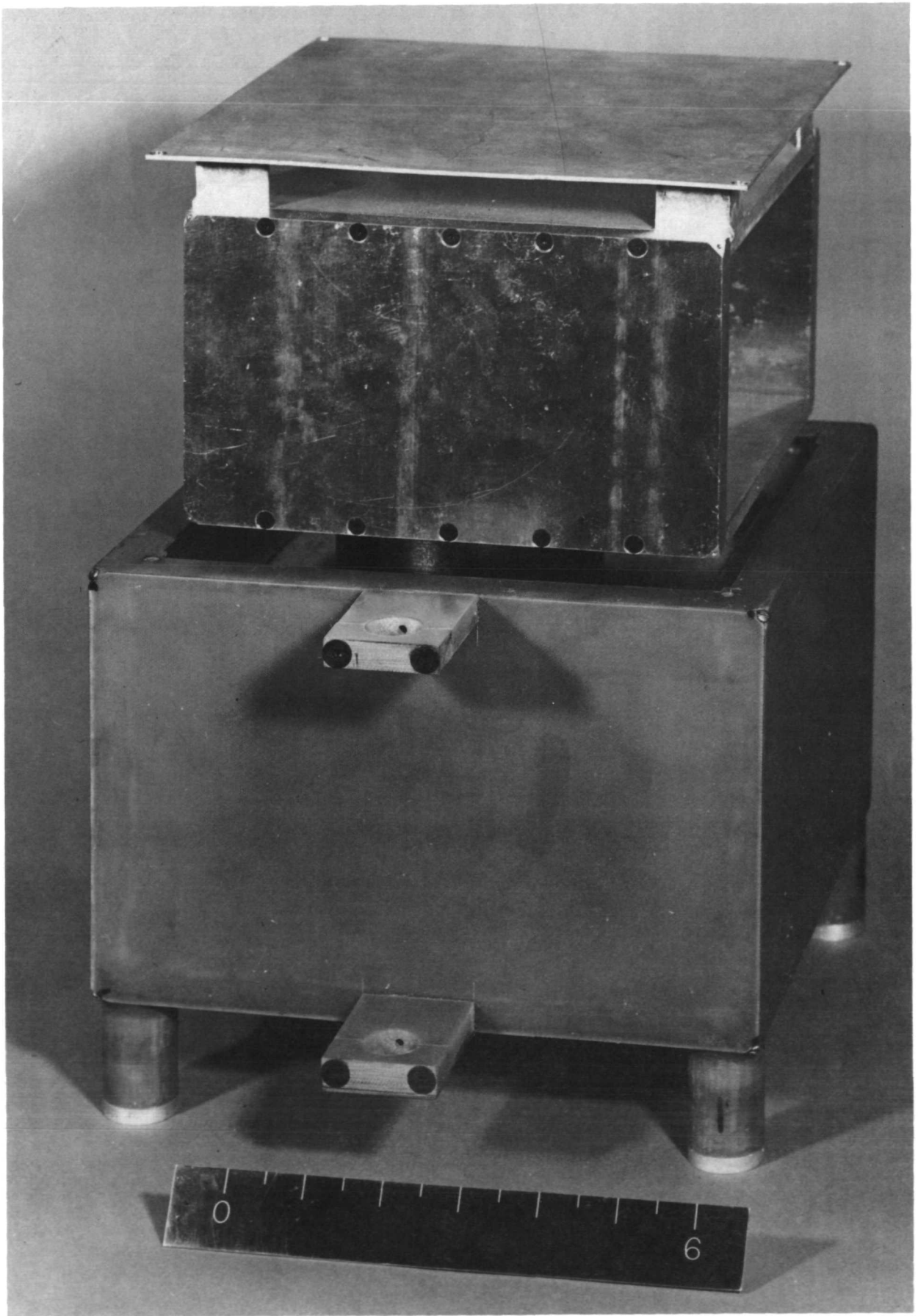






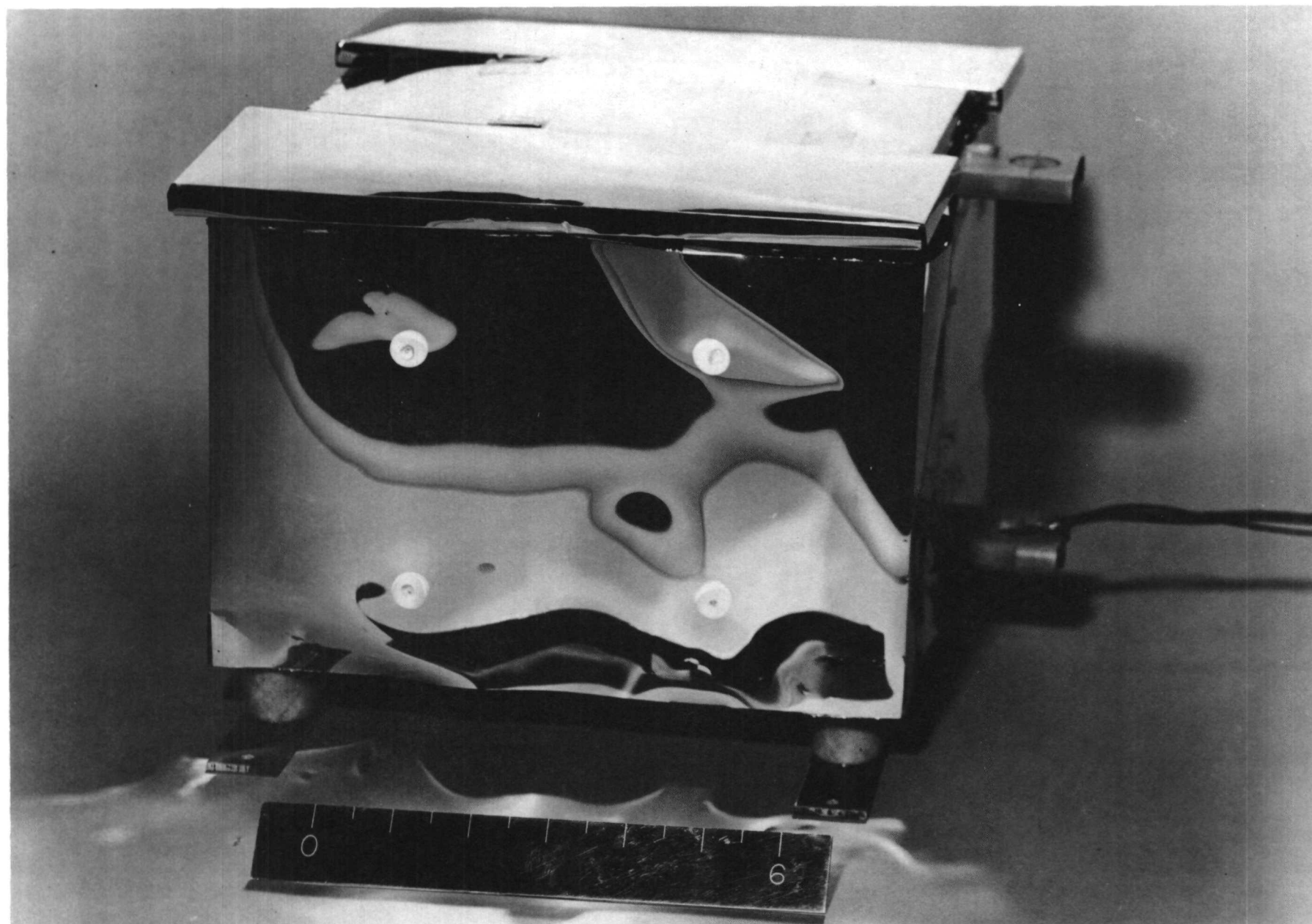


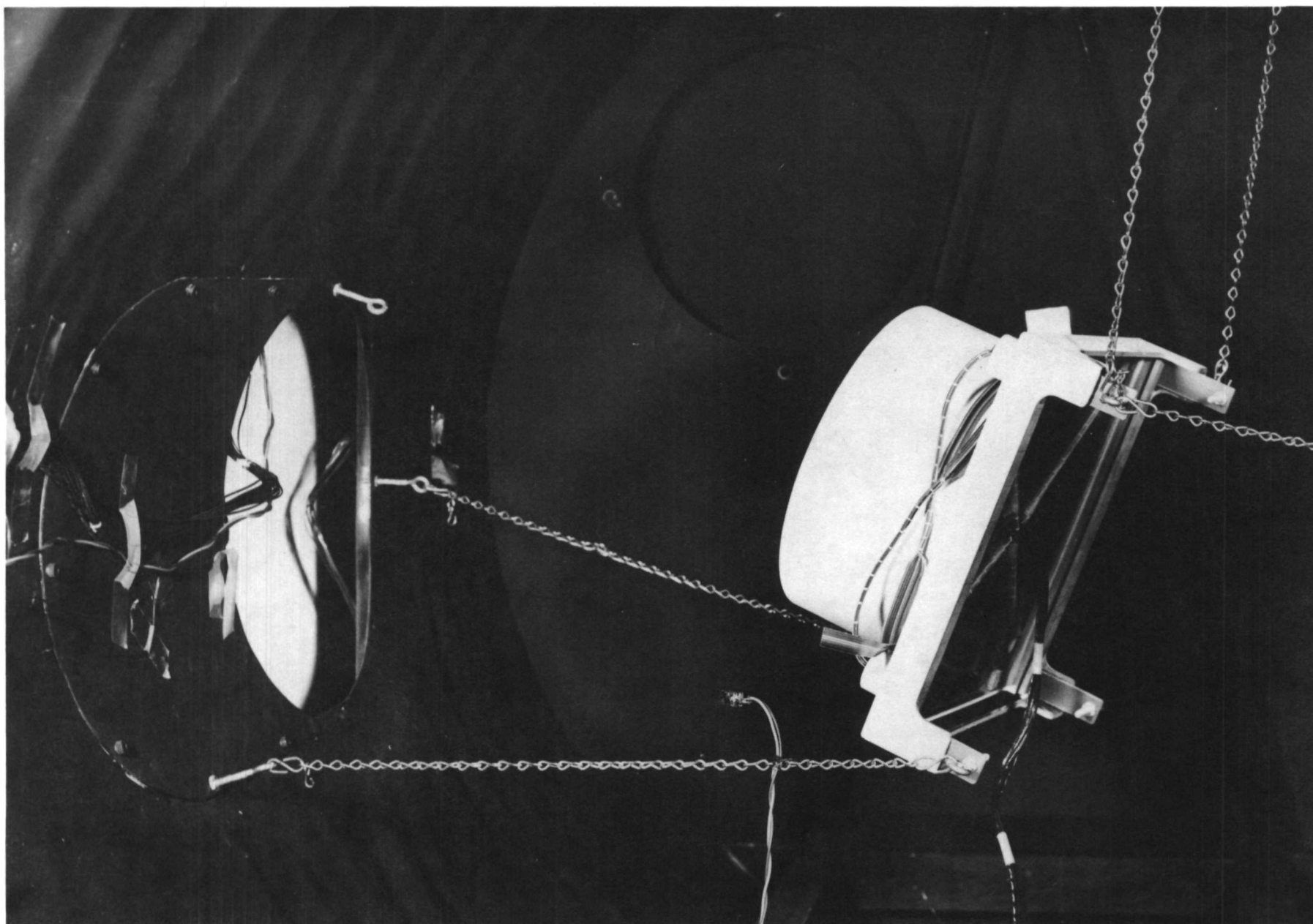




THERMAL BALANCE

1. HEAT GENERATED IN THE EQUIPMENT
2. HEAT ABSORBED FROM DIRECT SOLAR RADIATION
3. HEAT ABSORBED FROM SOLAR RADIATION REFLECTED FROM LUNAR SURFACE
4. HEAT ABSORBED FROM IR RADIATION FROM LUNAR SURFACE
5. HEAT ABSORBED FROM MAN PLACED OBJECTS
6. HEAT CONDUCTED TO OR FROM THE LUNAR SURFACE
7. HEAT LOSS FROM EQUIPMENT BY RADIATION
8. HEAT STORAGE OR LOSS THROUGH EQUIPMENT TEMPERATURE CHANGE





SYSTEM INTEGRATION

- THE ROLE OF SYSTEM INTEGRATION IS TO ASSURE THAT SYSTEM MEETS THE CRITERIA DEFINED IN THE END ITEM SPECIFICATIONS.
- THE CURRENT END ITEM SPECIFICATION IS PRELIMINARY. IT REQUIRES EXPANDED COVERAGE, MORE DETAILED QUANTATIVE SPECIFICATIONS, AND WILL PROBABLY BE SUBJECT TO REVISIONS.
- RECENT SYSTEM INTEGRATION EFFORT HAS BEEN DIRECTED TOWARD OBTAINING INFORMATION FOR COMPLETION OF THE EIS.
- EFFORT HAS CONSISTED OF ERROR ANALYSES AND THE IDENTIFICATION OF POTENTIAL SYSTEM DESIGN PROBLEM AREAS.

EIS ADDITIONS

- TYPICAL ADDITIONS TO SPECS ARE:

- DEFINITION OF OPERATING ENVIRONMENT

THERMAL ENVELOPE

EXPECTED RANGE OF SURFACE ELECTRICAL PROPERTIES

TIME BASELINE

- DEFINITION OF OPERATIONAL REQUIREMENTS

- MECHANICAL AND THERMAL SPECIFICATIONS

- TOLERANCES

POTENTIAL EIS REVISIONS

ENGINEERING DATA FROM THE INTEGRATION STUDIES, BREADBOARD SUB ASSEMBLY EVALUATIONS, AND THE GLACIER FIELD TESTS, INDICATE THE NEED FOR REVIEW OF SEVERAL ORIGINAL DESIGN CONCEPTS TO ALLEVIATE POTENTIAL HARDWARE DESIGN PROBLEMS:

THE AREAS FOR REVIEW INVOLVE:

- (1) REQUIREMENT FOR BEAM ROTATION REDUCED TO 5 HIGHEST FREQS.
- (2) POSSIBLE REDUCTION IN RESOLUTION ALLOWABLE IN RECEIVED ENVELOPE.
- (3) NEED FOR AN ANTENNA DESIGN ALTERNATIVE TO THE MULTI-ELEMENT DIPOLE DESIGN.
- (4) DEFINITION OF A 1% RELATIVE ACCURACY RATHER THAN ABSOLUTE ACCURACY REQUIREMENT.

SUMMARY

1. CSDL Phase I Output 7/23/70
Preliminary work statement and specification.
2. CSDL Conceptual Design Report 7/23/70
Preliminary recorder specification, mechanical configuration, power estimates, and deployment estimates.
3. Tape Recorder Survey Complete 6/23/70
Recommends DSEA.
4. Initiate Electrical and Mechanical Detail Design 9/16/70
5. Preliminary Rover Noise Test Report 11/2/70
6. Tape Recorder Procurement Package (Leach DSEA) At Contract Office 11/27/70
7. SEP Proposal Delivered 12/11/70

APPENDIX 5.5

SEP MEMO SEP-10-T EMI TESTS
ON THE ROVER TRACTION MOTOR DRIVE.

Eldon

THE CHARLES STARK DRAPER LABORATORY
A DIVISION OF MASSACHUSETTS INSTITUTE OF TECHNOLOGY
88 ALBANY STREET
CAMBRIDGE, MASSACHUSETTS 02139

SEP-10-T

Digital Dev. Memo #571

To: Eldon Hall
From: Don Bowler & George Jones
Date: 2 November 1970
Subj: EMI Tests on the Rover Traction Drive Motor

Tests were run at the Marshall Space Flight Center on October 26 and 27 on a Rover Traction Drive Motor. The cooperation and help received from the Space Flight Center people was greatly appreciated.

TEST CONFIGURATION

The tests were run in three configurations: with the electronics unshielded, shielded, and outside the screen room. Figure 1 shows a diagram of the physical arrangement of the equipment.

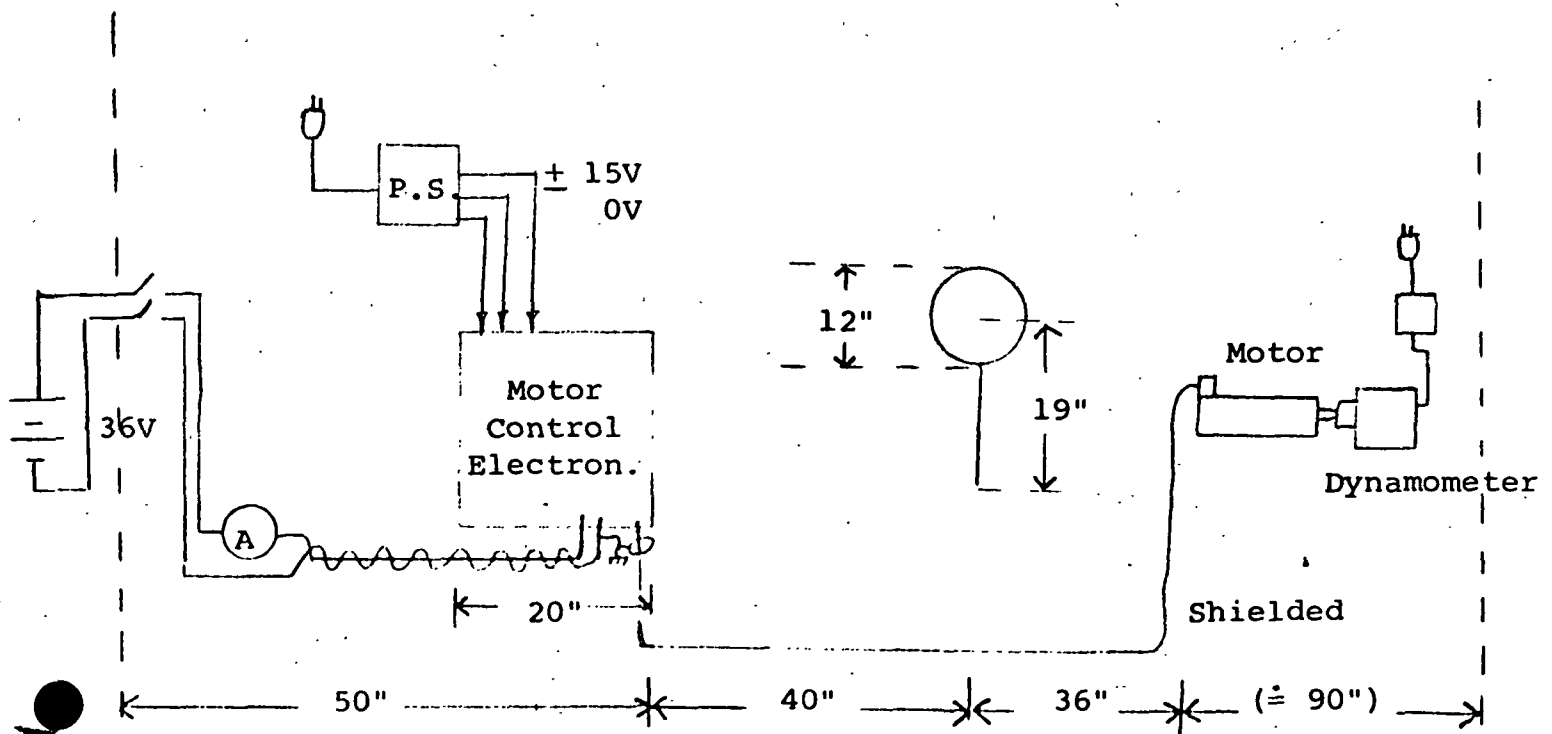
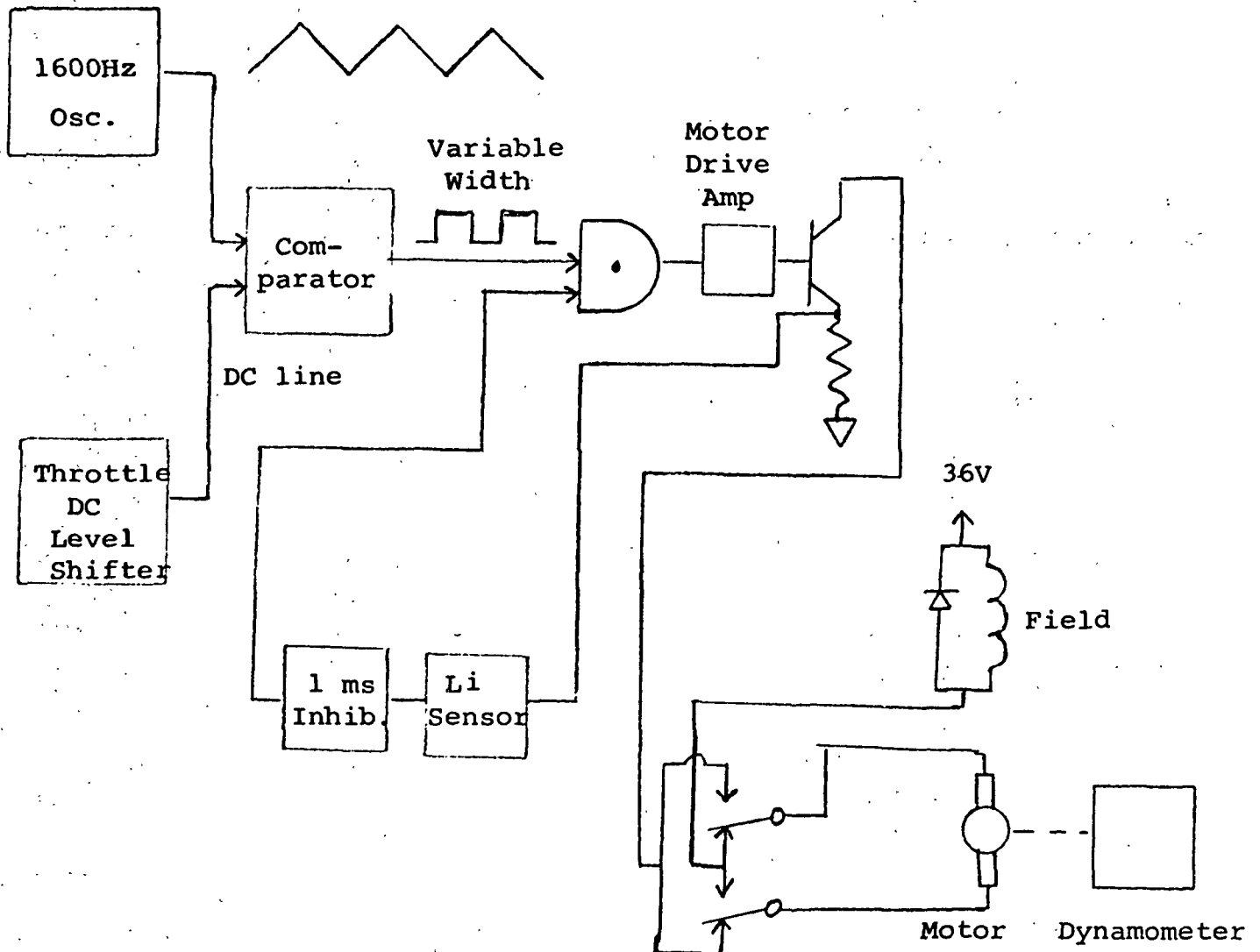


Fig. 1. Test Configuration.

TEST ITEM

The motor control electronics was in a breadboarded configuration and a functional drawing is shown in Figure 2.



Level 1
Level 2
Output Wave L1
Output Wave L2

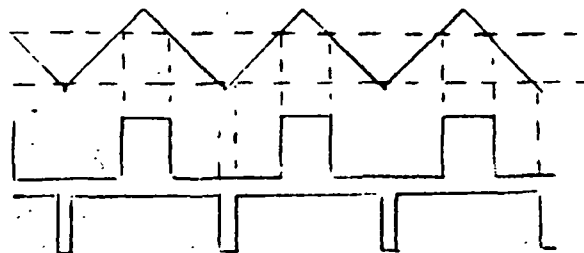


Fig. 2. Motor Control Electronics.

Essentially the throttle control varies the DC reference level into a comparator whose output is positive when the triangular input signal input exceeds the reference level. The width of the output pulse therefore varies as shown in the figure. The 36 volts is applied to the motor during the positive part of the waveform and the resulting motor current is a function of the pulse width and the dynamometer torque setting. The motor speed varies inversely with the dynamometer torque and the current varies directly with the torque.

There are several variables to monitor during the test and this aspect of the test could have been better controlled. There is a current sensor that shuts the torque off for approximately one millisecond when the current gets too high (25 amps).

The motor is 3-1/2 inches in diameter by 5-1/2 inches in length.

TEST PROCEDURE

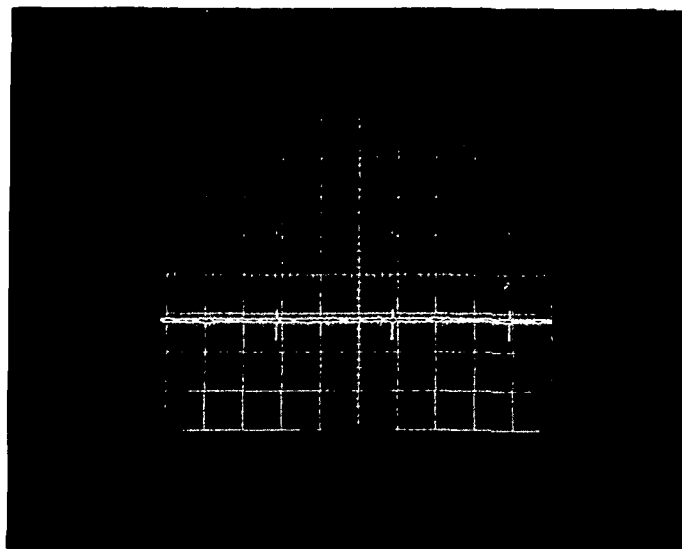
The purpose of the test was to find out how much interference the drive motor would generate that could be detected by the SEP receiver. The SEP receiver is in the process of being designed and presently plans to utilize a Motorola MC-1553 video amplifier in the front end. Accordingly, the amplifier (Fig. 4) was breadboarded and packaged in a metal box with its own 6 volt battery. Two BNC connectors for input and output and a power switch were also provided. The video amplifier was used in a qualitative manner to assess the radiation from the test item.

With everything unshielded and set up in the screen room as shown in Figure 1, the amplifier output, as seen on a Tektronix type 454 scope, was saturated by spikes at 1.6 KHz and there appeared to be quite a bit of noise besides the 1600 Hz component. Accordingly, the power leads were twisted and shortened and shielded with aluminum foil. The control electronics was also shielded with aluminum foil. This appeared to reduce the amount of noise and a picture of the video output during test 2 is shown in Figure 3.

This figure indicates that the amplifier is saturated by a 1600 Hz component. The video amplifier circuit along with a gain vs frequency plot is shown in Figures 4 and 5.

Test 1 and 2 were run with this configuration and in the middle of test 2 a drive transistor in the motor drive electronics burned out due to the fact that the heat sinks were not able to radiate in the shielded enclosure and overheated.

This ended the shielded type tests.



Vertical 0.5 V/cm
Horizontal 200 μ sec/cm

Fig. 3. Video Amplifier Output.

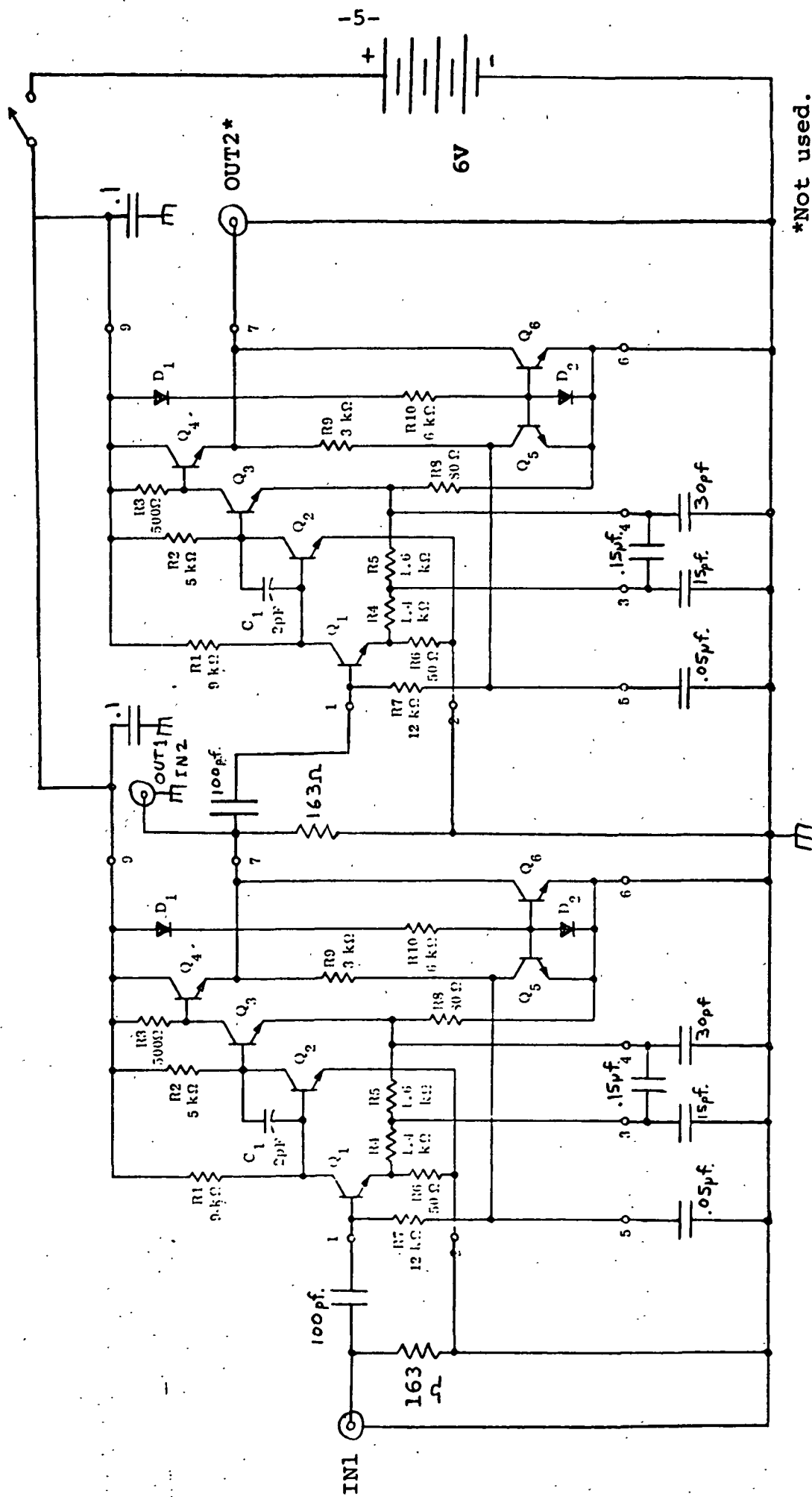
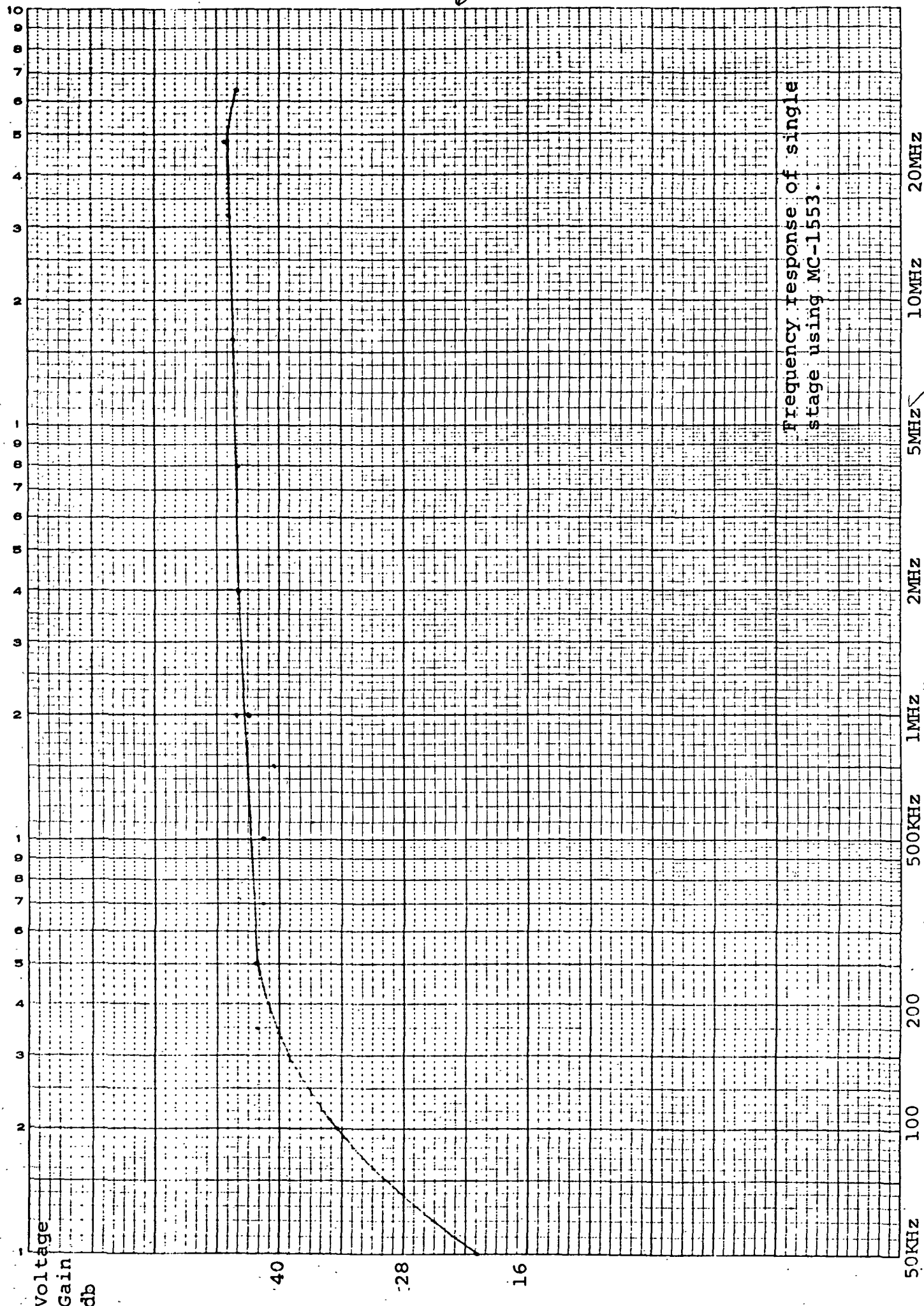


Fig. 4. Wide Band Preamplifier Using Two MC-1553's. Only First Stage was Used in Tests.

6



Frequency response of single stage using MC-1553.

Fig. 5.

Test 4 was run with the equipment as shown in Figure 1. While tests 5-16 were run with only the motor, its cable, and the dynamometer in the screen room. The electronics was placed outside and to the right of the motor rather than to the left as shown in Figure 1.

Test 5 was the last test run on October 26th and while a photograph of the video amplifier output was not taken, measurements were made and the peak amplitude of the 1600 Hz noise had been reduced from 1.1 volts shown in Figure 3 to 0.25 volts. The ambient amplifier noise was 10 mv peak to peak white noise.

Additional pictures would have been taken but the battery ran down and the video amplifier didn't work the next day. The decrease in amplitude just noted is not felt to be due to the battery drop but this possibility has not been excluded.

Tests 6-17 were run on October 27th and Table 1 summarizes all the tests. It would have been desirable to have measured the speed of the motor and its current but the voltage waveform applied to the motor driver is shown in the table.

The average current shown is that measured by the ammeter in the 36 volt supply and the pulses to the motor are not filtered on the breadboard.

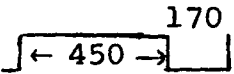
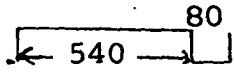


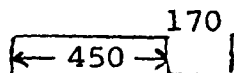
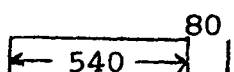
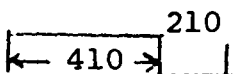
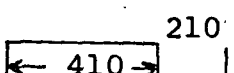
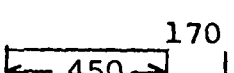
Data was taken using the Stoddart NM22A receiver with a 20 foot cable connecting the loop antenna to the receiver. The cable was a two conductor coax with one side tied to the shield at the receiver end. The loop antenna was electrostatically shielded with the shield returned through the cable shield. Both broad band and narrow band measurements were made over the frequency range of 500 KHz to 32 MHz.

The noise was not sharply tunable. The bandwidth of the NM22A is 10 KHz for the broad band position and 3 KHz for the narrow band position. Noise levels between the measured frequencies were checked for the first few tests and were not found to vary significantly from the straight line data.

Data was also taken using the standard 41 inch rod antenna in the vertical position in order to provide reference data for comparison with standard EMI radiated measurements.

The broad band data are plotted in Figure 6-9 and some narrow band data is shown in Figure 10.

TABLE I

TEST NO.	DYNAMOMETER TORQUE IN OZ	AVG. CURRENT AMPS	MOTOR DRIVE ELECTRON.	MOTOR SPEED	DRIVER VOLT. WAVEFORM (μ sec)
1	80	9	Shielded	Fast	
2	14	4	Shielded	Very fast	
3	ambient	-	---	---	---
4	80	5	Unshielded	Slow	
5	80	5	outside screen rm.	Slow	
6-8	80	9	outside screen rm.	Fast	
9-11	14	4	"	Very Fast	
12-14	176	12	"	Slow	
15	176	12	"	Slow	
16	80	9	"	Fast	
17	Ambient	-	---	--	---

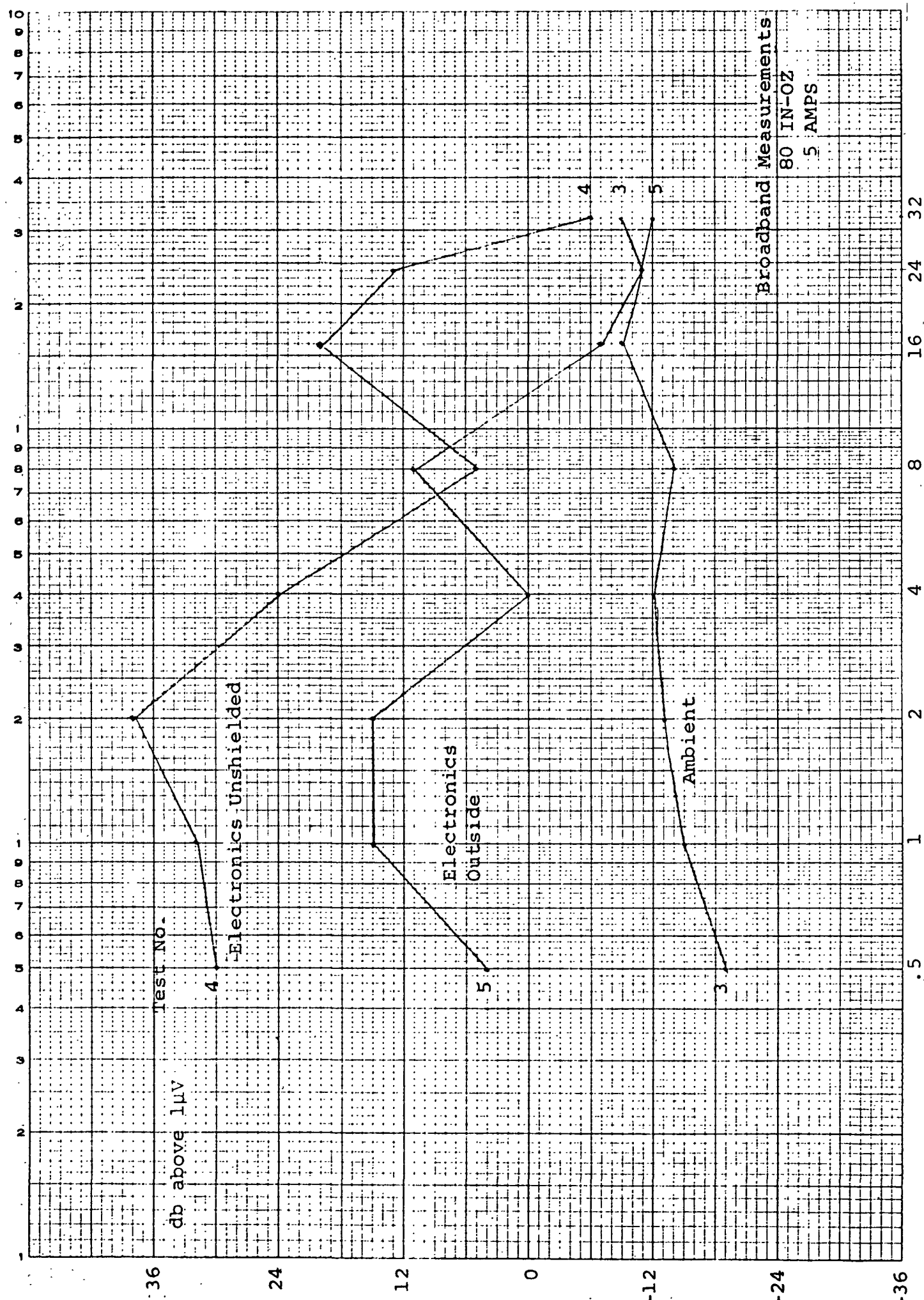


Fig. 6.

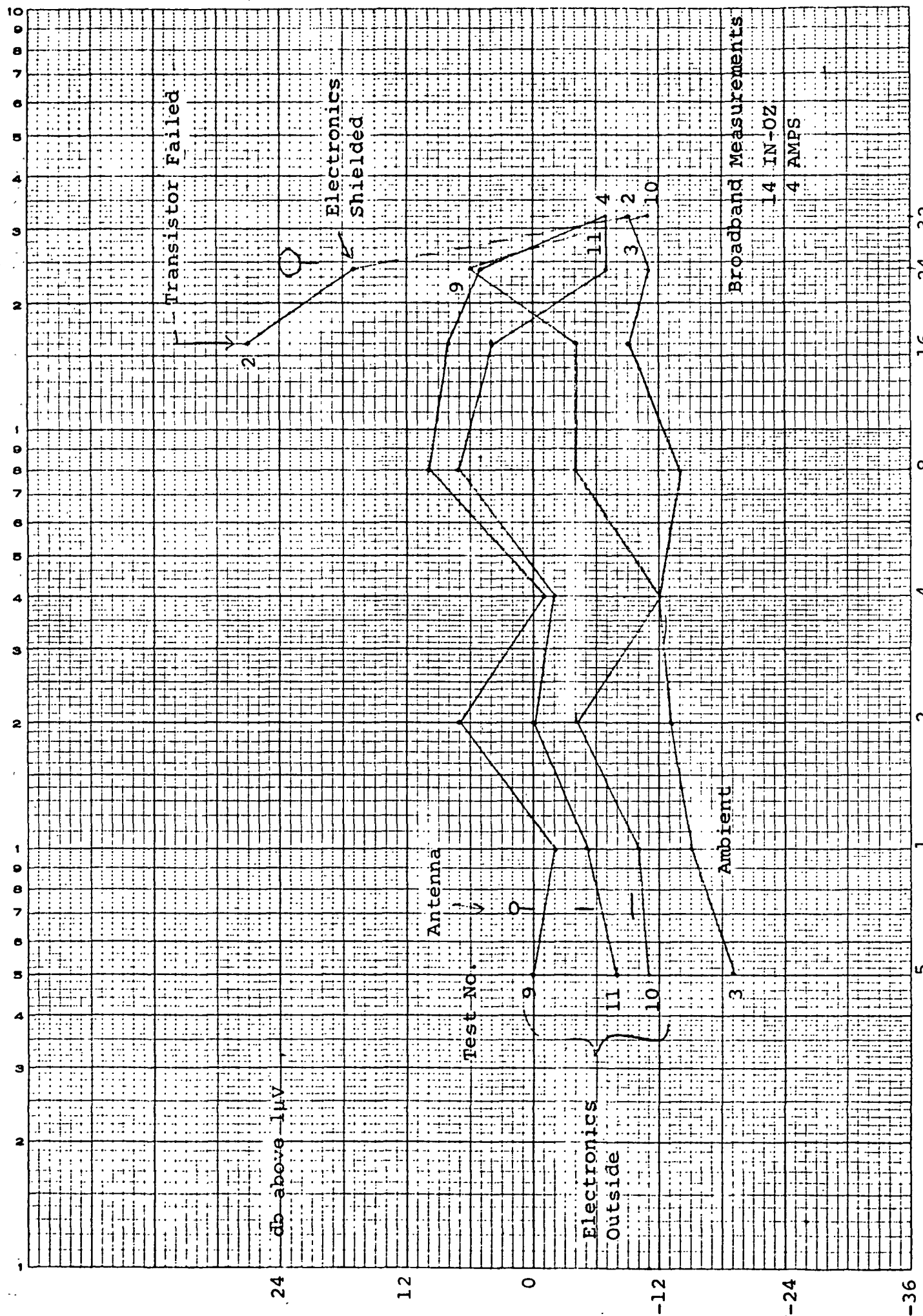


Fig. 7.

Frequency - MHz

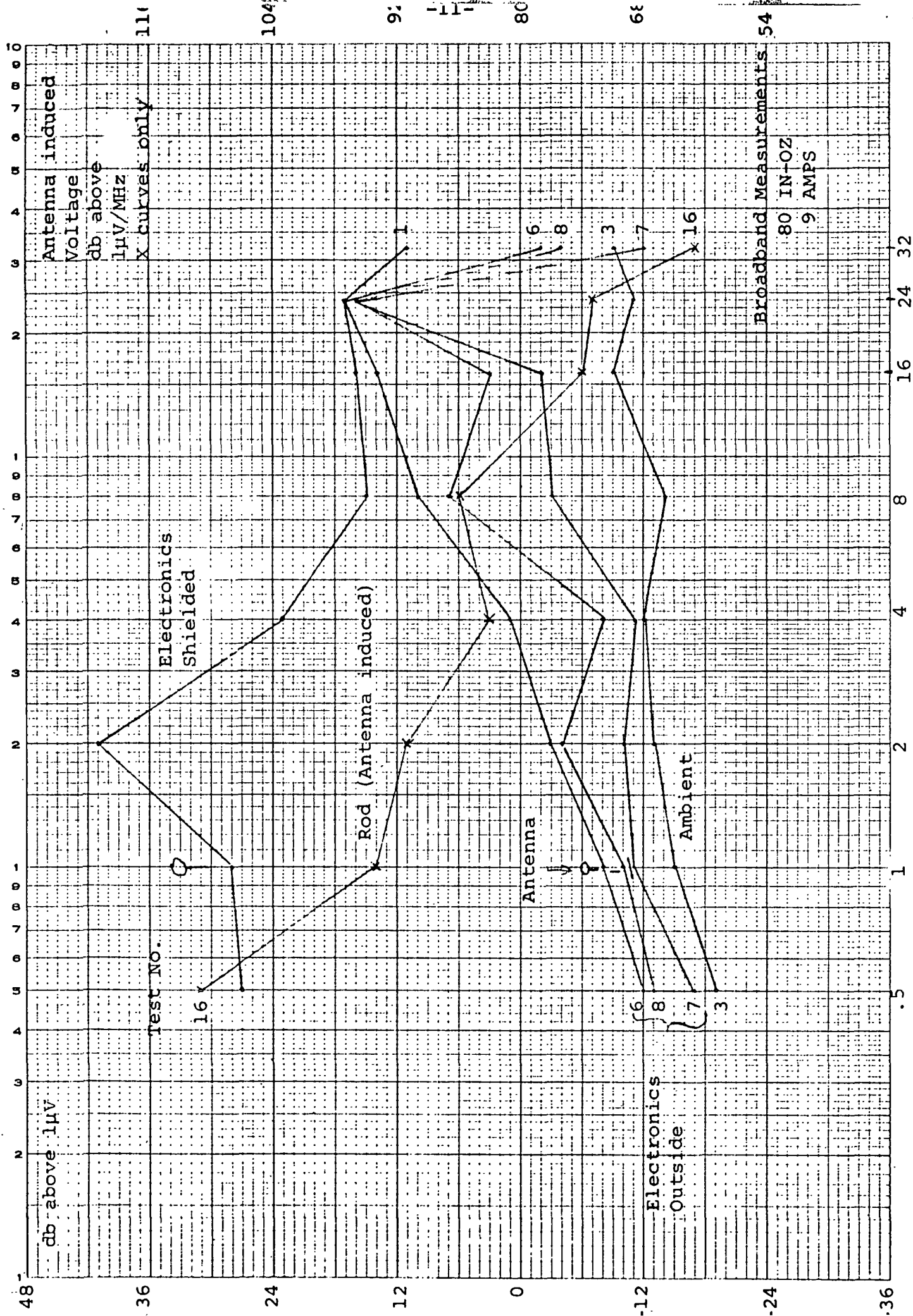


Fig. 8.

Frequency - MHz

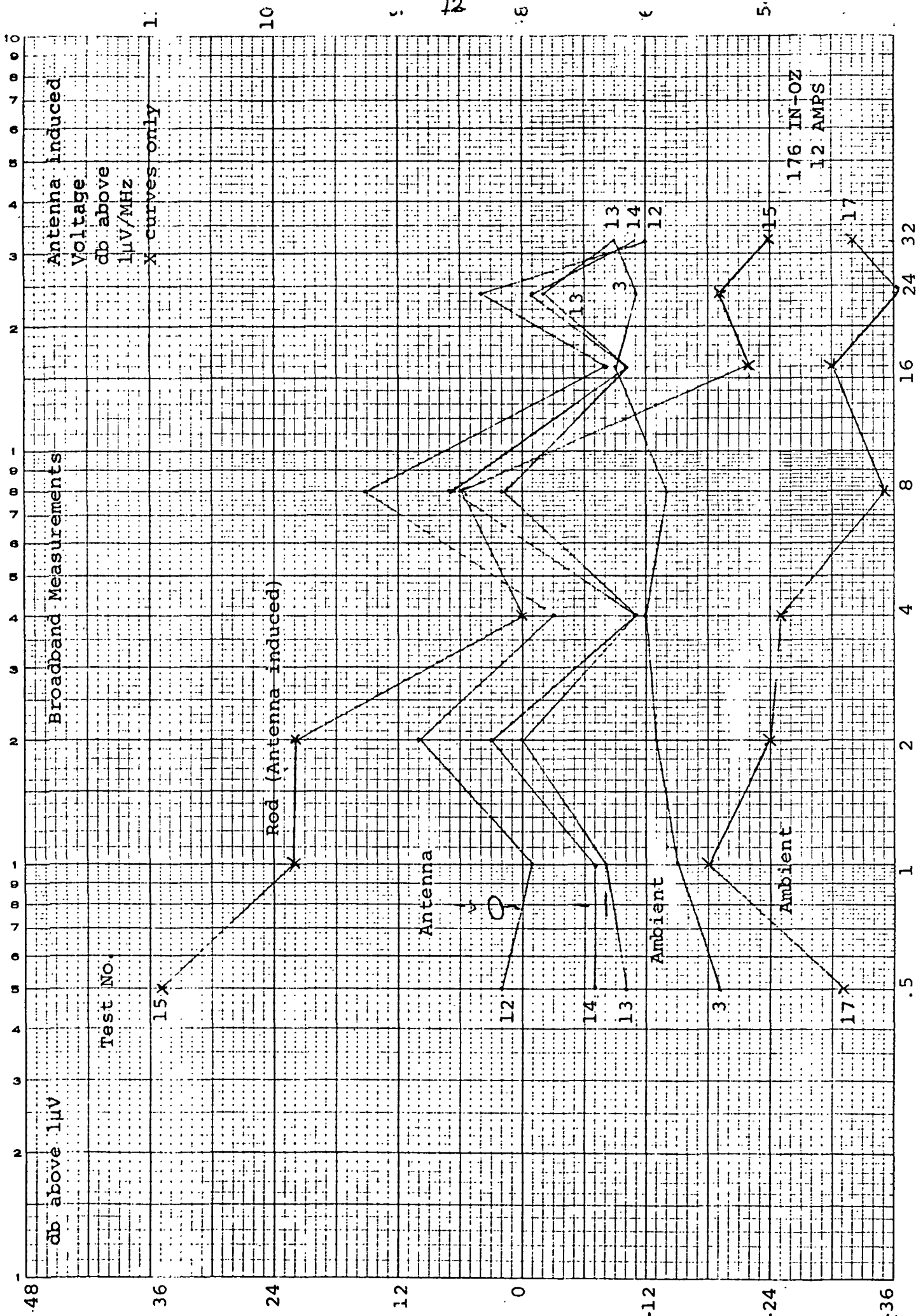


Fig. 9.

Frequency - MHz

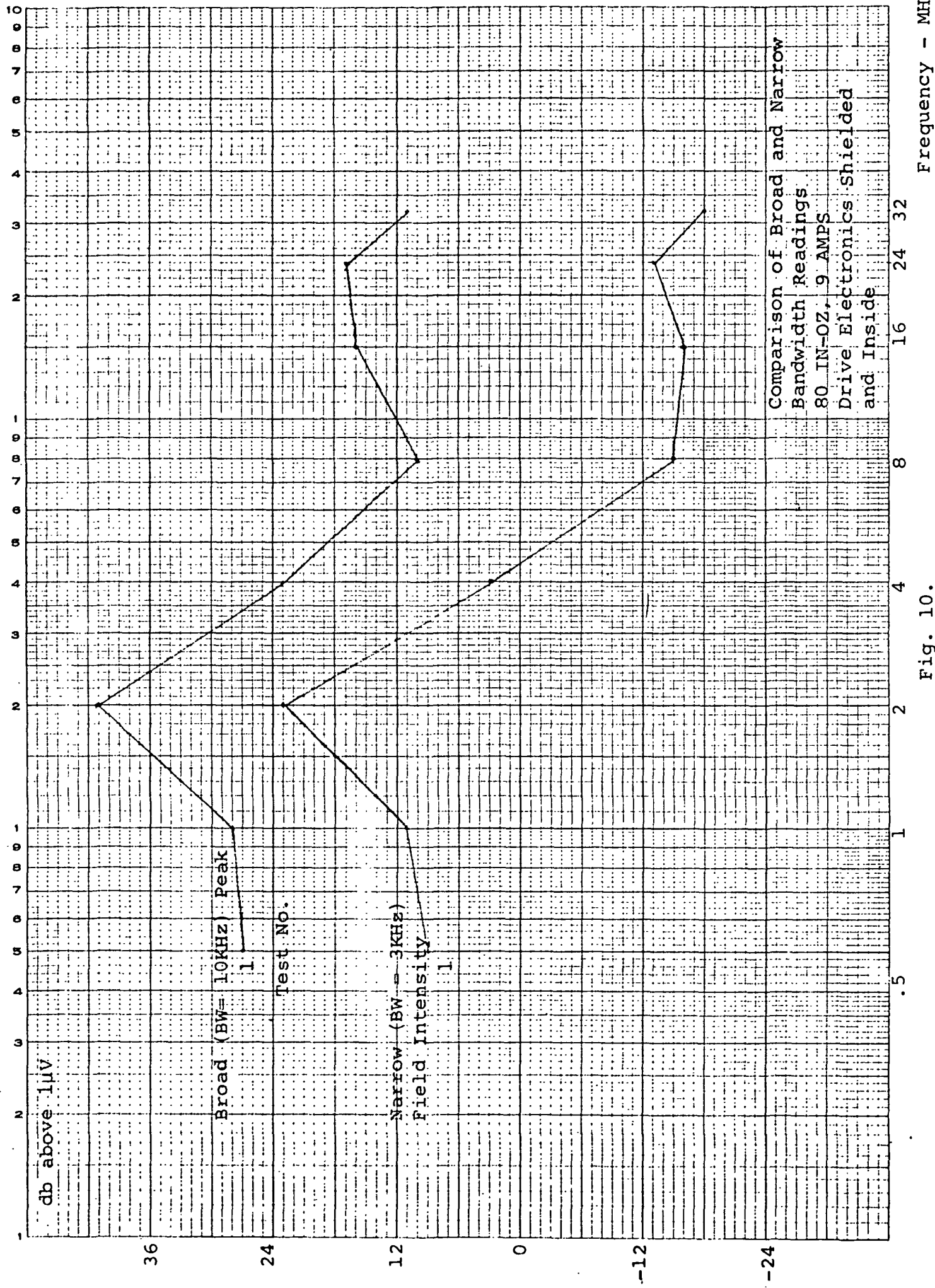


Fig. 10.

14

1034

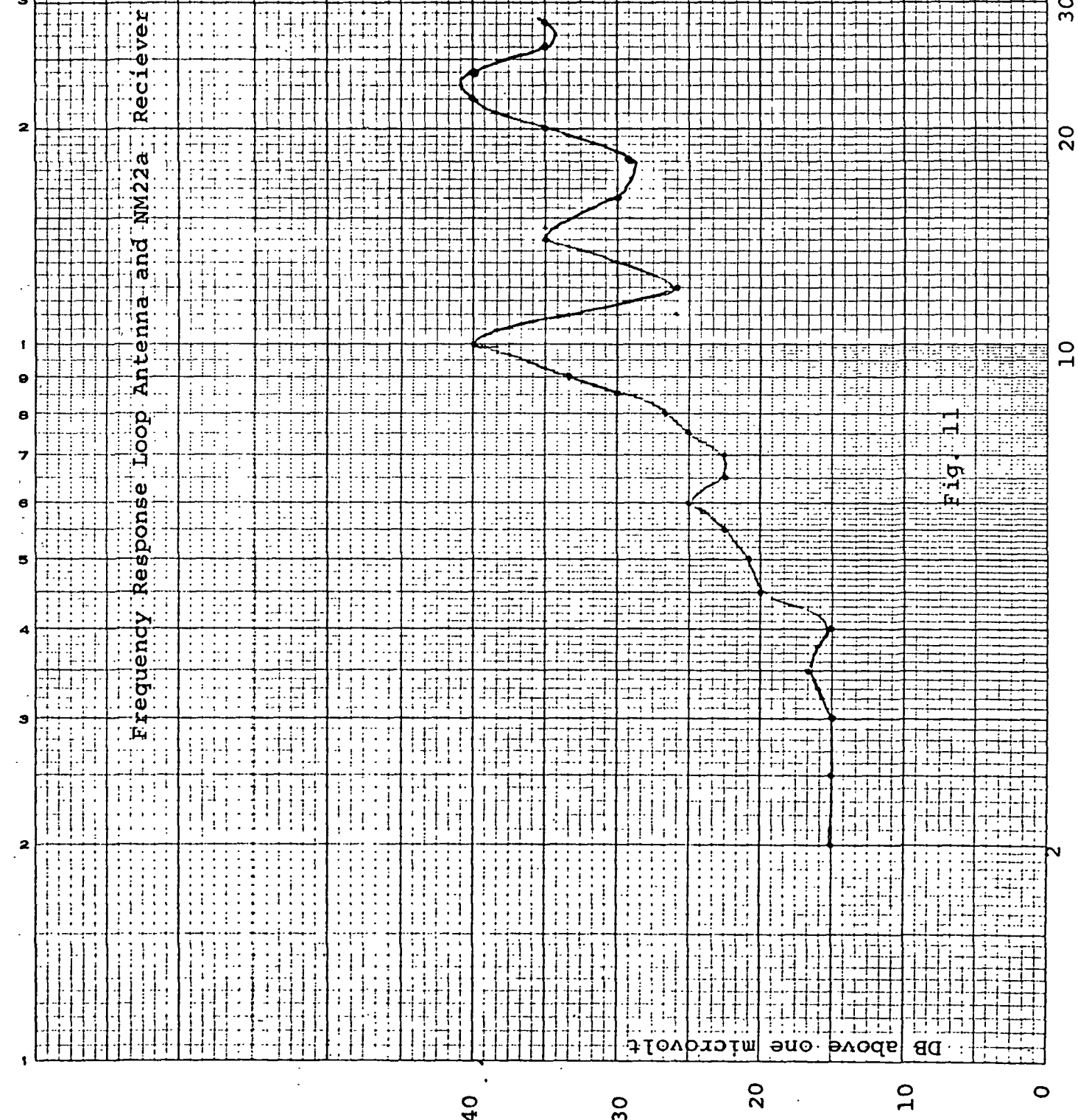


Fig. 11

Dist.

Ross Evans MSFC
Fred Cagle "
Harry Reid "
R.H. Baker
L. Bannister
J. Barker
R. Cushing
E.C. Hall
D. Hanley
D.G. Hoag
E.A. Johnston
L.B. Johnson
J. Martin
J. McKenna
A. Metzger -2
M. Murley
J. Partridge
R. Ragan
L. Schnee
W. Stameris
G. Trousil
C. Files

APPENDIX 5.6

EMI TEST RESULTS QUICK LOOK
(USING M.I.T. EMI RECEIVER)

APRIL 12, 1971

00097 7

RECEIVED

APR 12 1971

SEP-PMO

MEMORANDUM

TO: L. Johnson
FROM: W. Saltzberg
DATE: 12 April 1971
SUBJECT: EMI Test Results, Quick-look (using MIT EMI Receiver) -- PDR Action Item #21
REFERENCE: 1. Test Plan for Lunar Surface Experiments, Electromagnetic Compatibility Program, dated 19 Feb 1971 prepared by MSC, Houston

1. Introduction

Reduction of EMI Data, collected during test runs delineated in reference 1, is proceeding at this writing at MSC, Houston. This memo contains the results of a partial analysis of data obtained with the MIT EMI Receiver during the test runs performed on 29 March 1971.

The primary purpose - quick look test results to assist in establishing SEP receiver design parameters.

2. Brief review of test conditions

The test receiver was mounted on the LRV (Lunar Roving Vehicle) aft pallet and was operated during test runs which encompassed approximately 70 minutes of operation.

Fig. 1 is a chart which briefly shows the pertinent circumstances of the five test runs performed. The circled designations refer to data reduced in this report.

Receiver antenna loops #1 and 2 were connected to two of the receiver three inputs; antenna loop #3 was routed to a spectrum analyzer at a remote location to provide complementary data. Accordingly, no data were collected from channel 3 of the EMI receiver.

The tests were conducted at MSC, Houston in the anechoic chamber in Bldg 14. As indicated in Fig. 1, the five test runs included simulated conditions of LRV operation in various communication configurations; the last two runs also included simulated LRV motion and steering.

The orientation of the antenna loops with respect to the LRV is as follows:

1. The plane through antenna loop 1 was "athwartships" on the LRV and vertical.
2. The plane through antenna loop 2 was along the fore and aft center line of the LRV and vertical.
3. The plane through antenna loop 3 was horizontal.

3. Brief review of EMI Rcvr characteristics

The MIT EMI Receiver is a battery-operated unit incorporating a commercial tape recorder for data storage. Fig. 2 is a simplified functional block diagram.

It basically consists of a three channel broad-band front end (one for each of the three one-foot diameter electrostatically-shielded loops) with multiple detection incorporated.

Three modes of detection are established:

1. PEAK DETECTION of the broad band front end (each channel)
2. "AVERAGE" DETECTION of broad band front end (each channel)
3. Base band detection of each of eight frequency regions (.5 to 32 MHz in octave steps plus 24 MHz at four bandwidths)

The resulting detected levels are converted to a frequency (300 Hz to 6 KHz) in the VCO and are recorded on the tape recorder (a Sony TC-50).

Built-in timing and switching circuitry establishes the sequencing of data collection.

Fig. 3 shows the timing sequence established. Each loop of the receiver is cycled through a timing sequence that:

1. Introduces a frame identification signal (twenty pulses - loop 1; 2 pulses - loop 2; 4 pulses - loop 3).
2. Records the output of the broad band average and peak detectors.
3. Cycles the local oscillator excitation frequencies (eight) into each of four post detection filters.

The time required for a full loop sequence is 140 seconds. All three loops complete their cycles in 420 seconds (seven minutes)

3.1 Calibration

Calibration of the receiver was performed at MIT prior to shipment to MSC. The calibration procedure utilized a signal generator with an output impedance of 50 Ω , terminated by the input impedance of each receiver channel in turn. These calibration data are used in the data reduction at MIT.

Additional calibration data were taken at MSC prior to the test runs. Stimulation of the receiver channels was performed using a current probe at each antenna in turn at the frequencies of interest. Data reduction utilizing this calibration technique is being performed at MSC at this writing. In addition, electric field strength data of the EMI using conventional equipment is being processed at MSC.

3.2 Receiver Bandwidth

The receiver bandwidths are established by active filters with design cutoff frequencies at the bandwidths indicated.

The actual bandwidths are somewhat different than the nominal values shown and are indicated in Fig. 4. The reasons are the following:

1. The lower bandwidths are approximately $3.14 (\pi)$ times the active filter cutoff frequency conversion due to the fact that the method of detection after frequency conversion utilizes both the upper and lower base-band spectra and the 12db/octave filter roll off .
2. Higher bandwidths are less than π times the cutoff frequency because the gain of the preamplification ($\times 500$) following the active filters was not sufficient to maintain flat-response closed loop operation over the full bandwidth; a simple solution to this problem would have been the addition of another pre-amplifier, but the possibility of a delay in receiver availability prevented this approach.

The receiver is limited in its operational length of time by the recorder tape cassette (one hour per cassette) and by the built-in batteries of both the receiver and tape recorder (up to three hours depending upon tolerable gain shifts).

Receiver sensitivity and overload levels decrease with accumulated battery time. Data reduction in this report assumes fresh batteries (calibration data were accumulated with fixed power supply terminal voltages at the levels of fresh batteries) and is a reasonable assumption for the length of time operated in these tests.

4. Available data for quick-look reduction

The data available from the EMI RECEIVER was recorded on the magnetic tape of the receiver tape recorder. The VCO (voltage controlled oscillator) output of the receiver was recorded; the frequency recorded is indicative of the signal level detected.

The recorded outputs were fed to a frequency discriminator at MSC and recorded as a DC level on a chart recorder. A copy of this data was used in the MIT evaluation.

Fig. 5 (2 sheets) shows the nature of the available data; a sample of the chart recorder is shown under nominal conditions. The scale factors for the frequency discriminator output and pen recorder deflection sensitivity were arranged so that one inch of pen deflection equals one Volt DC equals 1 KHz of frequency deviation of the receiver VCO (tape recorder output).

Calibration curves of the VCO output as a function of input signal levels at the frequencies of interest for the receiver channels involved were utilized to determine the equivalent sine wave rms levels at the receiver input.

Fig. 6 (two sheets) shows a sample of the chart recorder data under worst case conditions (LRV motion simulated in conjunction with other systems in operation - TEST RUN 4B). Reference will be made to this chart in Section 6 of this report.

5. Discussion of Reduction Data

Fig. 1 gives an indication of the operating conditions of the five test runs (Reference 1 details the conditions specifically). It was intended in this review that both nominal conditions and worst case conditions be evaluated.

Selected portions of Test Runs 1, 4 and 5 were evaluated.

Fig. 7 shows the results of Test Run 4A on channel 1 of the receiver. The responses are shown at eight frequencies and four bandwidths for each frequency (responses of .5 MHz and 24 MHz are shown in all of the results even though, at this time, it is intended that they not be incorporated in the SEP receiver).

The responses are shown as both noise power and equivalent voltage levels at the input to the receiver vs frequency. In calculating the voltage level with respect to noise power, a receiver noise figure of 6db in a 2Hz bandwidth was assumed; it was further assumed that the SEP RECEIVER would be matched to its antenna in the indication of the receiver noise floor at -135 dbm (.07 μ v into 150 Ω input impedance).

The voltage readings shown are those derived from the test data and EMI receiver calibration.

The responses at each of the four available bandwidths are shown in Fig. 7. No attempt was made to connect the points to form a smooth curve for each of the bandwidths though the pattern of responses suggest a defined trend.

Fig. 8 shows the results of Test Run 4A (channel 2 of receiver). In this run simulated motion (10Km/hr) of the LRV is incorporated (the simulated motion actually started while the receiver was being sequenced through the 100 Hz bandwidth of channel 1).

This run is indicative of worst case conditions and the responses can be seen to be somewhat higher than those of the previous test run; in comparing the two figures, it is to be noted that different antenna loops are involved.

Fig. 9 shows the results of a number of test runs in the 3 KHz bandwidth (1 KHz filter cutoff) of channel 1 of the receiver. This bandwidth is the closest to that of the proposed SEP receiver.

Fig. 10 shows a similar set of test results for channel 2 of the receiver in the same bandwidth. The interference levels in receiver 2 seem to be somewhat higher than those of channel 1.

Fig. 11 shows the responses of each of the two receiver channels in an early test run (TEST RUN 1A). Here, too, the responses in channel 2 appear to be higher than those in channel 1.

On comparing the responses in TEST 1A (earliest test run) with those of Test Runs 4 and 5 (later runs) there is no obvious difference in the levels shown; this indicates that the receiver responses were not markedly degraded in later test runs by such causes as battery rundown.

6. Validity of Test Results

The EMI Noise Test Receiver was specifically designed and built to assist in the collection of data relating to LRV Spurious outputs in the frequency bands of interest to the SEP lunar experiment. It's configuration relating to antenna design and location closely simulates the intended configuration.

It is intended to provide complementary data to that which can be obtained by more seasoned and conventional equipment (field intensity meters and spectrum analyzers).

A few of the pertinent characteristics of the receiver are considered in the context of their relation to the test results.

6.1 Receiver Sensitivity and Dynamic Range

The receiver by design has limited sensitivity in order to provide approximately 40db of dynamic range (sensitivity and dynamic range varies in different channels and bandwidths). Too much sensitivity would have compromised the extent to which the receiver could handle large signals without overload (no AGC techniques or logarithmic amplifiers are employed to simplify the data reduction techniques required).

Accordingly, it is to be noted that signals which appear on the recorder at all are some 23db above the internally generated noise of the proposed SEP Receiver (assuming matched antennas). Signals higher than nominally 50-100 μ v will overload the receiver and will not be recorded to the degree that they exist.

Analysis of the data indicates that the choice of design parameters was a good one, though there is evidence that receiver overload occurred under worst case conditions at wide bandwidths (which was not unexpected).

It is to be noted that the levels recorded are those that appear at the receiver input terminals through whatever inefficiencies are involved in the transfer of energy from the loop antennas to the receiver input terminals.

6.2 Antenna Mismatch

No antenna matching techniques are used in the EMI Noise Test Receiver to transform the antenna loop impedances (a variable with frequency) to that of the receiver input impedances (which is almost flat but falls off with frequency at the higher frequencies).

The calculation of magnetic field intensity imposed upon the loop antennas must include antenna correction factors (a variable with frequency).

6.3 Receiver Calibration

The receiver was calibrated using the output of a 50 Ω Signal Generator into the input impedance of the receiver. Such a technique results in an apparent increase in sensitivity at the lower frequencies of approximately 1.5db and a decrease at the higher frequency of approximately 1.5db. The data shown on the charts do not incorporate this discrepancy.

6.4 Cross-Talk

Channel 3 of the receiver was not connected to an antenna loop during the test runs. There is evidence on the chart recordings that signal levels in the band around 24 MHz were coupled into that channel (the receiver response has a peak in that frequency range). The source of the signal is not obvious because the channels used are disconnected during the timing sequence involving channel 3 response. The signal levels in other frequency ranges are imperceptible. Overall conclusion is that measurements were not degraded from this cause.

6.5 Effects of Battery Voltage rundown

The receiver/recorder combination ran on their fresh batteries approximately eight minutes prior to the test runs and seventy minutes during the test run. Best estimates on the effect on performance indicates a maximum of 2db of degradation and is not incorporated in the data.

During data transformation, the tape recorder speed should ideally be identical to the speed when the recording was made. Deviations would result in a change in apparent recorded frequency which would be interpreted in the data reduction as an input signal level change. Because of the limited dynamic

range of the recorded data, it is believed that errors introduced from this source would be small enough to ignore.

6.6 Effect of Impulse Noise and Chart Recorder Bandwidth

Figs. 5 and 6 show the results of the transformation of data from the magnetic tape to a pen-drawn chart recorder. It is obvious that impulse-type noise is considerably more vigorous in Fig. 6 (LRV simulated motion). "Average" values were used in the data reduction.

Fig. 12 shows a typical calibration curve used in the data reduction. The effect of noise peaks on the method of averaging leads to greater errors at the lower signal levels than the stronger signal levels due to the fact that the direct relationship between signal level and VCO frequency is non-linear at the lower levels.

The response of the pen driven recorder is probably in the neighborhood of 100 Hz max to the 3db point. In effect, it acts as a low pass filter to the impulse noise.

Such noise can be somewhat readily filtered in evaluating the data of the EMI Receiver. In the SEP Receiver, the intended time interval for examining each frequency from a particular antenna loop is 67 milliseconds as opposed to 4 seconds. Bandwidth reduction is still possible but definition of the level of desired signal will be disturbed by such impulses as appear to be present.

6.7 Effect of Switching Transients

No degradation of the data available from the EMI receiver results from the switching transients in changing antenna loops, bandwidths and local oscillators - in fact, if anything, they assist in separating operating conditions.

The transients are due to the fact that levels are capacitor-coupled in both the switching circuits and at the demodulator output and result in spikes appearing at the capacitor outputs.

In the SEP receiver, due to the limited time available in each operational time span (and depending on the method of data reduction), such transients are intended to be minimized.

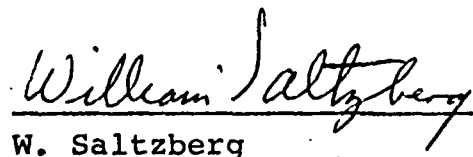
6.8 Test Equipment Calibration Errors

Any errors in the calibration of the equipment used to establish the calibration data (signal generator, voltmeter, frequency discriminator, chart recorder, etc) are presumed to be negligibly small.

7. Conclusion

The data collected by the EMI Receiver and reduced at MIT show that problems due to EMI, generated by the LRV operating systems, indeed exist in the frequency bands intended for operation of the SEP receiver.

A review of the adequacy and validity of the test data indicate that the receiver appears to have operated as designed and that results obtained cannot be treated as invalid. It is intended that this data be considered in conjunction with complementary tests performed at the same time using other analysis equipment to determine the adequacy of the proposed SEP design in the environment of the LRV.


W. Saltzberg

xc: G. Ogletree
J. McKenna
G. Jones
W.S. File

FIG 1 TEST RUN PROFILE

TEST No	TAPE No.	CHART No.	TAPE TIME	ACTUAL OPERATING TIME NOTE 1	TEST DATA COLLECTED (NOTE 3)			REMARKS (NOTE 2)
					Loop 1	Loop 2	Loop 3	
1	1	1	10 MIN 50 SEC	15:25:30 to 15:36:20	(1A) 1B	(1A) 1B PARTIAL	1A RESET	TEST E4A - LRV STOPPED; LCRU MODE 3 (FM/TV); NAV. SYSTEM ON TV UPLINK COMMANDS & DOWNLINK VOICE OPERATIONAL
2	2	2	11 MIN 20 SEC	16:65:00 to 16:16:20	2A 2B (PARTIAL)	2A	2A	TEST E3A - LRV STOPPED; LCRU MODE 1 (PM/WB) NAV SYSTEM ON DUPLEX VOICE ON VHF EVCS; DOWNLINK VOICE ON; TV UPLINK COMMAND ON
3	3	3	11 MIN 5 SEC	16:24:20 to 16:35:25	3A 3B	3A 3B	3A (RESET) 3B PARTIAL	TEST E3A - LRV STOPPED; LCRU MODE 2 (PM/NB) NAV SYSTEM ON VHF EVCS LIA & DOWNLINK OPERATION
4	4	4	12 MIN 10 SEC	16:43:20 to 16:55:30	(4A) (4B)	(4A) (4B)	4A 4B PARTIAL	TEST No E3a - LRV ON SIMULATED STRAIGHT RUN 10 KM/hr LCRU MODE 1 (PM 1/WB) EVCS (VHF) OPERATIONAL
4/5	4	4	14 MIN 14 SEC	16:55:30 to 17:09:44	4/5A 4/5B	4/5A 4/5B	4/5A 4/5B (RESET)	EMI RECEIVER & TAPE RECORDER WERE LEFT ON IN INTERIM PERIOD BETWEEN TEST RUNS 4 & 5.
5	4	4	11 MIN 6 SEC.	17:09:44 to 17:20:50	(5A) (5B)	(5A) (5B) (PART.)	5A	TEST No E3A - LRV ON SIMULATED STRAIGHT RUN 2 KM/hr LCRU (MODE 2) EVCS (VHF) OPERATIONAL

- NOTES: 1. DATE: 3/27/71 CENTRAL STD. TIME
 2. NOT ALL SYSTEMS WERE ON CONTINUOUSLY.
 3. TEST RUNS ENCIRCLED WERE REDUCED IN THIS REPORT

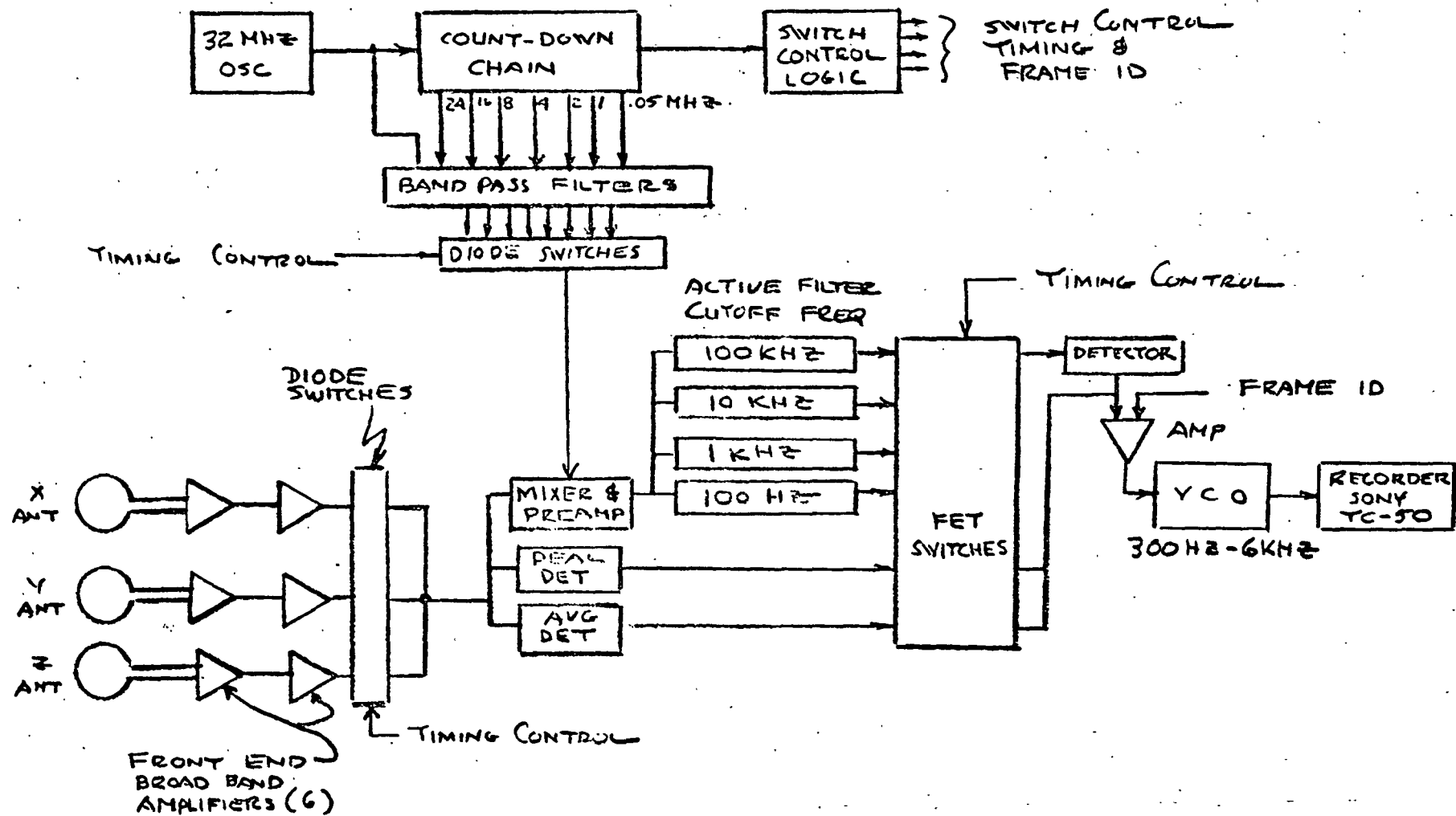
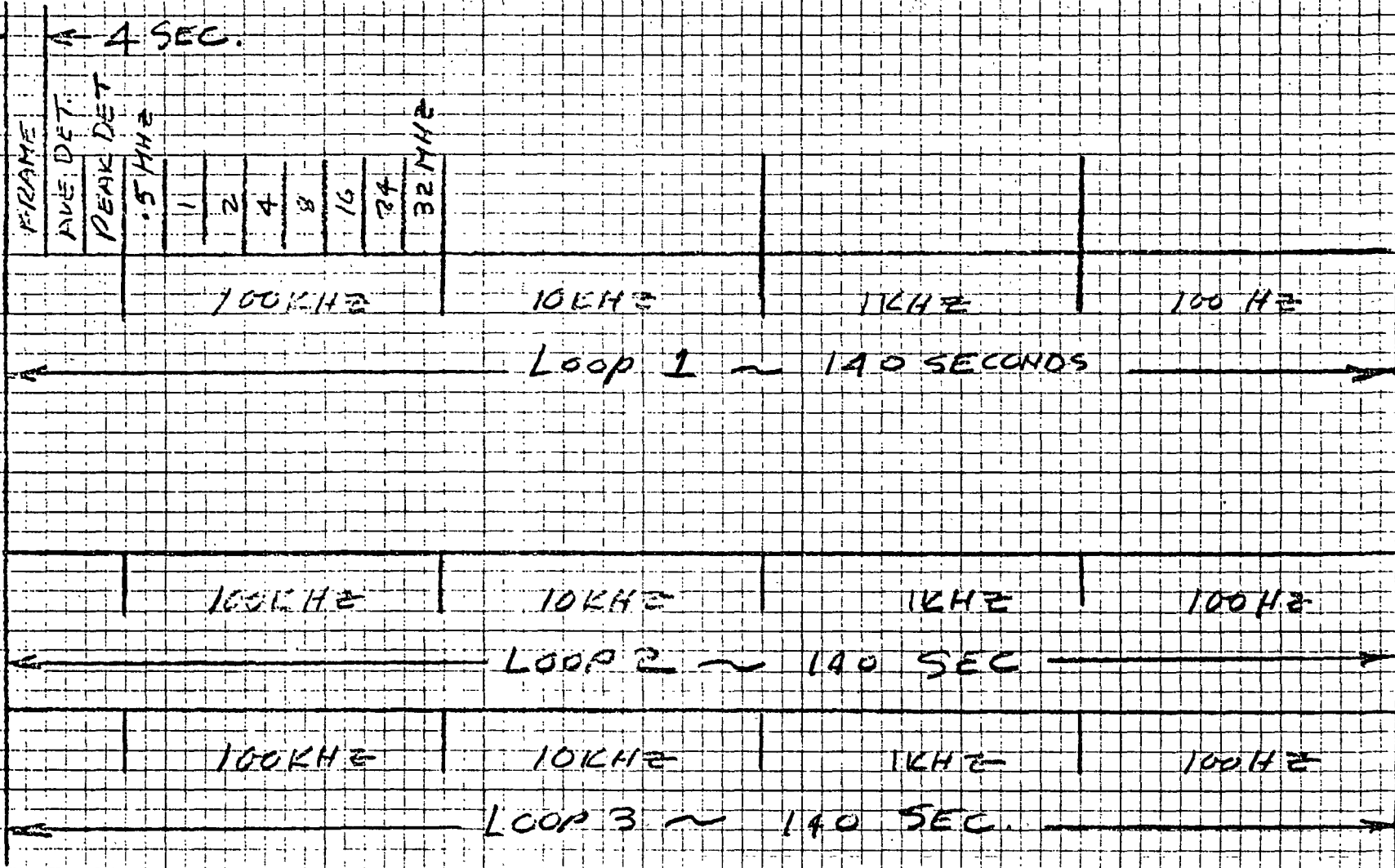


FIG 2 EMI NOISE TEST RECEIVER

FIG 3 REVERSE TIMING SEQUENCE



- 1 EACH TIME SPAN ~ 4 SECONDS
- 2 EACH LOOP CONNECTED FOR 140 SECONDS
- 3 FULL CYCLE: 420 SECONDS (7 MINUTES)

ACTIVE FILTER CUTOFF FREQ.	NOISE BANDWIDTH FROM ACTIVE FILTER	APPROX NOISE BW FROM FILTER & PREAMP.
100 Hz	300 Hz	300 Hz
1 KHz	3 KHz	3 KHz
10 KHz	30 KHz	21 KHz
100 KHz	300 KHz	25 KHz

FIG. 4 RECEIVER NOISE BANDWIDTHS

3:28:50
3 MIN.

BEGINNING of
TEST 1A LOOP 2 →

1 VOLT =
1 KHZ

1 SEC. →

LINE of ZERO VOLTS

10 KHZ

100 KHZ

PEAK DET

AV DET

FR.

TEST 1A

LOOP 2 (PARTIAL)

TV TURNED
ON →

FIG 5 DATA FORMAT -
TEST 1A LOOP 2 (Sheet 1 of 2)

3:29:50
4 MIN.

1 KHz
Loop 2

32 MHz

24

16

9

4

2

1

.5

END of TEST
1A, LOOP 2

100 Hz

1 KHz

LOOP 2

TEST 1A LOOP 2

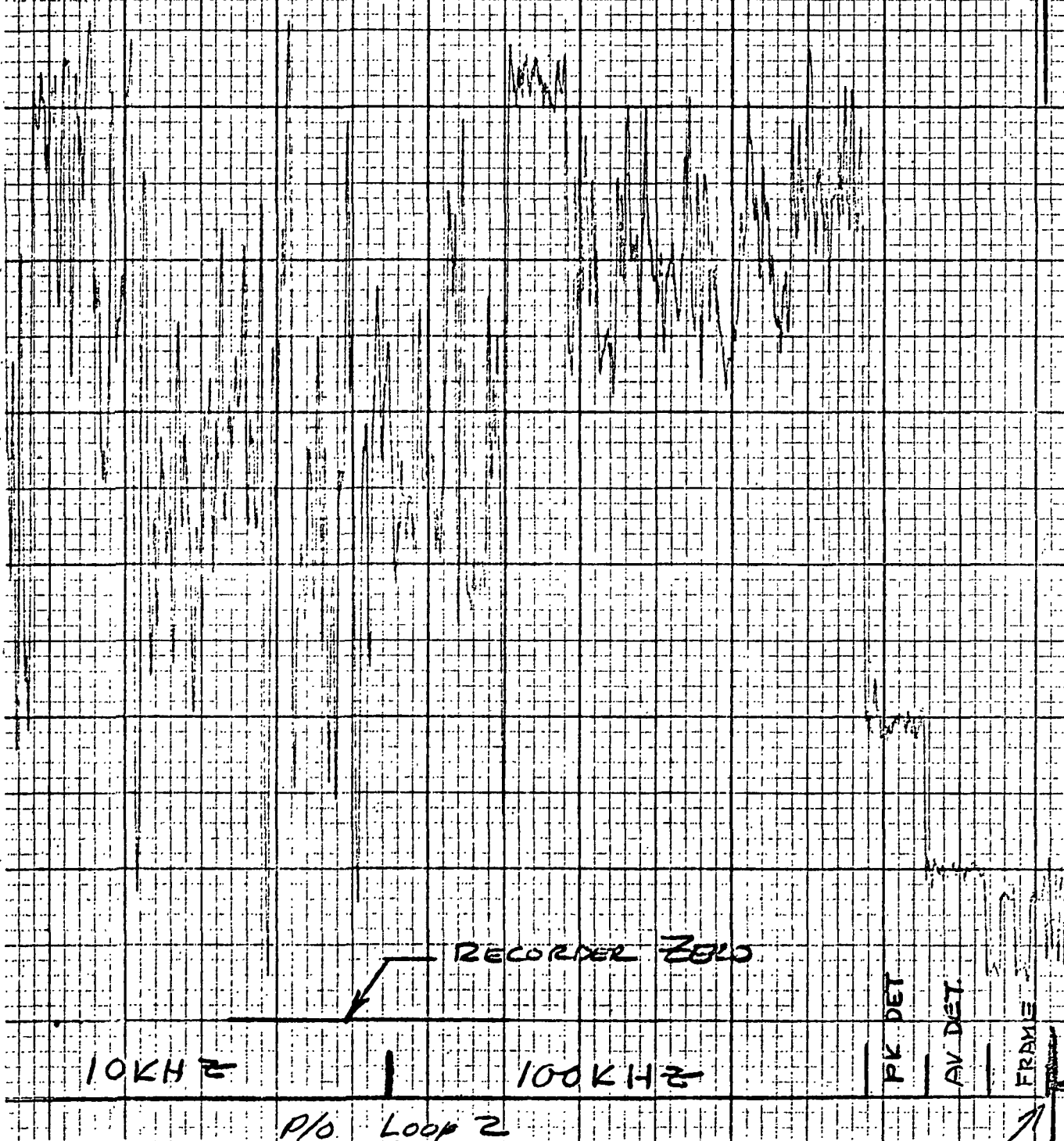
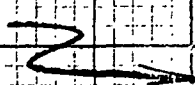
FIG 5 DATA FORMAT (Sheet 2 of 2)

4:53:20

8 MIN

START TEST RUN 4B
LOOP 2

CONDX:- LRV MOTION
SIMULATED



RECORDER ZERO

10 KHZ

100 KHZ

P/O LOOP 2

PK DET

AV DET

FRAME

TEST 4B LOOP 2 (PARTIAL)

FIG 6 DATA FORMAT TEST 4B LOOP 2
(Sheet 1 of 2)

← END TEST
RUN 4B

4:54:20
9 MIN

1 KHz
Loop 2

NOTE: FROM DATA, IT
SEEMS THAT DURING
THE PERIOD OF RECUR
SEQUENCING THRU 1 KHz
BANDWIDTH, THERE
WAS A PAUSE IN THE
SIMULATION OF MOTION!
NOTE HIGHER LEVEL
AT 32 MHz WHERE
MOTION SIMULATION WAS
APPARENTLY REINITIATED.

32 MHz

24

16

8

4

2

1

0.5 MHz

100 Hz

1 KHz

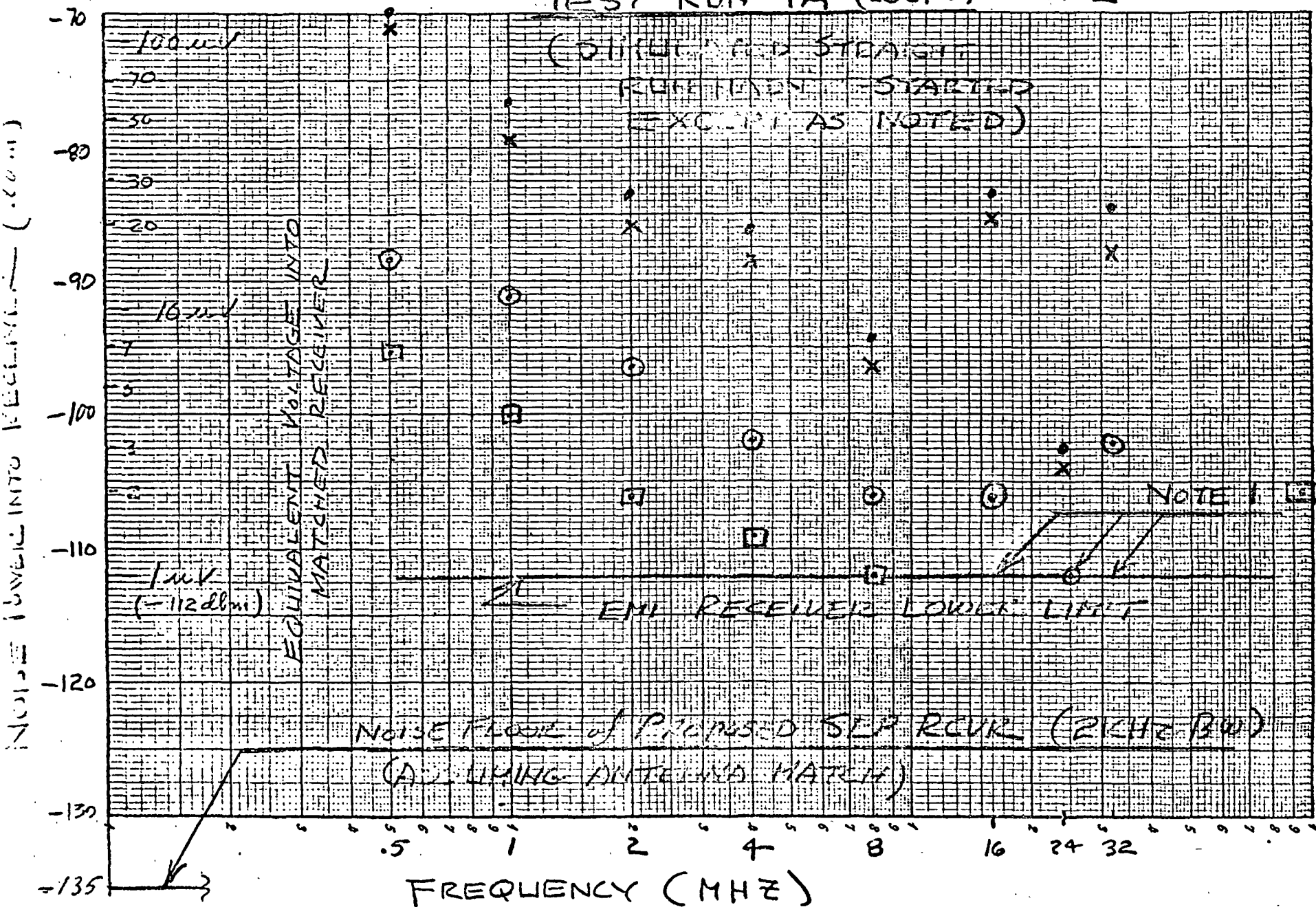
Loop 2

TEST 4B Loop 2
FIG 6 DATA FORMAT TEST 4B Loop 2
(SHEET 2 of 2)

NOTES: 1 SIMULATED STRAIGHT RUN
STARTED — DATA NOT SHOWN

• BW 20 KHz
x BW 21 KHz
○ BW 3 KHz
□ BW 300 Hz

TEST RUN 4A (LOOP 1)



TEST RUN 4A (LOOP 2) (SIMULATED STRAIGHT RUN - 10KM/HR)

• B.W. 2 KHz
X B.W. 21 KHz
○ B.W. 3 KHz
□ B.W. 300 Hz

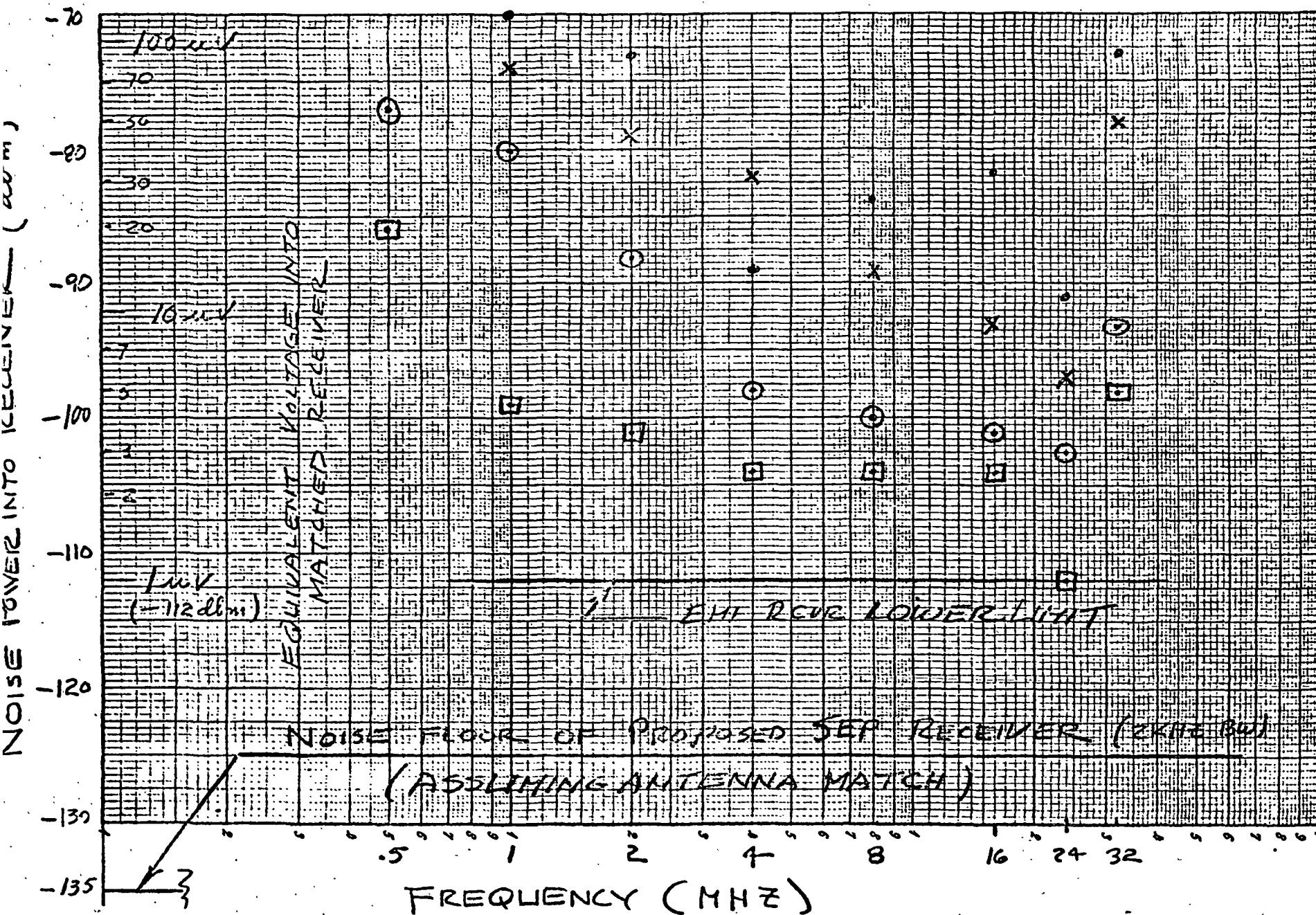


FIG 8

DATA of 3/29/71



○ RUN 4A
 ● RUN 4B
 □ RUN 5A
 x RUN 5B

TEST RUNS ~ 3 KHz BW (Loop 1)

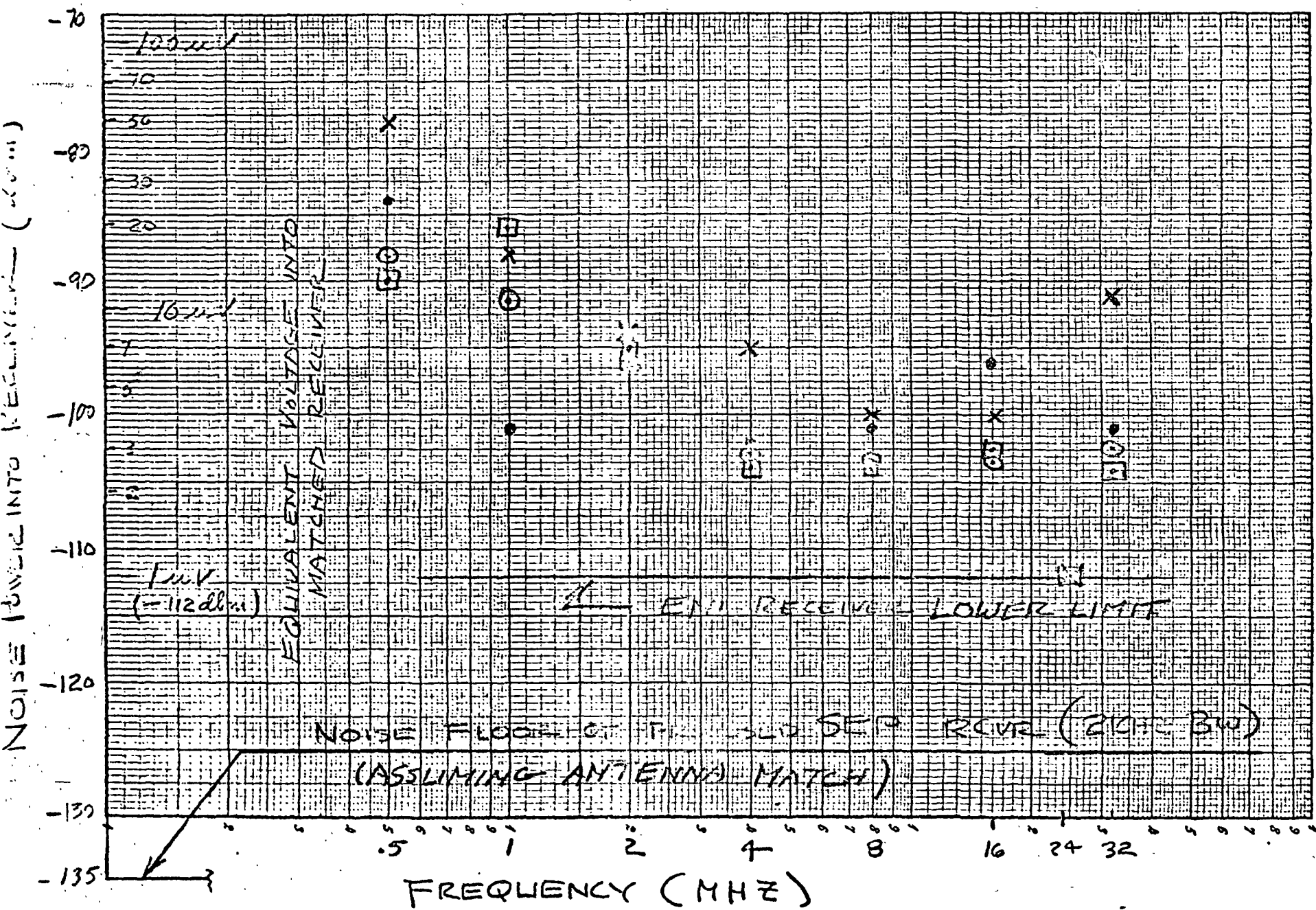


FIG 9

DATA of 3/11/11



TEST RUNS ~ 3KHz BANDWIDTH (LOOP 2)

- RUN 4A
- x RUN 4B
- RUN 5A
- RUN 5B

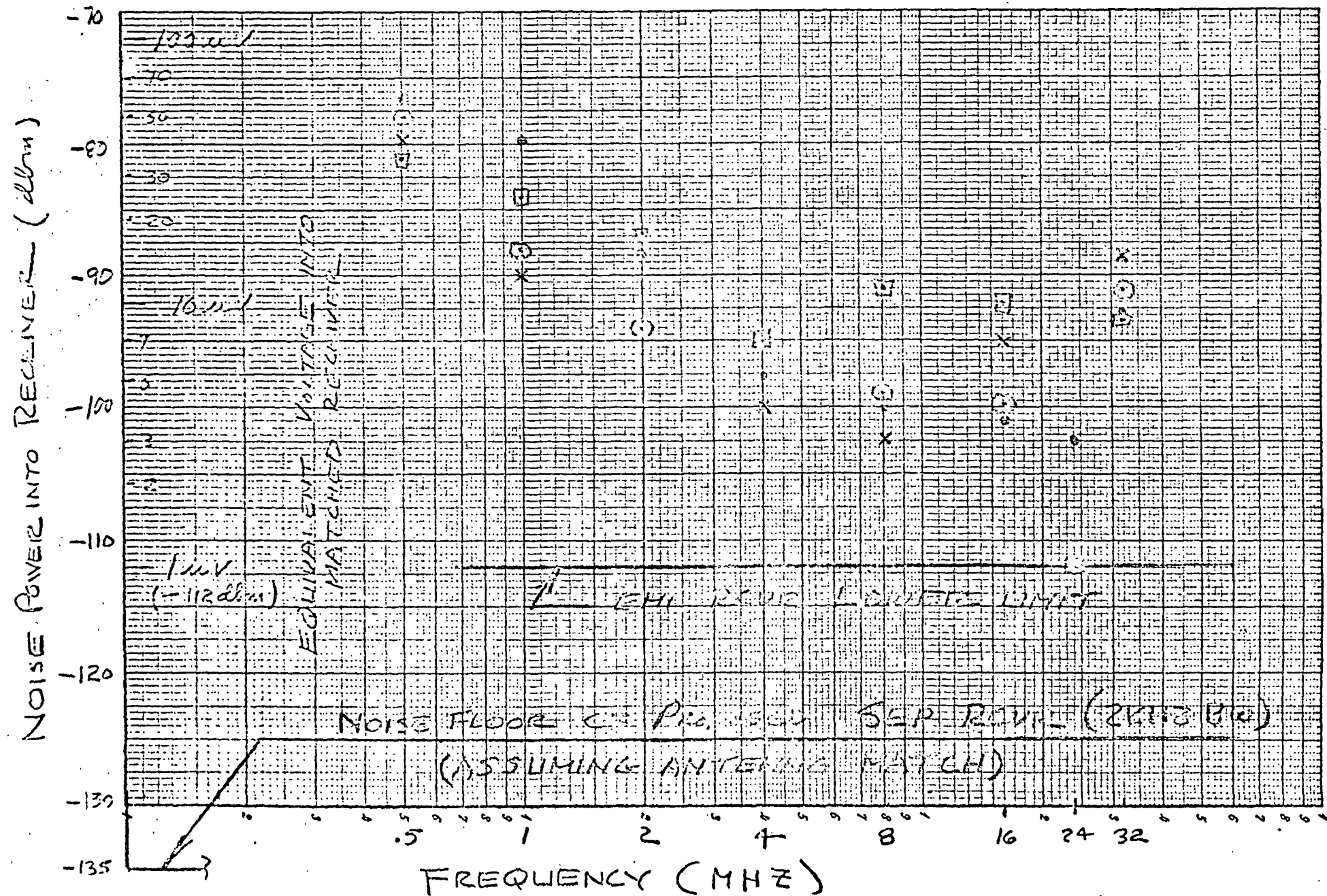


Fig 10



• RUN 1A Loop 1
 X RUN 1A Loop 2

TEST RUN 1A 3 KHZ BANDWIDTH

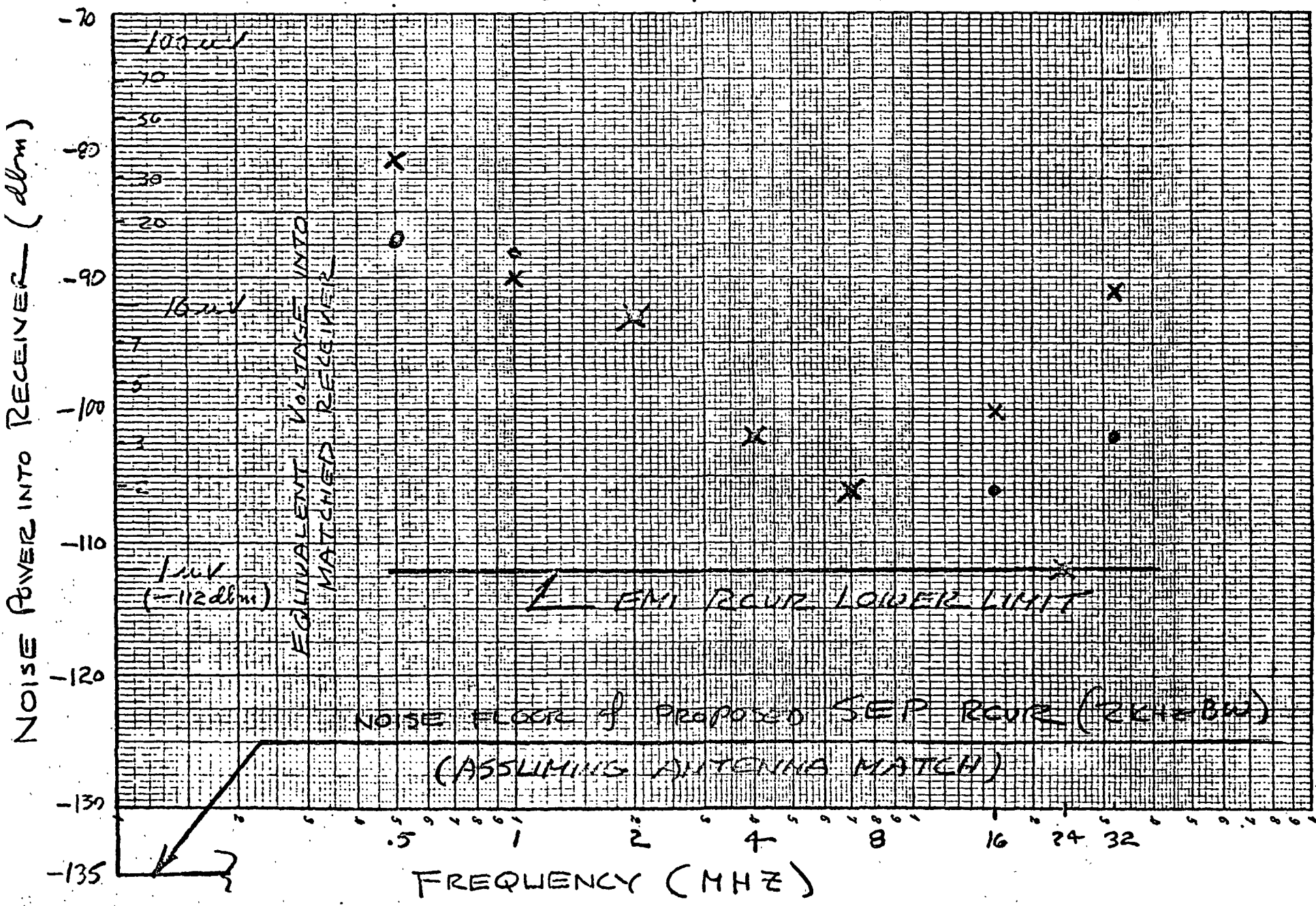


Fig 11

APPENDIX 6.1

PRELIMINARY END ITEM SPECIFICATION

Specification No. _____

Revision No. _____

Release Date _____

Page I-1

CONTRACT END ITEM SPECIFICATION

PART I

PRODUCT CONFIGURATION AND ACCEPTANCE TEST
REQUIREMENTS

Number _____

LUNAR SURFACE ELECTRICAL PROPERTIES EXPERIMENT

NOT SYSTEM EQUIPMENT

PRELIMINARY

DATE	REVISION LETTER	TDRR NO.	PAGES REVISED	APPROVALS	
				MIT	NASA

This specification consists of Pages 1 to _____ inclusive.

APPROVALS

NASA/FOLE	NASA/MSC	MIT/CSR	MIT/CSDL
-----------	----------	---------	----------

1. SCOPE

This part of this specification establishes the requirements for performance, design, test and qualification of one type-model-series of equipment identified as Lunar Surface Electrical Properties Experiment number _____. This CEI will be used to provide the means for an experiment the chief objectives of which are to determine layering in the lunar sub-surface, and to search for the presence of water at depth. In addition, the electrical properties of the lunar material will be measured in SITU. An attempt will be made to obtain an independent estimate of the lunar thermal flux and an indication of the number and size of subsurface scattering bodies.

2. APPLICABLE DOCUMENTS

The following documents, of exact issue shown, form a part of this specification to the extent specified herein. In the event of conflict between documents referenced here and other detail content of Section 3, 4, 5 and 10, the detail requirements of Sections 3, 4, 5 and 10 shall be considered a superseding requirement.

3. REQUIREMENTS

3.1 Performance

The primary function of the SEP apparatus is to radiate RF energy at the lunar surface and collect and record the characteristics given to this energy as it passes above and through the lunar surface to a receiver moved over the surface at prescribed distances radiation source.

The SEP apparatus shall consist of a transmitter assembly, a portable receiver assembly, and a recoverable data storage device. The transmitter will be small, low powered from its own source, and will radiate through a crossed dipole antenna laid on the lunar surface. The small receiver will consist of three orthogonal loop antennas, amplifying and signal timing electronics, and a magnetic tape recorder. The magnetic tape is to be returned to Earth for data analysis and interpretation.

Experimental data is the complex interference pattern between the surface wave and the subsurface and reflected waves. This interference pattern causes a variation in the received field strength as a function of range and frequency, the magnitude of the field components received by each of the three orthogonal loops is detected separately by the receiver and stored by the tape recorder. See Figure 1.

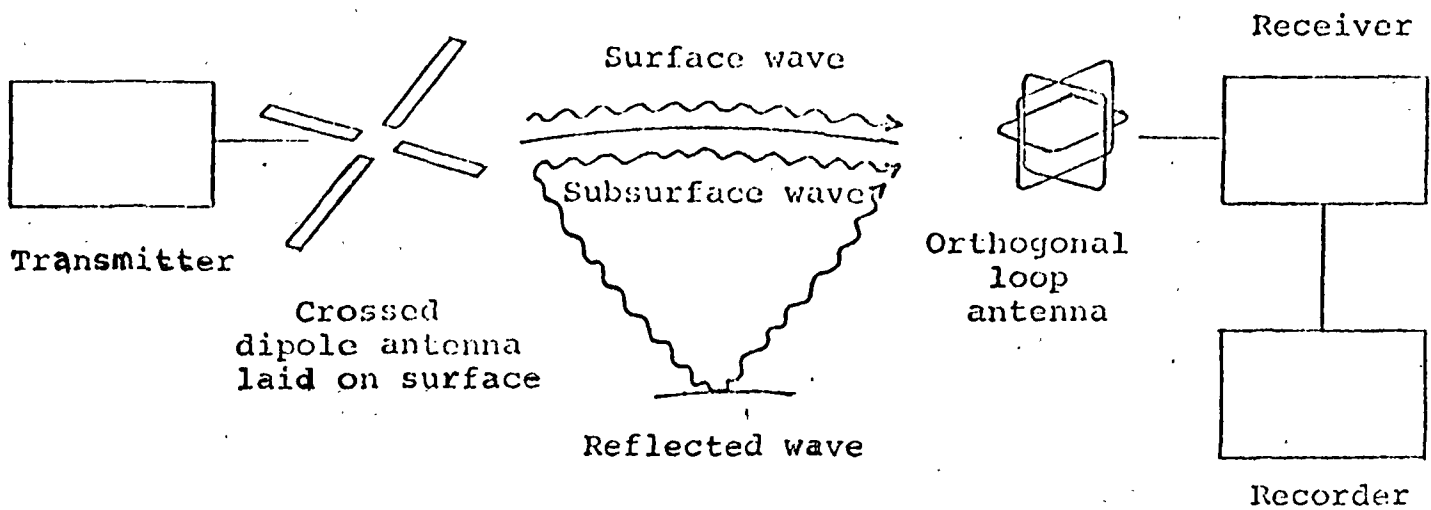


Figure I
Schematic Diagram of Experiment

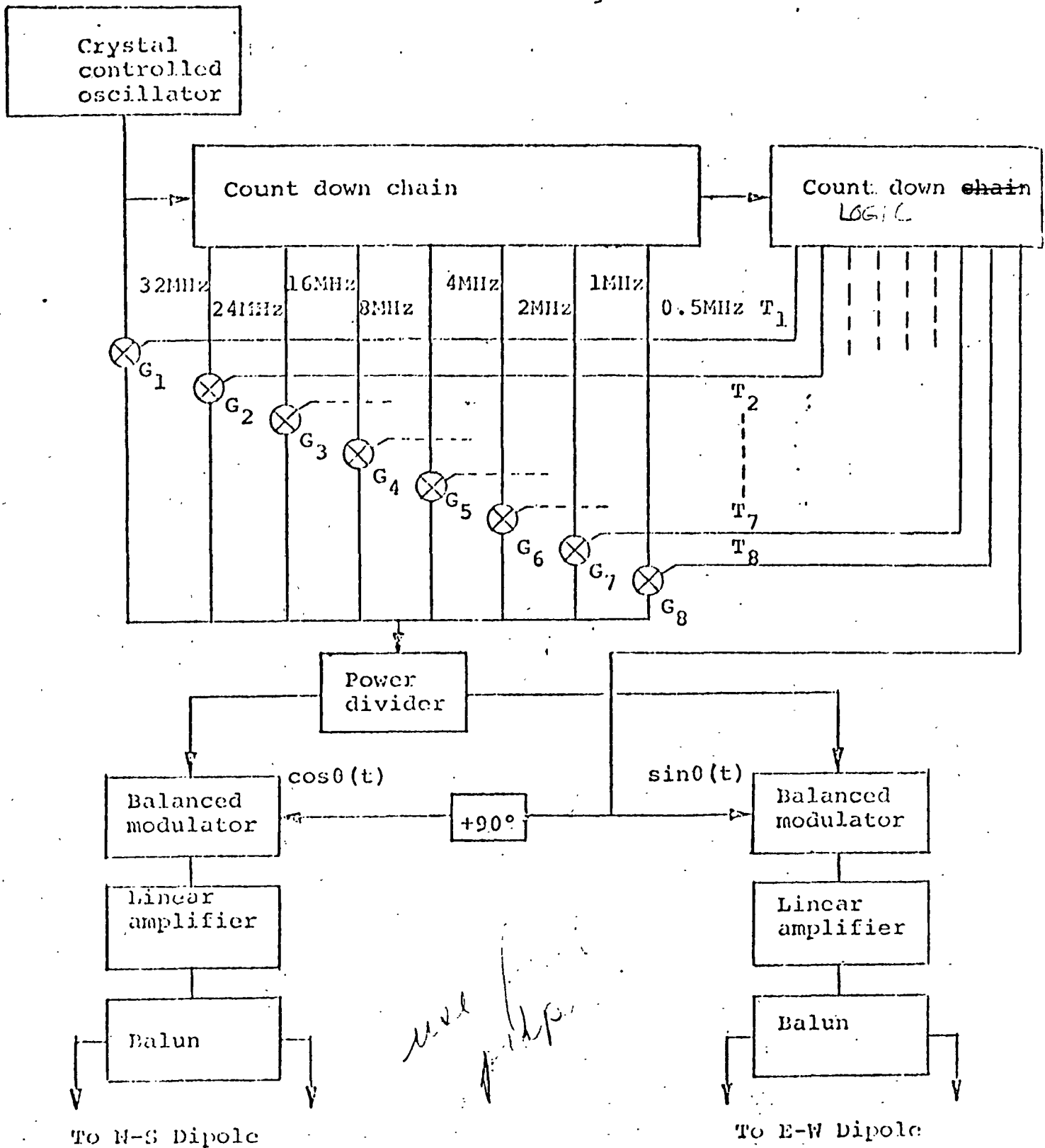


Figure 2

Transmitter Functional Diagram

Preceding page blank

0. TRANSMITTER FUNCTIONAL

The SEP transmitter contains two major functional subdivisions: the transmitter electronics subassembly and the transmitter antenna subassembly. The antenna subassembly consists of a pair of crossed dipoles (deployed) and the matching and balancing required to compensate for variations in driving-point impedance. The transmitter electronics subassembly contains all the electronics necessary for generating signals to drive the antenna subassembly.

0.1 TRANSMITTER ELECTRONICS SUBASSEMBLY

0.1.1 The Transmitter Electronics Subassembly (TES) shall provide modulated RF signals at each of two output ports designated "A" and "B".

0.1.2 FREQUENCY

The TES shall provide outputs at eight frequencies in accordance with Table 0-1.

0.1.2.1 STABILITY

The transmitter frequency stability shall be in accordance with Table 1.

0.1.2.2 COHERENCE

All frequencies generated by the transmitter shall be coherent.

TABLE 0-1

NOMINAL FREQ. MHz	ACTUAL FREQ. MHz	FREQ. TOL.	FREQ. STAB.	PEAK OUT- PUT POWER WATTS	TOLERANCE
32	31.94880		5 parts/10 ⁷	.125	± 1.5 db
24	23.96160	1 ppm	"	.125	"
16	15.97440	"	"	.125	"
8	7.98720	"	"	.125	"
4	3.99360	"	"	.250	"
2	1.99840	"	"	.5	"
1	0.99840	"	"	1.0	"
0.5	0.49920	"	"	2.0	"

0.1.3 OUTPUT POWER

Each TES output port shall provide a peak output power in accordance with Table 0-1 to a resistive load of 72 ohms.

0.1.3.1 OUTPUT POWER TOLERANCE

The tolerance on peak output power into 72Ω shall be in accordance with Table 0-1.

0.1.3.2 OUTPUT POWER STABILITY

The transmitter output power shall remain within ± 0.5 db of its initial value for a 15-hour period.

0.1.4 SEQUENCE OF TRANSMISSION

The sequence of outputs generated by the transmitter shall be in accordance with Figure 0-1.

0.1.4.1 STEPPING RATE

Each frequency shall be delivered to the output ports for 100 milliseconds each second.

0.1.5 MODULATION

The signal at each output port shall be modulated by a 15 Hz sinusoid. The modulator shall provide double side band suppressed-carrier modulation of the RF signal at each output port.

0.1.5.1 PHASING

The modulation of channel "A" shall lag the modulation of channel "B" by $90^\circ \pm 3^\circ$.

0.1.5.2 DISTORTION

The envelope of the modulated RF signal shall not deviate more than $\pm 1\%$ from that would be provided by perfect modulation by a pure sinusoid.

0.1.5.3 TOLERANCES

Modulation errors shall not result in peak power variations greater than specified under Section 0.1.3 of this specification.

0.1.6 OUTPUT PORT MATCHING

0.1.6.1 POWER

The peak power at each output port A shall be within ± 1.5 db of the power at output port B, when both ports are driving equal impedance.

0.1.6.2 PHASE

The phase of the RF signal at port A shall not differ from the phase of the RF signal at port B by more than $\pm 6^\circ$.

0.1.7 POWER SOURCE

The TES shall contain an energy source and necessary power conditioning apparatus to permit uninterrupted operation during each traverse.

1. RECEIVER FUNCTIONAL

The SEP receiver assembly collects and records field-strength data on traverses away from the lunar module and SEP transmitter deployment site. The receiver assembly has its own self-contained data storage capability, thermal control, and power source.

The receiver assembly contains the receiver antenna subassembly, which consists of three orthogonal loop antennas, a telescoping mast, and the necessary cabling for bringing signals from the loops to the receiver input terminals.

A diagram of the receiver assembly showing functional subassemblies appears in Fig. 1-1.

1.1 RECEIVER SUBASSEMBLY

1.1.1 Inputs

The receiver subassembly shall have three (3) input ports designated X, Y, and Z.

1.1.1.1 The input impedance at each port shall be between 120 and 200 ohms.

1.1.1.2 Sensitivity

The receiver sensitivity shall be in accordance with Table 1-1.

1.1.1.3 Noise Figure

The receiver noise figure shall not exceed 6 db through any input port.

1.1.1.4 Dynamic Range

The dynamic range of the receiver subassembly shall be 80 db minimum.

1.1.1.5 Resolution

The receiver shall resolve variations in field strength of $\pm 1\%$.

1.1.2 Frequency

The receiver shall receive and record field-strength data at eight actual frequencies per Table 1-1.

1.1.3 Bandwidth

The receiver bandwidth at each operating frequency shall be in accordance with Table 1-1.

1.1.4 Stepping

The receiver shall perform frequency switching consistent with that of the transmitter. Receiver stepping is shown in Fig. 1-2.

1.1.5 Synchronization

The receiver shall automatically achieve synchronization with the transmitter.

1.1.5.1 Method

The receiver assembly shall contain internal timing generation and circuitry that will maintain receiver time within 0.25 milliseoncds of transmitter time for a period of 50 seconds

following detection of a sync signal. Hard-line sync shall not be used.

1.1.5.2 The synchronizing signal shall be extracted from the 0.5 MHz transmitted signal and shall occur once per second when the receiver is not located in a null of the 0.5 MHz signal.

1.1.6 Data Storage Interface

1.1.6.1 Data

Field-strength data shall be represented by the frequency of a 0 dbn (+ 3, -7 dbn) signal between 300 Hz and 3 KHz.

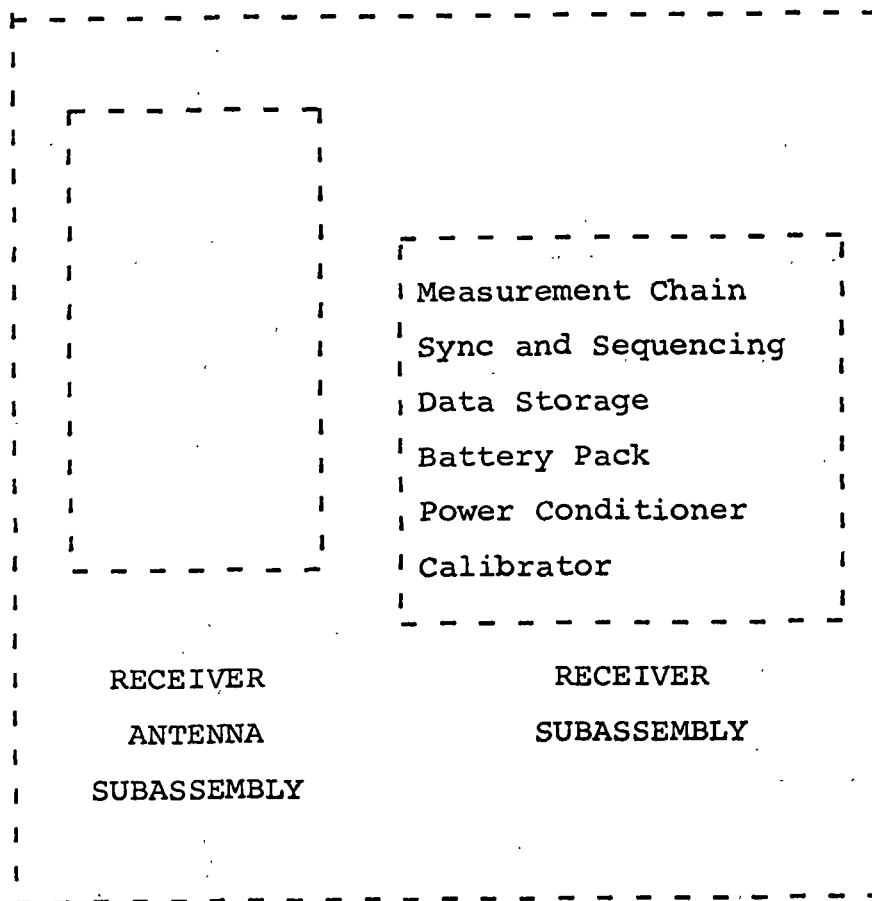
1.1.6.2 Reference

A 5.2 KHz reference signal shall be delivered to the recorder interface.

1.1.6.3 Power

The receiver subassembly shall provide power to operate the data storage device.

Revision No. _____
Release Date _____
Page 1



RECEIVER ASSEMBLY

Specification No. _____
Revision No. _____
Release Date _____
Page 1

TABLE 1-1
RECEIVER SUMMARY

NOMINAL FREQ. MHz	ACTUAL FREQ. MHz	TOL.	BANDWIDTH Hz (3dB)	MINIMUM SENSITIVITY μ V
0.5	0.49920	.005%	100	0.1
1	0.99840	.005%	200	0.1
2	1.99680	.005%	200	0.1
4	3.99360	.005%	400	0.1
8	7.98720	.005%	800	0.1
16	15.97440	.005%	1600	0.2
24	23.96160	.005%	2400	0.3
32	31.94880	.005%	3200	0.4

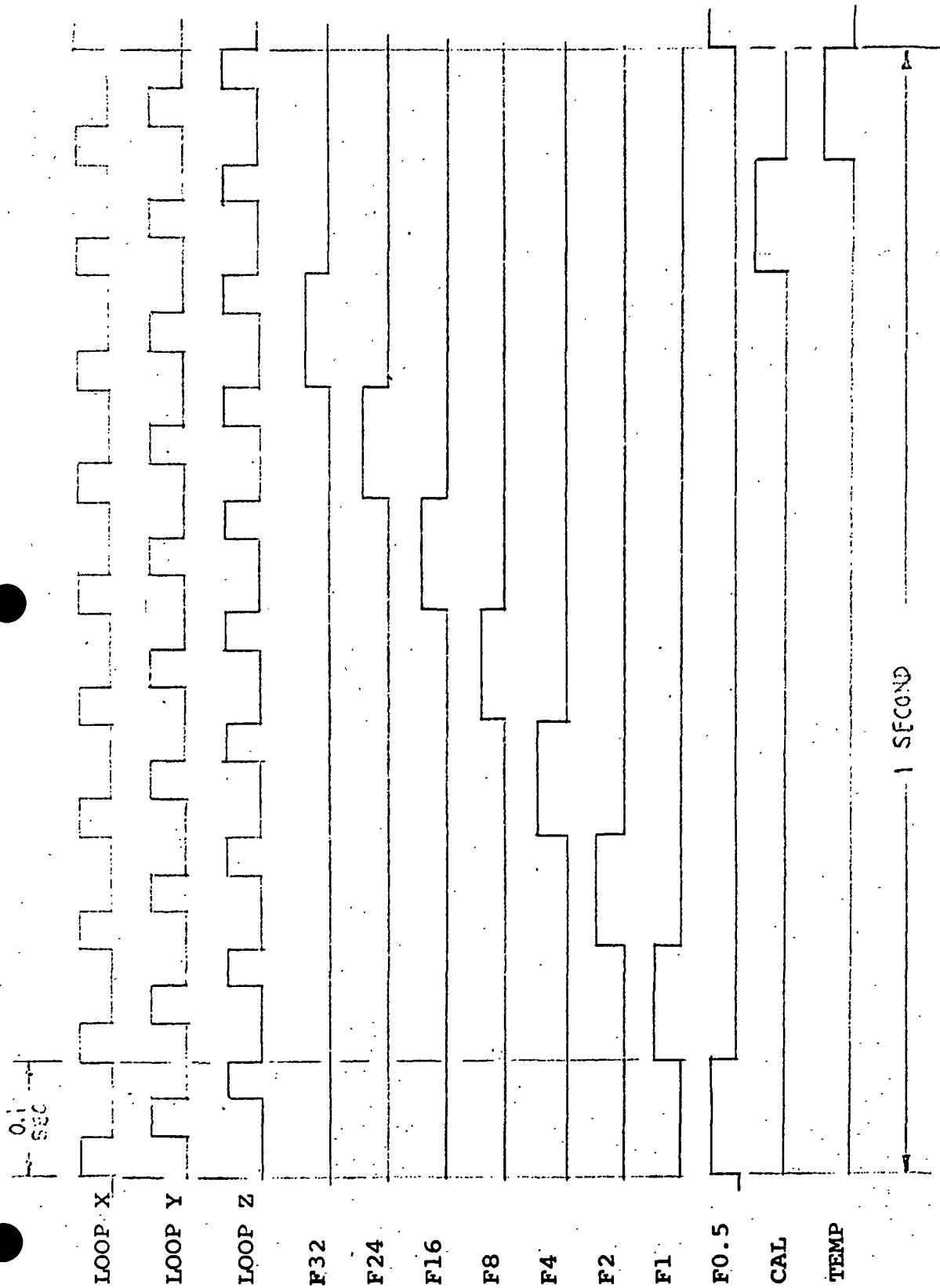


Fig. 1-2. RECEIVER TIMING.

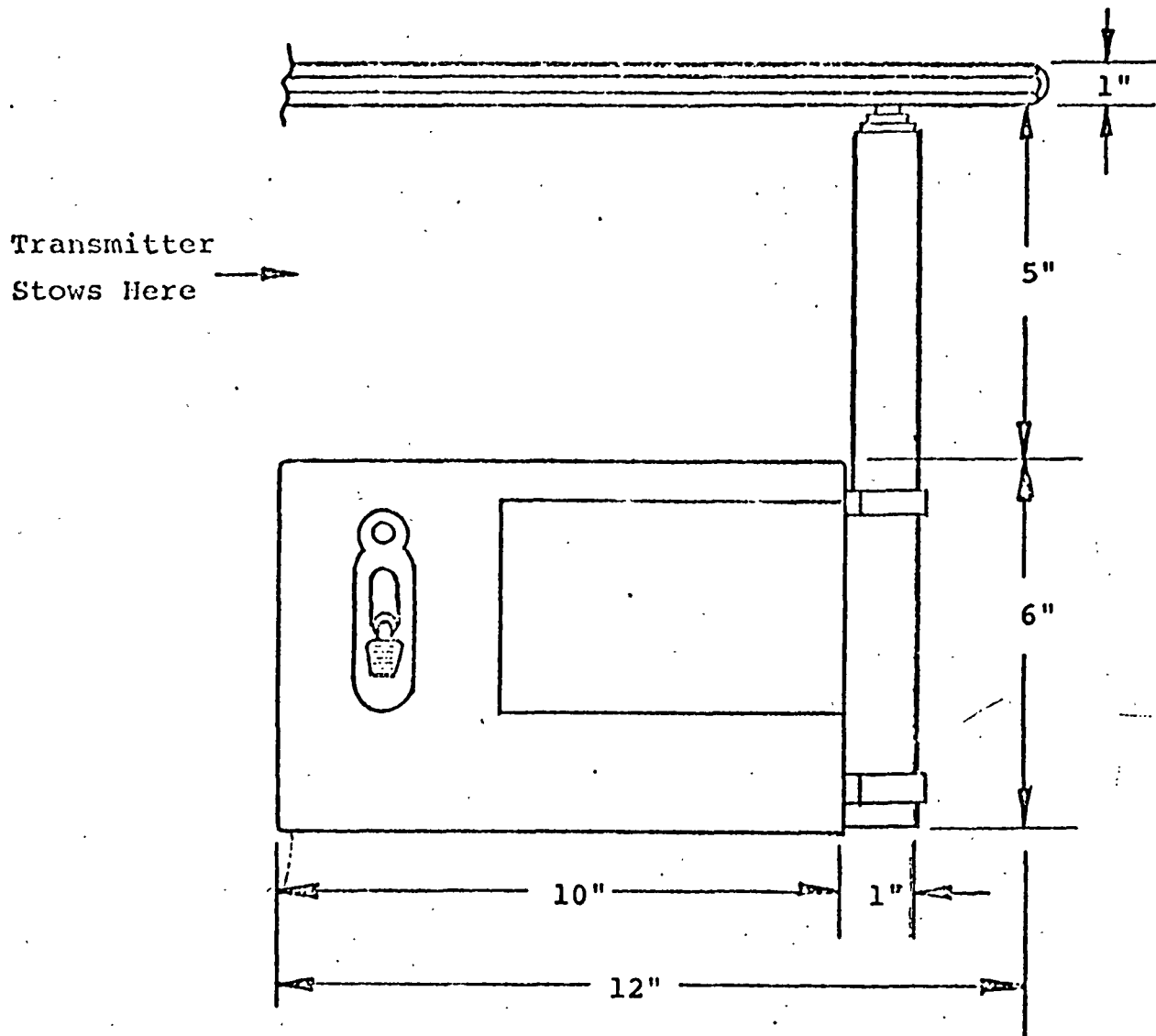


Figure 7 Receiver, Stowed

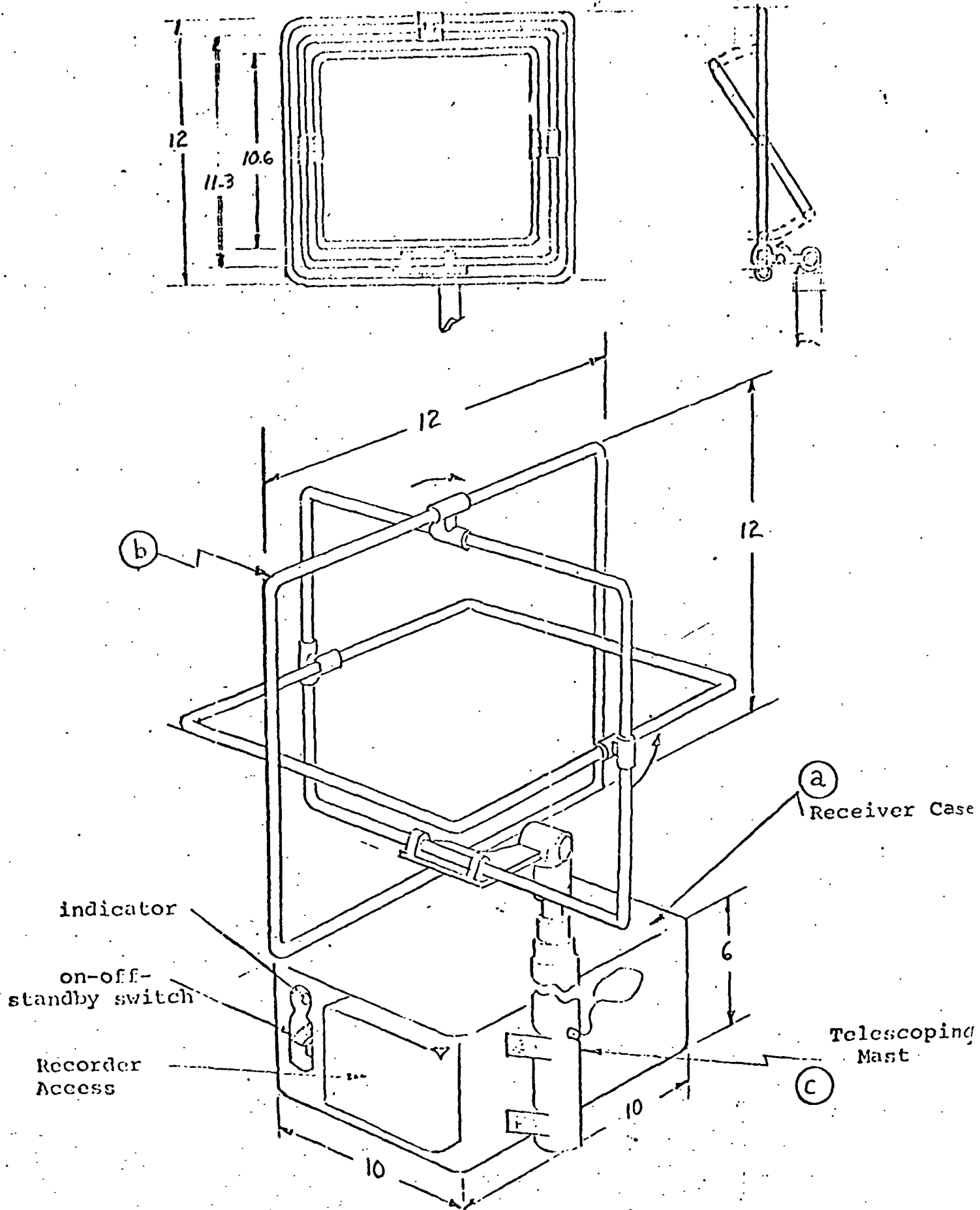


Figure 8 Receiver, Deployed

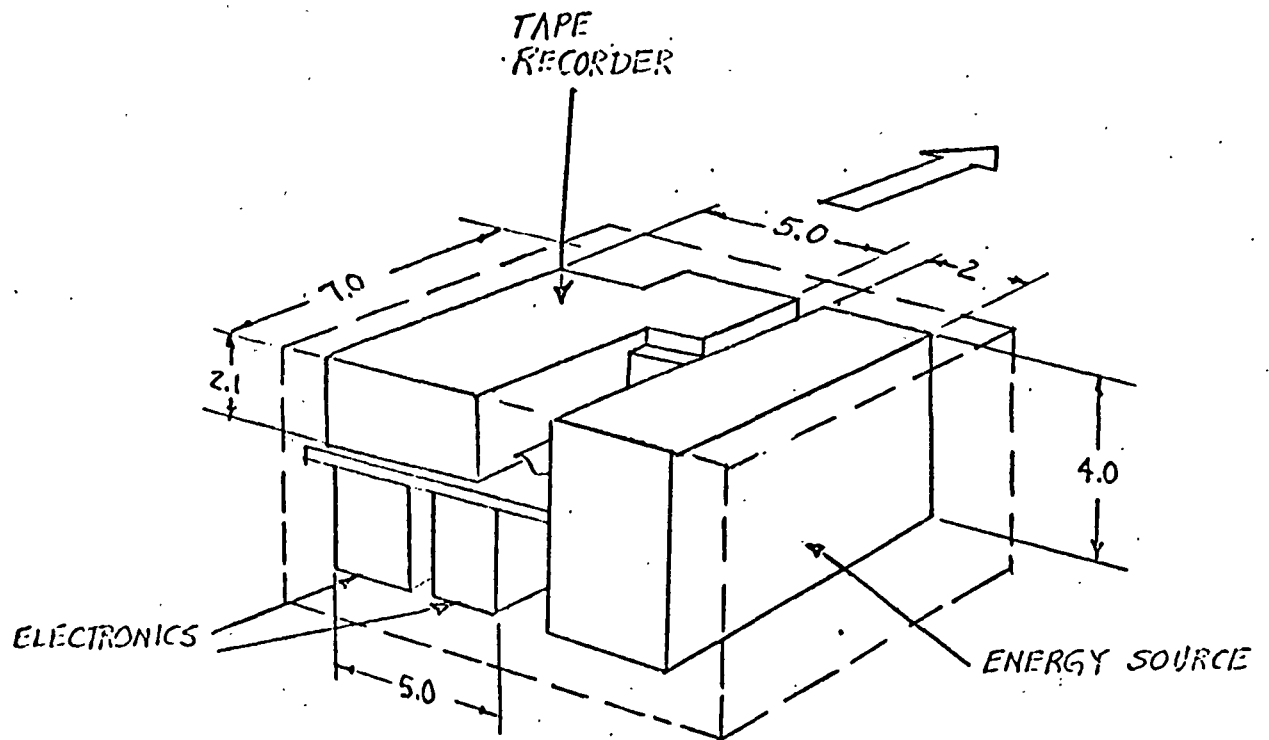


Figure 9

Receiver Electronic Subassemblies

"Page missing from available version"

I-20

and position 3 turns the receiver on. When the receiver is on, the indicator is illuminated when there is satisfactory output from the tape motion sensor. When the receiver is placed in the semi-active thermal control mode, the indicator remains lit for several seconds after the switch is thrown, and then is extinguished; and when the receiver is shut off, the indicator goes off immediately.

4. QUALITY ASSURANCE PROVISIONS (R&QA PLAN
APPENDIX F TO WORK STATEMENT)

4.1 Experiment and Design Verification Tests

4.1.1 Experiment Verification

4.1.2 Design Verification

4.2 Production Test Items

4.2.1 Component Test - Electrical

4.2.2 Component Test - Mechanical

4.3 Acceptance Test

4.4 Qualification Test

5. PREPARATION FOR DELIVERY

Not applicable to Part I of CEI Specification.

5. NOTES

Information included for administrative convenience only and not a part of the specification in the contractual sense.

APPENDIX 6.2

CONFIGURATION MANAGEMENT PLAN

E-2509

NASA EXPERIMENTS
CONFIGURATION MANAGEMENT
PLAN

by

M. G. Murley

August, 1970

Type I Document
NASA Approval Pending

CHARLES STARK DRAPER
LABORATORY

MASSACHUSETTS INSTITUTE OF TECHNOLOGY

CAMBRIDGE, MASSACHUSETTS, 02139

E-2509

NASA EXPERIMENTS
CONFIGURATION MANAGEMENT
PLAN

by

M.G. Murley

August, 1970

CHARLES STARK DRAPER LABORATORY
MASSACHUSETTS INSTITUTE OF TECHNOLOGY
CAMBRIDGE, MASSACHUSETTS 02139

Approved: *L. E. Larson Jr.* Date: 9/28/70
L. E. LARSON, DEPUTY ASSOCIATE DIRECTOR
CHARLES STARK DRAPER LABORATORY

Approved: *D. G. Hoag* Date: 28 Sep 70
D.G. HOAG, ASSOCIATE DIRECTOR
CHARLES STARK DRAPER LABORATORY

Approved: *Ralph R. Ragan* Date: 28 Sep 70
R. R. RAGAN, DEPUTY DIRECTOR
CHARLES STARK DRAPER LABORATORY

1-a

ACKNOWLEDGMENT

This report was prepared under DSR 55-42200 and 55-42300 sponsored by the Manned Spacecraft Center of the National Aeronautics and Space Administration through Contract NAS 9-10749 and 9-10748.

TABLE OF CONTENTS

<u>Chapter</u>		<u>Page</u>
	INTRODUCTION	9
1	DESIGN REVIEW BOARD	11
	1.1 Purpose	11
	1.2 Scope	11
	1.3 Function	12
	1.4 Organization	12
	1.4.1 Representation	13
	1.4.2 Responsibilities	13
	1.4.3 Schedule	13
	1.5 Applicable Documents	14
2	CONFIGURATION CONTROL BOARD	15
	2.1 Purpose	15
	2.2 Scope	15
	2.3 Function	15
	2.4 Procedure and Responsibilities	15
	2.5 CCB Membership	16
	2.5.1 CSDL Configuration Change Control Board Approval	17
	2.5.2 NASA Approval	18
	2.5.2.1 Participating Members	18
	2.5.2.2 NASA	18
	2.5.2.3 Manufacturing Contractor Approval	18
	2.5.2.4 CSDL	18
	2.5.2.5 Document Controller	18
	2.5.2.6 Recorder	19
	2.6 CCB Document Flow	19
	2.7 Identification of Data Subject to Change or Release Procedures	19
	2.7.1 Purpose	19
	2.7.2 Documents	19
	2.7.3 Identification of Document Release Classifications A and B	21

TABLE OF CONTENTS (Cont)

<u>Chapter</u>		<u>Page</u>	
2.7.3.1	Class A Release	21	✓
2.7.3.2	Class B Release	21	✓
2.7.4	Revisions to Class A and Class B Documents ...	22	✓
2.7.4.1	Class I Change (Reference NHB 8040.2)	23	✓
2.7.4.2	Class II Change (Reference NHB 8040.2)	24	✓
2.7.4.3	Determination of Revision Class	25	✓
2.7.5	Exceptions	25	✓
2.8	Engineering Change or Release Documents	25	✓
2.8.1	Introduction	25	✓
2.8.2	Engineering Change or Release Form	26	✓
2.8.2.1	ECR Form Rules	26	✓
2.8.2.2	Assignment of Effectivity	28	✓
2.8.2.2.1	Requirements for Effectivity	28	✓
2.8.2.3	Instructions for Preparation of ECR	29	✓
2.8.3	ECR Procedures	36	✓
2.8.3.1	Initial Release of Documents Maintained by CSDL	36	✓
2.8.3.1.1	CSDL Originator	36	✓
2.8.3.1.2	Contractor	36	✓
2.8.3.1.3	CSDL Design Group Leader	37	✓
2.8.3.2	Initial Release of Documents Maintained by the Contractor	37	✓
2.8.3.2.1	Contractor	37	✓
2.8.3.2.2	CSDL Design Group Leader	37	✓
2.8.3.3	Revisions to Documents Maintained by CSDL ...	37	✓
2.8.3.3.1	Originator	38	✓
2.8.3.3.2	Contractor	38	✓
2.8.3.3.3	CSDL Design Group Leader	38	✓
2.8.3.4	Revisions to Documents Maintained by the Contractor	38	✓
2.8.3.4.1	CSDL Design Group Leader	39	✓
2.8.3.4.2	Contractor, After CCB	39	✓
2.8.3.5	Procedure to Make Documents Obsolete	39	✓
2.8.3.5.1	No Title	40	✓
2.8.3.6	Procedure to Make a Document Inactive	40	✓
2.8.3.6.1	No Title	40	✓
2.8.4	ECR Corrective Actions	40	✓

TABLE OF CONTENTS (Cont)

<u>Chapter</u>		<u>Page</u>	
2.8.5	Documents	41	✓
2.8.5.1	The Project Document History Log	41	✓
2.8.5.2	End Item Configuration Family	43	✓
2.9	Special Instructions	43	✓
2.9.1	Nonconformance Documentation	43	✓
2.9.1.1	Material Review Board (MRB) Reports	43	✓
2.9.1.2	Waivers	43	✓
2.9.1.2.1	Contractual Waivers	43	✓
2.9.1.2.2	Engineering Waiver	47	✓
2.9.1.2.3	CSDL Waiver and Deviation Procedure	47	✓
2.9.1.2.3.1	Waivers	47	✓
2.9.1.2.3.2	Deviations	49	✓
2.9.1.2.3.3	Classification of Waivers and Deviations	49	✓
2.9.1.2.3.4	Procedure Definitions	50	✓
2.9.1.2.3.5	Preparation of the Nonconformance Authorization Format	51	✓
2.9.2	Engineering Change Proposal (ECP)	53	✓
2.9.2.1	ECP Recommendations	53	✓
2.9.2.2	ECP Preparation	53	✓
3	CHANGE CONTROL AFTER DELIVERY OF EQUIPMENT	55	
3.1	Retrofit Kit Release, Revision, and Marking	55	✓
3.1.1	Retrofit Kit Content	55	✓
3.1.1.1	Retrofit Instruction Bulletin (RIB)	55	✓
3.1.1.2	RIB Numbers	57	✓
3.1.1.3	Contractor In-House Retrofit	57	✓
3.1.2	Acceptance Data Package	57	✓
3.1.3	Drawings and Documents	57	✓
4	CONFIGURATION CONTROL IN MANUFACTURING	61	
4.1	Purpose	61	✓
4.2	Scope	61	✓
4.2.1	Design Review	61	✓
4.2.2	Parts Procurement Integrity	61	✓
4.2.3	Material Control and Traceability	61	✓
4.2.4	Manufacturing and Production	61	✓
4.2.5	Non-Conformance Monitoring	61	✓

TABLE OF CONTENTS (Cont)

<u>Chapter</u>		<u>Page</u>
4.2.6	Acceptance Data Collection	62 ✓
4.3	Operation Procedures	62 ✓
4.3.1	No Title	62 ✓
4.3.2	No Title	62 ✓
4.3.3	No Title	62 ✓
4.3.4	No Title	62 ✓
4.3.5	No Title	62 ✓
4.3.6	No Title	62 ✓
4.3.7	No Title	62 ✓
4.3.8	No Title	62 ✓
4.3.9	No Title	62 ✓
4.3.10	No Title	62 ✓
4.3.11	No Title	62 ✓
4.3.12	No Title	62
5	GLOSSARY OF TERMS AND ABBREVIATIONS	63
5.1	Glossary of Terms	63 ✓
5.2	Abbreviations	65 ✓

LIST OF ILLUSTRATIONS

<u>Figure</u>		<u>Page</u>
1	Configuration Control Organization Chart	17
2	Basic Documentation Flow Control Chart	20
3	ECR Form (Sheets 1 and 2)	30/31
4	Document History Log	42
5	Configuration Family Tree	44
6	Family Tree Legend	45/46
7	Deviation/Waiver Request	48
8	Retrofit or Repair Compliance Form	56
9	RIB Outline	58

INTRODUCTION

CONFIGURATION MANAGEMENT PLAN

Purpose

This document presents the CSDL plan for the establishment, implementation and maintenance of a configuration management system for NASA experiments.

It provides an operating plan and the necessary procedures to provide a common base for configuration management.

Organization and Function, Configuration Management Office

The objective of this document is to outline the overall functional organization of Configuration Management for NASA Experiments and to specify its responsibilities and basic authority. The CMO operates in a management capacity to identify the requirements, establish the procedures and assign responsibility for the establishment and maintenance of configuration control for NASA experiments and their related support equipment.

The following formally organized boards provide the basic coordination and control points for configuration management.

- (1) Design Review Board (DRB)
- (2) Configuration Control Board (CCB)

Preceding page blank

CHAPTER 1

DESIGN REVIEW BOARD DRB Organization and Procedures

1.1 Purpose

This Chapter defines in sufficient detail the Design Review activity undertaken by CSDL in connection with the design and development of NASA experiments and short term programs.

The concept is to provide the highest degree of assurance as early as possible so that maximum potential is realized for the design factors below, and any areas requiring additional improvement may be defined and acted upon in an expeditious manner. The intent is to make the DRB a beneficial endeavor to all concerned with the design of the experiment and its interface with associated systems. The degree of success depends on the attitude and cooperation it is afforded.

In each element of design the following factors are to be considered:

Reliability	Failure Effect Analysis
Producibility	Standardization
Maintainability	Optimization
Compatibility	Function and Operability
Interfaces	Parts Application
Material Usage	Mechanical Integrity
Safety	Cost
Format	Completeness

1.2 Scope

The Design Review shall be applicable to all initial design and engineering efforts. All documents describing the design of the experiment or important to its fabrication, assembly, test, use, and procurement of parts and material must be reviewed and approved by the DRB before submittal to and release by the CCB. In changes subsequent to Design

Preceding page blank

Review and Change Control Action, not effecting Reliability, Form, Fit or Function, that is to say, Class II changes (as defined in Section 2.7) need not go to Design Review, only to the Change Control Board.

1.3

Function

The Design Review will bring together representatives with specialized as well as general experience to evaluate the detail design for consideration of factors as aforementioned. Although the responsibility for design will continue to be that of the design engineer and no attempt will be made by Design Review Representatives to usurp the prerogatives of the designer, they can and will, by an unbiased and independent appraisal, assure that every consideration has been given toward the generation of an optimum design. Courses of action necessary to alleviate or correct any hazard areas will be recognized and implemented before costly malfunctions can be experienced. The result of Design Reviews will be adequately documented to ensure effective follow-up corrective action.

In order to realize the full benefit of the Design Review, it must take place in sufficient time to permit any corrective measures developed to be incorporated before release through the CCB. While it is highly desirable for the DRB to consider the design package in the final form in which it will be released, and every effort should be made to permit this, it is recognized that because of overall schedules and the need for releasing designs to start fabrication and procurement, such may be neither possible nor practical. It is far better to conduct a timely review on preliminary versions of the final design that may be nearly complete than to wait until everything is complete and no time is left for adoption of beneficial recommendations stemming from the Design Review.

Therefore, design groups shall carefully weigh their progress against release deadlines and suggest that the design reviews be scheduled at the earliest possible time that meaningful results can be obtained.

1.4

Organization

The DRB organization and individual responsibilities are as follows.

1.4.1 Representation

Chairman	:	Project Technical Director (or Designate)
Recorder	:	Secretary Clerk
Member	:	System Integration Staff Engineer
Member	:	Responsible Design Engineer
Member	:	Manufacturing Engineer
Member	:	Quality Assurance/Reliability Engineer
Others	:	Consultants as required

1.4.2 Responsibilities

Chairman.

- (1) Preside at DRB Meetings.
- (2) Provide DRB signature approval of an Engineering Change or Release (ECR).

Recorder

- (1) Assist Chairman in scheduling Design Review Meetings.
- (2) Determine scope of each review and notify particular members of date, time, place, subject and materials required.
- (3) Keep an accurate record of proceedings.
- (4) Maintain records and file of Design Review activities, prepare and distribute reports.

Members

- (1) Participate in reviews.
- (2) Present descriptions of the design or proposed changes thereto, reasons for the change along with any data and results of engineering evaluation as required.
- (3) Act on recommendation of the DRB.

1.4.3 Schedule

The DRB will meet as required to satisfy the needs of the program.

1.5

Applicable Documents

The following was used as source documentation in the generation of this plan which has utilized license toward meeting the specific goals of a NASA Experiment.

- | | | |
|-----|-----------------|--|
| (1) | NHB 8040.2 | Apollo Configuration Management Manual |
| (2) | E1167 | Apollo Drawing Standards |
| (3) | E1087 | Documentation Handbook |
| (4) | NHB 5300.4 (1B) | Quality Program |
| (5) | NPC 200-3 | Inspection System |
| (6) | NPC 250-1 | Reliability Program |

CHAPTER 2

CONFIGURATION CONTROL BOARD

2.1 Purpose

This procedure establishes the method for the release and revision of the technical data necessary to fulfill the design and configuration control responsibility assigned to CSDL on NASA experiments for Class I and II changes as related to these data. It establishes the method by which CSDL will control the design configuration as represented by the technical data released.

2.2 Scope

The procedures for release and revision of technical data require the

- (1) Establishment of the CCB as an adjunct of the CMO for the formal processing of documents
- (2) Identification and definition of documents which must be processed under this procedure
- (3) Establishment of responsibilities in processing the release and revision of technical data
- (4) Establishment of necessary forms and the distribution of data

2.3 Function

The CCB is the authorizing agency of CSDL for the initial release and subsequent revision of technical documentation for NASA experiments. This authority may be delegated to members as necessary to expedite the flow of technical documentation; however, the designated members must have approval authority commensurate with their responsibilities.

2.4 Procedure and Responsibilities

The formal and complete release of technical data requires the approval of the Authorizing Members of the CCB as specified in Section 2.5.1.

If any one approval is withheld, an agreement must be reached on the further action or disposition of the document, and responsibility for completing the action shall be assigned by the CCB Chairman.

The CCB functions on the assumption that complete coordination and understanding has been attained prior to presentation of the document for formal release. The formal meeting of the CCB presents the opportunity for the Authorizing Members to query in detail the other organizations involved as necessary before approval of the document.

The technical documents released by the CCB constitutes the authenticated sources of design data to be used in the manufacturing of the Experiment hardware.

The names of the Authorizing Members and their alternates designated by each organization shall be formally submitted to the chairman of the CCB for inclusion in the administrative record of the CCB.

2.5

CCB Membership

CCB membership is comprised of authorizing and participating members.

Authorizing members are the NASA representative and the CCB Chairman.

Participating members shall be as follows.

- Project Manager (or designate) (Chairman)

- Design group leader

- DRB, systems integration engineer, or other representation as required

- Document controller

- Recorder

- Contractor Support or observer personnel as required

The relationship of the CCB to the CMO is shown in the organization chart of Figure 1.

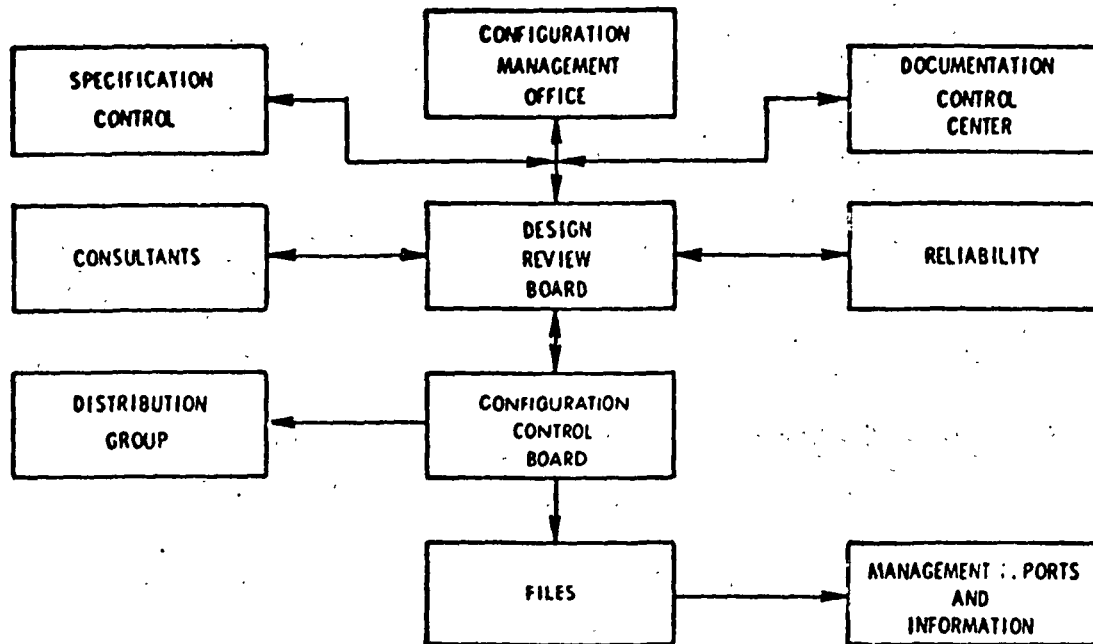


Figure 1 Configuration Control Organization Chart

2.5.1 CSDL Configuration Change Control Board Approval

The CSDL Configuration Change Control Board Approval indicates that the following CCB requirements have been fulfilled.

- (1) Proper CSDL coordination and design approval
- (2) Adequacy of information provided to fulfill requirements of the documentation control system
- (3) Design approval of planned effectivity for configuration control

In addition a CSDL Authorizing Member shall

- (4) Be chairman of the CCB
- (5) Establish time and place of meetings
- (6) Designate work load requirements
- (7) Notify the required Participating Members
- (8) Provide the support services (recorder and document controller)

2.5.2 NASA Approval

NASA Approval indicates the NASA Authorizing Member gives final approval to Class I and II changes to signify the Government's acceptance of the technical data and the possible program impact on cost, schedule and effectivity.

2.5.2.1 Participating Members

The Participating Members are in direct support of the Authorizing Members.

2.5.2.2 NASA

The NASA Participating Member shall act as requested by the Authorizing Member to support the Authorizing Member or to observe proceedings.

2.5.2.3 Manufacturing Contractor Approval (If Applicable)

The Manufacturing Contractor approval indicates that the contractor is:

- (1) Accepting the technical data as binding within the cost, schedule, and effectivity designated. If the impact cannot be fully recognized, modifying conditions may be made on the ECR form,
- (2) Presenting to the CCB any problems his organization foresees in carrying out the design intent, effectivity or any other consideration being imposed,
- (3) Accepting the documentation requirements for correctness and format.

2.5.2.4 CSDL

The Participating Member for CSDL shall be the cognizant design group leader, system integration engineer, and/or other personnel required to present documents and supply additional information to the CCB.

2.5.2.5 Document Controller

The Document Controller is a required Participating Member to support the CCB Chairman in:

- (1) Processing the approved CCB actions and documents into the documentation control system,
- (2) Coordinating the CSDL support function of reproducing and distributing documents,
- (3) Checking documents for completeness and accuracy of managerial information.

2.5.2.6 Recorder

The Recorder is a required Participating Member and provides services assigned by CSDL under the direction of the Document Controller. His activities will include, but not be limited to the following:

- (1) Preparing for the CCB meeting and coordinating the schedule by ascertaining the number and types of releases and communicating with CCB members,
- (2) Assisting the Document Controller,
- (3) Maintaining a complete log of all items brought before CCB and the actions resulting,
- (4) Assigning ECR numbers to completed CCB actions,
- (5) Maintaining and publishing a record of CCB actions after each meeting, indicating ECR actions completed and reasons for rejection or delays of any unfinished ECR action,
- (6) Providing typing and other clerical services at CCB as required,
- (7) Distribution of released documents.

2.6 CCB Document Flow

Figure 2 shows the general flow of documents to and through the CCB, for all changes.

2.7 Identification of Data Subject to Change or Release Procedures

2.7.1 Purpose

The purpose of this section is (1) to identify the documents which are subject to the CCB Procedure, (2) to define the release and revision classifications, and (3) to identify the requirements unique to each classification.

2.7.2 Documents

The following, and changes thereto, must be approved by the CCB to become authorized documents for use in the production, testing, and acceptance of the NASA Experiments and/or any related equipment.

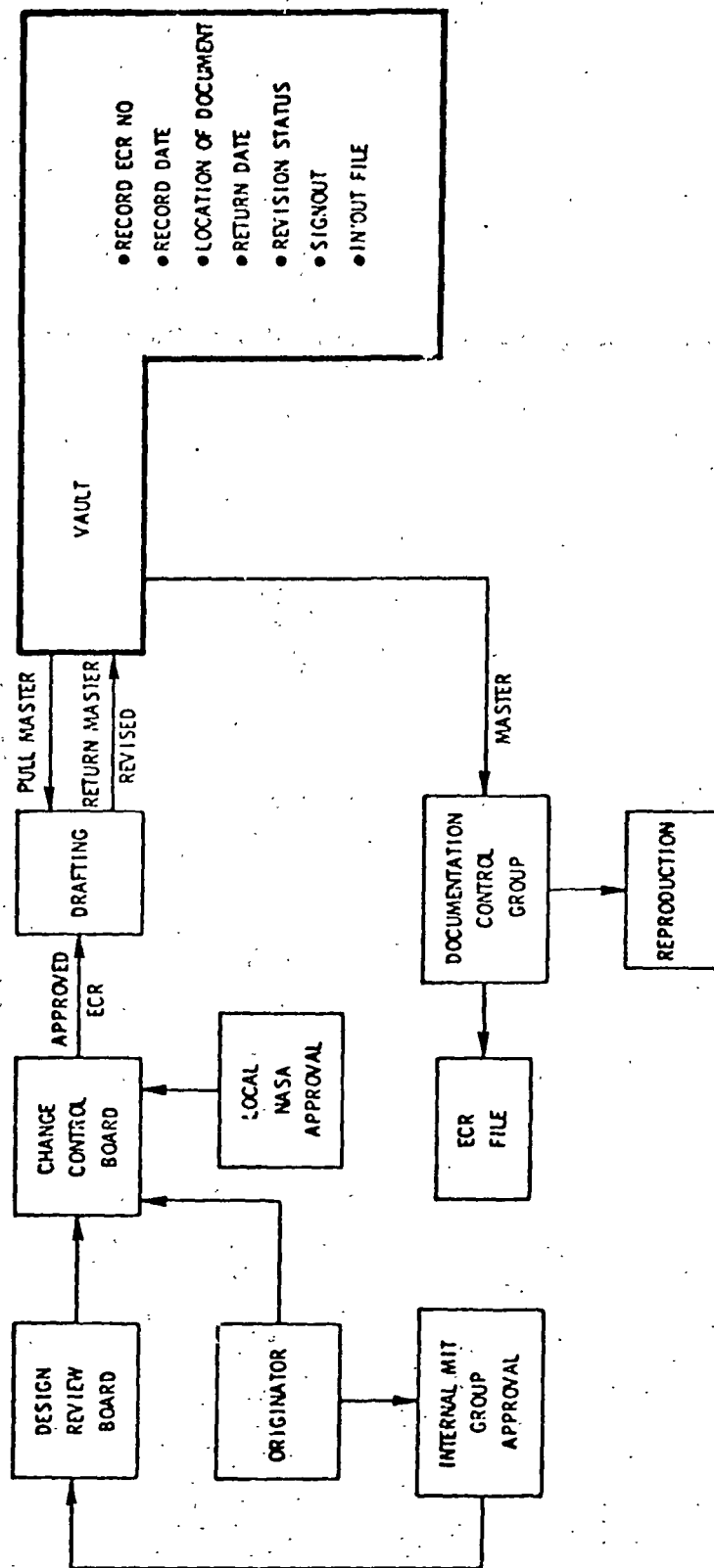


Figure 2 Basic Documentation Flow Control Chart

- (1) All drawings, schematics, assemblies, parts lists, layout, packaging, and the like
- (2) Procurement Specifications
- (3) Specification Control Drawings (SCD's)
- (4) Assembly Test Specification/ Procedures (ATS/ P)
- (5) Process and Material Specifications
- (6) Interface Control Documents (ICD's)
- (7) Waivers/ Deviations
- (8) Manuals
- (9) Approved Suppliers List
- (10) Computer Programs

This list does not preclude the addition of other documents for which a review cycle and document control may be desirable or mandatory.

2.7.3 Identification of Document Release Classifications A and B

Documents referred to herein are grouped into two classifications: Class A and Class B.

2.7.3.1 Class A Release

Class A documents are those which the project or design engineer designates as representing the design configuration to be used for operational hardware and supporting equipment. All documents that do not carry a Class B designation are to be considered Class A documentation. Changes to Class A documents must be rigidly controlled since such changes may affect interfaces, procurement specifications, tooling, and the like. Incomplete initial releases shall be subject to management approval prior to CCB action, and shall be approved only in exceptional cases. The DRB shall review and approve all initial Class A releases and Class I changes prior to CCB action. Class A documents are signed and authenticated releases.

2.7.3.2 Class B Release

Class B documents are essentially drawings and supporting documentation generated during the research and development stages of the program. They shall meet normal document standards and shall contain a Class B marking. Depending upon the phase of development, they may only partially fulfill the complete requirements of the document content.

Class B documents are representative of the current status of design development and are released in advance of completed design, prior to approval, in order to permit breadboarding and evaluation and to initiate planning and advance procurement in areas that are critical from a schedule standpoint.

It is normally expected that there may be numerous revisions to Class B documents, particularly drawings, before completion of design and Class A release. However, in order to meet schedules, Class B documents must be released at the earliest possible date. Limited advance procurement and/or fabrication of parts and assemblies built to Class B documents can be authorized whenever it is considered essential to maintain schedules. Acceptance testing and assembly of items procured, fabricated, or assembled for manned vehicles from this advance procurement based on Class B documentation shall meet the requirements of the resultant Class A releases. Drawings and documents issued as Class B releases for the purpose of breadboarding or evaluation of proposed design are continuously reviewed and should be upgraded to Class A releases as soon as possible.

The DRB shall review and approve all initial Class B releases and Class I changes prior to CCB action.

A Class B document can be upgraded to a Class A document when appropriate by approval of the DRB, removal of the Class B marking, and upon release by the CCB.

2.7.4 Revisions to Class A and Class B Documents

Since Class A and Class B documents represent two distinct phases of documentation, revisions to each class of document must of necessity be accomplished in such a manner as to support and implement the basic intent of the two classes of release. No changes to Class A documents can be made prior to CCB approval.

Changes to Class B documents are handled in the same way as changes to Class A documents, but special procedures may be devised by the CMO to handle special situations concerning Class B revisions.

In addition to the two classes of document release, revision to either class of document shall be divided into two broad categories, Class I and Class II, as defined below.

2.7.4.1 Class I Change (Reference NIIB 8040.2)

An engineering change shall be classified Class I when one or more of the factors listed below (subparagraphs (a) or (b) or any factor(s) listed under (c), (d) or (e)) is affected:

- (a) The functional or allocated configuration identification.
- (b) The product configuration identification as contractually specified (or as applied to Government activities), excluding referenced drawings.
- (c) Technical requirements below contained in the product configuration identification, including referenced drawings, as contractually specified (or as applied to Government activities).
 - (1) Performance outside stated tolerance.
 - (2) Reliability, maintainability or survivability outside stated tolerance.
 - (3) Weight, balance, moment of inertia.
 - (4) Interface characteristics.
- (d) Non-technical contractual provisions.
 - (1) Fee
 - (2) Incentives
 - (3) Cost
 - (4) Schedules
 - (5) Guarantees or deliveries
- (e) Other factors
 - (1) Government furnished equipment (GFE)
 - (2) Safety
 - (3) Electromagnetic characteristics
 - (4) Operational, test or maintenance computer programs
 - (5) Compatibility with support equipment, trainers or training devices/equipment.
 - (6) Configuration to the extent that retrofit action would be taken.
 - (7) Delivered operation and maintenance manuals for which adequate change/revision funding is not on existing contracts.
 - (8) Pre-set adjustments or schedules affecting operating limits or performance to such extent as to require assignment of a new identification number.
 - (9) Interchangeability, substitutability or replaceability, as applied to CI's, and to all subassemblies and parts or repairable CI's, excluding the pieces and parts of non-repairable subassemblies.
 - (10) Sources of CI's or repairable items at any level defined by source control drawings.

Class I changes must be approved by the DRB prior to the CCB. The effectivity for a Class I change must be specified prior to the review by CSDL DRB. Any change made to the effectivity at the CCB will require re-approval of the DRB. The effectivity stated at the time of CCB approval shall be mandatory.

All proposed Class I changes shall be prepared as complete package changes. The changes must be defined in all areas of the drawing structure through the highest assembly affected, including Process Specification.

2.7.4.2

Class II Change (Reference NHB 8040.2)

Any engineering change not falling within Class I as defined above shall be designated as a Class II change. Generally Class II changes are those changes which are desirable but not technically necessary from a system function standpoint. Changes required to comply with documentation format specifications would be in this class. A Class II change cannot change form, fit, function or reliability so as to affect interchangeability and will not result in the scrapping of any previously manufactured item. No effectivity is specified and the change is incorporated on the basis of no cost and no schedule impact.

The Inactivation or Obsoleting of documents shall be considered a Class II change. Inactivation and Obsoleting of documents are defined as follows.

- (1) Inactivated : Inactivation of a document shall prevent further use of a document which has been released through the CCB and used to build, procure, test, or otherwise support hardware. The fact that the document has been "used" requires the designation of being inactivated and not obsoleted.
- (2) Obsoleted : Obsolescence of a document shall prevent the use of a document which has been previously released through the CCB but never actually used to build, procure, test, or support hardware. Documents shall not be made Obsolete if any hardware has been built to the document.

When an ECR is prepared to incorporate a Class I change in a document, Class II changes are sometimes incorporated on the same ECR. Class II changes released in this manner automatically become Class I changes and are subject to all the requirements

imposed for a Class I change, including the DRB review and approval prior to the CCB. Care must therefore be exercised that true Class II changes processed by this method do not produce a cost or schedule impact or result in nonessential changes to hardware.

If any change on the ECR is considered by the CCB to be Class I or if any doubt should arise concerning the Class II designation for a change, the entire ECR shall be submitted to the CSDL DRB for evaluation and approval. Normally, Class II changes shall not require CSDL DRB approval.

2.7.4.3 Determination of Revision Class

It is the originator's responsibility to initiate the change as Class I or Class II. Final determination of the class of change rests with the CSDL DRB and the CCB. When designating any change, the effects on interface activities including logistics, training, operation, reliability, and the like must be considered. Any change in the revision class effected at CCB shall require approval by the DRB.

2.7.5 Exceptions

Some documents are processed through CCB for record purposes only and to insure distribution throughout the system. Documents falling into this category are Interface Control Documents (ICDs). When documents of this type are submitted to CCB, the ECR should be boldly marked in the "Description of Changes" column "For Information Only," thus indicating that the signatures of the Contractor and NASA are not required.

2.8 Engineering Change or Release Documents

2.8.1 Introduction

The purpose of this section is to relate the ECR form to the procedures required for the release, revision and recording of technical data.

The required ECR form provides the means of processing data and a record of approved technical data.

2.8.2

Engineering Change or Release Form

The ECR form is the sign-off form for the CCB. It is serialized and recorded when approved as part of the Board's record and provides the only authority for the release or revision of NASA Experiment Systems technical data.

All the documents listed in Section 2.7 of this procedure require processing by ECR's for approval. The person who prepares the ECR form is responsible for assuring that there is a mutual understanding of the reason for the change and the effect of the change by the responsible engineering personnel at the Charles Stark Draper Laboratory, the Contractor's facility and the Government Agency. If documents are applicable to other systems, the changes must be coordinated through the associated groups.

2.8.2.1

ECR Form Rules

An initial release is defined as the procedure followed the first time an identification number is assigned to a document, part or assembly and the document is processed through the CCB. Subsequent revisions to the document which do not affect interchangeability are called "revisions" and are indicated by using the same identification number with appropriate change made to the revision letter. If a document has already been released and must be revised in such a manner as to cause a noninterchangeability of parts, a new identification number or a new dash number is assigned. If a new identification number (seven digits) is assigned to a replacing part, the new drawing shall be released through the CCB as an initial release.

If a new dash number is assigned to a replacing part, the action on that drawing is a revision through the CCB.

The action of replacement with a noninterchangeable part is evidenced on the next higher assembly where a new dash number must also be added to show noninterchangeability at this level, and progressively up to the level where interchangeability is re-established. To alert those who are concerned with effectivity and spares provisioning, the ECR may emphasize by note that the revision adding a new dash numbered configuration creates a noninterchangeable replacement.

The following rules apply for ECR's:

- (1) Each ECR may include more than one document for initial release; however, when changes affect more than one drawing, a separate ECR shall be prepared for each revised drawing except in the following cases:
 - (a) All drawings to be made obsolete or inactive may be listed on one ECR Form.
 - (b) On package changes for which the effectivity and overall reason for the change are identical for several different drawings, even though the specific changes listed for each drawing may differ, a single ECR may be used for processing the entire release at CCB. The changes to each drawing itemized on the ECR must be completely described. The revision letter changes to each drawing shall be tabulated in the "Description of Changes" block.
- (2) Each ECR for a revision must carry a complete description of the proposed change (i. e. , FROM:, TO:) so that it is possible to effect the revision without further information. The change shall be fully described on the ECR and a marked-up reproducible shall accompany the ECR except when, in the judgment of the originator, the ECR is prepared in sufficient detail and clarity as not to be subject to misinterpretation, in which case the marked-up reproducible may be omitted.
- (3) When "non-interchangeable replacements" are being prepared, the part number of the replaced part should be referenced.
- (4) If a "reissue" of an ECR is used to correct errors which were present on it when it was originally issued, the original ECR is brought to CCB, where it is marked and initialed by those concerned to indicate the correction which is made. The document itself is not affected because the error exists only on the ECR. If the CCB review reveals a possible Class I change resulting from the correction (e. g. , "effectivity"), the ECR shall be boldly marked at the top "REISSUE" and the minutes of the CCB Meeting shall record the action. (See Section 2. 8. 4).

(5) All ECR's are consecutively numbered by the CCB upon approval. The configuration control data contained in the approved ECR is recorded and released for distribution and documentation.

(6) All ECR's are to be typed.

2.8.2.2 Assignment of Effectivity

The following rules apply for assigning effectivity on ECR's.

- (1) Effectivities associated with equipment shall be assigned in accordance with the sequence of system or subsystem (as applicable) end-item serial numbers. If "cut-in" only is indicated on the ECR, the effectivity applies to the serial number entered and to all subsequent hardware.
- (2) The "cut-out" effectivity must be supplied whenever it is necessary to limit procurement or usage to an amount less than the total contract buy. The omission of a "cut-out" will be interpreted as indicated in paragraph (1) above.
- (3) To change the effectivity specified for a previous revision without a documentation change will be handled by reissuing the latest applicable ECR.
- (4) Contract End Item Serial numbers will be assigned in accordance with NHB 8040.2.

2.8.2.2.1 Requirements for Effectivity

The following ground rules identify the minimum requirements for the assignment of effectivity and do not preclude conformance with additional requirements, not stated herein, which are also contractually imposed.

- (1) Effectivity shall be specified for all Class I changes. Revisions to "mechanization drawings" shall be exempted from this requirement.
- (2) If the effectivity of a Class I change affects spares, it shall be indicated on the ECR in such a way as to clarify the required changes to spares.
- (3) If a change results in a non-interchangeable item, the identification number of the non-interchangeable item and of its next higher assembly, and of all progressively higher assemblies shall be changed up to but not including the level where interchangeability is re-established. The effectivity

changes shall be assigned as required to identify the new configuration or application. These changes shall be processed as a package change.

- (4) The total applicability of a document when considering a particular change to its use shall include all related documents. All affected documents shall be processed as a package change.
- (5) Effectivity of a change to a dash-number type of document applied only to the dash-number specified on the ECR, and does not affect the effectivity of the other dash-number configurations on the drawings. When more than one dash-number is affected by the revision, the effectivity for each of the affected dash-numbers shall be indicated.
- (6) No effectivity shall be assigned to Class II changes.
- (7) No effectivity shall be assigned when a new item is released. Effectivity for such items is determined by reference to the assembly drawings which call out the new items.

2.8.2.3 Instructions for Preparation of ECR

Instructions for preparing ECR's are detailed below (see Figure 3 for the sample ECR form). All items on the form will be completed. "NA" (not applicable) or NONE will be used if necessary.

- Item 1 ECR No.
A five digit ECR number will be assigned by CCB for each approved ECR.
- Item 2 ORIGINATOR CONTROL No.
This block is used for an in-house control identification number when needed prior to release by CCB.
- Item 3 PROGRAM
Title or letter abbreviation of NASA Experiment or project.
Enter the Customer contract number and the document number or CEI number.
- Item 4 DOCUMENT No.
Enter the identification number of the document being processed by the ECR. (See Item 28 for multiple document numbers.)

CHARLES STARK DRAPER
LABORATORY
ENGINEERING CHANGE OR RELEASE

ORIGINATOR CONTRACT NO. <u>2</u>		SHEET 1 of <u> </u>	
PROJECT NAME <u>3</u>		CONTRACT NO. <u>3</u>	
EFFECTS NO. <u>3</u>		ECR NO. <u>1</u>	

DOCUMENT NO. <u>4</u>		REVISION <u>5</u> <u>5</u>		DOCUMENT TITLE <u>6</u>		TYPE DOCUMENT <u>7</u>	
ORIGINATOR <u>8</u>		SYSTEM/SUBSYSTEM <u>9</u>		EFFECTIVITY <u>10</u>			
ORGANIZATION <u>8</u>		DATE <u>8</u>					
DESCRIPTION OF CHANGE (S) RELEASE (S)							
<u>11</u>							
<u>12</u>							
CHANGE CLASS <u>13</u>		NEXT HIGHER ASST <u>14</u>		MASTER DOCUMENT LOCATION <input type="checkbox"/> CSDL <u>15</u> <input type="checkbox"/> <u> </u>		DOCUMENT NO. REPLACES <u>16</u>	
AFFECTED DOCUMENTS <u>17</u>		RELATED ECR NO'S <u>18</u>		AFFECTED INTERFACES <u>19</u>			
AFFECTED CONTRACTS <u>20</u>		REMARKS <u>21</u>					
CSDL ENGINEERING APPROVAL <u>22</u>				MIL. CONTRACTOR APPROVAL <u>26</u>			
DATE <u> </u>				DATE <u> </u>			
R & QA APPROVAL <u>23</u>				NASA APPROVAL <u>27</u>			
DATE <u> </u>				DATE <u> </u>			
CSDL DESIGN REVIEW APPROVAL <u>24</u>							
DATE <u> </u>							
CSDL CHANGE CONTROL BOARD APPROVAL <u>25</u>							
DATE <u> </u>							

TP22924-1

ECR NO. 1

Figure 3

CHARLES STARK DRAPER
LABORATORY

ENGINEERING CHANGE OR RELEASE

SHEET ____ OF ____

PROGRAM	3	CONTRACT NO.	3
CTI NO.	3	ECO NO.	1

DOCUMENT NO.	4	REVISION	FROM	TO	DOCUMENT TITLE	6	TYPE DOCUMENT	7
			5	5				

DESCRIPTION OF CHANGE, PRELIMINARY COMMENT

12

TP22924-2

ECO NO. 1

Figure 3 cont.

Item 5 REVISION

Enter the current revision letter under "FROM" and the new revision letter under "TO. " In the case of the initial release of a document a "-" shall be entered in the "TO" column. If the document is being initially released with a revision status, "-A", "-B", etc., shall be entered in the "TO" column. (See Item 28 for revisions to multiple documents.)

Item 6 DOCUMENT TITLE

Enter the complete title of the document. (See Item 28 for multiple document titles.)

Item 7 TYPE DOCUMENT

Indicate the type of document being released or changed by the ECR. Example: Dwg., SCD, PS, etc.

Item 8 ORIGINATOR

Indicate the name of the individual preparing the ECR, the organization he represents and the date of preparation.

Item 9 SYSTEM/SUBSYSTEM

Enter the name of the assembly or subassembly on which the item appearing under "DOCUMENT TITLE" will be used. For example, if the item listed under "DOCUMENT TITLE" were "Directional Gyro," the subsystem would be the "Gyro Assembly. "

Item 10 EFFECTIVITY

Enter the serial number of the first and last contract end item that will have the change incorporated. If only one serial number is specified, then the effectivity applies to that serial number and all subsequent serial numbers. The last serial number must be supplied whenever it is necessary to limit procurement to an amount less than total contract buy. When a new item is released, this block will be left blank. The effectivity of the new item will be determined by reference to the assembly drawing which calls for the new item. Effectivity must be specified for all Class I changes. Some examples: "1 - 6"

Item 10 (Cont) Indicates that this change will be effective for serial numbers 1 through 6 inclusive. "3" indicates that the change is effective for serial number 3 and all subsequent serial numbers. "4 only" indicates that this change is effective for serial number 4 only.

Item 11 REASON(s) FOR CHANGE/RELEASE

Enter the precise reason for the change. This reason must be complete enough to permit the evaluation of the proposed change. If the ECR is releasing a new item, "Initial Release" shall be entered here.

Item 12 DESCRIPTION OF CHANGE(s)/RELEASE(s)

Supply a complete description of the changes indicating the present condition (FROM) and the specific way the document is to be revised (TO). Supplementary reproducible sheets 8 - 1/2 by 11 inches in size may be included to amplify the description when the change involves extensive modifications. In certain cases, a reduced-size, marked, reproducible copy of the drawing is permitted to serve as a second page of the ECR. The ECR number is required on the reproducible. The description of the desired change must be complete enough to allow incorporation without any further clarification or interpretation. (See Item 28 for multiple documents.)

Item 13 CHANGE CLASS

Indicate the appropriate change classification, i.e.: Class I or Class II.

Item 14 NEXT HIGHER ASSEMBLY

Indicate the next higher assembly for the document being processed by the ECR. (See Item 28 for multiple documents.)

Item 15 MASTER DOCUMENT LOCATION

Indicate the location of the master document and the activity responsible for incorporating the document revision completely as outlined on the ECR.

Item 16 **DOCUMENT NUMBER REPLACED**

If the ECR is releasing or revising a document that falls into the category of establishing a new non-interchangeable replacement part, the part number of the old part shall be indicated.

Item 17 **AFFECTED DOCUMENTS**

Indicate all other drawings, specifications, or documents that are affected as a result of this change. If the revision resulted in a change to these documents, indicate the revision at which this change took place. If the revision is still under preparation and the revision letter cannot be forecast, indicate this by the letters "UR" (under revision). When possible, associated documents which must be revised as a result of the described revision shall be submitted simultaneously with the original change; the complete revision shall then be submitted as a "Package".

Item 18 **RELATED ECR NUMBERS**

The ECR number for those documents listed in Item 17 that are submitted as a "Package" will be assigned by CCB.

Item 19 **AFFECTED INTERFACES**

If a physical or electrical change affects the interface with another subsystem, indicate the document title and number of the affected subsystem. Also enter the title and number of the Interface Control Document or Specification if affected.

Item 20 **AFFECTED CONTRACTS**

Indicate the MIT Sub-Contract or Industrial Contract number affected either directly or through an interface, by issuance of the ECR.

Item 21 REMARKS

This should be accomplished at the time of CCB approval.

Item 22 ENGINEERING APPROVAL AND DATE

The signature of the responsible design engineer and the date must be entered. This must be accomplished at or prior to submission to the DRB and CCB.

Item 23 QA/RELIABILITY APPROVAL AND DATE

The signature of the responsible QA/Reliability engineer and the date (when specified).

Item 24 DESIGN REVIEW APPROVAL AND DATE

The signature of the chairman of the DRB, or his designated representative and the date will be entered to indicate design approval. This must be accomplished prior to submission to CCB.

Item 25 CONFIGURATION CONTROL BOARD APPROVAL AND DATE

The signature of the Configuration Control Board authorizing member and date are affixed during the CCB meetings.

**Item 26 MANUFACTURING CONTRACTOR APPROVAL AND DATE
(where applicable)**

The signature(s) of the appropriate contractor(s), his affiliation and the date when applicable. This should be accomplished at the time of CCB approval.

Item 27 NASA APPROVAL

Authorization of contracting agency or designate, as required.

Item 28 MULTIPLE CHANGES/RELEASES

One ECR form may be used to process multiple changes/releases whenever the information contained in Items 3, 7, 8, 9, 10, 11 and 13 pertain to all of the changes/releases. This may be accomplished by listing the following information in Item 12.

<u>Item</u>	<u>Document No.</u>	<u>Revision</u>		<u>Document Title</u>	<u>Next Higher Assy</u>
		<u>From</u>	<u>To</u>		

When the ECR is processing multiple changes the following additional information will be furnished following the above listing.

Item 1 Document No.
 (Description of change)

Item 2 Document No.
 (Description of change)

etc.

2.8.3 ECR Procedures

ECR forms and the documents being processed for approval may be originated by CSDL or the Contractor responsible for the manufacture of the equipment in question.

2.8.3.1 Initial Release of Documents Maintained by CSDL

Class A and Class B documents shall be released by the following procedure.

2.8.3.1.1 CSDL Originator

The CSDL originator of the document shall provide blue-line copies (or reproducible on request) to the Contractor and to the CSDL DRB members of each document to be released. These copies should be provided at the earliest possible date prior to submission to DRB and CCB. The ECR forms shall be prepared by the originator.

2.8.3.1.2 Contractor

The Contractor shall review the blue-line copies of drawings prior to CCB action and prepare any pertinent comments relative to, but not limited to, production, design, interface, cost, effectivity, or schedule impact. He must be prepared to complete an Engineering Change Proposal (ECP) form, even though it may only be an ECP of record.

2.8.3.1.3 CSDL Design Group Leader

The design group leader shall

- (1) Process copies of the proposed Class A documents through DRB
- (2) Coordinate with the CSDL Reliability Group for SCDs, procurement specifications, assembly test specifications and procedures, and process and material specifications.
- (3) Consolidate DRB, Contractor and Reliability Group recommendations and submit documents and ECR's to CCB after DRB approval.

2.8.3.2 Initial Release of Documents Maintained by the Contractor **(When applicable)**

Class A and Class B documents shall be released by the following procedure.

2.8.3.2.1 Contractor

When the Contractor is the originator, he shall prepare the proposed documents to be released by CSDL in accordance with CSDL procedure. Blue-line copies of each document to be released shall be provided to the cognizant CSDL engineer and to the DRB members. These blue-lines should be provided at the earliest possible time. The Contractor shall prepare and submit the ECR and the document master to the CSDL design group leader and prepare ECP forms if necessary.

2.8.3.2.2 CSDL Design Group Leader

The CSDL design group leader shall

- (1) Review the drawing prior to submission to DRB and and CCB and prepare any pertinent comments relative to, but not limited to, production, design, interface and effectivity
- (2) Process the proposed documents through DRB for release
- (3) Consolidate DRB CSDL Engineering and Reliability Group recommendations, and submit document masters and the ECR's to CCB.

2.8.3.3 Revisions to Documents Maintained by CSDL

Revisions to documents maintained by CSDL shall be accomplished in the manner described below.

2.8.3.3.1 Originator

Prior to DRB and CCB meetings, the CSDL originator of the proposed revision shall supply copies of each revision, in order to provide advance information, to the following.

- (1) One reproducible copy to the Contractor for planning purposes and cost estimation.
- (2) One blue-line copy for reliability review when applicable. This copy then goes to DRB for review.

2.8.3.3.2 Contractor

The Contractor shall review a copy of the revision prior to CCB action and prepare any pertinent comments relative to, but not limited to, production, design, interface, cost, effectivity, or schedule impact and prepare an ECP if necessary.

2.8.3.3.3 CSDL Design Group Leader

The design group leader shall

- (1) Process the proposed document revision through DRB if necessary.
- (2) Coordinate with the Reliability Group for PS's, SCD's and ATS/P.
- (3) Consolidate DRB, Contractor and Reliability Group comments.
- (4) Group recommendations and submit documents with their ECR's to CCB.

After the CCB approval, the drafting department shall

- (1) Incorporate the document revision completely as outlined on the signed ECR
- (2) Add the CSDL ECR number to the document, raise the document revision to the next sequential revision (must agree with the ECR), and deliver the revised document to the chairman of the CCB within one week after the signed ECR is received from CCB.
- (3) Deliver the signed documents to the Document Controller for distribution.

2.8.3.4 Revisions to Documents Maintained by the Contractor

Prior to DRB and CCB meetings, the Contractor who originates the proposed revision shall provide copies of each drawing in order to provide advance information to the following.

- (1) One reproducible copy or marked-up reproducible to the cognizant engineer at CSDL for evaluation of the proposed revision.
- (2) One copy for Reliability Group review when applicable. This copy then goes for system interface review at DRB.
- (3) If the revision originates at CSDL, the procedure is similar to that described in Section 2.8.3.3 except that the Contractor will finally incorporate the change as specified in this section.

For actual submittal to CCB, the Contractor shall prepare the proposed revision package and submit it to the CSDL cognizant engineering group through the CSDL CMO. The package shall contain a reproducible or marked-up reproducible of all revised documents and a completed ECR form. He shall also prepare an ECP if necessary.

2.8.3.4.1 CSDL Design Group Leader

The CSDL design group leader shall

- (1) Process the proposed documents through DRB if necessary
- (2) Coordinate with the Reliability Group for PS's and SCD's.
- (3) Consolidate DRB, cognizant engineer, and Reliability Group recommendations and submit documents with the associated ECR's to CCB.

2.8.3.4.2 Contractor, after CCB

Upon receipt of the approved ECR's, the Contractor shall perform the following.

- (1) Incorporate all approved changes as specified by the signed-off ECR and supported by a marked-up drawing or specification when necessary.
- (2) Add the CSDL ECR number to the document, raise the document revision to the next sequential letter (must agree with the ECR), and affix his initial. The initial indicates that the approved revision has been incorporated completely and accurately in the master document.
- (3) Deliver a reproducible copy of the updated document to CSDL for distribution.

2.8.3.5 Procedure to Make Documents Obsolete

An ECR shall be prepared to make documents obsolete only when a sufficient quantity has accumulated to make a worthwhile package.
The ECR shall be reviewed and approved by the DRB and CCB.

- 2.8.3.5.1 The revision letter on a document which is made obsolete shall not be changed to effect the obsolescence; however, the word "OBSOLETE" and the date of obsolescence shall be written above the title block on the master of the document. The document is submitted with the ECR to CCB.

Identification of the obsolete documents shall appear in the Document History Log (See Figure 4). No document distribution will be prepared to reflect obsolescence.

The identification number assigned to a document shall not be re-assigned after the document is made obsolete.

2.8.3.6 Procedure to Make a Document Inactive

A document shall be inactivated only if one of the following conditions exists.

- (1) The document is being released by another document which shall be used for all former applications of the inactive document, or
- (2) All hardware supported by the document has been retrofitted and subjected to the requirements of a new document, scrapped or otherwise removed from use.

- 2.8.3.6.1 When an ECR is processed to release a replacement document as described in Items (1) and (2) above, the document which is inactivated shall be identified on the same ECR as a separate action item.

Identification of inactive documents shall appear in the Document History Log.

The identification number assigned to a document shall not be reassigned after the document is made inactive.

2.8.4 ECR Corrective Actions

This procedure outlines the corrective action to be followed when the issued ECR and drawing are not in accordance with each other at the same revision letter.

The two situations and the applicable procedures are identified as follows.

(1) New ECR. If the ECR is correct but the drawing does not reflect the change shown on the ECR:

(a) Make out a new ECR.

(b) Cross-reference should be made to the old ECR by stating in the "Reason for Change" block that "above changes listed on ECR _____ were not incorporated on the drawing at Rev ____."

(c) List on the new ECR only those changes that were omitted on the drawing.

(2) Reissue ECR. If drawing is correct but the ECR is not correct:

(a) Mark up a copy of original ECR to correct the ECR errors for reissue of ECR.

(b) In the "Remarks" block give reason why ECR is being reissued. Mark "Reissue" into border of ECR. At least one day prior to the next scheduled CCB meeting a list of all the ECR numbers being reissued will be given to the CCB recording secretary. This will give the secretary ample time to have original ECR's available for the CCB meeting.

During the CCB meeting a marked-up copy of the ECR will be presented to the board by the design group representative. If approved, a CCB member will transfer this information to the original ECR with the reason for being reissued and the cognizant CSDL engineer will initial the change for processing through the CCB.

2.8.5 Documents

2.8.5.1 The Project Document History Log

The Project Document History Log is the official design release record for those documents which are issued to implement technical direction. (See Figure 4 Sample Format). It identifies all drawings, specifications and other documents released by the CCB for the production, procurement, assembly, inspection and use

of Project hardware, including test equipment.

2.8.5.2 End Item Configuration Family

The End Item Configuration Family Trees may be a pictorial representation of the hardware configuration for each end item. The level of preparation shall be down to the piece part level and also include all other associated documentation such as specifications, schematics, etc. (See Figures 5 and 6).

2.9 Special Instructions

2.9.1 Nonconformance Documentation

2.9.1.1 Material Review Board (MRB) Reports

The reports of MRB's are usually in the form of Variation Permits, requested by a Contractor and submitted for approval to CSDL. The CSDL CMO controls format and procedure.

2.9.1.2 Waivers

All waivers are identified to part number and serial or lot number of the part, assembly, or end item involved. No waiver may be written to cover more than one single system or subsystem. No "blanket waivers" are permitted. If more than one system incorporates the same nonconformance, separate waivers are required for each of the systems. No additional changes shall be made to the face of the waiver after it has been put in process. If substantiating technical data are considered necessary, attachments shall be made to the waiver. A sepia copy of the complete waiver shall be furnished to the CSDL Project Director, who will insure the listing of the waiver in the CSDL documentation control system.

2.9.1.2.1 Contractual Waivers

A Contractual Waiver is originated by the Contractor when a nonconformance exists that adversely affects the safety, reliability, performance, interchangeability, weight or any other basic objective of the contract.

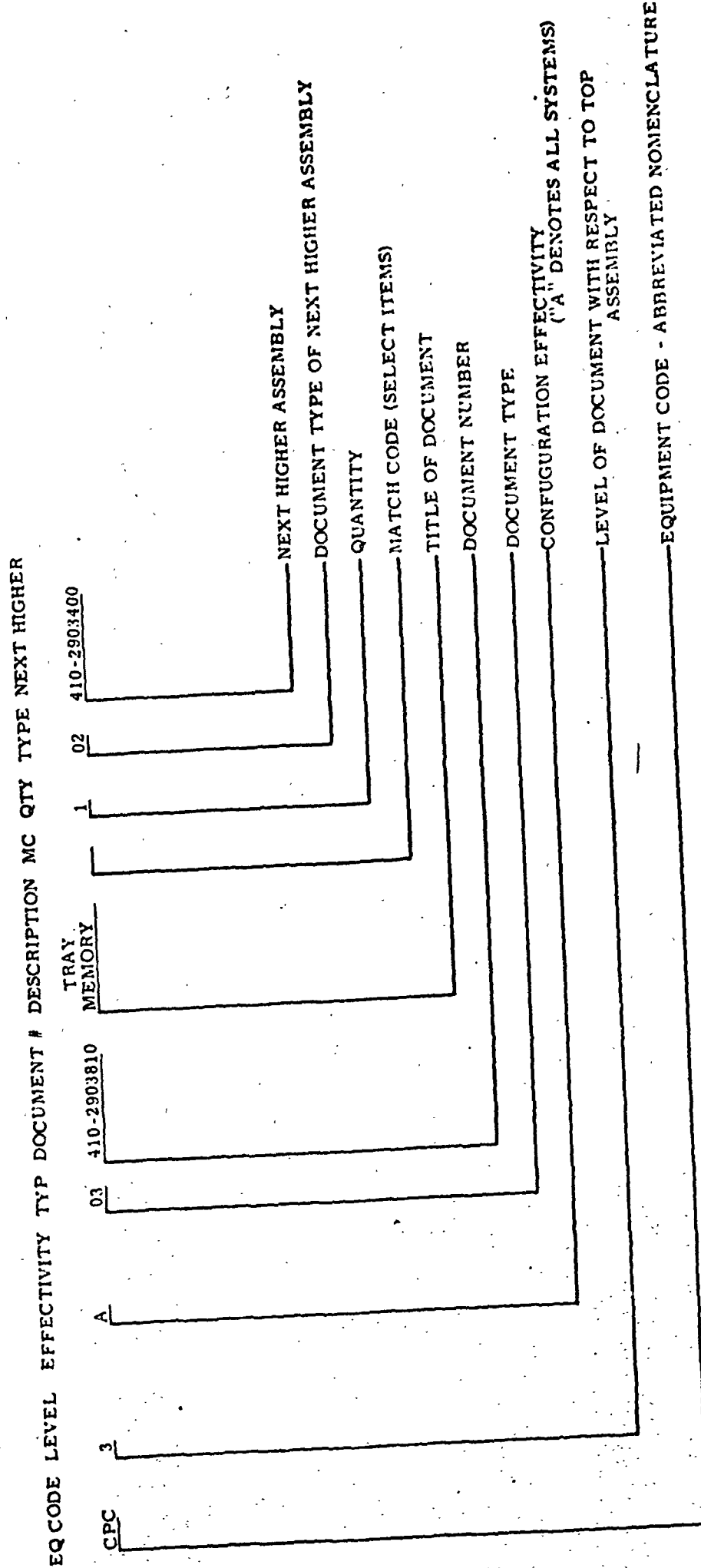


Figure 5 Configuration Family Tree

Figure 6 Glossary

CONFIGURATION FAMILY TREES

Equipment Code:	abbreviated title of the equipment
Level:	<p>pertains to the level of a document with respect to the top assembly.</p> <p>Example: level 1 - top assembly level 2 - items called out on top assembly level 3 - documents called out on level 2 items level 4 - documents called out on level 3 items</p> <p>The computer will list all information on top drawing and parts list and then break each item down to its lowest level.</p>
Effectivity:	where equipment "cuts-in" to the CEI serialization ("A" denotes all systems)
Type:	part number (Document number and dash number)
Part #:	part number (Document number and dash number)
Description:	title of document
M C:	match code (select items)
Qty:	quantity on next higher assembly
Type:	document type of next higher assembly
Next Higher:	next higher assembly (NHA) (used on)

Figure 6 (cont.) Glossary

DATA BANK DOC TYPE CODES

CODE

01	ASSEMBLY
02	PARTS LIST
03	DETAIL OR PART
04	ELECTRICAL SCHEMATIC
05	INTERCONNECT DIAGRAM
06	RUNNING LIST
07	SOURCE CONTROL (SCD)
08	SPEC CONTROL (SCD)
09	INTERFACE CONTROL
10	DATA LIST
11	INDEX LIST
12	REVISION NOTICE
13	MIL SPECS (MIL-D-XXXX, MIL-Q-XXXX, MIL-M-XXXX)
14	FED SPECS (UU-P-XXXXX, CCC-C-XXX)
15	BU WEPS SPECS (JAN)
16	KIT CONTENTS LISTING
17	MIL STANDARDS (MIL-STD-XXX)
18	AN SPECS (AN, NAS, MS)
19	INDUST ASSOC STDS (ASTM)
20	MIT SPECS (S-SC-XXXX)
21	NASA SPECS (OD XXXXX)
22	PROCUREMENT SPECS (PS 410-290XXXX)
23	FACTORY ACCEPTANCE TEST
24	INSTALLATION PROCEDURE
25	CONTRACT END ITEM (CEI 410-290XXXX)

Coordination of the waiver is accomplished with CSDL through the CMO via telephone and/or datafax. CSDL concurrence or non-concurrence is to be accomplished within 48 hours. Format, routing, distribution and designation of authorizing signatures are a CSDL responsibility. This type of waiver requires CSDL signature approval (design cognizance and DRB).

2.9.1.2.2 Engineering Waiver

Engineering Waivers shall have no contractual implications; therefore cost and schedule impact are not a consideration. These waivers are initiated by CSDL or a Contractor.

This type of waiver is initiated when material or items are to be used "as is" and when they possess the following kinds of nonconformance.

- (1) Functional nonconformances other than those defined in Section 2.9.1.2.1 provided that there is no adverse effect on the safety, performance, weight, interchangeability, durability, reliability, or system performance for customer acceptance of demonstrable parameters and the nonconformances do not have an unsatisfactory contract cost or schedule impact.
- (2) When PS's, ATS/P's or drawing errors exist for which an ECR request has been initiated.
- (3) Performance of the deliverable equipment is out-of-tolerance and the condition is defined to be caused by a test equipment inadequacy.

2.9.1.2.3 CSDL Waiver and Deviation Procedure

The purpose of this procedure is to define the responsibilities of CSDL personnel in the initiation, preparation and processing of waivers and deviations.

2.9.1.2.3.1 Waivers (See Figure 7)

A waiver is a written, approved authorization to enable the inspector to accept designated items which are found not to meet contract requirements during production or during inspection.

CHARLES STARK DRAPER LABORATORY

DEVIATION / WAIVER REQUEST

CATEGORY A ☐ B ☐ C ☐ D ☐

DATE _____

SHEET ____ OF ____

PART NUMBER _____	NOMENCLATURE _____
NEXT ASSEMBLY _____	FINAL ASSEMBLY _____
SERIAL NUMBER _____	QUANTITY INVOLVED _____
VENDOR _____	CONTRACT NUMBER _____
PURCHASE ORDER NUMBER _____	TYPE FP <input type="checkbox"/> CPFF <input type="checkbox"/> CPIF <input type="checkbox"/>

DETAILS OF NON-CONFORMITY:

REASONS FOR NON-CONFORMITY:

ACTION THAT MIGHT BE TAKEN TO CORRECT DEFECT IN EXISTING ITEM, IF ANY:

ACTION TAKEN TO PREVENT RECURRENCE OF NON-CONFORMITY:

EFFECT ON PRODUCTION SCHEDULE/COST IF REQUEST NOT APPROVED:

LIMITATIONS OF USAGE: YES ☐ NO ☐

APPROVALS

RELIABILITY

ORIGINATOR

DESIGN ENGINEERING/DRB

CNO

CUSTOMER REPRESENTATIVE

TP22925-1

Figure 7

All waivers are identified to part number and serial or lot number of the part, assembly, or end item involved. No waiver shall be written to cover more than one single system or subsystem. No blanket waivers shall be permitted. If more than one system incorporates the same nonconformance, separate waivers are required for each of the systems. No additional changes shall be made to the waiver after it has been put in process. Whenever substantiating technical data is necessary, attachments shall be made to the waiver.

2.9.1.2.3.2 Deviations (See Figure 7)

A deviation is a written approved authorization, granted prior to the production, procurement or performance, of the affected item, allowing noncompliance with or variance from a contract requirement.

The second paragraph of Section 2.9.1.2.3.1 (Waivers) shall also apply to deviations.

2.9.1.2.3.3 Classification of Waivers and Deviations

In order to facilitate the delegation of authority to act on waiver and deviation requests, the following categories of requests are established.

- (1) Category A includes requests which concern material, process or equipment characteristics which, if defective, do one or more of the following.
 - (a) Could or would result in hazardous or unsafe conditions for individuals during use, handling, stowage, shipment or maintenance of the product.
 - (b) Conflict, directly or indirectly, with Project Coordination Drawings or Systems specifications or otherwise affect coordination or compatibility with other equipment.
 - (c) Would result in failure or degradation of performance to the extent that the system fails to meet minimum performance.
 - (d) Would materially degrade the reliability of the system or subsystem.

- (2) Category B includes requests, other than those in Category A, which concern material or equipment characteristics which, if defective, do one or more of the following.
 - (a) Would result in failure or degradation of performance, but not of such magnitude as to fail to meet System requirements.
 - (b) Affect interchangeability of replaceable components.
 - (c) Would measurably reduce the expected life of the affected equipment.
- (3) Category C includes requests other than those in Category A or B, that could reduce, but not materially, the useability of the materials or equipment, or that could delay further processing or assembly.
- (4) Category D includes requests other than those in Category A, B or C which in no way affect the useability of the item, or of other equipment with which it is used.

2.9.1.2.3.4 Procedure Definitions

For the purpose of this procedure the following definitions shall apply.

(1) Coordination

Coordination attributes of an equipment are those features that affect or are affected by the physical and functional mating (including weight) of the equipment with other parts or equipments in the system in which it is used.

(2) Life

Requirements that contribute to life design objectives are those features created to resist fatigue and deteriorating conditions of environment and wear in use and in storage. In general, pertinent life design characteristics are:

- (a) Specific physical, electrical and chemical characteristics such as hardness, tensile strength, and related criteria.
 - (b) Protective coatings, plating and surface treatments and finishes.
- (3) Interchangeability

The requirements that contribute to interchangeability are those pertaining to functional and physical characteristics that will assure proper mating of repair parts at point of service use without selective fitting.
- (4) Function

Function characteristics are those that affect the operation and use of the item. They are generally those that define such things as mechanical or electrical output or chemical action, or other performance criteria.
- (5) Safety

Safety characteristics are those features that reduce the hazard to personnel handling, using, or maintaining the equipment.

2.9.1.2.3.5 Preparation of the Nonconformance Authorization Format

Whenever a nonconformance exists which requires a deviation or waiver, the cognizant engineer shall inform his group leader of this condition. If it is obvious that this condition cannot be corrected by standard documentation changes (such as Engineering Change Request or Specification Change Notices) before "sell-off", the engineer shall request a nonconformance form from the documentation group. The documentation group shall decide if a waiver or deviation is applicable and shall assign a number to the form. The engineer shall then fill out the applicable sections and return the form to the documentation group which shall then complete the form and obtain necessary signatures.

A detailed instruction for preparation of the Nonconformance Authorization action is included below.

a. Firm Name and Address

b. Nonconformance Authorization

When it has been determined whether the nonconformance is a deviation or a waiver the nonapplicable term shall be crossed out.

c. Number

The documentation group shall assign consecutive numbers beginning with 001. There shall be separate numbers for waivers and for deviations.

d. Sheet of

Insert 1 in first blank and total number of sheets required in second blank.

e. Prepared By

Originating or cognizant Engineer shall sign his name.

f. Date

Insert date when number is assigned.

g. Contract No.

The number of the Prime Contract shall be entered.

h. Type of Contract

Enter type of contract.

i. Component/System Affected

Component nomenclature and system nomenclature shall be entered.

j. Serial No. Affected

Serial numbers of component and system shall be entered.

k. Impact

Documentation Schedule Cost Certification

Place a check mark in those areas which are affected. Define on an additional sheet(s) why and to what extent these areas are affected.

l. Category

Check the applicable category. See Section 2.9.1.2.3.3 for definition of categories. Define on additional sheet(s), the consequences of not correcting nonconformance.

m. Present Condition -- Provide a description of the existing condition.

Reasons for Existing Condition -- State the reason the nonconformance condition exists.

n. **Recommended Corrective Action**

Existing Units -- Provide a solution to correct the deficiency in the existing unit(s).

Future Units -- Provide a solution to correct the deficiency in future unit(s).

o. The remaining blocks are for approval signatures. The responsible personnel shall sign their name and the date of signature.

2.9.2 **Engineering Change Proposal (ECP)**

NIIB 8040.2 is the governing document for the ECP procedure. Those changes which require ECP action shall be prepared in accordance with this document. Whenever an ECP involves a change to a specification, a specification Change Notice shall be prepared and attached to the ECP.

2.9.2.1 **ECP Recommendations**

Recommendation for ECP action may be originated by NASA, CSDL or any sub-contractor. In each case, CSDL will initiate the ECP and submit it as stated above.

2.9.2.2 **ECP Preparation**

The MIL-STD-480 ECP procedure shall be used as a guide in the preparation and submission of all ECP's. The ECP coordinator shall assist in the preparation of ECP's, and shall establish coordination meetings as required.

CHAPTER 3

CHANGE CONTROL AFTER DELIVERY OF EQUIPMENT

3.1 Retrofit Kit Release, Revision, and Marking

When it is proposed that a retrofit modification is required or desired in delivered equipment, action is necessary to insure proper documentation of the change. This procedure identifies the necessary documentation and approvals for retrofit actions. Every retrofit action will carry an ECP as defined by NASA procedures (ref., NHB 8040.2) to recognize any required work requirements for contract purposes.

3.1.1 Retrofit Kit Content

The retrofit kit will contain all the necessary parts, unique tools, and necessary engineering drawings required to accomplish the modification. In addition, each kit will contain a Retrofit Instruction Bulletin (RIB) when the retrofit is to be accomplished at field locations.

3.1.1.1 Retrofit Instruction Bulletin (RIB)

The Retrofit Instruction Bulletin shall be prepared by the Contractor for modification of hardware for which he has cognizance. The RIB shall contain all required instructions (special disassembly or assembly techniques, and the like) for installation of the kit. It shall also contain descriptions of the required retesting to insure that the modified equipment adheres to all specification requirements. The retesting requirements may be specified as certain paragraphs of applicable specifications. However, if special retest procedures are required, they shall be detailed in the RIB.

Retrofit or Repair Compliance forms are to be completed when the retrofit (or repair) is accomplished: see Figure 8. These forms are used to give detailed information regarding parts added and/or removed from NASA equipment.

NASA EXPERIMENT

RETROFIT OR REPAIR COMPLIANCE REPORT

The following information must be submitted to the CSDL NASA Experiments Configuration Management office upon completion of any retrofit performed on _____ equipment.

[illegible][illegible]

	KIT INSTALLED	Q.A. VERIFICATION
DATE		
SIGNED		

Figure 8

3.1.1.2 RIB Numbers

Each RIB number shall be a seven-digit NASA Production number (from a series assigned by the CMO). The RIBs will be written for the level of a highly skilled technician. Figure 9 is an outline of the format and types of information required in a RIB.

3.1.1.3 Contractor In-House Retrofit

RIBs are not required for contractor in-house retrofit. However, a retrofit kit drawing listing all parts and/or assemblies required to accomplish the retrofit must be processed through DRB and CCB. The elimination of RIBs for contractor in-house retrofit is predicated on the following actions:

- (1) The Contractor is responsible to insure that adequate procedures are instituted and followed both internally and at subcontractors to properly accomplish these in-house retrofits.
- (2) Retrofit kits with RIBs are still required for all field retrofits.
- (3) Retest of modified equipment which consists of a complex functional test to the level of assembly modified is required.
- (4) Deviation to item 3 shall be with the written prior concurrence of the NASA/MSC.
- (5) All critical processing which has depotting, weld repairs, etc., shall be accomplished per CCB released ND documents or the procedure must be approved by the NASA/MSC.

3.1.2 Acceptance Data Package

Each deliverable retrofit kit shall require an Acceptance Data Package (ADP) to be delivered with the hardware. In addition, a Unit History Record shall accompany each article in accordance with MIT Report E-1087, "Documentation Handbook and Plan".

3.1.3 Drawings and Documents

All new drawings and revisions to documents necessary for the retrofit kit shall be prepared in accordance with MIT Report E-1167, "Drawing Standards", and shall be released through CCB by means of the ECR Procedure. The agency responsible for

RETROFIT INSTRUCTION BULLETIN (RIB) OUTLINE

- I. PURPOSE
(A brief description of what the retrofit is to accomplish.)
- II. AUTHORITY
(The ECP number.)
- III. UNITS affected
(Name, part number, serial number, and new part number of the units to be modified, in indenture order.)
- IV. PRIORITY CHANGES
(Any modification which must be incorporated prior to the incorporation of this retrofit.)
- V. RELATED CHANGES
(Any other RIBs for the same ECP.)
- VI. MATERIAL REQUIRED
(List of kit contents and a list of required, but not supplied, items, in indenture order of equipment affected.)
- VII. PROCEDURE
(Instructions for accomplishment:
 - A. General - Applies to all sections if required or top kit retrofit procedure (Console, system, etc., of ECP); Statement of re-test requirements and procedures.
 - B., C., etc. - Section for each affected assembly of a console or specific instructions for the item for which there is a retrofit kit. Statement of re-test requirements and procedures.))
- VIII. MODIFICATION DESIGNATION
(Application of new nameplates, marks, or harness tags for the console or end item. Console subassemblies will be given modification designation in their respective procedures.)
- IX. DISPOSITION OF PARTS REMOVED
(Scrap, return to stock, etc.)
- X. REPORT OF ACCOMPLISHMENT

Figure 9

maintenance of the master drawings shall establish two "top retrofit kit drawings" against which all retrofit kits will be released, i. e. , one top kit drawing will be established for the release of all flight hardware kit assemblies and the other top kit drawing will be established for the release of all ground support equipment kit assemblies. The top retrofit kit drawings will list all applicable subkits necessary to modify components, assemblies, subassemblies, and spares. For each retrofit, a retrofit kit assembly drawing shall be established which shall contain a listing of all the subkit part numbers applicable to the ECP.

CHAPTER 4

CONFIGURATION CONTROL IN MANUFACTURING

4.1 Purpose

This chapter refers to the Reliability and Quality Assurance system and procedures, the implementation of which will assure continuity of configuration control during the manufacture and production of hardware under NASA Experiment contracts.

4.2 Scope

This system is designed to provide the NASA with a high degree of confidence that the product, as represented by the delivered hardware, is of known and documented quality and free of problems associated with workmanship defects. This system provides for the accomplishment of the following objectives:

4.2.1 Design Review

That the design is reviewed for engineering excellence, quality, and reliability; and is subsequently controlled.

4.2.2 Parts Procurement Integrity

That parts and materials are procured from quality sources under appropriate quality requirements and that significant characteristics of this procured material are verified by inspection.

4.2.3 Material Control and Traceability

That material destined for inclusion in deliverable hardware is controlled and traceability maintained as to its history and status.

4.2.4 Manufacturing and Production

That fabrication and assembly operations are conducted in an organized and orderly fashion, with quality inspection of important hardware characteristics and workmanship, and that documented evidence

exists of fabrication operations and inspections performed on hardware as it is processed.

4.2.5 Non-Conformance Monitoring

That non-conforming, discrepant material, and problems encountered throughout the process are documented, resolved, and corrective action effected.

4.2.6 Acceptance Data Collection

That hardware configuration, test data, and history, important to the sponsor's acceptance and uses, are accumulated and delivered with the units or collected for future availability.

4.3 Operation Procedures

The procedures listed hereafter are selected from the standard quality system developed at CSDL for implementation in an Engineering Research and Development environment. They have been selected to respond to the NASA requirements and special needs as imposed by the nature of the experiment projects.

4.3.1 Material Procurement, Supplier and Sub-Contractor Control - QOP 003 Revised June 9, 1970

4.3.2 Receiving, Inspection, Stocking, Issuance and Kitting - QOP 004 Revised June 9, 1970

4.3.3 Serialization and Lot Control - QOP 005 October 1969

4.3.4 Production and Inspection Planning and Control of Fabricated Articles - QOP 006 October 1969

4.3.5 Non-Conforming Material/Waivers - QOP 007 October 1969

4.3.6 In Process Inspection and Test - QOP 008 Revised May 13, 1970

4.3.7 Acceptance Data Package - QOP 010 Revised June 9, 1970

4.3.8 Handling of Government Furnished Equipment - QOP 014 Revised June 9, 1970

4.3.9 Calibration and Standards - QOP 012 October 1960

4.3.10 Failure Reporting and Corrective Action - QOP 011 Revised June 9, 1970

4.3.11 Qualification and Special Testing - QOP 016 May 15, 1970

4.3.12 Personnel Training and Certification - QOP 017 May 15, 1970

CHAPTER 5

GLOSSARY OF TERMS AND ABBREVIATIONS

5.1 Glossary of Terms

The following definitions shall apply to the use of terms as they appear in this publication.

Cancelled	"Cancelled" denotes any document which has been removed from potential use and which had not been released through the CCB at CSDL. The identification number of a cancelled document shall not be reassigned, and will not appear in formal documentation records.
Class of Changes	The classification of changes shall be in accordance with Section 2.7 of this publication
Dash Number	An identification suffix used to indicate a unique configuration of the hardware.
Deviation	A specific authorization, granted by NASA and CSDL before the fact, to depart from a particular requirement of specifications or related documents.
Effectivity	Effectivity identifies the application to stated designed CEI serial numbers.
ECP Form	The ECP form described in MIL-STD-480 shall be used as required. Refer to Section 2.9.2.
ECR Form	The ECR form (Figures 3 and 4) is used to authorize and release documentation through the CCB at CSDL.
Inactive	"Inactive" denotes any document which has been formally removed from use and the document had been previously released through the CCB at CSDL, and the document had previously been used to build, procure, test or otherwise support hardware.

Interchangeable Item	When two or more items possess such functional and physical characteristics as to be equivalent in performance, reliability, durability and capable of being exchanged one for the other without alteration of the items themselves or of adjoining item except for adjustment, and without selection for fit or performance, the items are interchangeable. Reference MIL-STD-447.
Obsolete	"Obsolete" denotes any document which has been formally removed from use, and the document had been previously released through the CCB at CSDL, build, procure, test or in any way support hardware.
Replacement Item	An item which is functionally interchangeable with another item, but which differs physically from the original part in that the installation of the replacement part required operations such as drilling, reaming, cutting, filing, shimming, etc., in addition to the normal application and methods of attachment, is known as a replacement item. Reference MIL-STD-447.
Revision Letter	An identification of the status of the document.
Schedule	Schedule is interpreted in accordance with the delivery requirements established by the contracts of the Contractors. Schedule impact identifies the fluctuation about these contractual delivery requirements.
Substitute	Where two or more items possess such functional and physical characteristics as to be capable of being exchanged only under certain conditions or in particular applications and without alterations of the items themselves or adjoining items they are substitute items. This includes the definition of one-way interchangeability such as, Item B can be interchanged in all applications for Item S, but Item A cannot be used in all applications requiring Item B. Reference MIL-STD-447.
Waiver	Granted use or acceptance by NASA and CSDL of an article which did not meet specified requirements. Reference NPC 200-2.

5.2

Abbreviations

The following abbreviations are used in this publication.

AGE/SE	Aerospace Ground Equipment/Support Equipment
APL	Advanced Parts List
ATS/P	Assembly Test Specification/Procedure
CCB	Configuration Control Board
CMO	Configuration Management Office
CSDL	Charles Stark Draper Laboratory
DRB	Design Review Board
ECP	Engineering Change Proposal
ECR	Engineering Change or Release
FSN	Federal Stock Number
FTM	Final Test Method
GFE	Government Furnished Equipment
ICD	Interface Control Document
JDC	Job Description Card
MRB	Material Review Board
NA	Not Applicable
PS	Procurement Specification
QA	Quality Assurance
RIB	Retrofit Instruction Bulletin
SCD	Specification Control Drawing

E-2509

DISTRIBUTION LIST

Internal

R. Ragan	W. Beaton
D. Hoag	D. Hanley
L. Larson	J. McKenna
N. Sears	J. Partridge
J. Harper	R. Baker
P. Bowditch	M. Murley (30)
S. Buck	W. Stameris
J. Hursh	J. Barker
E.C. Hall	K. Whitney
G. Silver	Apollo Library (2)
G. Mayo	Central Files (2)
D. Grief	Tech Doc Center (12)
R. Weatherbee	

External

A. Metzger (2) NASA/FOLE

NASA/MSC: M. Krisberg JC931
J. T. Wheeler BM7
D. Cubley EE3 (2)
J. Vyner PP7
A. Carraway EH
M. Holley EG14